THE HONG KONG POLYTECHNIC UNIVERSITY

INSTITUTE OF TEXTILES AND CLOTHING

PRODUCTION, PROPERTIES AND STRUCTURES OF SHORT STAPLE LOW TORQUE SINGLES RING YARN FOR WEAVING

HUA Tao

A thesis submitted in partial fulfillment of the requirements for the Degree of

DOCTOR OF PHILOSOPHY

September, 2006

CERTIFICATE OF ORIGINALITY

I herby declare that this thesis is my own work and that, to the best of my knowledge and belief, it reproduces no material previously published or written, nor material that has been accepted for the award of any other degree or diploma, except where due acknowledgement have been made in the text.

_____(Signed)

HUA Tao (Name of student)

This Thesis is Dedicated to My Family

to my wife for her encouragement and constant support

and

to my parents and my son for their understanding and support

ABSTRACT

One of the disadvantages related to the conventional ring spinning process is that ring spun yarn possesses high residual torque, which may cause distortion in knitted fabric and woven fabric, bring about difficulties in handling any post-spinning operation, and also produce defects in fabrics. The project is thus conducted with an aim to probe the possibility of producing low torque ring weaving yarns for industrial application by a torque reduction device attached on the conventional ring machine.

A preliminary study of the torque reduction device was made. The torque reduction device was composed mainly of a false-twisting system including a pair of spaced rotors, a false-twister in tangential frictional contact with each of rotors and magnetic means. The experimental results show that the resultant yarns had reduced residual torque through modifying yarn structure directly during yarn formation, which eliminates any additional step after the spinning process. In addition, with a false-twister installed between the front roller and the yarn guide, the yarn spinnability is improved.

As one of the most important parts for yarn spinning mechanism investigation, a study is conducted on the geometry of ring spinning triangle and its effect on the yarn torque. The observation of spinning triangle indicates that the geometry of spinning triangle in low torque ring yarn exhibits some unique characteristics such as

symmetric structure, short height and multi-bundle of fibers. A modified energy approach is presented to study the distribution of fiber tension force in the spinning triangle under the applied of yarn spinning tension. The shape of spinning triangle is represented by a shape parameter newly introduced in the analysis. The effects of shape of spinning triangle on the fiber stress distribution at the spinning triangle are investigated including fiber distributed in the form of multi-bundle and without multi-bundle fibers. The simulated results indicate that the distribution of fiber tension force is influenced obviously by the shape of spinning triangle. A theoretical analysis of the fiber tensile stress distribution within the yarn and its effect on the yarn torque is thus conducted on the basis of the translation of fiber tension at the spinning triangle into the fiber tensile stress within the yarn.

A system for investigation of the fiber configuration in staple yarns has been developed in this study. The main feature of the system is that it can capture and store consecutive images of single tracer fiber, thus the image acquisition becomes faster and more accurate. It is also helpful for the analysis and processing of the tracer fiber image information. The investigation of yarn structures demonstrated that low torque ring yarn possesses ring like appearance, compact structure, wrapper fibers in vertical or opposite direction, some parts of fibers arranging in opposite direction to the yarn twist and higher rate of fiber migration, which contributes to the reduction of yarn residual torque and yarn hairiness, as well as to the increase of yarn strength when low twist level was adopted in low torque ring yarns.

Statistic models have been developed for the relationship between yarn properties

and spinning parameters with the help of Fractional Factorial Methodology and Response Surface Methodology. The model adequacy assessment of Response Surface Methodology demonstrated that the developed model exhibits a good predicating accuracy and this model can reflect the actual relationship between yarn properties and yarn twist and speed ratio. The optimum spinning parameters are found, based on the developed models coupled with the desirability function and overlaid contour plot.

The properties of low torque ring yarn and the resultant fabric are comprehensively investigated. The test and analysis exhibit some exciting results of low torque ring yarn with great reduction of yarn snarling and yarn hairiness. Even using low twist level, low torque ring yarn can still maintain its comparable yarn tenacity and evenness to conventional ring yarn with normal twist level. The results also demonstrate that low torque ring yarn fabric exhibits improved denim fabric and twill fabric appearance, a fuller, thicker and more smooth hand.

The investigation of the effect of yarn torque on the surface smoothness of denim fabric was conducted theoretically and experimentally. The theoretical analysis results indicate that reducing yarn residual torque, particularly weft yarn residual torque will decrease the difference of the angle of twist between warp yarn sections. As a result, the yarn buckling unevenness may be decreased, which endows denim a more smooth surface and thus decrease the problem of 'small snake' pattern on denim fabric. The experimental study demonstrates that the appearance of the denim fabrics has been greatly improved by using the low torque ring yarns as weft yarns.

PRESENTATION AND PUBLICATION LIST

1. Tao Hua, Bin Gang Xu, Ka Fai Choi, Kwok-Po Cheng and Xiao Ming Tao, A System for Measuring Fiber Configuration in Staple Yarns, Proceedings of The Fiber Society International Fiber Conference 2006, Seoul, Korea, May, 2006

2. Hua, T., Murrells, C.M., Wong, K.K., Xu, B.G., Yang, K., Wong, S.K., Choi, K.F, Cheng, K.P.S. and Tao, X.M. Application of Nu-Torque^{TM} Singles Ring Yarns on Woven Fabrics, Textile Asia, 36(1), 28-30 (2005).

3. T. Hua, K.P.S. Cheng, X.M. Tao, S.K. Wong, K.K. Wong, B.G. Xu, Characterization of Woven Fabrics Produced from Nu-Torque^{TM} Singles Ring Spun Yarn, Proceedings of The Textile Institute 84th Annual World Conference, Raliegh NC, USA, March, 2005

4. Hua, T., Tao, X. M., Cheng, K.P.S., Wong, K.K., and Xu, B.G., Study on New Method Spinning Nu-Torque^{TM} Yarn for Weaving, Journal of Textile Research, 25(5), 38-40 (2004).

5. Wong, K.K., Hua, T., Leung, C.L., Murrells, C.M., Xu, B.G., Yang, K., Wong, S.K., Choi, K.F., Yip, Y.K., Cheng, K.P.S. and Tao, X.M., A New Ring-Spinning Technology, Textile Asia, 35(6), 27-28 (2004).

6. Wong, K.K., Hua, T., Murrells, C.M., Xu, B.G., Yang, K., Wong, S.K., Choi, K.F., Cheng, K.P.S. and Tao, X.M., Production Technology and Applications of Nu-Torque^{TM} Singles Ring Yarns, The 33rd Textile Research Symposium, Fuji, Japan, August, 2004

7. Hua, T., Cheng, K.P.S., Tao, X.M., Choi, K.F., Wong, S.K., Wong, K.K., Xu, B.G., Murrells, C.M., Yang, K. and Leung, C.L., A Method For Improvement of Denim Fabric Appearance by Using Nu-Torque^{TM} Singles Ring Spun Yarns, The 83rd Textile Institute World Conference, Shanghai, P R China, May, 2004

8. Wong, K.K., Hua, T., Leung, C.L., Murrells, C.M., Xu, B.G., Yang, K., Wong, S.K., Choi, K.F., Yip, Y.K., Cheng, K.P.S. and Tao, X.M., Development of Nu-Torque^{TM} Singles Ring Yarn for Industrial Application, The 83rd Textile Institute World Conference, Shanghai, P R China, May, 2004

9. Murrells, C.M., Wong, K.K., Hua, T., Yang, K., Cheng, K.P.S. and Tao, X.M., Study of Yarn Snarling in Nu-Torque^{TM} Singles Ring Yarn, The 83rd Textile Institute World Conference, Shanghai, P R China, May, 2004

10. Xu, B.G., Tao, X.M., Cheng, K.P.S., Yip, Y.K., Choi, K.F., Wong, S.K., Wong, K.K., Leung, C.L., Hua, T., Yang, K. and Murrells, C.M., Nu-Torque^{TM} Singles Ring Yarn and Its Production Technology, The 83rd Textile Institute World Conference, Shanghai, P R China, May, 2004

11. Yang, K., Yip, Y.K., Tao, X.M., Wong, S.K., Wong, K.K., Murrells, C.M., Xu, B.G., Hua, T. and Leung, C.L., Developing Torque-free ring^{TM} Singles Ring Yarn to Reduce Spirality of Single Jersey Knitted Fabric, The 83rd Textile Institute World Conference, Shanghai, P R China, May, 2004

12. T. Hua, X.M. Tao, K.P.S. Cheng and B.G. Xu, Effects of Geometry of Ring Spinning Triangle on Yarn Torque: Part I: Analysis of Fiber Tension Distribution, submitted to Textile Research Journal

13. T. Hua, K.P.S. Cheng, X.M. Tao and B.G. Xu, Effects of Geometry of Ring Spinning Triangle on Yarn Torque: Part II: Distribution of the Fiber Tensile Stress within a Yarn and Its Effect on Yarn Torque, to be submitted to Textile Research Journal

14. T. Hua, K.P.S. Cheng, X.M. Tao and B.G. Xu, Investigation on the Effects of Spinning Processing Parameters on Properties of Low Torque Ring Yarn by Statistic Design Method, to be submitted to Journal of Materials Processing Technology

15. K.P.S. Cheng, T. Hua, X.M. Tao, B.G. Xu, and K. K. Wang, Properties of Low Torque Ring Yarn and Characteristics of Resultant Woven Fabric, to be submitted to Textile Research Journal

16. T. Hua, X.M. Tao, K.P.S. Cheng, and B.G. Xu, An Experimental Study of Improving Fabric Appearance of Denim by Using Low Torque Singles Ring Spun Yarn, to be submitted to Textile Research Journal

ACKNOWLEDGEMENTS

Firstly, I would like to express my deepest gratitude and sincere appreciation to my chief supervisor Dr. Kwok-po Cheng, Associate Professor of Institute of Textiles and Clothing, The Hong Kong Polytechnic University, for his valuable and professional guidance throughout this research. Without his constant help, constructive criticism and encouragement, I will not be able to complete my PhD study successfully.

I would like to express my deepest gratitude and sincere appreciation to my supervisor Prof. Xiaoming Tao, Head and Chair Professor of Institute of Textiles and Clothing, The Hong Kong Polytechnic University, for providing me the opportunity to study here. Her critical discussion and comments, professional guidance and consistent support are invaluable for me in the course of my PhD study.

My sincere appreciation is given to Mr. Sing-kee Wong for his valuable advice and great help in the research study. My sincere thanks are given to Dr. Ka-fai Choi for his valuable advice and help on the investigation of yarn structures. My sincere thanks to Dr. Bingang Xu for his valuable suggestions and great help in the study particularly on the theoretical aspects in the thesis. My sincere thanks to Mr. Man Chi Yan for his great help on the experimental set-up for investigation of spinning triangle.

My grateful thanks are given to my project team members for their support in research and study, particularly to Dr. Ka Kee Wong for her great support, Mr. Kun Yang for his helpful discussion and Ms Murrells Charlotte, Ms. Suk Yee Chen, Mr. Alan Ho and Mr. Paul Leung for their support in the research and PhD study.

My sincere thanks are given to Mr. Wai-man Chu and Mr. Fan in the Spinning Workshop, Mr. Wong in the Weaving Workshop, Ms. Mow-nin Sun and Mr. Choi in the Physical Lab and Ms. Ching-yee Lung and Mr. Wai Kong Ho in the Chemical Lab for their technical support and help.

Special thanks are given to my wife, Qian Jinjuan, and my son, Hua Wei, and my parents, for their constant encouragement, understanding and great support. Leaving home around four years, I am deeply indebted to them too much. Without their continuous support and love, I could not complete my PhD study successfully.

Table of Contents

Abstract I

Presentation and Publication List IV

Acknowledgements VII

Table of Contents IX

List of Tables XVI

List of Figures XIX

CHAPTER 1 General Introduction 1

1.1 Ring Spinning Systems 1

1.2 Research Background 3

1.3 Aim and Objectives 6

1.4 Significance 7

1.5 Methodology 10

1.5.1 Investigation of Spinning Mechanism by the Geometry of Ring Spinning Triangle and Its Effect on the Yarn Torque 10

1.5.2 Analysis of Low Torque Ring Yarn Structure Characterized by Geometrical Arrangement of Fibers in the Yarn 10

1.5.3 Experimental Probe of the Relationship between Low Torque Ring Yarn Properties and Spinning Processing Parameters 11

1.5.4 Characterization of Low Torque Ring Yarn and Resultant Woven Fabric 11

1.5.5 Study of the Effects of Yarn Torque on the Surface Smoothness of Denim Fabric 12

1.6 Scope of Work 12

CHAPTER 2 Spinning Process of Low Torque Ring Yarn 16

2.1 Introduction 16

2.2 Yarn Torque Reduction 17

2.2.1 Nature of Yarn Torque 17

2.2.2 Factors Affecting Yarn Residual Torque 19

2.2.3 Existing Methods for Yarn Torque Reduction 21

2.2.4 Principles of Yarn Torque Reduction during Yarn Formation 22

2.3 Preliminary Investigation 26

2.3.1 Yarn Snarling 29

2.3.2 Yarn Tenacity 29

2.3.3 Yarn Hairiness 30

2.4 Summary and Conclusion 30

CHAPTER 3 Geometry of Ring Spinning Triangle and Its Effects on Yarn Torque 32

3.1 Introduction 32

3.2 Experimental Study on the Geometry of Spinning Triangle 34

3.2.1 Materials and Experimental Set-up 34

3.2.2 Characteristics of the Geometry of Spinning Triangle 36

3.3 Retrospect of Ring Spinning Triangle Study 41

3.4 Effect of Shape of Spinning Triangle on the Stress Distribution of Fibers at the Spinning Triangle 43

3.4.1 Theoretical Considerations 44
3.4.2 Various Cases of Distribution of Fiber Stress at the Spinning Triangle 47
3.4.2.1 Case I 47
3.4.2.2 Case II 53
3.4.3 Effect of Shape of Spinning Triangle on the Distribution of the Fiber Tensile Stress at the Spinning Triangle 55
3.4.3.1 Case I 55
3.4.3.2 Case II 60
3.5 Distribution of Fiber Tensile Stress Within a Twisted Yarn and Its Effect on Yarn Torque 63
3.5.1 Distribution of Fiber Tensile Stresses within a Twisted Yarn 64
3.5.1.1 Assumptions 65
3.5.1.2 Distribution of Fiber Tensile Stresses within a Twisted Yarn 67
3.5.2 Yarn Torque due to Residual Fiber Tensile Stress 72
3.6 Summary and Conclusion 76

CHAPTER 4 Structures of Low Torque Ring Yarn for Weaving 79

4.1 Introduction 79
4.2 Retrospect of Yarn Structure Study 80
4.3 Measuring System 84
4.3.1 System Configuration 84
4.3.2 Measurement Procedure 92
4.4 Experimental 93
4.4.1 Preparation of Yarn Sample for SEM Observation 93

4.4.2 Preparation of Yarn Sample with Tracer Fibers 93

4.5 Results and Discussion 97

4.5.1 Yarn Surface Structure 97

4.5.2 3D Configuration and Radial Position Variation of Tracer Fiber 102

4.5.3 Analysis of Migration Behavior 109

4.6 Summary and Conclusion 111

CHAPTER 5 Statistic Models for Relationships between Yarn Properties and Spinning Parameters **114**

5.1 Introduction 114

5.2 Experimental Work 116

5.2.1 Yarn Sample Preparation 116

5.2.2 Test Methods 116

5.3 Determination of Effect Significance of Spinning Parameters 117

5.3.1 Design of Experiment 117

5.3.2 Results and Discussion 119

5.4 Development of Statistical Models for the Relationship between Yarn Properties and Yarn Twist Level and Speed Ratio 124

5.4.1 Theoretical Consideration 125

5.4.2 Design of Experiment 127

5.4.3 Results and Discussion 129

5.4.3.1 Effects of Yarn Twist and Speed Ratio on the Tenacity of Low Torque Yarns 137

5.4.3.2 Effects of Yarn Twist and Speed Ratio on the Snarling of Low Torque Yarns 138

5.4.3.3 Effects of Yarn Twist and Speed Ratio on the Hairiness of Low Torque Yarns 141

5.4.3.4 Effects of Yarn Twist and Speed Ratio on the Evenness of Low Torque Yarns 142

5.5 Deviation of the Estimated Value of Yarn Properties from Statistical Models to Experimental Results 143

5.6 Optimization of Spinning Processing Parameters 146

5.6.1 Optimization Using the Desirability Function 146

5.6.2 Optimization Using Overlaid Contour Plot 150

5.7 Summary and Conclusion 153

CHAPTER 6 Properties of Low Torque Ring Yarn and Characteristics of Resultant Woven Fabric 155

6.1 Introduction 155

6.2 Experimental 156

6.2.1 Sample Preparation 156

6.2.1.1 Yarn Sample Preparation 156

6.2.1.2 Fabric Sample Preparation 158

6.2.2 Test Methods 160

6.2.2.1 Yarn Test 160

6.2.2.2 Fabric Test 161

6.3 Results and Discussion 163

6.3.1 Yarn Properties 163

6.3.1.1 Yarn Diameter 163

6.3.1.2 Yarn Twist 164

6.3.1.3 Yarn Hairiness 165

6.3.1.4 Yarn Evenness 167

6.3.1.5 Yarn Torsional Property 167

6.3.1.6 Yarn Tensile Property 169

6.3.1.7 Yarn Bending Property 171

6.3.2 Fabric Properties 172

6.3.2.1 Structure Characteristics 172

6.3.2.2 Mechanical Characteristics 174

6.3.2.3 Fabric Performance 180

6.4 Subjective Evaluation of Denim Jeans and Twill Trousers 187

6.4.1 Methods 188

6.4.1.1 Clothing and Subjects 188

6.4.1.2 Procedures 189

6.4.2 Results and Discussions 193

6.4.2.1 Subjective Evaluation of Appearance and Performance 193

6.4.2.2 Measurement of Dimensional Stability and Skewness 204

6.4.2.3 Overall Subjective Evaluation 206

6.5 Summary and Conclusion 208

CHAPTER 7 Effect of Yarn Torque on Surface Smoothness of Denim Fabric 211

7.1 Introduction 211

7.2 Theoretical Study of Surface Smoothness of Denim Fabric 213

7.3 Experimental Study of Surface Smoothness of Denim Fabric 223

7.3.1 Yarn and Fabric Sample Preparation 224

7.3.2 Test Methods 226

7.3.3 Results and Discussion 227

7.3.3.1 Yarn Properties and Comparison 227

7.3.3.2 Fabric Properties and Appearance 230

7.4 Summary and Conclusion 237

CHAPTER 8 Conclusion and Recommendation 239

8.1 Conclusion 239

8.1.1 The Process and the Torque Reduction Device 240

8.1.2 Investigation on the Geometry of the Ring Spinning Triangle and Its Effect on Yarn Torque 242

8.1.3 Structures of Low Torque Ring Yarn for Weaving 244

8.1.4 Statistic Models for the Relationship between Yarn Properties and Spinning Parameters 245

8.1.5 Characteristics of Low Torque Ring Yarn and Its Woven Fabric 247

8.1.6 Effects of Yarn Snarling on Surface Smoothness of Denim Fabric 249

8.2 Recommendation for Future Work 249

References 251

Appendices A-1

Appendix A A-2

Appendix B A-3

Appendix C A-11

Appendix D A-17

Appendix E A-25

LIST OF TABLES

Table 2-1	Specifications of Yarn Samples	27
Table 2-2	Properties of Low Torque Ring Yarns and Conventional Ring Yarns	28
Table 3-1	Calculated Yarn Torque for 58tex Cotton Yarn	75
Table 4-1	Specifications of the Automatic Moveable Platform	88
Table 4-2	Specifications of Tencel Fiber	94
Table 4-3	Spinning Parameters and Yarn Specifications	94
Table 4-4	Specifications of Liquid Mixture	95
Table 4-5	Parameters Characterizing Low Torque and Conventional Ring Yarn Structure	111
Table 5-1	Experimental Variables and Levels of Low Torque Ring Yarn for Weaving	119
Table 5-2	Design Matrix and Response Data of Low Torque Ring Yarn for Weaving	121
Table 5-3	Experimental Variables and Levels of Low Torque Ring Yarn	128
Table 5-4	Design Matrix of Low Torque Ring Yarn	129
Table 5-5	Response Table of Low Torque Ring Yarn (84tex)	130
Table 5-6	Response Table of Low Torque Ring Yarn (58tex)	131
Table 5-7	Percentage Error between the Estimated Values and the Experimental Values of Yarn Properties	145
Table 5-8	Target and Boundaries of Each Response	149
Table 5-9	The Optimized Spinning Parameters and Yarn Properties	153
Table 6-1	Fiber Properties and Process Parameters of Spinning	157
Table 6-2	Specifications of Yarn Samples	158

Table 6-3	Fabric Specifications	159
Table 6-4	Yarn Hairiness	166
Table 6-5	Yarn Evenness	167
Table 6-6	Yarn Snarling	169
Table 6-7	Yarn Torsional Property	169
Table 6-8	Yarn Tensile Property	171
Table 6-9	Yarn Bending Property	172
Table 6-10	Dimensional Stability and Skewness of Fabric Samples	174
Table 6-11	Fabric Tensile and Tear Properties	175
Table 6-12	Fabric Mechanical Characteristics Measured by KESF	179
Table 6-13	Objective Evaluated Handle Values for Men's Winter Jacket and Slacks	181
Table 6-14	Air Permeability of Fabric Samples	182
Table 6-15	The Amount of Water Absorbed by Fabric Samples during Wicking	184
Table 6-16	Background of the Subjects	189
Table 6-17	Attributes of Jeans and Trousers	191
Table 6-18	Scale of the Level of Agreement	192
Table 6-19	Results of Multiple Comparisons LSD Test for Jeans' Subjective Evaluation	200
Table 6-20	Results of Multiple Comparisons LSD Test for Trousers' Subjective Evaluation	201
Table 6-21	The Consistency of the Subject's Ratings of Jeans	202
Table 6-22	The Consistency of the Subject's Ratings of Trousers	203
Table 6-23	Dimensional Stability and Skewness of Jeans	205
Table 6-24	Dimensional Stability and Skewness of Trousers	205

Table 6-25	Questions Given to Subjects and Summary of Their Answers on Jeans	207
Table 6-26	Questions Given to Subjects and Summary of Their Answers on Trousers	208
Table 7-1	Specifications of Yarn Samples	225
Table 7-2	Fabric Specifications	226
Table 7-3	Properties of Low Torque Ring Yarns and Conventional Ring Yarns	229
Table 7-4	Fabric Properties	236
Table 7-5	Results of Multiple Comparisons LSD Test	237

LIST OF FIGURES

Figure 1-1	Schematic of the Process of the Ring Spun Yarn Formation	2
Figure 2-1	Torque Reduction Device Fitted onto Ring Spinning Frame	24
Figure 2-2	Schematic of the Low Torque Ring Yarn Spinning	25
Figure 3-1	General View of the Transparent Roller for Photographic Experiment	35
Figure 3-2	General View of the Transparent Roller Mounted on the Spinning Frame	35
Figure 3-3	Consecutive Photographs of Geometrical Variation of Spinning Triangle in Conventional Ring Yarn	38
Figure 3-4	Consecutive Photographs of Geometrical Variation of Spinning Triangle in Low Torque Ring Yarn	38
Figure 3-5	Consecutive Photographs of Geometrical Variation of Spinning Triangle in Conventional Ring Yarn	39
Figure 3-6	Photograph of Spinning Triangle of Conventional Ring Yarn	40
Figure 3-7	Photographs of Spinning Triangle in Low Torque Ring Yarn	40
Figure 3-8	Photograph of Spinning Triangle in Conventional Ring Yarn	41
Figure 3-9	The Geometry of Spinning Triangle	44
Figure 3-10	Force on Fibers at the Spinning Triangle	45
Figure 3-11	Spinning Triangle Model for Fiber Tension (Geometry A)	46
Figure 3-12	Spinning Triangle Model for Fiber Tension (Geometry B)	56
Figure 3-13	Spinning Triangle Model for Fiber Tension (Geometry C)	57
Figure 3-14	Fiber Tension at Different Spinning Triangles	60
Figure 3-15	Fiber Bundle Tension at Different Spinning Triangles	62
Figure 3-16	Fiber Tension in Bundles at Different Spinning Triangles	63

Figure 3-17	The Distribution of Fiber Tensile Stress as a Function of Radial Position in a Twisted Yarn of Radius R_y	71
Figure 4-1	Yarn Geometry. a. Ideal Helical Yarn Geometry; b. Yarn Structure with Fiber Migration	83
Figure 4-2	a. The Whole Set of Tracer Fiber Measuring System;	84
	b. Configuration of Tracer Fiber Measuring System	85
Figure 4-3	General View of Tracer Fiber Observation Device	87
Figure 4-4	Modified Technique for Observing Two Images of A Tracer Fiber	87
Figure 4-5	a. Surface Structure of Low Torque Ring Yarn (TF=3.2, FTT=0.43);	99
	b. Surface Structure of Low Torque Ring Yarn (TF=3.8, FTT=0.43);	100
	c. Surface Structure of Conventional Ring Yarn (TF=3.2);	101
	d. Surface Structure of Conventional Ring Yarn (TF=4.2)	101
Figure 4-6	a. Typical Images of Tracer Fibers in Low Torque Ring Yarn (10Ne, TF=3.2, FTF=0.43);	103
	b. Typical Images of Tracer Fibers in Conventional Ring Yarn (10Ne, TF=4.2);	104
	c. Typical Images of Tracer Fibers in Conventional Ring Yarn (10Ne, TF=3.2)	104
Figure 4-7	a. 3D Configuration and Radial Position Variation of Tracer In Low torque Ring Yarn (10Ne, TF=4.2, FTF=0.43);	105
	b. Tracer Sections with Opposite Arranging Direction to the Yarn Twist In Low torque Ring Yarn (Section A and B) (10Ne, TF=4.2, FTF=0.43);	106
	c. 3D Configuration and Radial Position Variation of Tracer In Conventional Ring Yarn (10Ne, TF=4.2);	107
	d. 3D Configuration and Radial Position Variation of Tracer In Conventional Ring Yarn (10Ne, TF=3.2)	108
Figure 5-1	The Strategy of Experiment Research	115
Figure 5-2	Schematic of the Position of the Torque-reduction Device	118
Figure 5-3	The Effects of Factors on Yarn Tenacity	122
Figure 5-4	The Effects of Factors on Yarn Elongation	122

Figure 5-5	The Effects of Factors on Yarn Snarling	123
Figure 5-6	The Effects of Factors on Yarn Hairiness	123
Figure 5-7	The Effects of Factors on Yarn Evenness	124
Figure 5-8	A Central Composite Design in k = 2 Variables	128
Figure 5-9	a. Residual Analysis for Model Adequacy Checking of Yarn Tenacity and Snarling (84 tex)	133
	b. Residual Analysis for Model Adequacy Checking of Yarn Hairiness and Evenness (84 tex)	134
Figure 5-10	a. Residual Analysis for Model Adequacy Checking of Yarn Tenacity and Snarling (58 tex)	135
	b. Residual Analysis for Model Adequacy Checking of Yarn Hairiness and Evenness (58tex)	136
Figure 5-11	Contour and Surface Plot of Yarn Twist and Speed Ratio on Yarn Tenacity (84tex)	138
Figure 5-12	Contour and Surface Plot of Yarn Twist and Speed Ratio on Yarn Tenacity (58tex)	138
Figure 5-13	Contour and Surface Plot of Yarn Twist and Speed Ratio on Yarn Snarling (84tex)	140
Figure 5-14	Contour and Surface Plot of Yarn Twist and Speed Ratio on Yarn Snarling (58tex)	140
Figure 5-15	Contour and Surface Plot of Yarn Twist and Speed Ratio on Yarn Hairiness (84tex)	142
Figure 5-16	Contour and Surface Plot of Yarn Twist and Speed Ratio on Yarn Hairiness (58tex)	142
Figure 5-17	Contour and Surface Plot of Yarn Twist and Speed Ratio on Yarn Evenness (84tex)	143
Figure 5-18	Contour and Surface Plot of Yarn Twist and Speed Ratio on Yarn Evenness (58tex)	143
Figure 5-19	Response Optimization of 84tex Yarn	149
Figure 5-20	Response Optimization of 58tex Yarn	150
Figure 5-21	Overlaid Contour Plot of Yarn Properties (84tex)	151
Figure 5-22	Overlaid Contour Plot of Yarn Properties (58tex)	152

Figure 6-1	Yarn Diameter Profile	164
Figure 6-2	Yarn Twist Profile	165
Figure 6-3	Average Wicking Curve for Fabric Samples	184
Figure 6-4	'Small Snake' Pattern on the Fabric Surface	186
Figure 6-5	Photographs of Denim Fabric Appearance	186
Figure 6-6	Subjective Evaluation on Smoothness of Jeans	196
Figure 6-7	Subjective Evaluation on Fuzz of Jeans	196
Figure 6-8	Subjective Evaluation on 'small snake' Pattern of Jeans	196
Figure 6-9	Subjective Evaluation on Prominent Slub Effect in Warp Direction of Jeans	197
Figure 6-10	Subjective Evaluation on Softness of Jeans	197
Figure 6-11	Subjective Evaluation on Overall Quality of Jeans	197
Figure 6-12	Subjective Evaluation on Luster of Trousers	198
Figure 6-13	Subjective Evaluation on Smoothness of Trousers	198
Figure 6-14	Subjective Evaluation on Fuzz of Trousers	198
Figure 6-15	Subjective Evaluation on Fullness of Trousers	199
Figure 6-16	Subjective Evaluation on Acceptable Stiffness of Trousers	199
Figure 6-17	Subjective Evaluation on Overall Quality of Trousers	199
Figure 7-1	Denim Fabric Surface in the Closeup View	215
Figure 7-2	Typical Shape of Denim Fabric (3/1 right hand-twill)	216
Figure 7-3	Geometry of Woven Fabric	217
Figure 7-4	Schematic Diagram of a Fixed-ends Rod for Warp Yarn with Weft Yarn Contacting at Point B	218
Figure 7-5	Photographs of Denim Fabric Appearance (84tex weft yarns)	233
Figure 7-6	Photographs of Denim Fabric Appearance (58tex weft yarns)	234

Figure 7-7	Grade of 'Small Snake' Pattern of the Denim Fabrics	234
Figure 7-8	Relationship between Weft Yarn Snarling and Fabric 'Small Snake' Pattern	235

CHAPTER 1 GENERAL INTRODUCTION

1.1 Ring Spinning Systems

Spinning technology plays a very important role in the textile industry. From hand spinning to today's modern spinning technologies enormous human inventive efforts have been spent to develop better twist insertion mechanisms in terms of production speed and yarn quality. A major breakthrough came with the invention of the ring spinning machine more than 160 years ago (Klein, 1987). In the past few decades, many new spinning methods such as rotor spinning, air-jet, friction and vortex spinning have been developed, which were aimed at achieving higher production per spinning units. However, ring spun yarn has always been, and still is, the undisputed quality benchmark. On one hand, ring spinning possesses higher yarn quality and is more flexible in application compared to other new spinning systems. On the other hand, with the improvement of ring spinning itself, much modification on the basis of traditional ring spinning has given rise to Compact Spinning (CTI, 1990; Fehrer, 2000; Cheng and Yu, 2003), JetRing Spinning (Wang, Miao and How, 1997; Cheng and Li, 2002), Siro Spinning (Plate and Lappage, 1982; Emmanuel and Plate, 1983) and Solo Spinning (TWC, CSIRO and WRONZ, 1998). These new spinning techniques have contributed greatly to the improvement of ring spun yarn quality and end-use style.

Figure 1-1 shows a schematic of the process of the ring spun yarn formation (Grosberg and Iype, 1999), during which a roving is fed into drafting zone. Emerging from the front drafting rollers, the drafted strand is twisted and wound onto a bobbin by an arrangement of a traveler, ring and spindle. The traveler is a small clip, which rotates freely on the ring. The twisted strand of fibers passes through the traveler before being wound onto the bobbin on the spindle. Yarn from the rotating bobbin drags the traveler around the ring, forming a balloon, thereby simultaneously inserting twist and winding the yarn on the bobbin.

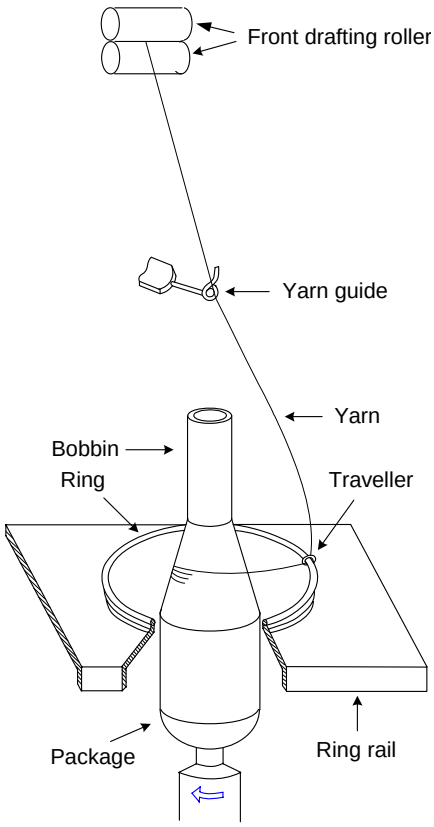

Figure 1-1 Schematic of the Process of the Ring Spun Yarn Formation

1.2 Research Background

As revealed by the paragraphs above, the ring spinning technology is still the most widely used spinning method, and it seems that it will continue to dominate the long- and short-staple spinning industries for some time due to its flexibility with respect to type of material and count range, and particularly its optimal yarn structure, which results in outstanding yarn strength (Klein, 1987; 1993). However, along with these positive aspects, there was a growing realization that this system still has imperfections that cause quality problems in yarns and thus influence some fabric performance. One of the disadvantages related to the conventional ring spinning process is that ring spun yarn possesses high residual torque or twist liveliness which builds up as twist is inserted.

In the ring spinning method, twisting plays an important role, which produces cohesive forces to hold the fibers together in the yarn by introducing interfiber three-dimensional crosslinking (Hearle, Grosberg and Backer, 1969; Goswami, Martindale and Scardino, 1976). The degree of twist in the yarn influenced properties of yarns and fabrics made from them such as yarn strength and elasticity, yarn hand and smoothness, and fabric durability and appearance (Yao, Zhou, Huang, Shao, An and Fan, 1988). As twist is inserted, the fibers become closer, yarn size is reduced and an internal force called torque builds up. Yarn torque is a force or a combination of forces, which tends to make yarn turn on itself, or kink, as a result of twisting. Fiber tension, fiber torsion, and fiber bending are three components contributed to yarn torque generated during yarn twisting.

A number of methods have been used to evaluate yarn torque. One of the simplest ways is to count the number of turns of snarling formed when the two ends of specified pre-tensioned length yarn segment are completely in contact and reach equilibrium. Other criteria also can reflect the residual torque in yarns, such as the distance between two approaching yarn ends at the moment the yarn just starts to snarl, and the length of the loop. A yarn with a higher residual torque will have a higher potential of snarling and thus can be considered more twist lively. For hydroscopic fibers, the residual yarn torque is measured in water as most of hydrogen bonds are broken, thus the residual torque measured will not be affected by temporary set (Milosavljevic and Tadic, 1995; Tavanai, Denton and Tomka, 1996; Primentas, 2003). Recently, a direct technique developed for measuring yarn torque is explored for the case of worsted yarns by Mitchell, Naylor and Phillips (2006).

Yarn torque has practical significance for a number of the characteristics of yarns, fabrics, and carpets. The magnitude of initial torque and the residual torque or twist liveliness of a twisted yarn have a considerable effect on the yarn properties and subsequently influence fabric performance. For example, the tendency of singles yarns to snarling, yarn twist instability and the twist balance in ply yarns depend on yarn torque in whole or part. The twisted yarn with residual torque or twist liveliness will have a tendency to untwist and release the torsional strain inside it to acquire the natural configuration of a minimum energy state. An effect of the residual torque or twist liveliness on yarns is their tendency to snarl, which may cause distortion in knitted and woven fabric such as spirality of knitted fabrics and skewness of woven fabrics, bring about difficulties in handling any post-spinning operation such as

winding, sizing, dyeing and weaving, and also produce defects like pucker in fabrics. Therefore, reducing yarn torque and producing low torque yarn even torque-balanced yarn have important practical meaning for weaving process and woven fabric. Low torque yarn exhibits low tendency to double, snarl or kink when held in the form of an open loop or suspended without tension, which is desirable in order to obtain stability in the resulting fabric and make yarn manageable for further processing.

In the past, various techniques were developed to reduce or eliminate residual torque in textile yarns. In terms of the underlying principle, these techniques can be divided into two major categories—permanent setting of yarn and physically balanced residual torque (Lau, Tao and Dhingra, 1995). Setting of yarn using resins, heat, steam or mercerization can reduce yarn residual torque by relaxing the stresses induced during spinning and twisting (Miles, 1971). Ageing of the yarn for prolonged periods is also useful in allowing torque stresses to decay until the yarn reaches equilibrium. In addition, torque-free in yarns can be obtained by setting up special yarn geometry of structure such as plying two singles yarns with the right amount of plying twist in the direction opposite to that in the singles yarns. The balancing methods have obvious advantages over the setting process, especially for natural fibers. However, several drawbacks are associated with these techniques, such as unsatisfactory fabric performance and high production costs.

According to the underlying principle, a technique has been developed for production of low torque or even torque balance single yarns by ring, rotor and

friction systems (Tao, Lo and Lau, 1997; Tao and Xu, 2003; Tao, Xu and Wong, 2004). In order to further develop this technology, the research work focuses on studying low torque single ring weaving yarn for industrial applications.

The requirements of low torque single ring weaving yarns are different from knitting yarns. Low torque single ring weaving yarns require higher tensile strength with acceptable lower snarling. In conventional ring spinning, it is well known that staple yarn with no twist has no strength, and before critical twist is reached the yarn strength increases with increase in yarn twist. On the other hand, usually the greater the amount of twist in the yarn, the greater is its tendency to snarl. Hence a modification on ring spinning technology is ideally to be made to produce low torque singles ring weaving yarns for industrial application.

1.3 Aim and Objectives

The aim of this project is to study and develop low torque single ring weaving yarn for industrial applications. The principle objectives of the project are as follows:

(1) To study the spinning mechanism and structure of low torque single ring yarns for weaving;

(2) To optimize processing technology with special emphasis on spinning;

(3) To investigate properties of low torque single ring weaving yarns and characterization of woven fabric from low torque single ring yarns; and

(4) To investigate the effect of yarn torque on the surface smoothness of woven fabric.

1.4 Significance

Yarn torque has practical significance for a number of the characteristics of yarns, fabrics, and carpets. Low torque yarn or even torque-balanced yarn is desirable in order to obtain stability in the resulting fabric and make yarn manageable for further processing. In the past, various techniques have been used to reduce or eliminate residual torque in textile yarns. However, several drawbacks like high production costs and unsatisfactory fabric performance are related to these techniques. In the present work, a technology for producing low torque ring yarn in a single step on ring spinning machine has been developed, which uses a modification system attached to an existing ring spinning machine. The principal mechanism of this method is to produce modified yarn structure, wherein the yarn residual torque can be counteracted partly because of the introduction of false-twisting operation during yarn formation. The feature of the technology is that it produces yarns with reduced residual torque through modifying yarn structure directly during yarn formation, which eliminates any additional step after the spinning process and makes this technology more practical and economical for industrial application. In addition, with a false-twister installed between the front roller and the yarn guide, the yarn strength at the spinning triangle zone can be enhanced, thus the yarn spinnability is improved. Hence, this method can spin yarn using low twist, which is unable to be obtained by normal ring spinning method.

As a spinning technology of producing low torque ring yarn, low torque ring yarn possesses its characteristics different from those of conventional ring yarn.

Investigation of spinning mechanism, structures and properties of low torque single ring yarn for weaving is helpful to understand yarn structures and properties in depth, optimize yarn spinning process and make low torque ring yarn better applied on woven fabric. In this respect, a shape parameter of spinning triangle is firstly introduced and its effect on the distribution of fiber tension is newly studied in the ring spinning triangle. This study, together with a new attempt to relate the fiber tension stress at the spinning triangle to yarn residual torque, provides a new concept in the area of textile structures and mechanics which has been previously neglected. In the study of yarn structure, the development of the measuring system for capturing and storing consecutive images of single tracer fiber is of great importance, with which the image acquisition becomes quicker and more accurate, and the problems in manual operation such as slow movement, larger random error can be solved. It is also helpful for the analysis and processing of the tracer fiber image information such as transfer of the obtained images into a set of data. Moreover, the regeneration of the 3D configuration and radial position variation of the tracer fiber in a real yarn and the analysis of yarn structural characteristics can be achieved.

Yet, little research has been carried out on investigating the effect of yarn residual torque on the woven fabric performance and application of low torque ring yarn on woven fabric, particularity on denim fabric. The experimental results demonstrated that the appearance of the denim fabrics has been improved significantly using the low torque ring yarns as weft yarns. The present study provides a new approach to improve appearance of denim fabric.

The reduction of yarn residual torque has positive significance on the improvement of yarn property and fabric performance. In this respect, the project is intended to study and develop low torque single ring weaving yarn production technology and its industrial application. This technology produces yarns with reduced residual torque through modifying yarn structure directly during yarn formation, which eliminates any additional step after the spinning. The adoption of the modified spinning technology for producing low torque ring yarn can reduce yarn snarling and improve surface appearance of denim fabric produced, resulting in improved yarn and fabric performance characteristics and hence products of high quality. These will enable local cotton spinners, weavers and garment manufacturers to remain competitive in the world market. Based on the previous work done by other researchers and my current investigations, the project will lead to some new developments in ring spinning technology and bring improvements in products quality and efficiency.

The benefits from this research work to the textile industry would be as follows:

(1) Development of a modified ring spinning technology to produce low torque singles ring yarns by a single step on ring spinning machines;

(2) Improvement of spinning productivity and efficiency;

(3) Improvement of yarn quality with lower yarn residual torque, less yarn hairiness and normal yarn tenacity and evenness;

(4) Improvement of woven fabric performance such as flatter fabric surface and better appearance and a solution of the ‘small snake’ problem of denim fabric;

(5) Easier weaving preparation and processing; and

(6) Good prospect to enter new markets and develop new woven products and therefore increase in the competitive power in the market.

1.5 Methodology

1.5.1 Investigation of Spinning Mechanism by the Geometry of Ring Spinning Triangle and Its Effect on the Yarn Torque

Theoretical probe is very instructive since it can provide an in-depth understanding of the spinning mechanism. This work starts with the study on the geometry of spinning triangle with the help of an experimental device for spinning triangle observation. Following that, a theoretical investigation of the effect of geometry of spinning triangle on the distribution of the fiber tensile stress is carried out using the principle of stationary total potential energy. In addition, a study on linking the fiber tension stress at the spinning triangle to yarn properties particularly on yarn torque is also included.

1.5.2 Analysis of Low Torque Ring Yarn Structure Characterized by Geometrical Arrangement of Fibers in the Yarn

With the help of SEM, tracer fiber technique and a newly developed measuring system for the investigation of the fiber configuration in staple yarns, structure of low torque single ring weaving yarn is investigated. The measuring system can

capture consecutive images of single tracer fiber with the help of the automatic moveable platform and a program written by the National Instruments LabVIEW 5.1 language for grabbing images of the tracer fiber. Thus, yarn surface structure, 3D configuration of tracer fiber in the yarn, fiber migration behavior of the yarn are determined and used to understand yarn structure and mechanics in depth.

1.5.3 Experimental Probe of the Relationship between Low Torque Ring Yarn Properties and Spinning Processing Parameters

Based on the fundamental investigation of effect significance of spinning processing parameters such as yarn twist level, yarn speed ratio, traveler and the position of yarn false-twister using Fractional Factorial Methodology, the effects of processing parameters on yarn properties are investigated using Response Surface Methodology (RSM) with Minitab statistical software. Second-order polynomial response surface models are set up to predict and explain the relationship between yarn properties and processing variables. In addition, the developed RSM model is further coupled with the desirability function and overlaid contour plot to find the optimum spinning parameters leading to the desirable yarn properties.

1.5.4 Characterization of Low Torque Ring Yarn and Resultant Woven Fabric

The yarn properties investigated include structural properties such as yarn diameter, yarn twist, yarn hairiness and yarn evenness, and physical properties with emphasis on torsion property, tensile property and bending property. Besides, the low torque

single ring yarns were woven into fabrics to investigate the yarns' processability as well as the potential changes or benefits brought about to their fabrics. Characterization of woven fabric from low torque single ring yarns investigated includes fabric structural characteristics, mechanical characteristics and fabric performance. KES apparatus is the main device for fabric testing. Particularly, subjective evaluation is carried out to evaluate the comparative performance of the end-product (Jeans and Trousers) produced by low torque ring yarns to conventional ring yarns and rotor yarns through actual wearing and washing trials.

1.5.5 Study of the Effects of Yarn Torque on the Surface Smoothness of Denim Fabric

Theoretical probe and experimental study are of great significance since they can provide an in-depth understanding for the effect of yarn residual torque on surface smoothness of denim fabric, and may help to optimize low torque single ring weaving yarns process, structures and properties with which low torque ring weaving yarns could be best applied on woven fabric.

1.6 Scope of Work

There are eight Chapters in the thesis. Chapter 1 introduces the background, aim and objectives, significance and methodology of the research project. The outline of the thesis is also provided.

Details of the process of low torque ring yarn spinning are presented in Chapter 2. It starts with an explanation of the torque reduction device principle, covering nature of yarn torque, the factors responsible for yarn residual torque, existing method for yarn torque reduction and the reasons of considering yarn torque reduction device. Following this, the preliminary investigation was conducted to asses the feasibility of the torque reduction device, by not only the yarn spinnability but also yarn properties. The experimental results demonstrated the success of the low torque ring yarn spinning technology in terms of significant yarn torque reduction and yarn hairiness decrease as well as maintenance of normal yarn tenacity when low twist level is used in low torque ring yarns.

Theoretical probe is very instructive since it can provide an in-depth understanding of the spinning mechanism. Thus, the investigation on the geometry of the ring spinning triangle and its effect on the yarn torque become the subject of Chapter 3. This work starts with the study on the geometry of spinning triangle with the help of an experimental device for spinning triangle observation. Following that, a theoretical investigation of the effect of geometry of spinning triangle on the distribution of the fiber tension stress is carried out using the principle of stationary total potential energy in this Chapter. In addition, a study on linking the fiber tension stress at the spinning triangle to yarn properties particularly on yarn torque is also included.

The investigation of low torque ring yarn structure characterized by geometry of fibers in the yarn is discussed in Chapter 4. In order to analyze yarn structure faster

and more accurately, a system for investigation of the fiber configuration in staple yarns, based on the tracer fiber technique, has been developed in this study, which can capture consecutive images of single tracer fiber with the help of the automatic moveable platform and a program written by the National Instruments LabVIEW 5.1 language for grabbing images of the tracer fiber. Besides, with the help of SEM, tracer fiber technique, structures of low torque ring yarn were analyzed and characterized by yarn surface structure, 3D configuration of tracer fiber in the yarn and fiber migration behavior of the yarn in this Chapter.

Chapter 5 provides statistic models for predicting and explaining the relationship between low torque ring yarn properties and spinning processing parameters, in which the Fractional Factorial Methodology (FFM) was used for experiment design and to determine those processing parameters having significant effects on yarn properties. Then a two-factor Response Surface Methodology (RSM) was used to investigate the effects of yarn twist and speed ratio on low torque ring yarn properties and Second-order Polynomial Response Surface Models were set-up to predict and explain their relationship. The developed RSM model was further coupled with the desirability function and overlaid contour plot to find the optimum spinning parameters leading to the desirable yarn properties.

Yarn properties are determined by not only fiber properties but also spinning methods. In this respect, the introduction of false-twisting operation during yarn formation gives low torque ring yarn a new fiber and yarn configuration, and thus causes different characteristics of low torque ring yarn from that of conventional ring

yarn, which forms the subject in Chapter 6. In addition, the new characteristics of low torque ring yarn will no doubt be brought into downstream fabrics in subsequent production. Therefore, fabric characteristics become another focus of the investigation in this Chapter. With results of objective measurements on fabrics, a study was carried out to evaluate the comparative performance of the end-product (jeans and trousers) produced by low torque ring yarns to conventional ring yarns and rotor yarns through actual wearing and washing trials in this Chapter.

In Chapter 7 the effect of yarn torque on the surface smoothness of denim fabric was conducted theoretically and experimentally. Firstly, a theoretical analysis on the effect of yarn residual torque on the surface smoothness of denim fabric was conducted based on woven fabric with typical 3/1 twill structure. Secondly, the low torque ring yarns were applied on the denim fabric to improve fabric smoothness appearance.

Chapter 8 provides a general discussion of the present study. Recommendations for further study based on the present work are also proposed.

CHAPTER 2 SPINNING PROCESS OF LOW TORQUE RING YARN

2.1 Introduction

The most common method of staple yarn production is the insertion of twist into a parallel array of fibers, which produces cohesive forces to hold the fibers together in the yarn. However, as twist is inserted, residual torque or twist liveliness is also introduced in the yarn simultaneously. The torsional stresses or torque generated by such a process have a considerable effect on the stability and mechanical characteristics of the yarn and may subsequently influence fabric properties. Therefore, low torque yarn or torque-balanced yarn is desirable in order to obtain stability in the resulting fabric and make yarn manageable for further processing.

In the past, various techniques were used to reduce residual torque in textile yarns. However, several drawbacks like high production costs and unsatisfactory fabric performance are related to these techniques. In this Chapter, a technology for producing low torque ring yarn in a single step on ring spinning machine is introduced, which uses a modification system attached to an existing ring spinning machine. A preliminary study of the torque reduction device was also made.

2.2 Yarn Torque Reduction

2.2.1 Nature of Yarn Torque

In the past, researchers investigated the nature of yarn torque from filament yarn to staple yarn. Platt, Klein and Hamburger (1958) developed a quantitative theory of tornsional stress of formation of the singles yarn. By using elastic theory and relating singles yarn torque to fiber elastic properties, fiber geometry, and singles yarn structure, they showed that the torque created in twisted singles yarns is due to fiber bending, fiber torsion and their combination. When the yarn tension is low, the treatment is reasonable.

In accordance with the results obtained from yarn torsion experiments under tension reported by Hickie and Chaikin (1960), considering not only fiber bending and fiber torsion but also fiber tension in estimating the torque in a twisted yarn, Postle, Burton and Chaikin (1964) gave a much more realistic result than that if fiber tension was ignored. In fact, they found that the contribution to the yarn torque due to fiber tension was far greater than the contributions due to fiber bending and fiber torsion, the torque component due to fiber torsion being negligible.

Based on a force method, Bennett and Postle (1979) carried out a theoretical and experimental analysis to study the dependence of yarn torque on the nature of the fiber tensile stress distribution within a yarn. They found that the level of torque generated in a yarn is highly dependent on the fiber tensile-stress distribution, which

is determined not only by the yarn geometry but also the mode of twisting.

Recently, based on discrete-fiber modeling principle, an energy method, and a 'shortest-path' hypothesis, Tandon, Carnaby, Kim and Choi (1995) developed a theoretical analysis and experimental evaluation to gain an insight into the torsional behavior of singles yarns, which may be bulky and have non-uniform fiber packing density distribution. This modeling confirmed that the contribution to yarn torque due to fiber tension is much greater than the sum of the contribution due to fiber bending and fiber torsion. The fiber tensile-strain distribution used here is different and is more realistic for bulky yarn than that in previous modeling.

It can be seen that without considering the interfiber friction, the total yarn torque generated during yarn twisting is contributed by three components: due to fiber bending, fiber torsion and the internal fiber tensile stress, which can be expressed as:

$$L=L_e+L_t+L_b \qquad (2\text{-}1)$$

where L is total yarn torque, L_e is yarn torque component due to fiber tension, L_t is yarn torque component due to fiber torsion, and L_b is yarn torque component due to fiber bending.

Of these three components, the contribution to yarn torque due to fiber tension is much greater than the sum of the contribution due to fiber bending and fiber torsion. Therefore, the instantaneous torque may be estimated simply by calculating the

torque due to fiber tension as follows (Postle, R., Burton, P., and Chaikin, M., 1964):

$$L=\frac{\pi R^3 E_f e_y \tan\theta_s}{2} \tag{2-2}$$

where L is total yarn torque, R is yarn radius, E_f is fiber tensile modulus of elasticity, e_y is yarn strain, and θ_s is yarn surface helix angle.

In order to further understand the nature of yarn torque, the effects of inter-fiber friction and the fiber migration during yarn forming on the yarn torque need to be considered.

2.2.2 Factors Affecting Yarn Residual Torque

Yarn residual torque is a complex phenomenon arising from many factors influencing the nature and degree of torsional behavior of yarns. Yarn torque depends on the fiber types used in yarn. Fiber mechanical properties such as fiber tensile modulus, torsional modulus and bending modulus, fiber stress-strain relation of tensile, torsion and bending, and fiber resiliency have significant effects on yarn torque. Yarn torque also depends on fiber friction, fiber dimension and fiber cross-section shape. Textile fibers are viscoelastic materials. Stress relaxation in fibers results in the reduction of yarn torque with time. Hence, the property of fiber stress relaxation affects the level of residual torque in yarns to some extent.

Yarn structure also has a significant influence on yarn torque. Yarn twists, yarn

radius, the arrangement of fibers in the yarn and fiber migration are major yarn structure features related to yarn torque. In staple yarns, twist is essential to hold the fibers together and to impart some degrees of cohesiveness to the structure. When twist is inserted in yarns, the fibers will be bound into a helical path along the yarn. Fiber internal stress and strain are created in the yarn. The theoretical analysis and experimental study on yarn torque demonstrated that the yarn torque, under certain conditions, increases with increase in yarn twist (Postle, Burton and Chaikin, 1964; Postle, Carnaby and Jong, 1988; Hearle, Grosberg and Backer, 1969). Yarn twist is one of the most important factors governing the magnitude of yarn torque and the tendency of yarn to snarl. The arrangement of fibers in the yarn affects the twist imparted to the yarn and the distribution of fiber stress in the yarn, thus greatly influences the level of torque generated in a yarn (Buhler and Haid, 1986; Araujo and Smith, 1989). The distribution of fiber stress, as a function of the position in the yarn, depends largely on the facility with which fibers can migrate throughout the yarn cross-section. Fiber migration and interfiber entanglement affect interfiber friction within a yarn, and thus affect the residual torque in a yarn. Wu, Wang, F., and Wang, S.Y. (2001) studied the torsional properties and torque-relaxation behavior of wool/PET composite yarns. They found that the special structures of composite yarns mainly cause the high residual torque.

Different spinning technologies produce yarns with different geometrical and physical properties (Lord, 1971; Louis, Salaun and Kimmel, 1985; Kim, Huh and Ryu, 1995; Huh, Kim and Oxenham, 2002). Friction-spun yarns possess the highest residual torque and snarling tendency, followed by ring spinning yarns, rotor

spinning yarns, and air-jet spinning yarns (Lord, and Mohamed, 1974; Araujo and Smith, 1989; Barella and Manich, 1989; Sengupta and Sreenivasa, 1994).

2.2.3 Existing Methods for Yarn Torque Reduction

In the past, various techniques have been developed to reduce or eliminate residual torque in textile yarns. Based on their principles, these techniques can be divided into two major categories: permanent setting of yarn to reduce its residual torque and balancing the yarn torque by various means.

Yarns can be set by various means depending on fiber type. In the case of thermal plastic fibers, heat treatment is applied while the yarn or fabric is held under stress at temperatures above the glass transition but below the melting point. Araujo and Smith (1989) reported that thermal setting of cotton/polyester blended yarns greatly reduced residual torque. For natural fibers such as cotton and wool, setting progresses are more complicated, for example, steaming, setting in hot water, and chemical treatments such as mercerization for cotton yarns. However, Araujo and Smith (1989) found that the setting process for natural fibers cannot completely eliminate the residual torque of singles yarns, and fiber damage and deterioration in yarn properties may occur. Torque balanced yarn can also be obtained by plying two singles yarns with the right amount of plying twist in the direction opposite to that in the singles yarns.

Some novel approaches have been reported to produce torque free singles yarns by

direct spinning method. Sawhney, Robert and Ruppenicker (1992) introduced the technique of producing ring spun cotton covered/polyester core yarn that can be torque-balanced by using a core yarn with a twist direction opposite to that of the resulting core-wrap yarn. Sawhney and Kimmel (1995) also developed the tandem spinning system for producing a torque-balanced yarn. With this method, the core and sheath components of the resultant yarns usually have opposite twist/torque directions. Taking advantage of the core-sheath structure of unconventional spun yarns, Tao, Lo and Lau (1997) developed a yarn modification process and applied it to pure cotton singles yarns spun by friction spinning and rotor spinning, producing torque free singles yarns. According to a concept similar to false twist texturing, Primentas and Iype (2003) developed a technique to reduce yarn residual torque. In this method, highly twisted yarns were steam-set and counterbalancing torsional force was introduced by partially detwisting the steam-set yarns to a level of 15-30% of their initially introduced twist.

2.2.4 Principles of Yarn Torque Reduction during Yarn Formation

Based on the above facts, it is known that yarn torque generated during yarn twisting is mainly determined by the fiber bending, fiber torsion and internal fiber tensile stress, particularly their distribution within the yarn. Yarn surface helix angle increases with the amount of twist inserted in a yarn and yarn twist level is directly responsible for the magnitude of the three components of yarn torque-fiber bending, fiber torsion and tension, while the distribution of fiber stress in the yarn depends on the arrangement of fibers in the yarn. Besides, the distribution of fiber stress, as a

function of the position in the yarn, depends largely on the facility with which fibers can migrate throughout the yarn cross-section, as well as interfiber friction within a yarn.

Therefore, the possible method to reduce yarn torque can be based on the following aspects. Firstly, reducing yarn twist level may result in the reduction of the magnitude of the fiber bending, fiber torsion and fiber tension created during yarn twisting and thus reduces yarn torque and the tendency of yarn to snarl. Secondly, changing fiber tensile stress distribution within the yarn to avoid its radial bias and to bring about some fibers and fiber sections arranging in the opposite direction to the yarn twist, through altering fiber arrangement in the yarn, i.e. modifying yarn structure, probably also reduces yarn torque. In addition, the increase of fiber migration which improves the equalization of fiber tensile stress and interfiber friction within the yarn, and the forming of a more compact yarn structure will contribute to the reduction of yarn residual torque.

With these in mind, a torque reduction device was introduced into ring spinning process. The torque reduction device is composed mainly of a false-twisting system which is fitted onto a Ring Spinning Frame (See Figure 2-1). Figure 2-2 is a schematic of the modified ring spinning technology for low torque ring yarn developed by Tao and Xu (2003) and Tao, Xu and Wong (2004). Installed between the front roller and the yarn guide, the torque reduction device of the present invention comprises a pair of spaced rotors, a false-twister in tangential frictional contact with each of rotors and magnetic means. One of the rotors is positively

driven rotor and the other runs passively driven by friction force, and the false-twister is pressed against the rotors by means of magnets so as to ensure a higher level contact force and steady friction to rotate at high speed. The electric motor drives the driving rotor via the transmission shaft assembly. During the spinning process, the strand of fibers emerged from the front-drafting-roller nip enters a rapidly spinning false-twister from the entrance direction and is twisted by the turning effort of the false-twister. Twisted yarn is drawn out from the exit direction, and then passes through a guide and down through a traveler, and finally winds onto a package inserted into the spindle.

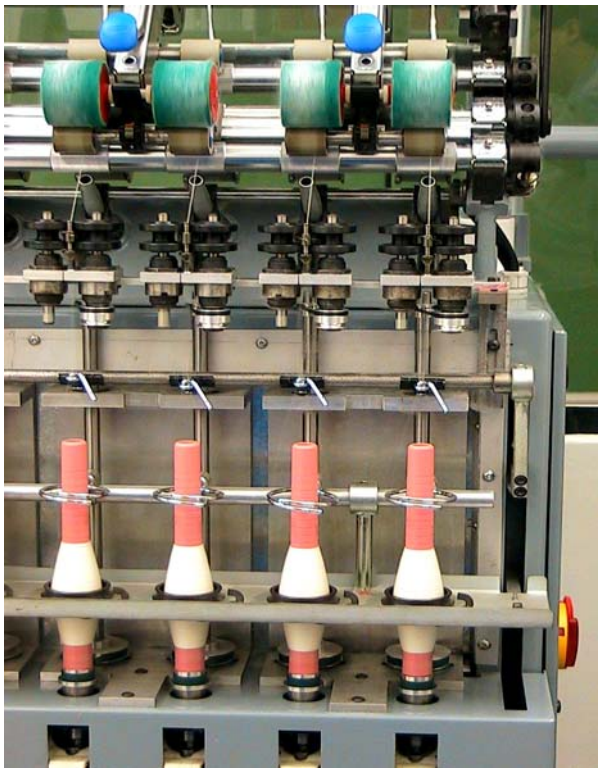

Figure 2-1 Torque Reduction Device Fitted onto Ring Spinning Frame (SDL Spin Tester)

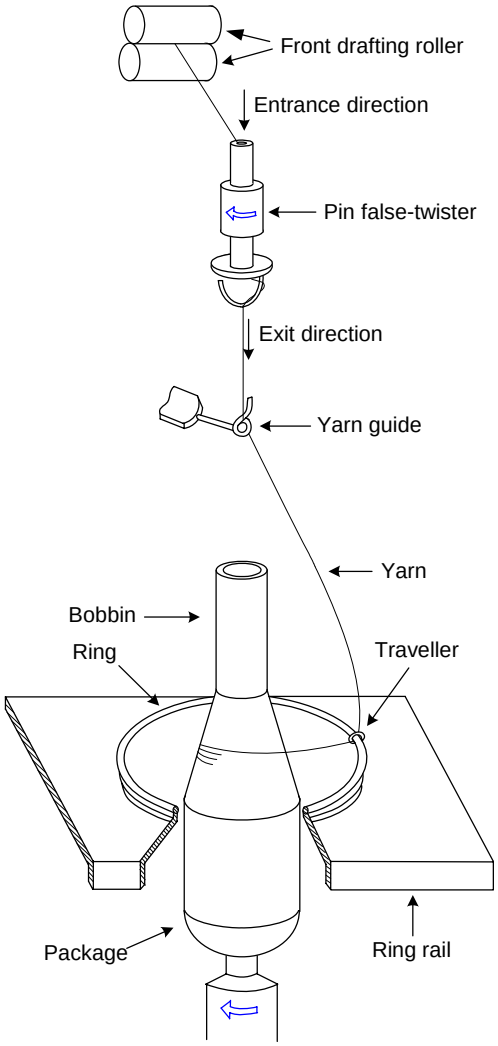

Figure 2-2 Schematic of the Low Torque Ring Yarn Spinning

2.3 Preliminary Experiment

A preliminary experiment was conducted on a ring spinning machine with the torque reduction device as an attachment. The investigation was conducted to asses the feasibility of the torque reduction device, by not only the yarn spinnability but also yarn properties.

A carded cotton roving of 952tex (0.62 Ne) was used to spin 84tex (7Ne) conventional ring yarns(C) and low torque ring yarns (NS) with twist factors 4.2, 4.0, 3.8 and 3.2 on the modified Ring Spinning Machine. Details of processing conditions adopted in preliminary test are listed in Table 2-1. The cotton fibers had a micronaire value of 4.0, a 2.5% span length of 28.7mm, a bundle strength of 22cN/tex, and a breaking extension of 5.3%, all parameters were measured by Spinlab 900. Here, the speed ratio (FTF) which relates to the level of yarn false-twisting during spinning is defined as follows:

$$\text{FTF}=\frac{S_r}{S_s}=\frac{S_p\times\tau}{S_s} \tag{2-3}$$

where S_r (rpm) is the false-twister rotor speed, S_s (rpm) is the spindle speed, S_p (rpm) is the false-twister (pin) speed and τ is the transmission ratio of the false-twister rotor speed to the false-twister (pin) speed. In this study, τ took value of 0.15.

Yarn codes ‘Ne-TF-A’ for conventional yarn samples and ‘Ne-TF-NS_{FTF}’ for low torque yarn samples were used in the study where Ne is yarn count, TF is yarn twist

factor, A is conventional yarn, NS is low torque yarn and FTF is the speed ratio.

Table 2-1 Specifications of Yarn Samples

Yarn sample	Yarn type	Yarn count		Twist factor	Speed ratio
		Ne	Tex		
7-3.2-A	C	7	84	3.2	-
7-3.2-NS $_{0.33}$	NS	7	84	3.2	0.33
7-3.2-NS $_{0.38}$	NS	7	84	3.2	0.38
7-3.2-NS $_{0.43}$	NS	7	84	3.2	0.43
7-3.8-NS $_{0.33}$	NS	7	84	3.8	0.33
7-4.0-NS $_{0.33}$	NS	7	84	4.0	0.33
7-4.2-NS $_{0.33}$	NS	7	84	4.2	0.33
7-4.2-A	C	7	84	4.2	-

A yarn snarling tester was used to measure yarn twist liveliness or residual torque by referring to a principle similar to ISO Standard 3343-1984. In this test, the yarn was drawn from a yarn package holder through a tension device to ensure consistent tension (0.06cN/tex). Then the yarn was secured by the two screws and a weight of 0.003cN/tex was added to the bottom. Then, the yarn sample was put into a water bath for relaxation until it reached equilibrium. The numbers of snarling turns per 25cm length of yarn were measured to indicate the yarn residual torque. Since a yarn with a higher residual torque will have a higher potential of snarling and thus can be considered more twist lively. Thirty readings were taken on each sample.

Yarn tensile properties were tested on an Uster Tensorapid instrument at a speed of

5,000mm/min and a specimen length of 500mm. Fifty readings for each sample were recorded. A Zweigle G566 hairiness tester was used to measure the hairiness of yarns at different length groups. For each yarn bobbin, three different parts, small bobbin, middle bobbin and full bobbin, were measured and the average value for each bobbin was calculated.

Table 2-2 presents the experimental results of low torque ring yarn (NS) and conventional ring yarn (C).

Table 2-2 Properties of Low Torque Ring Yarns and Conventional Ring Yarns

Yarn sample	Tenacity (cN/tex) [CV%]	Elongation (%) [CV%]	Snarling (turns/25cm) [CV%]	Hairiness (S3/100m) [CV%]	Evenness (%) [CV%]
7-3.2-A	15.65 [6.8]	6.71 [7.1]	33 [6.2]	1989 [12.3]	12.02 [1.3]
7-3.2-NS $_{0.33}$	16.21 [5.6]	6.15 [3.9]	29 [3.8]	1298 [15.5]	11.19 [0.9]
7-3.2-NS $_{0.38}$	16.75 [5.5]	6.38 [6.4]	27 [5.8]	645 [14.6]	11.09 [2.1]
7-3.2-NS $_{0.43}$	16.44 [6.1]	6.42 [7.8]	23 [3.5]	551 [15.2]	11.13 [1.2]
7-3.8-NS $_{0.33}$	16.42 [3.9]	6.19 [4.6]	31 [4.6]	419 [12.1]	10.85 [1.2]
7-4.0-NS $_{0.33}$	15.90 [5.1]	6.17 [6.6]	31 [6.1]	440 [10.6]	10.81 [2.3]
7-4.2-NS $_{0.33}$	16.23 [6.2]	6.59 [3.9]	33 [6.6]	413 [12.3]	10.72 [2.4]
7-4.2-A	17.58 [5.5]	7.14 [5.8]	39 [4.2]	1049 [13.6]	11.43 [1.6]

2.3.1 Yarn Snarling

As revealed in Table 2-2, yarn snarling decrease is clear due to the introduction of the torque reduction device. In more details, low value of yarn residual torque can be very clearly observed for the yarns with a low twist level and high speed ratio. In the case of low torque ring yarn with a twist factor of 3.2 and a speed ratio of 0.43, when compared with conventional ring yarn with normal twist factor 4.2, the yarn has a snarling reduction of around 40% from 39 to 23 turns/25cm. Using normal twist level and low speed ratio, low torque ring yarn exhibits a less obvious yarn torque reduction such as Sample 7-4.2-NS $_{0.33}$. With a lower twist level, conventional ring yarn can also achieve yarn snarling reduction to some extent, but the level of snarling reduction is less than that of low torque ring yarn.

2.3.2 Yarn Tenacity

In order to achieve a great reduction of yarn residual torque, a low twist level was adopted in the low torque ring yarn spinning. Strength may be reduced. Table 2-2 shows that the tenacity of low torque ring yarns is only slightly lower than that of conventional yarns with a normal twist level (Sample 7-4.2-A). The lowest value of yarn tenacity of low torque ring yarn is around 16.2cN/tex among the eight 7Ne yarn samples, which is acceptable for industrial application.

2.3.3 Yarn Hairiness

Yarn hairiness is a key factor affecting yarn and fabric processes and properties. Previous research (Pillay, 1964; Barella, 1957) revealed that yarn hairiness may be due to the materials and processes. Table 2-2 shows a discernible decrease in the hairiness of most generated low torque ring yarns by comparison with that of conventional ring yarns. Even though a lower twist level is used in low torque ring yarn spinning, the hairiness of low torque ring yarns is still close to or even less than that of conventional ring yarns with a normal twist level; while the conventional ring yarns using a lower twist level show a significant increase in yarn hairiness after yarn twist decrease. This was brought about by the tighter yarn structure and more wrapper fibers.

2.4 Summary and Conclusion

This Chapter describes a technology for producing low torque ring yarn in a single step on ring spinning machine, which uses a modification system attached to an existing ring spinning machine.

A preliminary study of the torque reduction device was made. The torque reduction device was composed mainly of a false-twisting system including a pair of spaced rotors, a false-twister in tangential frictional contact with each of rotors and magnetic means. The experimental results show that the resultant yarns had reduced residual torque through modifying yarn structure directly during yarn formation, which

eliminates any additional step after the spinning process and makes this technology more practical and economical for industrial application. In addition, the yarn strength at the spinning triangle zone can be enhanced, thus the yarn spinnability is improved. Moreover, false-twisting operation probably results in a higher migration effect in low torque ring yarn and endows low torque ring yarn more fiber entanglement as well as a tight yarn structure even though the final yarn twist level is low. Positive results were achieved in the preliminary experiment where low torque ring yarn exhibits lower yarn snarling, less yarn hairiness and normal yarn tenacity. Though the results are promising, the structure of low torque ring yarns and its relationship with processing conditions require further investigation. Even more importantly, the process needs to be optimized.

CHARPTER 3 GROMETRY OF RING SPINNING TRIANGLE AND ITS EFFECTS ON YARN TORQUE

3.1 Introduction

In the ring spinning process, the drafted fiber strand leaves the front roller at the nip with a width, and then the fibers enter the twisting zone and are tied into a yarn by twisting the strand. The twisting area between the front roller nip and the yarn twist point is known as the spinning triangle or twisting triangle. It is in this zone that individual or bundles of fibers are twisted and consolidated to form a yarn structure. Therefore, the spinning triangle or the dynamics of yarn formation has a significant and crucial effect on yarn structure and thus yarn property.

During ring spinning process, the fiber tension is created at the spinning triangle due to the spinning tension and the twist propagation. Moreover, it was postulated that different fibers have different tensions depending on their position in the spinning triangle. It is known that fibers at the center of the triangle are usually slack and those in the outer layers are under maximum tension. Yarn properties such as yarn tensile property and torsion property are related to the internal fiber tensile stress and

its distribution in the yarn.

As a modified ring spinning method, a false-twisting operation is induced during low torque ring yarn spinning technology and thus yarn structure is modified accordingly. The introduction of false-twisting operation during yarn formation might give low torque ring yarn a new geometry of spinning triangle and cause different distribution of strain and fiber arrangement in the yarn compared with conventional ring yarn, and thus affect yarn properties including yarn torsional behavior. Therefore, as one of the most important parts for yarn spinning mechanism study, an investigation of the spinning triangle of low torque ring yarn spinning is of great importance from the view of understanding the spinning mechanism, structures and properties of low torque ring yarn.

Thus, the investigation on the geometry of the ring spinning triangle and its effect on the yarn torque become the subject of this Chapter. This work starts with the study on the geometry of spinning triangle with the help of an experimental device for spinning triangle observation. Following that, a theoretical investigation of the effect of geometry of spinning triangle on the distribution of the fiber tension stress is carried out using the principle of stationary total potential energy in this Chapter. In addition, a study on linking the fiber tension stress at the spinning triangle to yarn properties particularly on yarn torque is also included.

3.2 Experimental Study on the Geometry of Spinning Triangle

The spinning triangle is formed continuously as the tension and torsion are simultaneously imparted into the fibers. With different spinning conditions, the spinning triangle shows different geometry such as the height, width and shape of the spinning triangle. It is likely that the yarn twist, yarn tension, spinning geometry, spindle speed, the roving width and the mechanical properties of fibers are the most important factors affecting the geometry of spinning triangle. Under the influence of spinning tension and twist, the distribution of fiber tension stress created in the spinning triangle partly depends on the geometry of spinning triangle. In this Section, an experimental device is set up in order to photograph the geometry of the spinning triangle. The fiber twisting behavior and the geometry of the spinning triangle are then investigated and compared between conventional ring spinning and low torque ring yarn spinning.

3.2.1 Materials and Experimental Set-up

A carded cotton roving of 952tex (4.0 in micronaire value and 28.7mm in 2.5% span length) was used to spin 58tex conventional yarns with normal twist level and high twist level and low torque ring yarn on the modified Ring Spinning Frame in this study.

A special transparent roller was designed and used in place of the top rubber roller to observe the full length of the spinning triangle. Figure 3-1 illustrates a general view

of this designed transparent roller which consists of the transparent and the bearing units. The transparent roller is made of an acrylic material with an outer diameter of 30 mm similar to that of the original top rubber roller. In addition, in order to provide a reasonable friction between the rollers and to avoid optical reflections during the photographic procedure, the fluted surface of the bottom roller was covered by a black rubber material (Figure 3-2).

The CCD Micro-Camera (Canon EOS 300D) was mounted on the top of the transparent roller and used to photograph the geometry of the spinning triangle. In order to make the photographing process more stable, a frame for camera-mounting and photo-taking was set up, which makes the geometry measurement and comparison of spinning triangle between conventional ring yarn and low torque ring yarn more accurate and comparable.

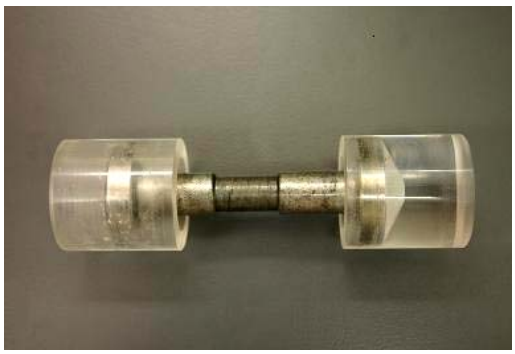

Figure 3-1 General View of the Transparent Roller for Photographic Experiment

Figure 3-2 General View of the Transparent Roller Mounted on the Spinning Frame

3.2.2 Characteristics of the Geometry of Spinning Triangle

Figures 3-3, 3-4 and 3-5 show a random selected set of 9 consecutive photographs of the spinning triangle in frame rate around 5 frames per second for cotton fibers during conventional ring yarn and low torque ring yarn spinning. It can be seen that coming out from the front roller, the drafted fiber strand enters the spinning triangle area and then turns around the yarn-axis due to yarn twist and spinning tension. Meanwhile, the drafted fiber strand gradually narrows its width with fibers' flowing downward to the point of yarn formation and its cross section changes from a two dimensional thin ribbon to a three dimensional roughly circular shape and finally forms into yarn.

In the previous studies on the spinning triangle, the shape of spinning triangle was usually assumed to be a symmetric triangle for simple analysis and discussion. However, the photos taken in the experiment show that in the conventional yarn spinning process, the twist point probably deviates from the symmetric axis of triangle due to the frictional contacts of fibers with the bottom roller which interferes the twist propagation to the spinning triangle zone. Thus, the spinning triangles of conventional yarns with normal twist level and high twist level (similar to twist level of yarn part above the point of the false-twisting in the low torque ring yarn spinning) show the asymmetric geometry (Figures 3-6 and 3-8). Contrast to the conventional ring yarn, the spinning triangle of low torque ring yarn presents a symmetric structure due probably to a small reflection arc at the front bottom roller (Figure 3-7). From the Figures, it can also be seen that during the course of yarn formation, the

fiber distribution at the spinning triangle is not always in the form of single fiber. Inversely, multi-bundle of fibers appeared at the spinning triangle before twisting into the point of yarn formation in the low torque ring yarn and high twist conventional ring yarn spinning (Figures 3-7 and 3-8). In filaments twisting and wool yarn spinning research conducted by Hearle and Goswami (1970) and Shaikhzadeh Najar (1994) respectively, they also observed this phenomenon when yarn was spun at high twists and twisting tensions. In addition, the spinning triangle heights of the high twist conventional ring yarn and low torque ring yarn are both shorter than those of normal conventional ring yarn. The photos of spinning triangle also indicate that there are less floating fibers near the spinning triangle in the low torque ring yarn spinning and high twist conventional ring yarn spinning compared with those in normal conventional ring yarn spinning probably due to the good fiber control in the spinning triangle of low torque ring yarn and high twist conventional ring yarn, which brings benefits for the reduction of yarn hairiness and fiber fly during yarn spinning.

The observation of spinning triangle as shown above indicates that the geometry of spinning triangle may exhibit different characteristics under the various spinning conditions, which will affect the distribution of the fiber tension stress at the spinning triangle.

Figure 3-3 Consecutive Photographs of Geometrical Variation of Spinning Triangle in Conventional Ring Yarn
(Spinning speed = 7000rpm, yarn count = 58tex, yarn twist = 523tpm)

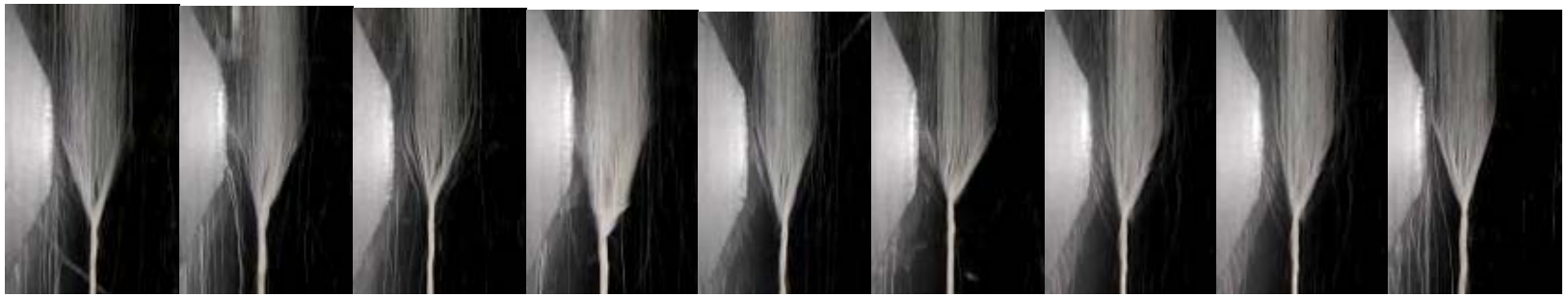

Figure 3-4 Consecutive Photographs of Geometrical Variation of Spinning Triangle in Low Torque Ring Yarn
(Spinning speed = 7000rpm, yarn count = 58tex, yarn twist = 398tpm)

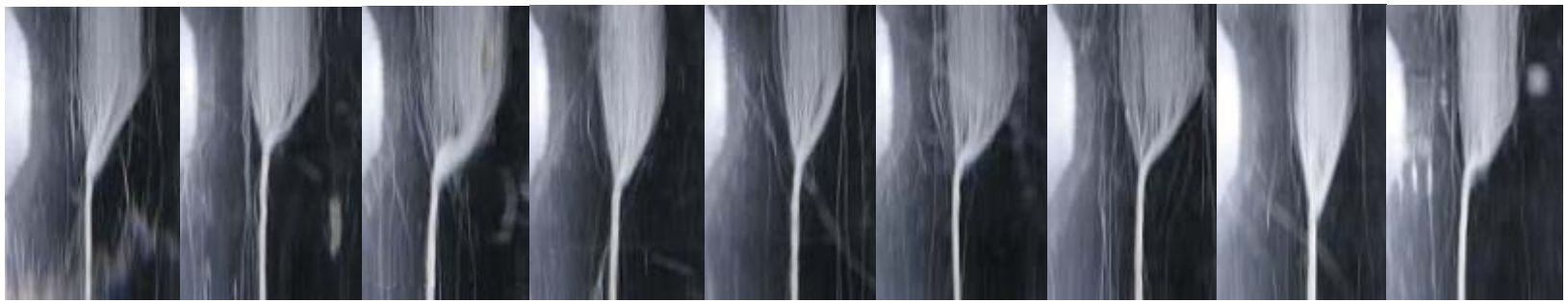

Figure 3-5 Consecutive Photographs of Geometrical Variation of Spinning Triangle in Conventional Ring Yarn (Spinning speed = 7000rpm, yarn count = 58tex, yarn twist = 1193tpm)

Asymmetric structure of the spinning triangle

Figure 3-6 Photograph of Spinning Triangle in Conventional Ring Yarn
(Spinning speed = 7000rpm, yarn count = 58tex, yarn twist = 523tpm)

Symmetric structure of the spinning triangle

The spinning triangle with multi-bundle

Figure 3-7 Photographs of Spinning Triangle in Low Torque Ring Yarn
(Spinning speed = 7000rpm, yarn count = 58tex, yarn twist = 398tpm)

Asymmetric structure of the spinning triangle

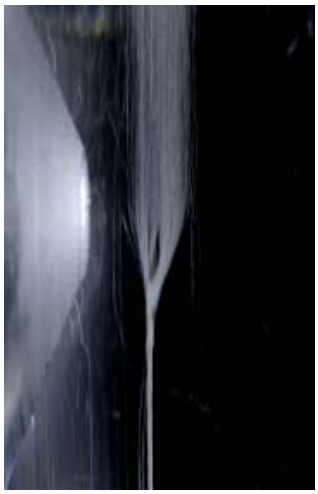

The spinning triangle with multi-bundle

Figure 3-8 Photographs of Spinning Triangle in Conventional Ring Yarn (Spinning speed = 7000rpm, yarn count = 58tex, yarn twist = 1193tpm)

3.3 Retrospect of Ring Spinning Triangle Study

In the past, various researches were made relating to the spinning triangle. Fujino (1962) studied the twist irregularity of yarns spun on the ring spinning frame, which included a theoretical investigation on the balance of force at the spinning triangle. In 1965, Pavlov carried out a theoretical analysis to study the structural transformations in the fiber assembly at the twist threshold at the instant of rupture. Considering two cases of fiber extension in the spinning triangle, Krause (1991) investigated theoretically the strength of the spinning triangle in ring spinning. In the study of spinning geometry and its significance, Klein (1993) pointed out that the spinning geometry on the ring frame has had always a certain influence on the

process, as well as on the end breakages and yarn structure. Based on the principle of stationary total potential energy, Shaikhzadeh Najar (1996) developed a theoretical model to predict and explain the tension forces of the fibers in the different positions of the spinning triangle. An experimental method was also set up for the measurement of fiber tension at the spinning triangle in his research. Shaikhzadeh Najar's model focused on the fiber tension stress at the spinning triangle in which he only considered a symmetric geometry of spinning triangle. In the study of reducing yarn hairiness with a modified yarn path in worsted ring spinning conducted by Wang and Chang (2003), it was pointed out that the twist triangle is the critical region in ring spinning and changes in its geometry affect yarn properties. Based on the examination of left diagonal and right diagonal yarn arrangement, the reduced yarn hairiness was achieved when the right diagonal yarn path was adopted.

Regarding the spinning triangle in the real situation, the spinning triangle shows different geometry under different spinning conditions. Thus, there is a need to develop a model for predicting the individual fiber strain at the twist triangle under the influence of the tension. The effect of geometry of spinning triangle on the distribution of the fiber tension stress was investigated and is reported in this Chapter. It must be emphasized that the study, particularly on linking the fiber tension at the spinning triangle to yarn properties with focus on yarn torque, is for the first time carried out in yarn modeling and reported in the present work.

3.4 Effects of Shape of Spinning Triangle on the Stress Distribution of Fibers at the Spinning Triangle

In the present research, the typical shape of spinning triangle (Geometry A in Figure 3-9) is adopted for modeling the stress distribution of fibers at the spinning triangle. Then two special cases of spinning triangle (Geometry B - symmetric triangle, and Geometry C - right-angled triangle in Figure 3-9) are analysed in this study. An energy approach is developed to analyze the distribution of fiber tension force at the spinning triangle under the yarn spinning tension. The analytical approach is similar to that presented by Shaikhzadeh Najar (1996), while some important modifications were made to improve it. Firstly, the free-body for analysis is a spinning triangle in the typical shape instead of a simplified symmetric geometry of spinning triangle to simulate the spinning triangle in real situation. A shape parameter (β) is firstly introduced for better describing the symmetric level of the geometry of spinning triangle and analyzing its effects on the fiber tension force distribution at the spinning triangle. Secondly, multi-bundle form of fibers is analyzed for the distribution of the fiber tension stress at the spinning triangle. The response of the spinning triangle system is determined by the principle of minimum potential energy. To evaluate and simulate the theoretical results, a case study is carried out on the study of the distribution of fibers tension stress in the spinning triangle of 58tex cotton yarn.

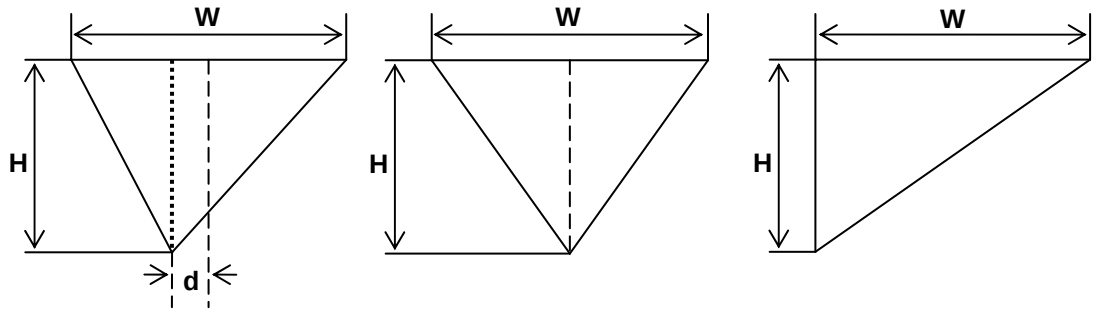

Geometry A Geometry B Geometry C

Figure 3-9 The Geometry of Spinning Triangle

3.4.1 Theoretical Considerations

The free-body diagram of force on fibers at the spinning triangle is shown in Figure 3-10. During ring yarn spinning, the spinning tension causes an unequal loading of the fibers due to fiber path length differences in the spinning triangle. We assumed that the elastic spinning triangle structure is deformed under the applied yarn spinning tension where both ends of the fibers are gripped between the front roller nip and the twist point. The spinning tension force will be transferred to fiber tension in the spinning triangle. In addition, some of the assumptions have to be further made, as listed below:

a. The system is assumed to be conservative under pure spinning tension.
b. A constant tensile force in the form of spinning tension is applied to the spinning triangle at the convergence point.
c. The frictional contacts of fibers with the bottom roller are ignored.

d. Fibers or fiber bundles are uniformly distributed in the spinning triangle.

e. Fibers exhibit pure linear elasticity.

f. Fiber migration and slippage are ignored.

g. During yarn formation, the velocity of fibers is constant.

h. Both of fiber displacement due to axial tension and axial compression obey the same fiber deformation-load relation.

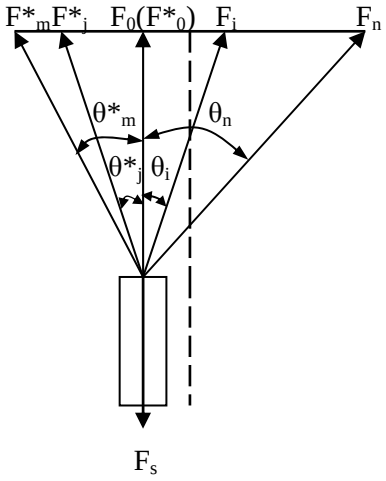

Figure 3-10 Forces on Fibers at the Spinning Triangle

With these assumptions, the energy method can be employed to obtain analytical expressions for the distribution of fiber tension at the spinning triangle. Figure 3-11 shows the diagram of the spinning triangle model for fiber tension. In this model, an imaginary twist point is assumed at the original state where the fiber ends are joined together, and the central fibers are slack and the outer fibers are straight at zero

extension. Then an external force in the form of spinning tension is exerted on the spinning triangle and the central fibers and the outer fibers are extended concurrently. The energy method of analysis requires the development of the total potential energy functional for the spinning triangle which is the sum of the strain energy U and the total work done by external loads W. The minimization of the total potential energy functional with respect to the generalized coordinates yields the equation. Solving the equation yields value for the generalized coordinates. Finally, the fiber tension force at the spinning triangle can be obtained.

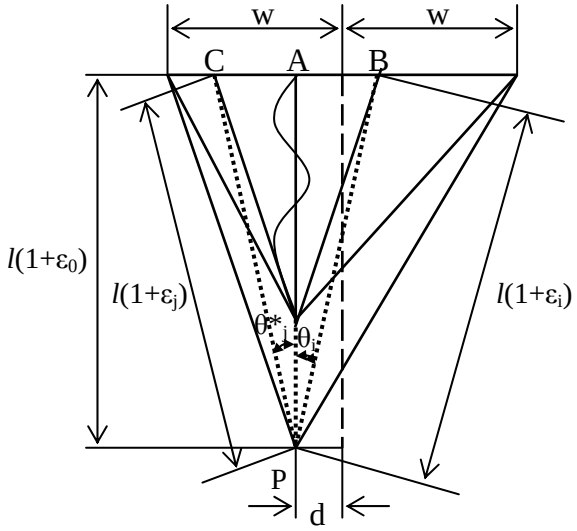

Figure 3-11 Spinning Triangle Model for Fiber Tension (Geometry A)

3.4.2 Various Cases of Distribution of Fiber Stress in the Spinning Triangle

Two cases of distribution of fiber stress at the spinning triangle are considered in the analysis below. These are Case I, uniformly distribution of fibers at the spinning triangle without multi-bundle form, and Case II, uniformly distribution of fibers at the spinning triangle with multi-bundle form. Though the present work is an extension of previous work by Shaikhzadeh Najar (1996), the shape of spinning triangle and the form of fibers distributed at the spinning triangle are important for the distribution of fiber stress at the spinning triangle which Shaikhzadeh Najar did not considered. However, we considered in the present model such as the typical shape of spinning triangle and multi-bundle form of fibers. Therefore, the main analysis procedures are outlined briefly for completeness in the following section:

3.4.2.1 Case I

According to the definition of Case I and considering the triangle ABP and the triangle ACP in Figure 3-11, it follows that:

$$a^2 + (l + u_o)^2 = (l + u_i)^2 \tag{3-1}$$

$$b^2 + (l + u_o)^2 = (l + u_j)^2 \tag{3-2}$$

where, a and b are fiber position at the roller nip; l is the initial length of fiber; u_o is centre fiber displacement; and u_i and u_j are outer fiber displacement.

According to the fiber strain, the equations become:

$$\frac{a^2}{2l^2} + \frac{\varepsilon_0^2}{2} + \varepsilon_0 = \frac{\varepsilon_i^2}{2} + \varepsilon_i \tag{3-3}$$

$$\frac{b^2}{2l^2} + \frac{\varepsilon_0^2}{2} + \varepsilon_0 = \frac{\varepsilon_j^2}{2} + \varepsilon_j \tag{3-4}$$

Considering the triangle ABP and the triangle ACP in Figure 3-11, it follows that:

$$a = l(1+\varepsilon_0)\tan\theta_i \tag{3-5}$$

$$b = l(1+\varepsilon_0)\tan\theta_j^* \tag{3-6}$$

where θ_i and θ_j^* denote the inclination of the individual fiber to the axial direction.

Since it is assumed that fibers are uniformly distributed at the spinning triangle, then we have:

$$\theta_i = i(\frac{\theta_n}{\mathrm{n}}) \tag{3-7}$$

$$\theta_j^* = j(\frac{\theta_m^*}{\mathrm{m}}) \tag{3-8}$$

where θ_n and θ_m^* are the maximum values of θ_i and θ_j^* respectively and

$m+n+1$ is the total number of fiber at the spinning triangle.

We then obtain the general relation between the central fiber strain (ε_o) and outer fiber strain (ε_i) and (ε_j) at the spinning triangle as follows:

$$\varepsilon_i = \varepsilon_0(1+\tan^2\theta_i)+\frac{1}{2}\tan^2\theta_i \tag{3-9}$$

$$\varepsilon_j = \varepsilon_0(1+\tan^2\theta_j^*)+\frac{1}{2}\tan^2\theta_j^* \tag{3-10}$$

Assuming the fibers following Hook's law, the elastic strain energy density of each fiber at the spinning triangle is given by:

$$U_i^* = \int \sigma d\varepsilon_i = \frac{E\varepsilon_i^2}{2} \tag{3-11}$$

$$U_j^{**} = \int \sigma d\varepsilon_j = \frac{E\varepsilon_j^2}{2} \tag{3-12}$$

where E is the fiber tensile modulus, ε_i and ε_j are the fiber strain and U_i^* and U_j^{**} are the elastic strain energy density of each fiber at the spinning triangle.

For linear elasticity, the elastic strain energy of each fiber U_i and U_j are given by:

$$U_i = U_i^* Vol_i \tag{3-13}$$

$$U_j = U_j^{**} Vol_j \tag{3-14}$$

where Vol_i and Vol_j are the volume of each fiber which is assumed to be equal to AL for all fibers and A is the cross-sectional area of each fiber.

Since the spinning triangle is treated as a conservative system, the total potential energy is the sum of the strain energy and the total work done by external loads. The total potential energy is given by:

$$V = U + W \tag{3-15}$$

where V is the total potential energy, U is the strain energy and W is the total work done by external loads.

Next, we have:

$$V(u) = Al[\frac{E}{2}(\frac{u}{l})^2] + Al\{\frac{E}{2}[\frac{u(1+\tan^2\theta_1)+\frac{1}{2}l\tan^2\theta_1}{l}]^2\}$$
$$+ Al\{\frac{E}{2}[\frac{u(1+\tan^2\theta_2)+\frac{1}{2}l\tan^2\theta_2}{l}]^2\}$$
$$+ ... + Al\{\frac{E}{2}[\frac{u(1+\tan^2\theta_n)+\frac{1}{2}l\tan^2\theta_n}{l}]^2\}$$
$$+ Al\{\frac{E}{2}[\frac{u(1+\tan^2\theta^*_1)+\frac{1}{2}l\tan^2\theta^*_1}{l}]^2\}$$

$$+ Al\{\frac{E}{2}[\frac{u(1+\tan^2\theta^*_2)+\frac{1}{2}l\tan^2\theta^*_2}{l}]^2\}$$

$$+ ... + Al\{\frac{E}{2}[\frac{u(1+\tan^2\theta^*_m)+\frac{1}{2}l\tan^2\theta^*_m}{l}]^2\} - F_s u \quad (3\text{-}16)$$

where u is the generalised coordinate.

By the principle of the minimum potential energy, the system is in stable equilibrium. That is $\frac{dV(u)}{du} = 0$.

We obtain:

$$u = \frac{F_s - \frac{AE}{2}[\sum_{i=1}^{n}(1+\tan^2\theta_i)\tan^2\theta_i + \sum_{j=1}^{m}(1+\tan^2\theta^*_j)\tan^2\theta^*_j]}{\frac{AE}{l}[1+\sum_{i=1}^{n}(1+\tan^2\theta_i)^2 + \sum_{j=1}^{m}(1+\tan^2\theta^*_j)^2]} \quad (3\text{-}17)$$

Since the outer fiber strain (ε_i and ε_j) is related to the central fiber strain ε_o, a general statement of the distribution of fiber tension forces at the spinning triangle can be given by:

$$F_{i=0,1,2,...,n} = \frac{F_s - \frac{AE}{2}[\sum_{i=0}^{n}(1+\tan^2\theta_i)\tan^2\theta_i + \sum_{j=0}^{m}(1+\tan^2\theta^*_j)\tan^2\theta^*_j]}{\sum_{i=0}^{n}(1+\tan^2\theta_i)^2 + \sum_{j=0}^{m}(1+\tan^2\theta^*_j)^2 - 1}(1+\tan^2\theta_i)$$

$$+ \frac{1}{2}AE\tan^2\theta_i \quad (3\text{-}18)$$

$$F^*_{j=0,1,2,...,m} = \frac{F_s - \frac{AE}{2}[\sum_{i=0}^{n}(1+\tan^2\theta_i)\tan^2\theta_i + \sum_{j=0}^{m}(1+\tan^2\theta_j^*)\tan^2\theta_j^*]}{\sum_{i=0}^{n}(1+\tan^2\theta_i)^2 + \sum_{j=0}^{m}(1+\tan^2\theta_j^*)^2 - 1}(1+\tan^2\theta_j^*)$$

$$+\frac{1}{2}AE\tan^2\theta_j^* \qquad (3\text{-}19)$$

Equations (3-18) and (3-19) express a general indication of the distribution of fiber tension forces at the spinning triangle, with which the tension forces of the fibers in the different positions of the spinning triangle can be predicted and explained by means of the principle of stationary total potential energy.

Based on Equations (3-18) and (3-19), it can be seen that the individual fiber tension at the spinning triangle is determined by yarn spinning tension (F_s), the cross-sectional area of fiber (A), the fiber tensile elastic modulus (E), number of fibers in the right side of spinning triangle (n) and left side of spinning triangle (m) according to the twist point axis, and the individual fiber angle with the twist point axis (θ_i) and (θ_j^*). The individual fiber angles (θ_i) and (θ_j^*) calculated from Equations (3-18) and (3-19) respectively for the uniform distribution of fibers at the spinning triangle depend on the fiber number on both side of spinning triangle and the maximum fiber angles with the twist point axis (θ_n and θ_m^*), which are related to the shape of spinning triangle and the yarn twist angle.

3.4.2.2 Case II

Based on the definition of Case II and adaptation of similar approach of the analysis as in Case I, the distribution of the tension forces of the fiber bundles at the spinning triangle can be expressed by:

$$F'_{i'=0,1,2,\ldots,n'} = \frac{F_s - \frac{A'E'}{2}\left[\sum_{i'=0}^{n'}(1+\tan^2\theta_{i'})\tan^2\theta_{i'} + \sum_{j'=0}^{m'}(1+\tan^2\theta^*_{j'})\tan^2\theta^*_{j'}\right]}{\sum_{i'=0}^{n'}(1+\tan^2\theta_{i'})^2 + \sum_{j'=0}^{m'}(1+\tan^2\theta^*_{j'})^2 - 1}(1+\tan^2\theta_{i'})$$

$$+\frac{1}{2}A'E'\tan^2\theta_{i'} \qquad (3\text{-}20)$$

$$F'^*_{j'=0,1,2,\ldots,m'} = \frac{F_s - \frac{A'E'}{2}\left[\sum_{i'=0}^{n'}(1+\tan^2\theta_{i'})\tan^2\theta_{i'} + \sum_{j'=0}^{m'}(1+\tan^2\theta^*_{j'})\tan^2\theta^*_{j'}\right]}{\sum_{i'=0}^{n'}(1+\tan^2\theta_{i'})^2 + \sum_{j'=0}^{m'}(1+\tan^2\theta^*_{j'})^2 - 1}(1+\tan^2\theta^*_{j'})$$

$$+\frac{1}{2}A'E'\tan^2\theta^*_{j'} \qquad (3\text{-}21)$$

where $F'_{i'=0,1,2,\ldots,n'}$ and $F'^*_{j'=0,1,2,\ldots,m'}$ are the tension forces of fiber bundles at the right side and the left side of the spinning triangle respectively. A' is the cross-section area of each fiber bundle and E' is the tensile modulus of fiber bundle. Based on the assumptions for fiber bundle, it can be reasonably assumed that: $A' = kA$ and $E' = E$, where A is the cross-section area of each fiber, E is the fiber tensile modulus and k denotes the number of fibers in each fiber bundle.

In addition, since it is assumed that fiber bundles are uniformly distributed in the spinning triangle, the inclinations of each fiber bundle to the axial direction $\theta_{i'}$ and $\theta^*_{j'}$ can be given by:

$$\theta_{i'} = i'(\frac{\theta_{n'}}{\mathrm{n'}}) \tag{3-22}$$

$$\theta^*_{j'} = j'(\frac{\theta^*_{m'}}{\mathrm{m'}}) \tag{3-23}$$

where $\theta_{n'}$ and $\theta^*_{m'}$ are the maximum values of $\theta_{i'}$ and $\theta^*_{j'}$ respectively and $\mathrm{m'+n'+1}$ is the total number of fiber bundles in the spinning triangle.

Assume all fibers in one bundle have equal tension, and then fiber tension force in each fiber bundle is given by:

$$\mathrm{F}_{i=0,1,2,...,\mathrm{n'}} = \frac{\mathrm{F'}_{i'=0,1,2,...n'}}{\mathrm{k}} \tag{3-24}$$

$$\mathrm{F}^*_{j=0,1,2,...,\mathrm{m'}} = \frac{\mathrm{F'}^*_{j'=0,1,2,...,m'}}{\mathrm{k}} \tag{3-25}$$

From Equations (3-24) and (3-25), it is obvious that the tension force of fiber bundle at the spinning triangle also depends on yarn spinning tension (F_s), the cross-sectional area of fiber bundle (A'), the fiber bundle tensile elastic modulus (E'), number of fiber bundles on the right side of spinning triangle (n') and left side of spinning triangle (m') according to the twist point axis, and the fiber bundle angle

with the twist point axis ($\theta_{i'}$) and ($\theta^*_{j'}$). In addition, the average fiber tension force can be simply calculated from the tensile stress of fiber bundles divided by the number of fibers in each fiber bundle.

3.4.3 Effects of Shape of Spinning Triangle on the Distribution of the Fiber Tensile Stress at the Spinning Triangle

3.4.3.1 Case I

As revealed by the paragraphs above, the distribution of the fiber tension stress at the spinning triangle depends in part on the shape of spinning triangle. In order to represent the shape of spinning triangle, a shape parameter (β) is adopted in the following analysis. In Figure 3-11, β can be given by:

$$\beta = \frac{w - d}{w + d} = \frac{\tan\theta^*_m}{\tan\theta_n} = \frac{m}{n} \tag{3-26}$$

The shape parameter β describes the symmetric level of the geometry of spinning triangle, and therefore is a more interesting variable. A greater β value indicates a more symmetric shape of spinning triangle. When $\beta = 1$, there will have a symmetric geometry of spinning triangle. In general, values of β are between 0 to 1 corresponding to the position of the twist point at the spinning triangle. In the following analysis, two typical examples are discussed.

In the first example, a symmetric triangle ($\beta = 1$) is assumed (Geometry B in Figure

3-9). Thus, based on Figures 3-11 and 3-12, we have:

$d = 0$, $\beta = 1$, and $\theta_n = \theta_m^*$;

Therefore, the tensile force of fibers at the spinning triangle is given by:

$$F_{i=0,1,2,...,n} = \frac{F_s - AE\sum_{i=0}^{n}(1+\tan^2\theta_i)\tan^2\theta_i}{2\sum_{i=0}^{n}(1+\tan^2\theta_i)^2 - 1}(1+\tan^2\theta_i) + \frac{1}{2}AE\tan^2\theta_i \qquad (3\text{-}27)$$

$$F_{j=0,1,2,...m}^* = \frac{F_s - AE\sum_{j=0}^{m}(1+\tan^2\theta_j^*)\tan^2\theta_j^*}{2\sum_{j=0}^{m}(1+\tan^2\theta_j^*)^2 - 1}(1+\tan^2\theta_j^*) + \frac{1}{2}AE\tan^2\theta_j^* \qquad (3\text{-}28)$$

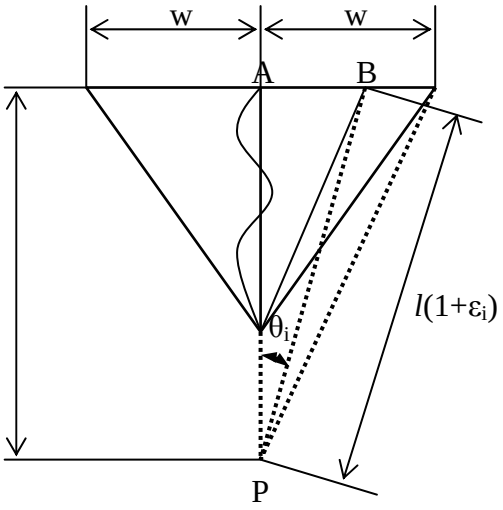

Figure 3-12 Spinning Triangle Model for Fiber Tension (Geometry B)

In the second example, we assume the geometry of spinning triangle resembles Geometry C ($\beta = 0$) in Figure 3-9.

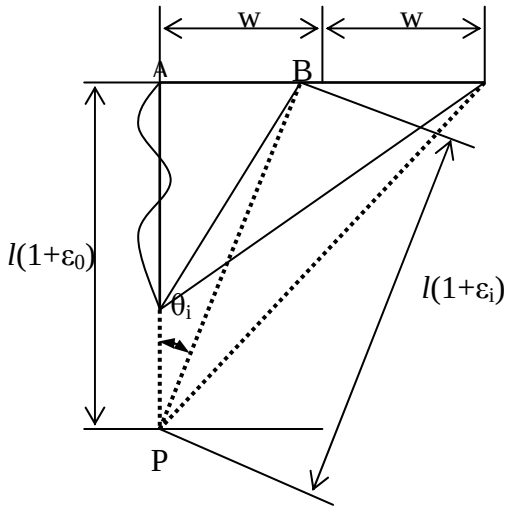

Figure 3-13 Spinning Triangle Model for Fiber Tension (Geometry C)

In this case, based on Figures 3-11 and 3-13, we have:

$d = w$, $\beta = 0$, thus $\theta_j^* = 0$;

The fiber stress distribution at the spinning triangle can be obtained by:

$$F_{i=0,1,2,\ldots,n} = \frac{F_s - \frac{AE}{2}[\sum_{i=0}^{n}(1+\tan^2\theta_i)\tan^2\theta_i]}{\sum_{i=0}^{n}(1+\tan^2\theta_i)^2}(1+\tan^2\theta_i) + \frac{1}{2}AE\tan^2\theta_i \quad (3\text{-}29)$$

$$F^{*}_{j=0} = \frac{F_s - \frac{AE}{2}[\sum_{i=0}^{n}(1+\tan^2\theta_i)\tan^2\theta_i]}{\sum_{i=0}^{n}(1+\tan^2\theta_i)^2} \quad (3\text{-}30)$$

In order to investigate the effects of the shape of the spinning triangle on the distribution of fiber force at the spinning triangle, a case of simulation of the tension force distribution of fibers at the spinning triangle was carried out as follows.

Since 58tex cotton yarn was mainly investigated in this study, the yarn parameters and fiber properties being used in the analysis are shown as follows - yarn twist factor: 4.2 and 3.2; number of fibers in the yarn: 385; spinning tension: 30cN; fiber elastic modulus: 50cN/dtex; and fiber linear density: 1.5dtex. The maximum fiber angles with the twist point axis in two typical examples of the spinning triangle ($\beta = 1$ and $\beta = 0$) are 26.5º and 30º for twist factor 4.2, and 20.8º and 23.6º for twist factor 3.2 based on experimental measurement. Besides, in order to simplify the analysis, it is assumed that the maximum fiber angle with the twist point axis is liner related to the shape parameter of the spinning triangle.

A computer programme using Matlab software was implemented, in the present work, to calculate the distribution of the fiber tension stress at the spinning triangle. In the following analysis, three different shapes of spinning triangle ($\beta = 0$, $\beta = \frac{1}{9}$ and $\beta = 1$) are compared and discussed.

Figures 3-14 and 3-15 show the tension distribution of fibers at the spinning triangles of three different types. The distribution of fiber tension depends on the shape of the spinning triangle. As the value of shape parameter β increases, the tension distribution of fibers at the spinning triangle becomes more uniform with the increase of symmetry of the spinning triangle. This may be due to the fact that an increase in the value of shape parameter β leads to a decrease of the maximum fiber angle with the twist point axis (θ_n) in the case of the same yarn twist angle, which results in a reduction of unevenness of fiber tension at the spinning triangle.

On the other hand, as yarn twist increases, more fiber tension is developed in the spinning triangle, as revealed by the comparison in Figure 3-14. Previous research (El-Shiekh, 1965; Pavlov, 1967; Klein, 1987) and present experimental study on the spinning triangle all support that the height of spinning triangle decreased with increase of the twist level. Thus the apex angle of the spinning triangle was increased and more fiber tension created. Across the width of the spinning triangle, different fibers show different fiber tensions depending on their position at the spinning triangle, as shown in Figure 3-14. The edge fibers present the highest fiber tension due to their long paths at the spinning triangle whereas central fibers are buckled under compression. When the shape of spinning triangle becomes asymmetric and yarn twist increases, more tension force of edge fibers are created and more compressive force are developed on the central fibers.

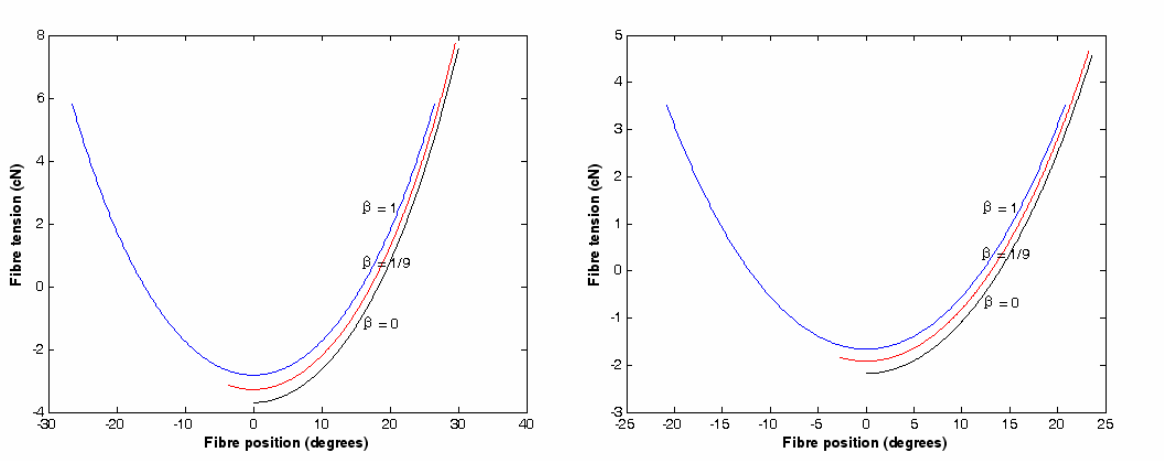

Yarn twist factor: 4.2 Yarn twist factor: 3.2

Figure 3-14 Fiber Tension at Different Spinning Triangles

3.4.3.2 Case II

Using similar approaches to those used in Case I, the distribution of the fiber bundle tension stress at the spinning triangles of different shapes can be obtained by:

$$F'_{i'=0,1,2,\ldots,n'} = \frac{F_s - A'E'\sum_{i'=0}^{n'}(1+\tan^2\theta_{i'})\tan^2\theta_{i'}}{2\sum_{i'=0}^{n'}(1+\tan^2\theta_{i'})^2 - 1}(1+\tan^2\theta_{i'}) + \frac{1}{2}A'E'\tan^2\theta_{i'} \quad (3\text{-}31)$$

$$F'^{*}_{j'=0,1,2,\ldots,m'} = \frac{F_s - A'E'\sum_{j'=0}^{m'}(1+\tan^2\theta^{*}_{j'})\tan^2\theta^{*}_{j'}}{2\sum_{j'=0}^{m'}(1+\tan^2\theta^{*}_{j'})^2 - 1}(1+\tan^2\theta^{*}_{j'}) + \frac{1}{2}A'E'\tan^2\theta^{*}_{j'} \quad (3\text{-}32)$$

where $d = 0$, $\beta = 1$, and $\theta_{n'} = \theta^{*}_{m'}$; and

$$F'_{i'=0,1,2,...,n'} = \frac{F_s - \frac{A'E'}{2}\sum_{i'=0}^{n'}(1+\tan^2\theta_{i'})\tan^2\theta_{i'}}{\sum_{i'=0}^{n'}(1+\tan^2\theta_{i'})^2}(1+\tan^2\theta_{i'}) + \frac{1}{2}A'E'\tan^2\theta_{i'} \qquad (3\text{-}33)$$

$$F'^{*}_{j'=0} = \frac{F_s - \frac{A'E'}{2}\sum_{i'=0}^{n'}(1+\tan^2\theta_{i'})\tan^2\theta_{i'}}{\sum_{i'=0}^{n'}(1+\tan^2\theta_{i'})^2} \qquad (3\text{-}34)$$

where $d = w$, $\beta = 0$, and $\theta^{*}_{j'} = 0$.

A case of simulation of the tension force distribution of fiber bundles at the spinning triangle was carried out using Matlab software to investigate the effects of the shape of the spinning triangle on the distribution of fiber bundle force and fiber force at the spinning triangle. In the following analysis, three different shapes of spinning triangle ($\beta = 0$, $\beta = \frac{1}{9}$ and $\beta = 1$) are compared and discussed.

For 58tex cotton yarn, the yarn parameters, fiber bundle and fiber properties being used in the analysis are shown as follows - yarn twist factor: 4.2 and 3.2, number of fibers in the yarn: 385, number of fiber bundle: 11, the number of fibers in each fiber bundle: 35, spinning tension: 30cN, fiber bundles elastic modulus: 50cN/dtex and fiber bundle linear density: 52.5tex.

Figures 3-15 and 3-16 show the tension distribution of fiber bundles and fibers of the fiber bundles at the spinning triangle of three different types. As shown in Figures

3-15 and 3-16, it can be seen that the effects of shape of spinning triangle and yarn twist level on the fiber tension distribution follow the same trend as that in Case I, in which more uniform distribution of fiber tension appears in the symmetry spinning triangle and lowing yarn twist level also makes great reduction of fiber tension at the spinning triangle. Based on the comparison between fiber distribution with and without multi-bundle form at the spinning triangle, it is also observed that the maximum value of fiber tension at the spinning triangle decreases when the fiber distribution takes the form of fiber bundle in the present proposed model. Meanwhile more compressive force is developed on the fibers in bundles distributed around yarn twist point.

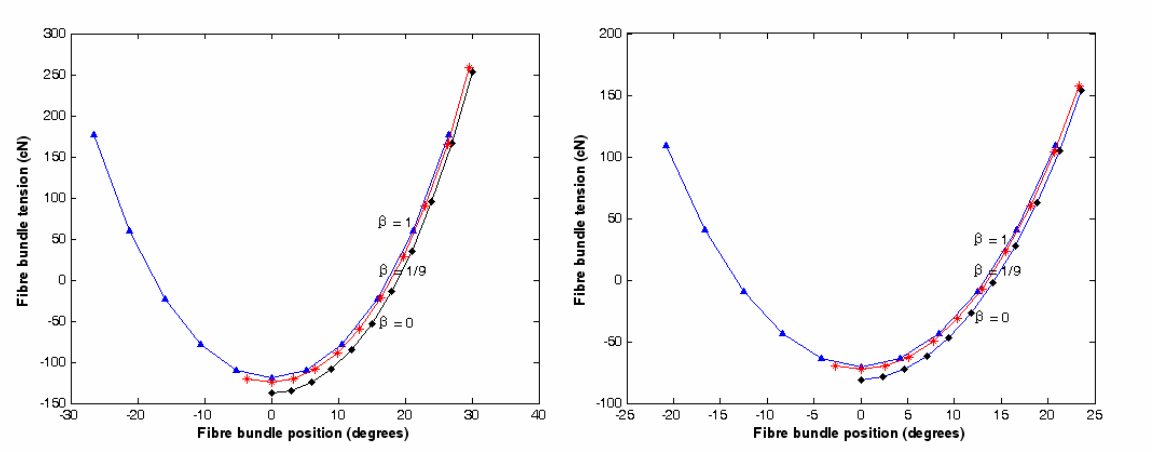

Yarn twist factor: 4.2 Yarn twist factor: 3.2

Figure 3-15 Fiber Bundle Tension at Different Spinning Triangles

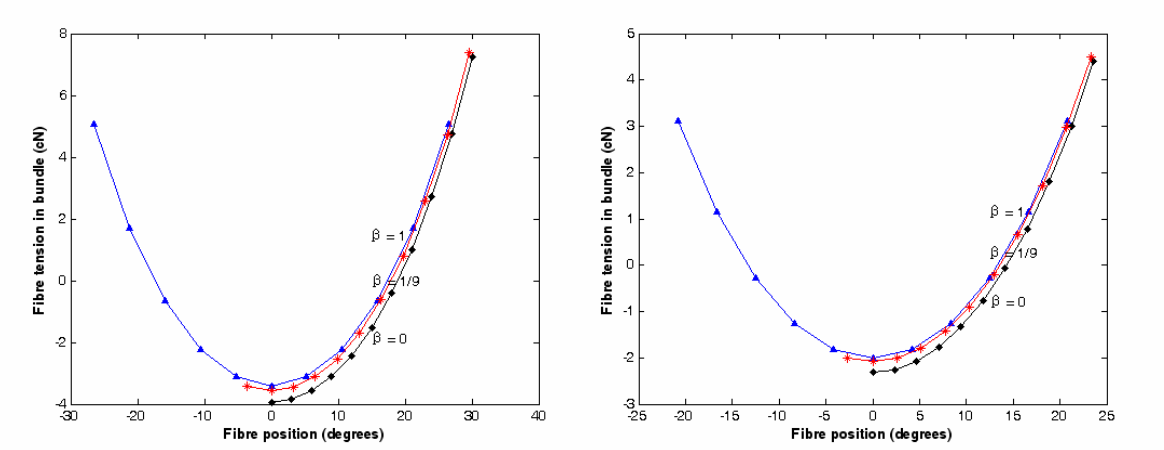

Yarn twist factor: 4.2 Yarn twist factor: 3.2

Figure 3-16 Fiber Tension in Bundles at Different Spinning Triangles

3.5 Distribution of the Fiber Tensile Stress within a Twisted Yarn and Its Effect on Yarn Torque

In a twisted structure such as a yarn, the mechanical state of the constituent fibers and their configuration in the yarn will determine the magnitude of the yarn torque. The mechanical states of fibers in tension, in torsion and in bending are three components contributing to yarn torque. The torsion strain and bending strain can be calculated from the helical-yarn geometry, while fiber tensile strain is difficult to be determined if only depending on yarn geometry. On the other hand, Postle, Burton and Chaikin (1964) and Bennett and Postle (1979) found that the fiber tension especially the fiber tensile stress distribution within a yarn is the most influential factor governing the magnitude of yarn torque. Despite of the difficulty, some research works were still done to find out internal fiber tensile strain in the yarn by

experimental study. Hickie and Chaikin (1960) investigated the configuration and longitudinal strain of single fibers in worsted yarn widely varying in count and twist using a radioactive fiber tracer technique. They found that the longitudinal strain of single fibers in yarns was a consequence of the spinning process and the twist is the main strain-inducing factor. In the study of yarn torque and its dependence on the distribution of fiber tensile stress in the yarn, Bennett and Postle (1979) presented an interpretation of the fiber tensile stress created during yarn twisting based on the retraction of twisted yarn when fiber migration was totally inhibited. In the present model, we seek to relate the distribution of fiber tensile stress in the yarn with the distribution of fiber tension force at the spinning triangle under the condition of Case I, uniformly distribution of fibers at the spinning triangle without multi-bundle form.

3.5.1 Distribution of Fiber Tensile Stresses within a Twisted Yarn

The distribution of fiber tensile stress in the yarn mainly depends upon the fiber tensile stress and the fiber arrangement within a yarn. In the present model, it is reasonably proposed that the fiber tensile stress within a yarn is related to the fiber tension created at the spinning triangle. Then how the fibers are arranged within a yarn under spinning tension and twisting becomes the key point for the solution of the distribution of fiber tensile stress in the yarn.

On the ring frame, the drafted roving silver is exported by the front roller and goes into the spinning triangle area. At the same time, the silver’s width gradually narrows with the forming of the twist spinning triangle and its cross section changes from flat

shape to a circular one. The form of yarn twist and migration of fibers in yarns were investigated in the previous investigation. Balls (1928) and Hearle, Gupta and Goswami (1965) proposed three possible ways of yarn twisting, namely the twisted cylindrical form, the twisted ribbon form and the wrapped ribbon form. They found that the individual fibers in the ribbon form will take up more favorable positions with shorter path lengths. In the experimental study on a 3-layer structure of 19 filaments twisting conducted by Hearle and Goswami (1970), it was observed that the filaments in the center of the ribbon try to run into the core of the yarn during the twisting.

The idealized packing of circular fibers in yarns was been discussed by Schwarz (1934, 1951). He proposed two basic forms: open-packing, in which the fibers lie in layers between successive concentric circles; and hexagonal close packing, in which the packing of fibers around a number of core fibers in a hexagonal configuration leads to a close packing manner. In the real yarn, it is difficult to achieve these two ideal forms and the yarn configuration obtained in real yarn is determined by some concentration and disturbing factors such as yarn twist (Hearle, Grosberg and Backer, 1969). However, these two ideal fiber packing forms are still useful in the study of yarn structure which in effect reduces the complexity of the yarn model.

3.5.1.1 Assumptions

Based on the findings in the previous study and above analysis, some reasonable assumptions are made in order to derive the mathematical equation for the

distribution of fiber tensile stress within a yarn as a function of the distribution of fiber tensile stress at the spinning triangle.

Firstly, we assume that the fiber tensile stress created in spinning triangle will be kept when fibers are transferred from the spinning triangle to the yarn, because the fiber is much longer than the height of the spinning triangle and the path length of fibers in the spinning triangle. Schonung (1989) found that the percentage of fibers whose both ends were gripped in the roller nip and the twist point reached 65% to 75% of fibers in the spinning triangle. Lord (1971) also mentioned that fibers were translated from a thin ribbon to a roughly circular shape in ring spinning, and usually fibers were gripped at the nip of the front rollers as well as the twisted structure. In addition, the act of twisting a number of components into a continuous strand during spinning was a continuous process in which fibers moved downward from spinning triangle to the yarn. This assumption is mostly true as long as the yarn is under the same tension and yarn geometry does not relax.

Secondly, during the fiber position transformation from the spinning triangle to the yarn, it is assumed that the central fibers at the spinning triangle will run into the core of the yarn, the fibers near the central of the spinning triangle will prefer to be arranged closely to the core of the yarn and the outer fibers of the spinning triangle will be transferred to the outside positions within a yarn correspondingly.

In addition, the fiber is assumed as circular in cross section. All the fibers are ideally

packed in the yarn cross-section in a packing manner. In a packing of components within the yarn there is a single core fiber at the centre around which six fibers are arranged. In this form, the fibers lie in layers between successive concentric circles. It is further assumed that the number of fibers arranged in each layer is given by the following equation:

$$N_{i'} = 6(i'-1) \quad (i' > 2) \tag{3-35}$$

where $N_{i'}$ is the number of fibers in each layer and i' is the layer number.

3.5.1.2 Distribution of Fiber Tensile Stresses within a Twisted Yarn

In order to investigate the effect of the geometry of the spinning triangle on the distribution of fiber tensile stresses within a twisted yarn, the typical shape of spinning triangle (Geometry A in Figure 3-11) and two special cases of spinning triangle (Geometry B-symmetric triangle, and Geometry C- right-angled triangle in Figures 3-12 and 3-13) are discussed and compared.

(1) It is assumed that the geometry of spinning triangle as Geometry A and the distribution of fiber tension forces at the spinning triangle can be expressed by Equations (3-18) and (3-19). If n>m, and $\Delta = n - m$; The two cases are investigated as follows.

a. If $2m = \sum_{i'=2}^{p} 6(i'-1)$, where i' is the layer number of fibers packing within a

yarn. Thus the 2m number of fibers are exactly arranged from 2-nd layer to p-th layer of yarns. Then, we have the average fiber tensile stress ($T_{i'}$) of every layer within the yarn from 2-nd layer to p-th layer of yarns.

1-st layer: $T_1 = F_0$, (3-36)

i'-th layer: $$T_{i'} = \frac{\sum_{i=1+3\sum_{k=2}^{i'}(i'-k)}^{3\sum_{k=1}^{i'}(i'-k)} F_i + \sum_{j=1+3\sum_{k=2}^{i'}(i'-k)}^{3\sum_{k=1}^{i'}(i'-k)} F_j}{6(i'-1)}; \quad (1 < i' \le p) \tag{3-37}$$

Then, the Δ number of fibers will be placed beyond the p-th layer. Hence, it follows that:

i'-th layer: $$T_{i'} = \frac{\sum_{i=1+6\sum_{k=2}^{i'-1}(i'-1-k)}^{6(i'-1)+6\sum_{k=2}^{i'-1}(i'-1-k)} F_i}{6(i'-1)}; \quad (i' > p) \tag{3-38}$$

b. If $\sum_{i'=2}^{p-1} 6(i'-1) < 2m < \sum_{i'=2}^{p} 6(i'-1)$, then the $2m$ number of fibers are not enough to be arranged completely from 2-nd layer to p-th layer of yarns. Other fibers such as (m+1)-th fiber, (m+2)-th fiber … (m+q)-th fiber at the spinning triangle will be arranged in the p-th layer for a completely ring. Then we have:

1-st layer: $T_1 = F_0$, (3-39)

i'-th layer: $$T_{i'} = \frac{\sum_{i=1+3\sum_{k=2}^{i'}(i'-k)}^{3\sum_{k=1}^{i'}(i'-k)} F_i + \sum_{j=1+3\sum_{k=2}^{i'}(i'-k)}^{3\sum_{k=1}^{i'}(i'-k)} F_j}{6(i'-1)}, \qquad (1 < i' \le p-1) \qquad (3\text{-}40)$$

i'-th layer: $$T_{i'} = \frac{\sum_{i=1+3\sum_{k=2}^{i'}(i'-k)}^{m} F_i + \sum_{j=1+3\sum_{k=2}^{i'}(i'-k)}^{m} F_j + \sum_{i=m+1}^{1-m+6\sum_{k=1}^{i'}(i'-k)} F_i}{6(i'-1)}, \quad (i' = p) \qquad (3\text{-}41)$$

i'-th layer: $$T_{i'} = \frac{\sum_{i=2-m+6\sum_{k=1}^{i'-1}(i'-1-k)}^{1-m+6(i'-1)+6\sum_{k=1}^{i'-1}(i'-1-k)} F_i}{6(i'-1)}; \qquad (i' > p) \qquad (3\text{-}42)$$

(2) It is assumed that the geometry of spinning triangle as Geometry B and the stress distribution of fiber at the spinning triangle can be expressed by Equations (3-27) and (3-28). Then, the average fiber tensile stress of every layer is given by:

1-st layer: $$T_1 = F_0, \qquad (3\text{-}43)$$

i'-th layer: $$T_{i'} = \frac{\sum_{i=1+3\sum_{k=2}^{i'}(i'-k)}^{3\sum_{k=1}^{i'}(i'-k)} F_i + \sum_{j=1+3\sum_{k=2}^{i'}(i'-k)}^{3\sum_{k=1}^{i'}(i'-k)} F_j}{6(i'-1)}; \qquad (i' > 1) \qquad (3\text{-}44)$$

(3) It is assumed that the geometry of spinning triangle as Geometry C and the

distribution of fiber tension forces at the spinning triangle can be expressed by Equations (3-29) and (3-30). The average fiber tensile stress of every layer can be expressed as follows:

1-st layer: $T_1 = F_0$, (3-45)

i'-th layer: $T_{i'} = \dfrac{\sum_{i=1+6\sum_{k=2}^{i'}(i'-k)}^{6\sum_{k=1}^{i'}(i'-k)} F_i}{6(i'-1)}$; $(i' > 1)$ (3-46)

In the following analysis, a case of simulation of the distribution of fiber tensile stresses within a twisted yarn are carried out based on the tension distribution of fibers at the spinning triangle discussed above when the shape of spinning triangle takes the form of Geometry B and C.

In Figure 3-17, two illustrations are given of the distribution of fiber tensile stress as a function of radial position in a twisted yarn of radius R_y for 58tex cotton yarn with twist factors of 4.2 and 3.2, respectively.

It is clear from the examples that the effect of the geometry of the spinning triangle on the distribution of fiber tensile stresses within a twisted yarn follows similar trend as the effect of the geometry of the spinning triangle on the distribution of fiber tensile stresses at the spinning triangle. In the form of symmetric spinning triangle, the yarn shows a more uniform tensile stress distribution of fibers within the yarn

while a higher radial bias of fiber tensile stress exists in the yarn when the spinning triangle takes the shape of a right-angled triangle.

From Figure 3-17, it can also be found that at lower yarn twist the yarn presents lower fiber tensile stress distributed across the whole yarn and a more uniform distribution of fiber tensile stress within the yarn regardless the spinning triangle takes a symmetric shape or not when compared to that of higher twisted yarn in the present example.

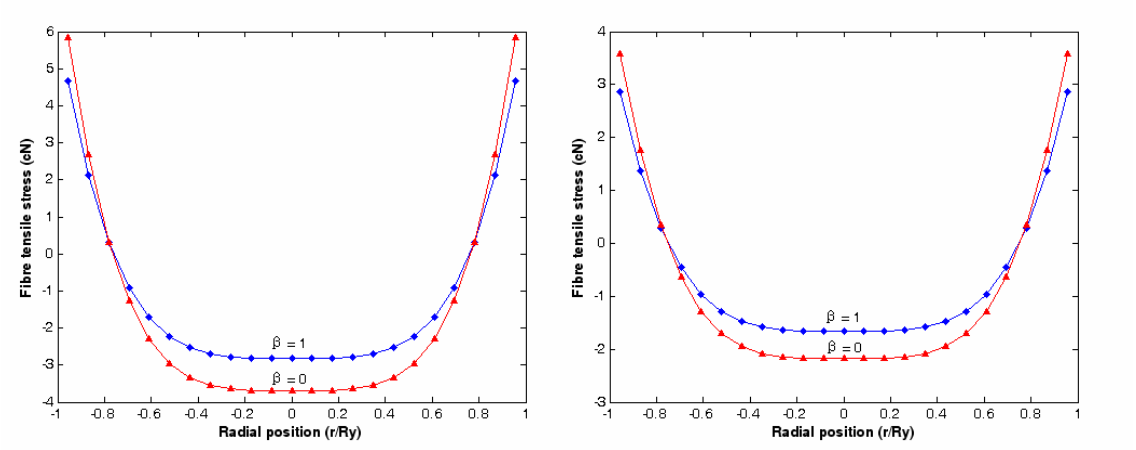

Yarn twist factor: 4.2 Yarn twist factor: 3.2

Figure 3-17 The Distribution of Fiber Tensile Stress as a Function of Radial Position in a Twisted Yarn of Radius R_y

3.5.2 Yarn Torque due to Residual Fiber Tensile Stress

In the previous study, it is proposed that the nature of the fiber tensile stress distribution within a yarn is likely to be the most influential factor governing the magnitude of yarn torque (Bennett and Postle, 1979). With the fiber tensile stress distribution within a yarn, the component of yarn torque due to these stresses is derived as follows.

It is initially assumed that the yarn will not buckle and the geometry will be fixed in the yarn. If a fiber has a tensile stress P_i along its axis with helix angle q_i as it lies in a yarn, each fiber tension contributes to the yarn torque component is given as follows:

$$L_i = P_i r_i \sin q_i \tag{3-47}$$

where L_i is the component of yarn torque due to each fiber tension and r_i is the distance of fiber from the yarn-axis.

Hence, the total yarn torque generated by fiber tension is obtained by:

$$L = \sum_{i=1}^{m+n+1} L_i = \sum_{i=1}^{m+n+1} P_i r_i \sin q_i \tag{3-48}$$

In the present model, fibers are ideally packed within the yarn cross-section in the packing manner as we assumed in the pervious section. The number of fibers ($N_{i'}$)

arranged in i'-th layer is given by:

$$N_{i'} = 6(i'-1) \quad (i'>2) \tag{3-49}$$

If $1+m+n = 1+\sum_{i'=2}^{\eta} 6(i'-1)$, the fibers will be packed completely within a yarn in which each layer contain an ideal number of fibers, where $1+m+n$ is the total number of fibers in yarn and η is the number of layers of fiber packing in yarn.

The contribution from tension of all fibers in a layer to yarn torque is determined by:

$$L_{i'} = 12(i'-1)^2 T_{i'} r \sin[\arctan(\frac{2i'-2}{2\eta-1}\tan\alpha)] \tag{3-50}$$

where $T_{i'}$ is the average fiber tensile stress of every layer, r is fiber radius and α is yarn surface helix angle.

Hence, the total yarn torque due to fiber tensile stress is given by:

$$L = \sum_{i'=1}^{\eta} L_{i'} \tag{3-51}$$

In another case, if $1+m+n = 1+\sum_{i'=2}^{\eta-1} 6(i'-1)+\delta$, it shows that the last layer (η) has not been assumed to have an ideal number of fibers, where δ is the number of fibers in the last layer of fiber packing in yarn.

Then, the yarn torque components contributed from tension of all fibers in a layer is given by:

$$L_{i'} = 12(i'-1)^2 T_{i'} r \sin[\arctan(\frac{2i'-2}{2\eta-1}\tan\alpha)] \quad (3\text{-}52)$$

where i' is given the value from 0 to $\eta-1$.

And the contribution from tension of all fibers in the last layer (η) to yarn torque is given by:

$$L_{\eta} = 2\delta(\eta-1) T_{\eta} r \sin[\arctan(\frac{2i'-2}{2\eta-1}\tan\alpha)] \quad (3\text{-}53)$$

where T_{η} is the average fiber tensile stress of the last layer.

The total yarn torque due to fiber tensile stress can be obtained by:

$$L = \sum_{i'=1}^{\eta-1} L_{i'} + L_{\eta} \quad (3\text{-}54)$$

According to the above analysis, a case of simulation of yarn torque was carried out based on the distribution of fiber tensile stresses within the yarn exhibited in Figure 3-17. Table 3-1 lists the calculated results of yarn torque for 58tex cotton yarn with twist factors of 4.2 and 3.2.

Table 3-1 Calculated Yarn Torque for 58tex Cotton Yarn

Yarn sample	Yarn twist factor	β	Calculated yarn torque (1×10^{-5} N ·m)
58 tex cotton yarn	4.2	1	7.5414
		0	9.0782
	3.2	1	4.0239
		0	4.9069

As revealed in Table 3-1, in the form of symmetric spinning triangle, the yarn exhibits a lower yarn torque because of a more uniform tensile stress distribution of fibers in the yarn when compared to that of yarn with shape of right-angled spinning triangle in the present examples. Besides, the torque of the yarn with twist factor 3.2 is much lower than that of the yarn using twist factor 4.2 due to lower fiber tensile stress and lower fiber helix angle in the yarn of twist factor 3.2.

Based on the results of theoretical analysis and case simulation, it is indicated that reducing yarn twist level results in the reduction of fiber tension created at the spinning triangle and within the yarn, and thus reduces yarn torque. For low torque ring yarn, low yarn twist level is mainly adopted in yarn spinning, thus low yarn torque can be achieved in the low torque ring yarn. Besides, the experimental observation showed that the spinning triangle of low torque ring yarn presents a symmetric structure, which creates a more uniform distribution of fiber force in the spinning triangle and within the yarn when compared with conventional ring yarn in an asymmetric geometry. Therefore, the symmetric structure of spinning triangle also

contributes to the low torque in the low torque ring yarn.

3.6 Summary and Conclusion

The work in this Chapter has been concerned with the investigation of the geometry of ring spinning triangle and its effect on the yarn torque. The study started with the geometry of spinning triangle with the help of an experimental device for spinning triangle observation. The experimental device includes a specially designed transparent roller, the CCD Micro-Camera and a frame for camera-mounting and photo-taking. The observation of spinning triangle indicates that the geometry of spinning triangle in low torque ring yarn exhibits some characteristics such as symmetric structure, short height and -bundle of fibers.

Following that, a theoretical investigation of the effect of shape of spinning triangle on the distribution of the fiber tension stress was carried out using the principle of stationary total potential energy in this Chapter. A shape parameter (β) which describes the symmetric level of the geometry of spinning triangle has been introduced in the analysis. The typical shape of spinning triangle (Geometry A in Figure 3-9) and then two special cases of spinning triangle (Geometry B - symmetric triangle, and Geometry C - right-angled triangle in Figure 3-9), as well as multi-bundle form of fibers were analysed for the distribution of the fiber tension stress at the spinning triangle.

The theoretical analysis indicates that the individual fiber tension at the spinning triangle is determined by yarn spinning tension, fiber properties, number of fibers, the shape of spinning triangle and the yarn twist angle. To evaluate and simulate the theoretical results, a case study was carried out on the investigation of the distribution of fibers tension stress at the spinning triangle of 58tex cotton yarn. The simulation results showed that the distribution of fiber tension force depends on the shape of the spinning triangle. As the value of shape parameter β increase, the tension force distribution of fibers at the spinning triangle becomes more uniform. Besides, as yarn twist increases, more fiber tension is developed at the spinning triangle. For fibers distributed at the spinning triangle in the form of multi-bundle, it was observed that the maximum value of fiber tension at the spinning triangle decreased when compared with that of fiber distribution without multi-bundle form in the present analysis.

On the basis of some assumption, an attempt on linking the residual fiber tension stress at the spinning triangle to yarn torque is also included in this Chapter. A case of simulation of the distribution of fiber tensile stresses within a twisted yarn suggested that the yarn shows a more uniform tensile stress distribution of fibers in the form of symmetric spinning triangle, and lower fiber tensile stress distributed across the whole yarn when lower yarn twist level is adopted. Besides, the calculated results of yarn torque for 58tex cotton yarn showed that in the form of symmetric spinning triangle, the yarn exhibits a lower yarn torque when compared to that of yarn with shape of right-angled spinning triangle, and the torque of the yarn with twist factor 3.2 is much lower than that of the yarn using twist factor 4.2 in the

present examples. For low torque ring yarn, low yarn twist level is mainly adopted in yarn spinning, thus low yarn torque can be achieved in the low torque ring yarn. Besides, the symmetric structure of spinning triangle also contributes to the low torque in the low torque ring yarn.

CHAPTER 4 STRUCTURES OF LOW TORQUE RING YARN FOR WEAVING

4.1 Introduction

Yarn structure has a significant influence on the properties and performance of yarns and the subsequent fabrics. The yarn structure is influenced not only by characteristics of fibers forming the yarn, but also by the spinning methods. In this respect, the introduction of false-twisting operation during low torque ring yarn spinning may give low torque ring yarn a new fiber and yarn configuration, while the configuration of the fibers and the fiber migration behavior in the yarn play a crucial role in determining yarn residual torque, yarn tenacity as well as other yarn structural and physical properties. Therefore, the investigation of low torque ring yarn structure characterized by geometrical arrangement of fibers in the yarn is of great importance and thus forms the subject of this Chapter.

In order to analyze yarn structure faster and more accurately, a system for investigation of the fiber configuration in staple yarns, based on the tracer fiber technique, has been developed in this study. The system can capture consecutive images of single tracer fiber with the help of the automatic moveable platform and a

program written by the National Instruments LabVIEW 5.1 language for grabbing images of the tracer fiber. Besides, with the help of SEM and tracer fiber, structures of low torque ring yarn will be analyzed and characterized by yarn surface structure, 3D configuration of tracer fiber in the yarn and fiber migration behavior of the yarn in the Chapter.

4.2 Retrospect of Yarn Structure Study

Yarn structure is determined mainly by the properties of the constituent fibers and the inherent characteristics of the processing system, while the physical properties and performance characteristics of yarns depend on the physical properties of the constituent fibers and on yarn structure. In this respect, the study of yarn structure and the positioning of the constituent fibers to form a continuous strand have attracted the attention of a lot of research work particularly the extensive work on the mechanical properties of yarns.

Although an excellent analysis of yarn mechanics was published by Gegauff (1907) as long ago as in 1907, work on yarns, particularly on yarn structures, had generally lagged behind comparable studies of fibers and fabrics (Hearle, Grosberg and Backer, 1969). Nevertheless since 1951, there has been a notable change, and many structural analysis of yarn have been carried out and published. Figure 4-1a illustrates the ideal helical geometry usually adopted in theoretical studies of the structural mechanics of yarns in which it is assumed that the yarn is circular in cross section and that the fibers are following helical paths around concentric cylinders of

constant radius. In staple-fiber spun yarns, such a highly idealized form of structure would be useless, if it existed. It could not survive any handling because there would be nothing to prevent the successive layers from peeling off at the slightest sign of surface abrasion due to the lack of cohesion of the fibers on the surface and hence lack of cohesion in the yarn as all. On the other hand, for both staple-fiber and continuous filament yarns, this structure would be difficult to achieve in practice. The difficulty of formation is due to the differences in the lengths of path followed by fibers at different radial positions in the yarn. It was first recognized by Pierce (1949) that there is a need for the interchange of the fiber position inside a yarn. In 1952 Morton and Yen discovered the change in the position of the single fiber along the length of a yarn and named this phenomenon “fiber migration”, as illustrated by Figure 4-1b. In order to study fiber migration they introduced the tracer fiber technique, which enables the path of a single tracer fiber to be observed under a microscope. This method is now widely used in yarn structure analysis. Later Morton (1956) proposed that one of the mechanisms causing fiber migration is the tension differences resulting from the different path lengths of the fibers. He also defined the “the coefficient of migration” to characterize the migration quantitatively. The second geometric mechanism of migration, suggested by Hearle and Bose (1965), is based on the assumption that the yarn is formed as a result of twisting a flat ribbon of fibers. For actual yarn, the conditions during formation are much more complicated because of the presence of the multiplicity of the parameters. Though two different mechanisms were introduced, Hearle, Gupta and Goswami (1965) pointed out that they are not mutually independent of each other. In 1964 Riding worked on filament yarns, and expanded the tracer fiber technique by observing the

fiber from two perpendicular directions by placing a plane mirror near the yarn in the liquid with the plane of the mirror at 45º to the direction of observation. Since the path followed by a fiber is actually in three dimensions, it can only be fully established if observations are made in more than one direction. Riding also applied correlogram analysis on characterizing the migration patterns and suggested that this analysis gave an over all statistical picture of the migration. Later a detailed theoretical study of the correlogram method of analysis on the migration of fibers in yarns was carried out by Hearle and Goswami (1968). In the mid 1960's Hearle and his co-researchers worked on a comprehensive theoretical and experimental analysis of fiber migration. They proposed various migration parameters such as Mean Fiber Position, RSM Deviation, Mean Migration Intensity and Equivalent Migration Frequency to characterize migration behaviour of an ideal yarn by considering ribbon-twist model. In the study of worsted-yarn structure, Hickie and Chaikin (1974) applied the technique of Finite Fourier analysis to traces of fibers with the aim of analyzing tracer fiber by decomposing the irregular periodic function into regular corresponding wave components with different periods. Alagha, Oxenham and Iype (1994) developed an image analysis system to assess the structural parameters of friction spun yarn, particularly on fiber migration, which offered significant benefits over the traditional tracer fiber technique. However, they recommended that improvements were required to refine the system so that it could be done automatically. A mathematical model of a helix with variable radius was developed to analyze geometric and mechanical properties of a migrating fiber by Tao (1996). The factors concerned include the frequency and amplitude of fiber migration as well as the equivalent radial position and equivalent helix height of the fiber, which

permitted the application of experimentally determined migration patterns defined by those factors. In 2001 Huh, Kim and Ryu described a visualization and analysis method for quantitatively analyzing the migration behaviour of stable fiber yarn. The analysis showed reproducibility and generated new information on yarn structure with efficiently automated analysis process. In the study on structural and physical properties of ring, rotor and frication spun yarns, Huh, Kim and Oxenham (2002) found that ring spun yarn exhibits the highest fiber migration followed by rotor spun yarn and friction spun yarn with the least. The ring spun yarn also shows a moderately uniform distribution of the fiber packing density among the three types of yarns.

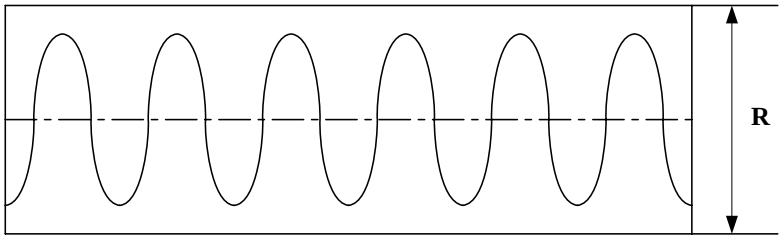

a. Ideal Helical Yarn Geometry

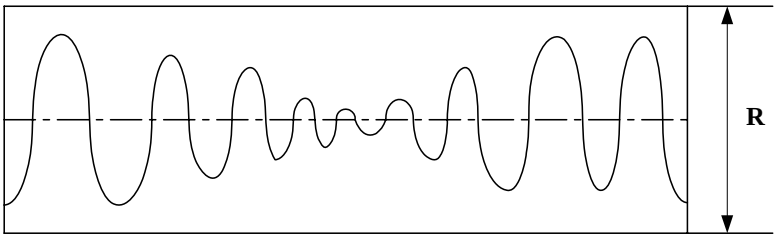

b. Yarn Structure with Fiber Migration

Figure 4-1 Yarn Geometry

4.3 Measuring System

4.3.1 System Configuration

A tracer fiber measuring system has been newly designed for the present work. The major components of the system include a tracer fiber observation device, an automatic moveable platform with motion velocity and length control system for specimen, a high resolution digital camera with high performance zoom lens, and the measuring procedure controller and data analysis system by a personal computer equipped with image capturing and analysis software, as shown in Figures 4-2a and 4-2b.

Figure 4-2a The Set-up of Tracer Fiber Measuring System

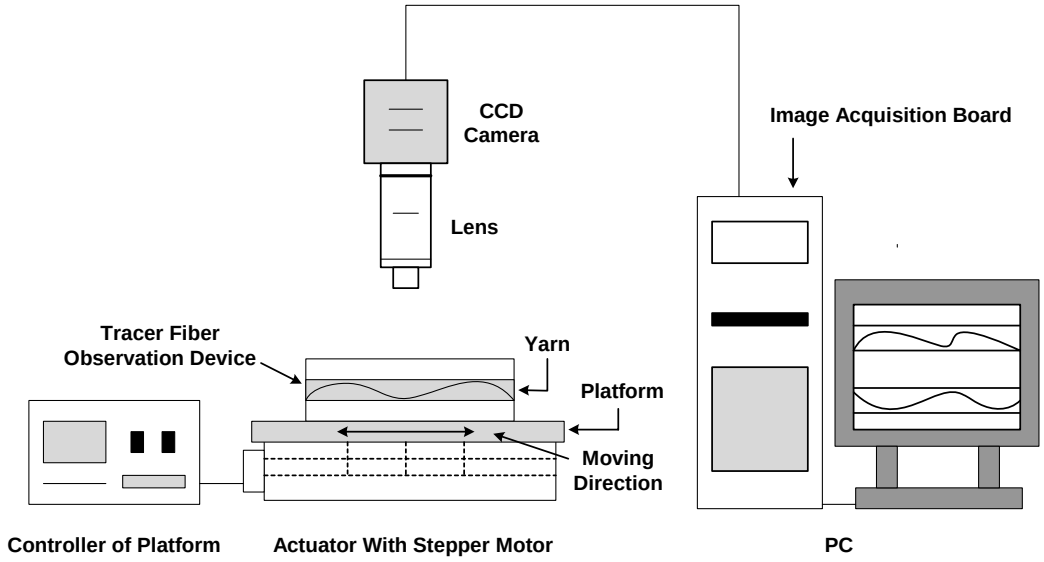

Figure 4-2b Configuration of Tracer Fiber Measuring System

The principle of measuring and analyzing the fiber configuration is based on the tracer fiber method invented by Morton and Yen (1952) and Riding (1964). In this method, a small amount of dyed fibers, known as tracers, are merged with normal undyed fibers in the carding process and all of them are fed into normal spinning process. The yarn produced is then immersed in a liquid medium having the same refractive index as that of the fibers. The undyed fibers almost disappeared from the view, and only the path of each of the dyed tracer fibers could be readily observed. In order to have a clear vision of the tracer fiber, a tracer fiber observation device was set up based on a modified version of tracer fiber method proposed by Choi (2003). Figure 4-3 illustrates a general view of this designed tracer fiber observation

device. Two smooth and shiny metal plates making an angle of 22.5º to the horizon were embedded in the metal box containing the liquid. Yarns for tracking the tracer fiber were mounted on the tension disks through the guides. The metal box was covered by a plastic sheet to avoid the irritating smell of the liquid diffusing out. The main features different from Riding' method is that two mirrors with the same angle 22.5º to the horizon were used in the present study. With the same distance from the lens to the two images of a tracer fiber, more clear images of yarns can be achieved. In addition, the position of yarn sample can be adjusted vertically and horizontally for better images of yarn, which is an improvement based on Choi's device. Figure 4-4 presents the modified technique for observing the two images of a tracer fiber. By measuring the distances of the fiber from the yarn axis in the two yarn images, namely x' and y', the distances of the fiber from the yarn axis by the x and y co-ordinates can be calculated as follows:

$$x = x'\cos\alpha - y'\sin\alpha \tag{4-1}$$

$$y = x'\sin\alpha + y'\cos\alpha \tag{4-2}$$

Since $\alpha = 45^{\circ}$, Then we have:

$$x = \frac{\sqrt{2}}{2}(x'-y') \tag{4-3}$$

$$y = \frac{\sqrt{2}}{2}(x'+y') \tag{4-4}$$

Figure 4-3 General View of Tracer Fiber Observation Device

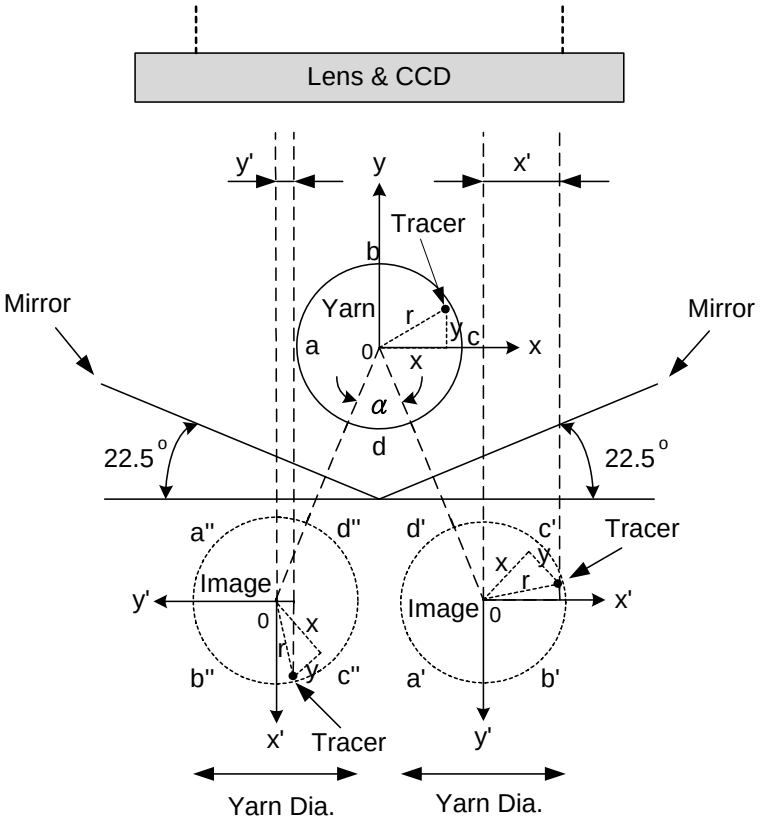

Figure 4-4 Modified Technique for Observing Two Images of A Tracer Fiber

In order to continuously capture the images of tracer fiber by the digital camera, an automatic moveable platform system for holding tracer fiber observation device was designed in the present study. A stepper motor (57BYG059) with a high step accuracy and resolution, together with its control systems including a driver (SH2034M), a programmable controller and a power supply, were used to drive the measurement platform. The stepper motor controller was specially designed to meet the requirements of the tracer fiber observation, which can display real time motion parameters and is capable of changing motion parameters such as motion velocity and motion length according to measuring requirements, and is easy to operate. The function of transmission mechanism is to change the rotary motion of the drive motor to the linear motion of the working platform. In this study, a LM Guide Actuator (THK KR 2001B) that combines guides and ball screws was used as the transmission mechanism which is characterized by the compact structure, high-precision ball screws, and highly precise smooth motion at a minimum frictional resistance. With the help of this system, the image acquisition is faster and more accurate, and the problems in manual operation such as slow movement, larger random error can be solved. The specifications of this automatic moveable platform are listed in Table 4-1.

Table 4-1 Specifications of the Automatic Moveable Platform

Parameter	Unit
Range of motion velocity	1-180 mm/min
Range of displacement	1-80 mm
Maximum load	1000 g

Images of tracer fibers were captured using a CCD camera (SK 2009) equipped with a 1/3 inch image sensor mounted on a bracket and perpendicular to the surface of platform. The resolution of digital camera was 640×480 pixel whose output has NTSC format. A hand-operated zoom lens with magnification of 10x-80x is attached to the CCD camera in order to acquire magnified images of the tracer fiber. The captured images were converted to 8 bits per pixel, 256 gray level, to enhance the analyzing speed and reduce the image file size. The CCD camera was connected to a COMPUCON computer equipped with two softwares, LabVIEW and IMAQ Vision image processing toolkit. LabVIEW (Laboratory Virtual Instrument Engineering Workbench) is a powerful instrumentation and analysis programming language developed by National Instruments (NI). With add-on toolkit LabVIEW covers anything from Internet connectivity and database access to fuzzy logic and image processing. The image-based on toolkit (called Vision) is particularly popular, simplifying the often-complex task of not only downloading appropriate quality images into a computer, but also making multifarious processing tasks much easier than many other packages and languages. IMAQ Vision is an image acquisition and manipulation add-on package for LabVIEW. IMAQ hardware includes the IMAQ 1408 series which is a high-accuracy image acquisition broad for analog monochrome and StillColor acquisition. By means of IMAQ 1408 acquisition broad the camera is connected to the computer. NI-IMAQ driver software gives high-level control of National Instruments IMAQ hardware. In addition, NI-IMAQ contains the NI-IMAQ Configuration Utility for configuring board and its VIs supply all functionality needed to acquire images with or without a trigger.

With NI-IMAQ and LabVIEW, the images of the yarn specimen can be grabbed and stored in the main memory of the computer if it is in a good position for measurement. Due to the high magnification employed in this process each captured picture covered only a part of the tracer fiber. Later, these images (approximately 6-10 images) need to be stitched to create composite images. In the previous image acquisition of tracer fiber, normally each time only one section of the tracer fiber image can be captured and stored into a memory buffer. Then it is needed to move the yarn specimen by hand to find the appropriate position for capturing next image. When a complete tracer fiber image is obtained in the form of several images of tracer fiber sections, these tracer fiber sections need to be linked together to get the panoramic image of the tracer fiber. During this process, some operation error probably occurred such as mistake in image stitching. Moreover, in practice it is not easy to move yarn to an appropriate position for each tracer fiber section being matched completely. The time consuming and tedious nature of this work is another problem which is needed to be considered. Therefore, it has become necessary to develop a system which can capture consecutive images of single tracer fiber at one time, thus avoiding fatigue while providing better reliability and improved accuracy. With the help of automatic moveable platform, a program is written by the National Instruments LabVIEW 5.1 language for capturing consecutive images of single tracer fiber (approximately 8 images). The accuracy and efficiency of measurement can be greatly improved. Besides, it is very helpful for the analysis and processing of the tracer fiber image information such as transfer of the obtained images into a set of data. Moreover, the regeneration of the 3D configuration and radial position variation of the tracer fiber in a real yarn and the analysis of yarn structural

characteristics can be achieved.

In the design of this measuring system, there are two issues specially considered. The first consideration is that the system can capture consecutive images of single tracer fiber and store them in the computer, which is realized by moving the yarn specimen with automatic moveable platform, and by setting up the procedure for continually capturing and storing images. In the wire diagram, three is the adoption of the IMAQ components: image create, snap, write, loop and sequence, to continually capture and store images of the tracer fiber as bitmap (BMP) files labeled chronologically. The second consideration is based on the time match between the motion of yarn specimen and the capture of the image in order to stitch tracer fiber sections for creating composite images. That means when the first section of tracer fiber is captured the camera is waiting till the second section of tracer fiber moves to an appropriate position and then capturing, and wait again for the third section and capturing, and actions repeat again until last section. This time match is achieved by adjusting the velocity of moveable platform and setting up control command ‘millisecond multiply’ which control the length of time that elapses between two successive pictures.

Since images are captured at the rate of 30 frames per second by an RS 170 CCD camera and the yarn specimen moves slowly, the displacement of yarn specimen is not appreciable during yarn image capturing.

4.3.2 Measurement Procedure

Before the formal measurement, a calibration is made for time match between movement of yarn specimen and the capturing of the tracer fiber image. In this procedure, a standard paper with known scale was used to determine the velocity of moveable platform and the setting of the control command ‘millisecond multiply’.

After calibration, the yarn specimen consisted of a few dyed tracer fibers was manually drawn through the tracer fiber observation box captaining a liquid medium having the same refractive index as that of the fibers until an appropriate tracer fiber was observed on the monitor.

When a tracer fiber came into view, the start button on platform controller was put on and the yarn specimen began to move. At the same time, the IMAQ program written for capturing consecutive images of single tracer fiber was executed. When the image capturing finished the obtained images of the tracer fiber were analyzed using a suitable algorithm to determine the yarn boundary and find the position of the tracer fiber, with which yarn structural parameters such 3D configuration of tracer fiber in the yarn and fiber migration behavior can be analyzed.

4.4 Experimental

4.4.1 Preparation of Yarn Sample for SEM Observation

As the first step on the study of low torque ring yarn structure, a carded cotton roving of 952tex (0.62 Ne) was used to spin 58tex (10Ne) conventional ring yarns (C) and low torque ring yarns (NS) with twist factors of 3.2, 3.8 and 4.2 on the modified Ring Spinning Frame. The surface structure of low torque ring yarn was then examined under the Scanning Electron Microscope (SEM) and compared to that of conventional ring yarn, which has the aim to identify some unique structural features of low torque ring yarn.

4.4.2 Preparation of Yarn Sample with Tracer Fibers

In the preparation of yarn sample for yarn structural investigation according to tracer fiber technique, Tencel fibers were selected for this experiment, since the proper immersion liquid for tracer fiber observation is easy to choose for Tencel fibers. In particular, the similar physical properties between Tencel and cotton yarns guarantee the reliability of the experimental results. The specifications of Tencel fiber is listed in Table 4-2.

Table 4-2 Specifications of Tencel Fiber

Fiber type	Fiber diameter (mm)	Fiber length (mm)	Fiber density (g/cm^3)
Tencel	0.0118	38	1.52

A small proportion (0.3%) of black-dyed tracer fibers was introduced in the carding stage, with the remaining undyed Tencel fibers. After carding, the materials were subjected to three passages of drawing and roving. Then the Tencel fiber roving with 0.3% black-dyed tracer fibers was used to produce 10Ne conventional ring yarn and low torque ring yarn on a small scale ring spinning machine with modification system. The main spinning parameters and yarn specification are shown in Table 4-3. The yarns produced were immersed in the tracer fiber observation box containing liquid, which is chosen so that its refractive index is very close to that of the Tencel fibers. In this study, the mixture of Turpentine oil and Bromonaphthalene at a proportion of 1:1 was used as immersion liquid in the tracer fiber technique since this chemical solution has the refractive index closer to that of Tencel as well as the toxicity is relatively low. Specifications of liquid mixture are shown in Table 4-4.

Table 4-3 Spinning Parameters and Yarn Specifications

Roving count (Ne)	Total draft	Spinning speed (rpm)	Twist factor	Speed ratio	Yarn count (Ne)
0.69	14.5	7000	3.2, 4.2	0.43	10

Table 4-4 Specifications of Liquid Mixture

	Turpentine oil	Bromonaphthalene (C10H7Br)
Refractive index	1.472	1.6575
Melting point (ºC)	-60 to -50	-2 to -1
Boiling point (ºC)	150 to 180	279 to 281
Relative density	0.9	1.4890

With the help of the developed tracer fiber measuring system, yarn structural parameters such as 3D configuration of tracer fiber in the yarn and fiber migration behavior can be analyzed.

Analysis of fiber migration necessitates some measures which can describe the location variations of fiber segments. The following parameters to characterize fiber migration behavior suggested by Hearle, Gupta and Merchant (1965) were used in this study, as shown in Equations 4-5 to 4-8.

a. Mean Fiber Position

$$\overline{Y} = \frac{1}{z_n}\int_0^{z_n} Y dz = \sum_{i=1}^{n} Y_i / n \qquad (4\text{-}5)$$

where $Y_i = (\frac{r_i}{R_i})^2$, r_i is the radial position of the fiber with respect to the yarn axis, R_i is the yarn radius at the yarn axis z_i and n is the number of the observation.

The mean fiber position gives the average radial position of fibers in yarn cross section and represents the tendency of fibers to be near the yarn surface or in the center of the yarn.

b. RSM Deviation

$$D = [\frac{1}{z_n}\int_0^{z_n}(Y-\overline{Y})^2 dz]^{\frac{1}{2}} = [\sum_{i=1}^{n}(Y_i-\overline{Y})^2/n]^{\frac{1}{2}} \quad (4\text{-}6)$$

RSM deviation is an expression of the migration amplitude, which gives the degree of the deviation from the mean fiber position.

c. Mean Migration Intensity

$$I = [\frac{1}{z_n}\int_0^{z_n}(\frac{dY}{dz})^2 dz = \{\sum_{i=1}^{n\text{-}1}[\frac{(Y_{i+1}-Y_i)}{(z_{i+1}-z_i)}]^2/n\}^{\frac{1}{2}} \quad (4\text{-}7)$$

Mean migration intensity represents the rate of change in radial position of a fiber.

d. Migration Frequency

$$f = \frac{I}{4\sqrt{3}D} \quad (4\text{-}8)$$

Migration frequency is the value of migration frequency when an ideal migration cycle is formed.

4.5 Results and Discussion

With the aforementioned experimental techniques and specially developed measuring system, several yarn structural parameters can be worked out.

4.5.1 Yarn Surface Structure

With the help of SEM, yarn surface structure can be easily observed. Figures 4-5a, 4-5b, 4-5c and 4-5d show the typical pictures of the surface structure of the low torque ring yarns in comparison with that of conventional ring yarns with normal twist level and low twist level. From the Figures, it can be seen that low torque ring yarns mainly have ring-yarn-like appearance but with wrapper-fiber features. Although the surface fibers arranged predominantly in Z direction, a number of wrapper-fibers wrapped yarn body vertically or even in S direction. Besides, more fiber wrapping occurred during low torque ring yarn spinning when compared to that of conventional ring yarn.

Figures of yarn surface structure also show that low torque ring yarn with low twist level has a tight structure which is close to or even tighter than that of conventional ring yarn with normal twist level, whereas conventional ring yarn using lower twist level exhibits a more loose yarn structure. Moreover, with tighter yarn structure and more wrapper-fibers, low torque ring yarns show similar or less hairiness on yarn surface in comparison with that of conventional ring yarn using normal twist level, but conventional ring yarn with lower twist level presents much more hairiness on

yarn surface.

Low torque ring yarn possesses ring-yarn-like appearance but some features different from conventional ring yarn which mainly results from low torque ring yarn spinning. During low torque ring yarn spinning, as a main part of the modification system, a false-twister is introduced into the spinning process, in which the high twist level of yarn section above the point of false-twisting endows low torque ring yarn a tight yarn structure even though the final yarn twist level is low. Meanwhile, this modification process influences the geometry of spinning triangle and thus the incidence of yarn hairiness (Rodiger, 1988; Stalder, 1991). In addition, the operation of false-twisting includes a process of twisting and detwisting. During detwisting, some edge fibers may be wrapped on the yarn body in vertical or even opposite direction to the original yarn twist direction. Thus the structural features exhibited in low torque ring yarns such as compact structure and wrapper fibers in vertical or opposite direction may contribute to the reduction of yarn residual torque and yarn hairiness, as well as to the increase of yarn strength when low twist level was adopted in low torque ring yarns.

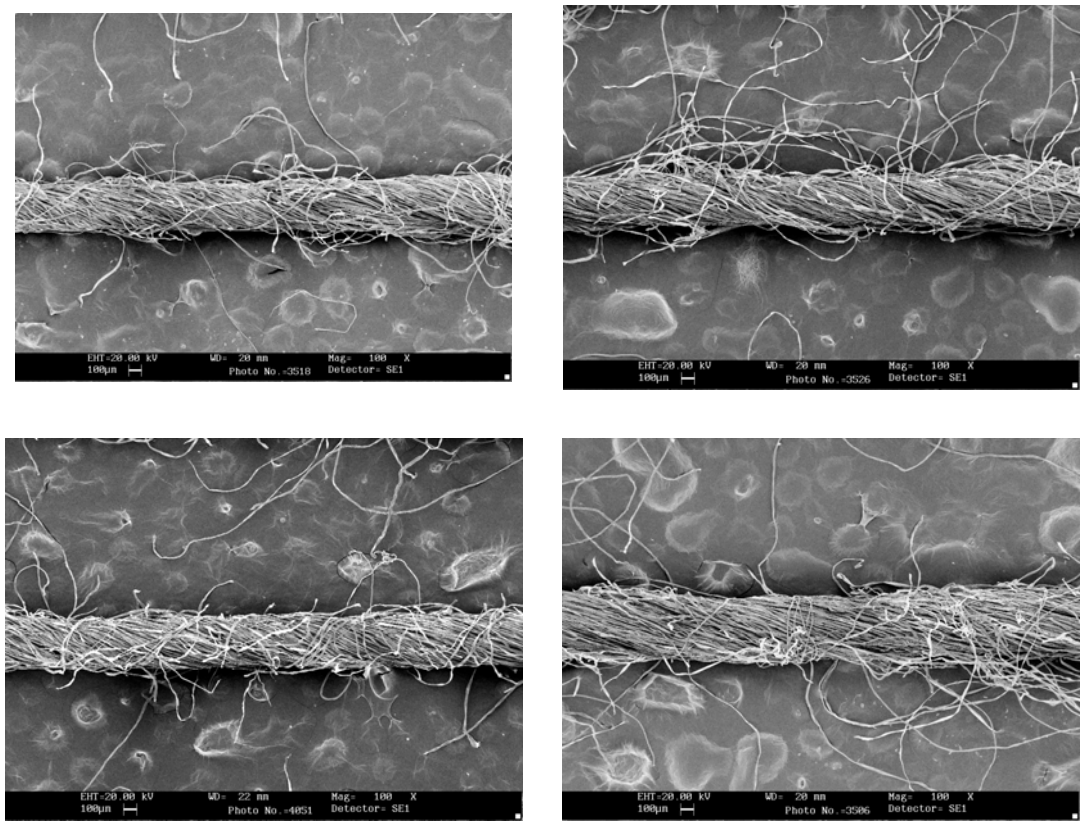

Figure 4-5a Surface Structure of Low Torque Ring Yarn (TF=3.2, FTF=0.43)

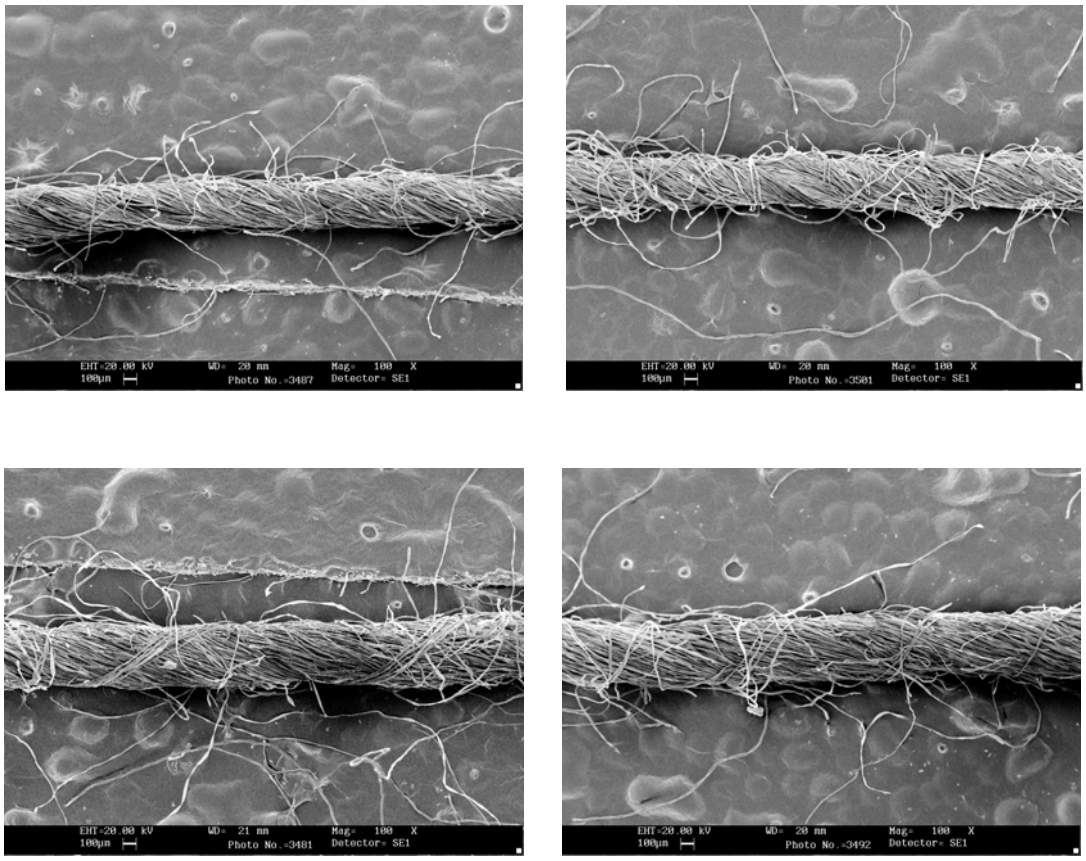

Figure 4-5b Surface Structure of Low Torque Ring Yarn (TF=3.8, FTF=0.43)

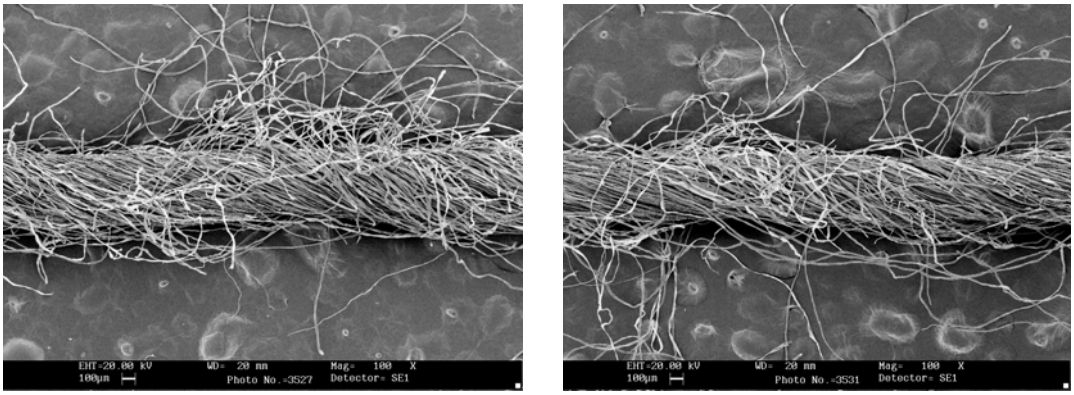

Figure 4-5c Surface Structure of Conventional Ring Yarn (TF=3.2)

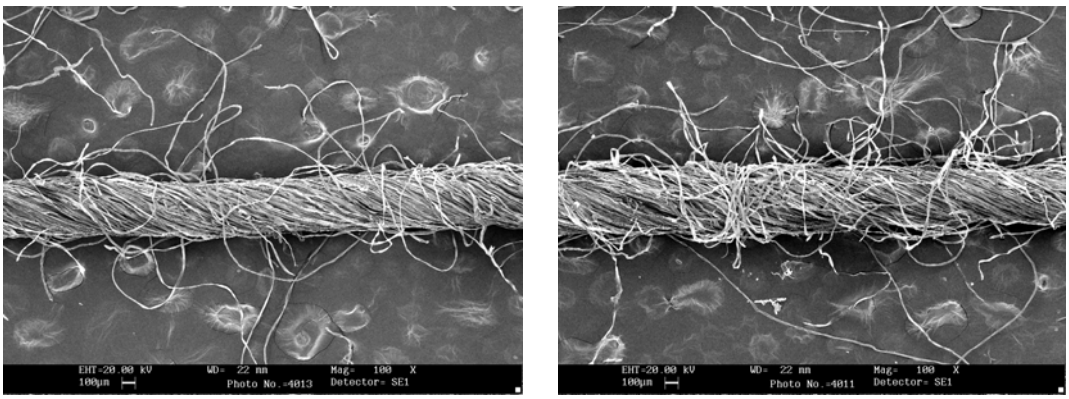

Figure 4-5d Surface Structure of Conventional Ring Yarn (TF=4.2)

4.5.2 3D Configuration and Radial Position Variation of Tracer Fiber

Figures 4-6a, 4-6b and 4-6c show portions of typical tracer images in the yarn, obtained during measurement. In order to give a general view of the structural characteristics of low torque ring yarns and compared to that of conventional ring yarns, trajectories of tracer fibers are visualized in a three-dimensional space on the basis of the data from tracer fiber technique. Figures 4-7a, 4-7b, 4-7c and 4-7d show the trajectories of tracer fibers regenerated by the developed program. It is revealed that the fibers in the low torque ring yarn aligned and interlocked inside the yarn and migrates from the surface to the center of the yarn and then back out, with some random features.

Compared with the configuration of tracer fiber in conventional ring yarns with normal twist level and low twist level, low torque ring yarns exhibit some unique features due to the yarn structure modification during low torque ring yarn spinning. The tracer fiber in the low torque ring yarn is located in the core area with more sections than that of conventional ring yarn and the migratory pattern shows apparently higher magnitude of fluctuation. Unlike conventional ring yarn, the low torque ring yarn exhibits different migratory pattern in which the big fiber migration includes some small fiber migration with various configurations. Moreover, some parts of tracer fibers in low torque ring yarns arrange in opposite direction to the yarn twist, which is rarely occurred in conventional ring yarn. These features of fiber configuration in low torque ring yarns can give some explanations to the properties exhibited in low torque ring yarns differing from that of conventional ring yarns.

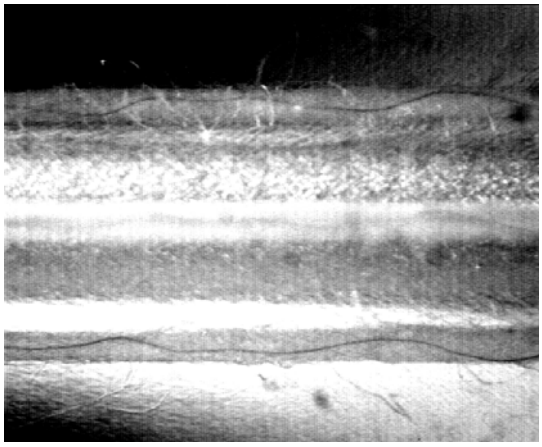

Portion 1

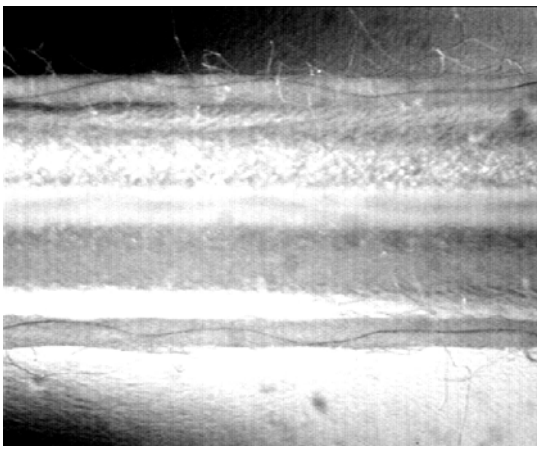

Portion 2

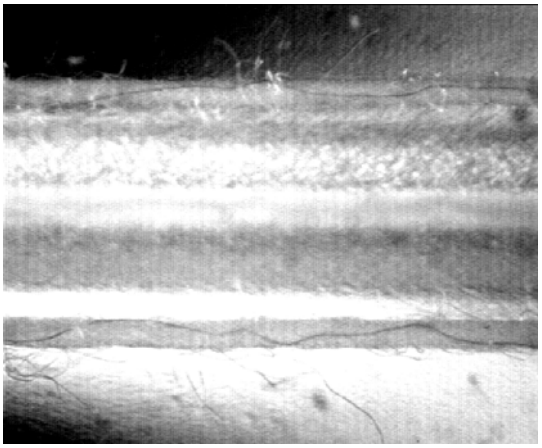

Portion 3

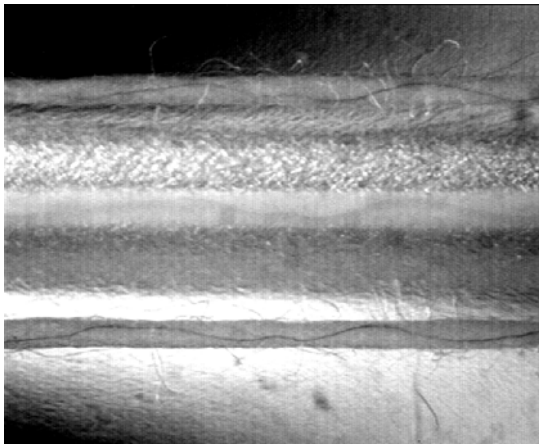

Portion 4

Figure 4-6a Typical Images of Tracer Fibers in Low Torque Ring Yarn (10Ne, TF=3.2, FTF=0.43)

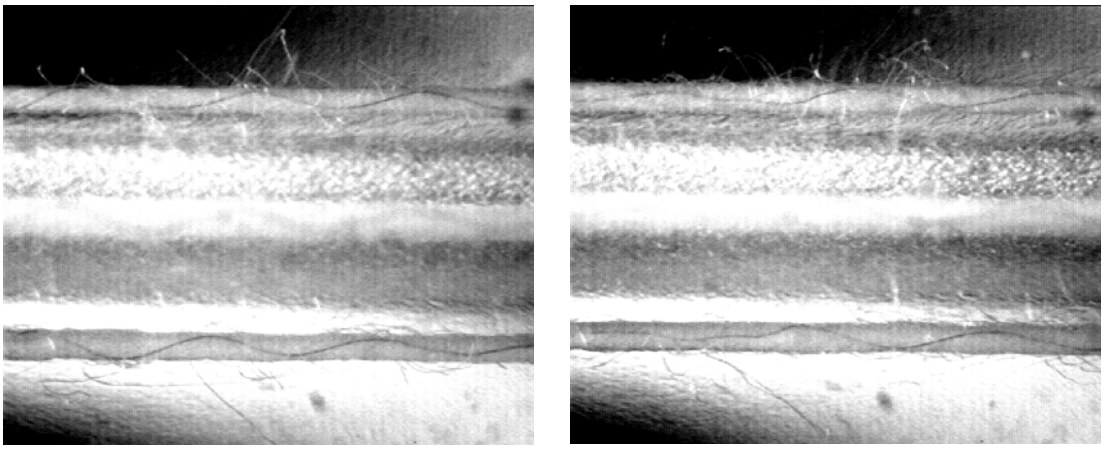

Portion 1 Portion 2

Figure 4-6b Typical Images of Tracer Fibers in Conventional Ring Yarn (10Ne, TF=4.2)

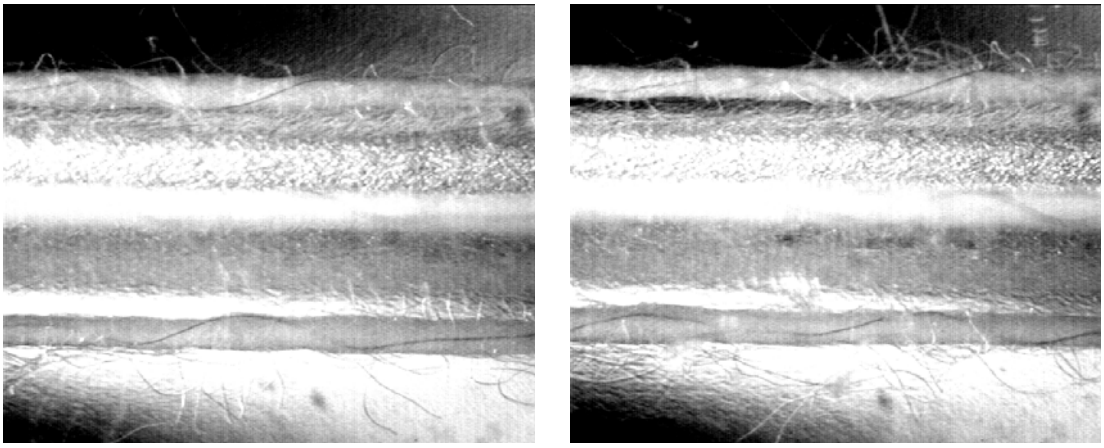

Portion 1 Portion 2

Figure 4-6c Typical Images of Tracer Fibers in Conventional Ring Yarn (10Ne, TF=3.2)

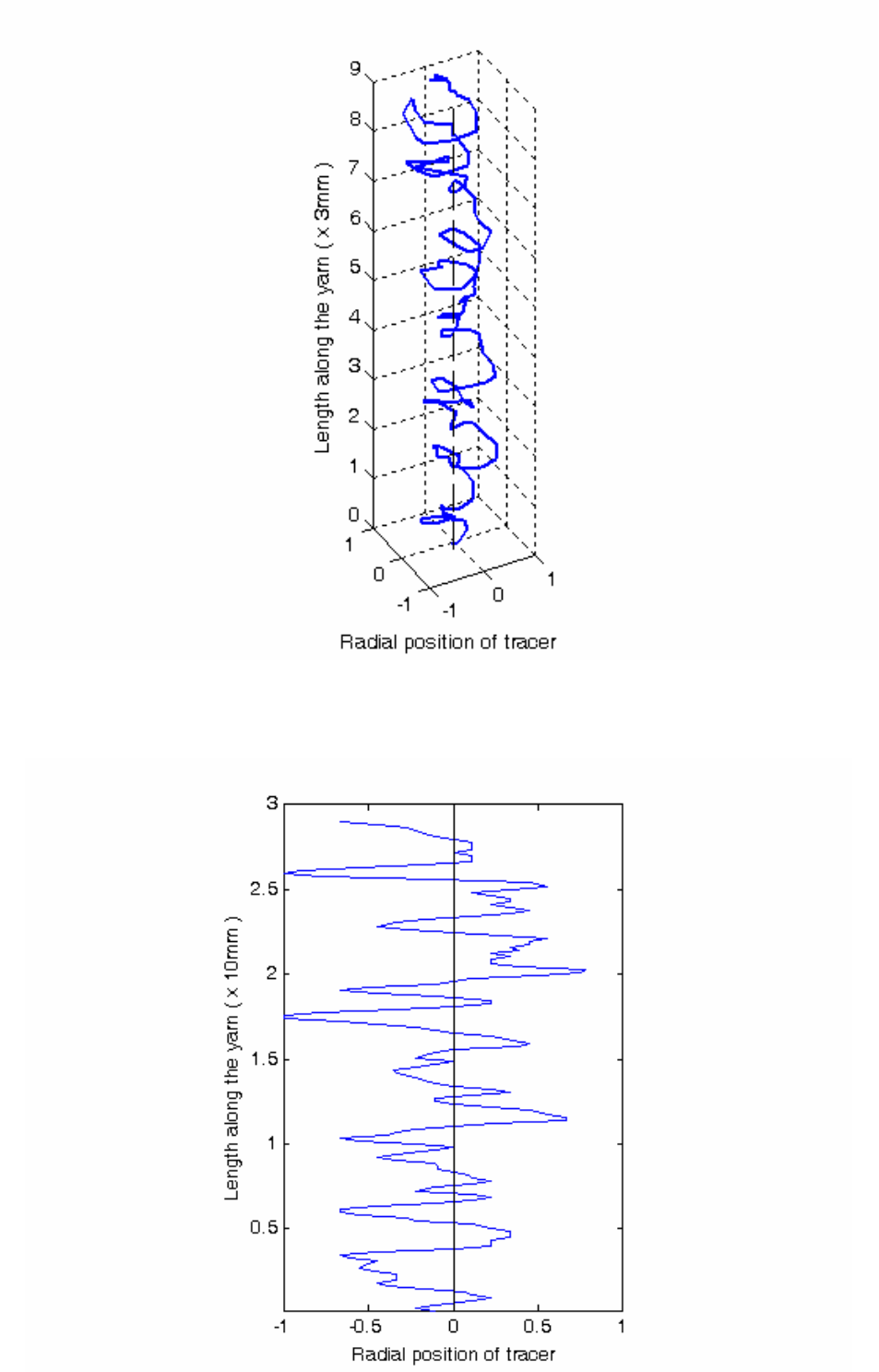

Figure 4-7a 3D Configuration and Radial Position Variation of Tracer in Low Torque Ring Yarn (10Ne, TF=4.2, FTF=0.43)

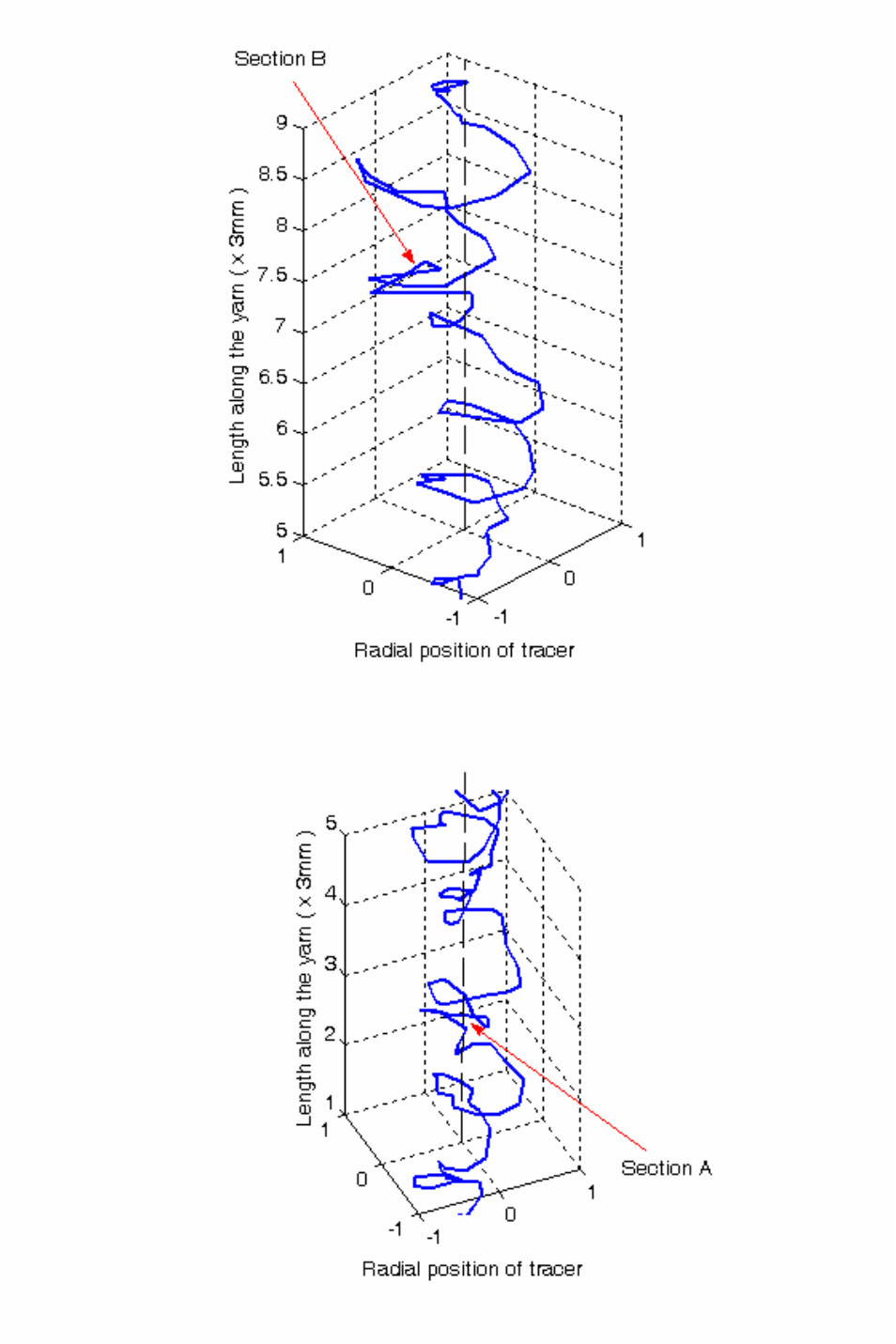

Figure 4-7b Tracer Sections with Opposite Arranging Direction to the Yarn Twist in Low Torque Ring Yarn (Sections A and B) (10Ne, TF=4.2, FTF=0.43)

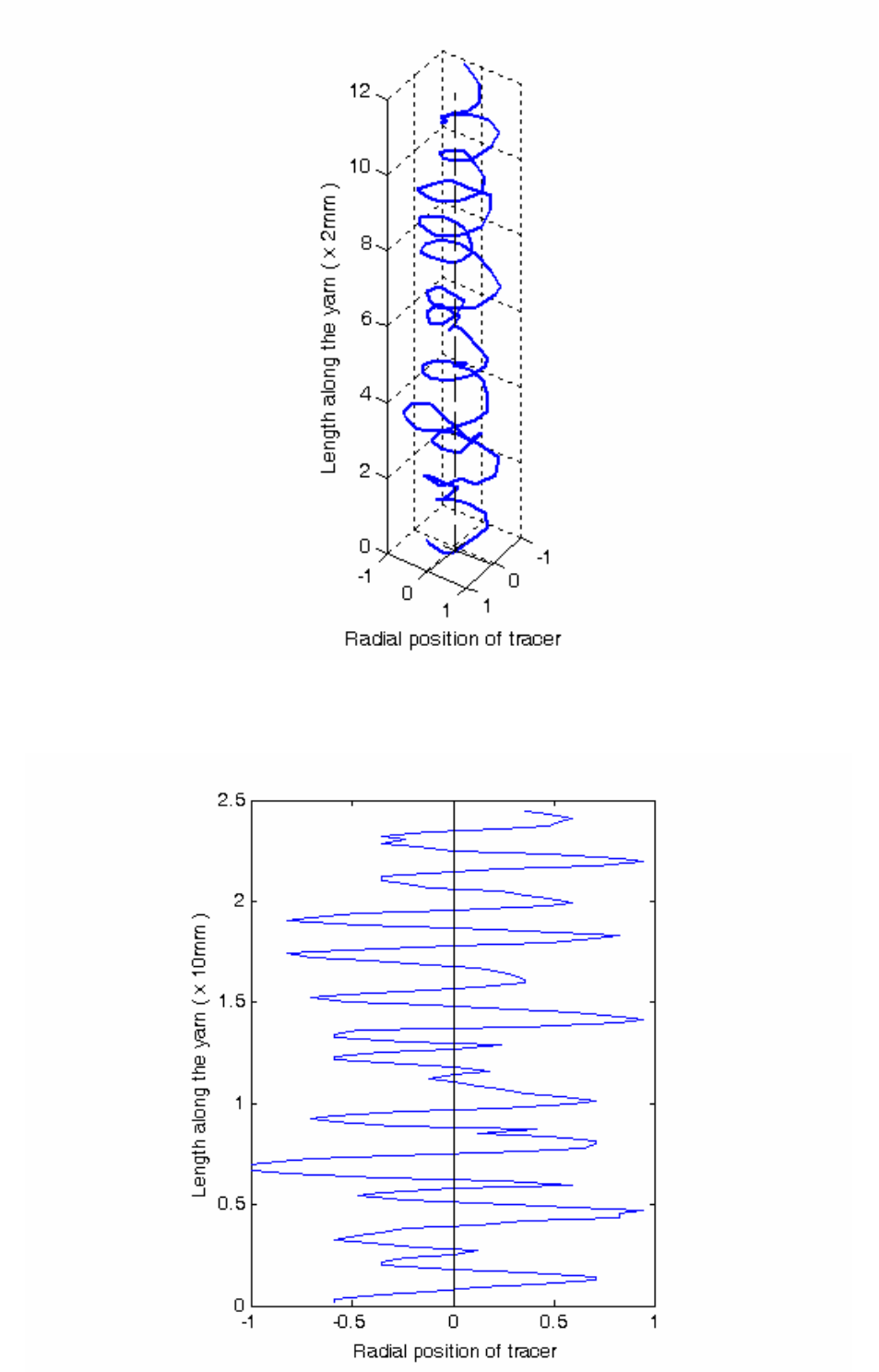

Figure 4-7c 3D Configuration and Radial Position Variation of Tracer in Conventional Ring Yarn (10Ne, TF=4.2)

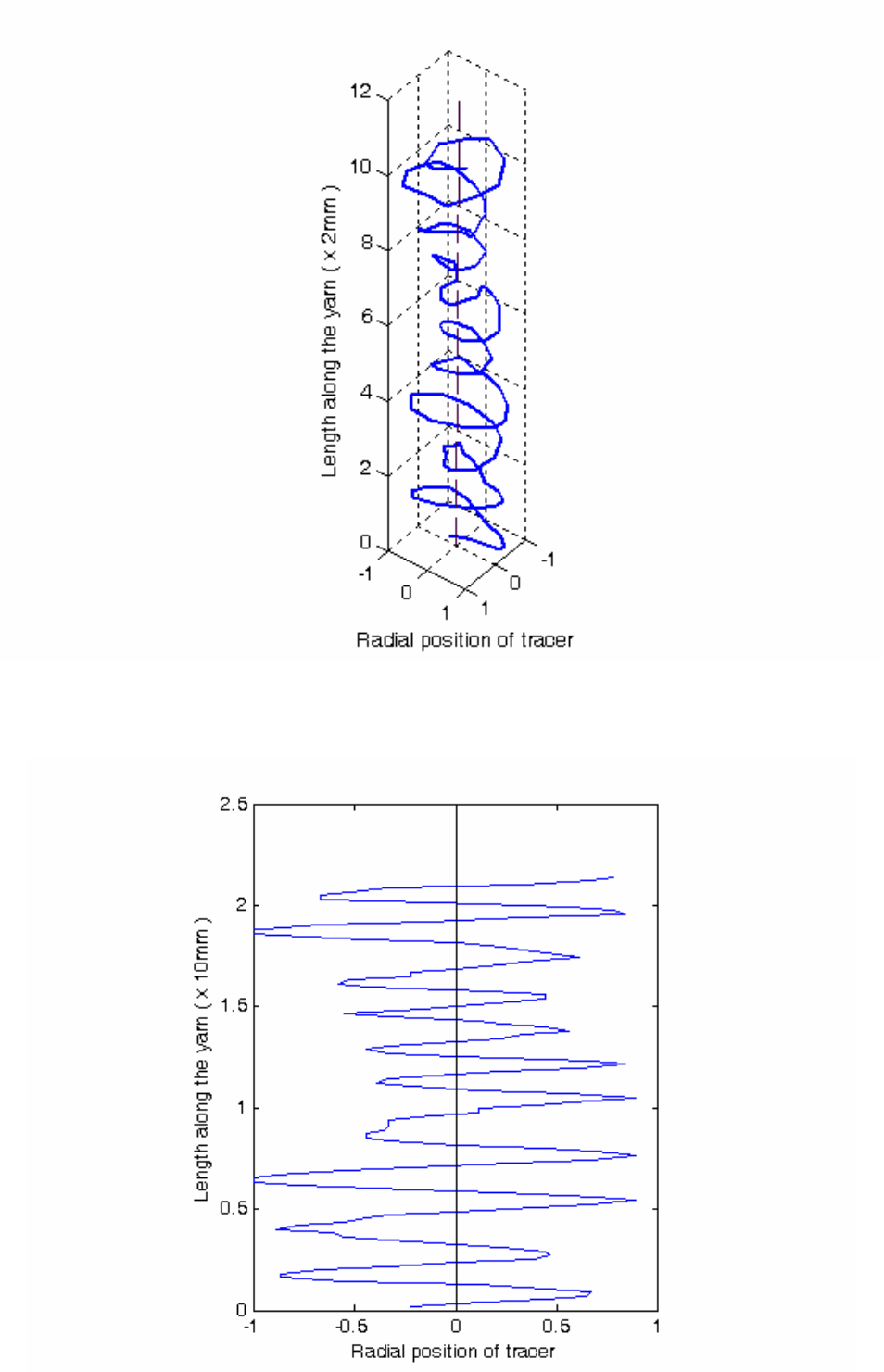

Figure 4-7d 3D Configuration and Radial Position Variation of Tracer in Conventional Ring Yarn (10Ne, TF=3.2)

4.5.3 Analysis of Migration Behavior

The yarn structure can be expressed in terms of the yarn surface structure and the geometric positions of the fibers. But it is very necessary to quantitatively characterize fiber arrangement in low torque ring yarns. Four parameters to characterize features of fiber migration behavior in low torque ring yarns were adopted in this study.

Table 4-5 shows the experimental results of the migration parameters calculated from the measured data. From the Table, it can be seen that the low torque ring yarn has the lowest value of mean fiber position among the three types of yarns. Thus, the fibers in the low torque ring yarn are located mostly near the yarn center, while those in the conventional ring yarn spread in the middle of the yarn cross section. In addition, when compared with the value of 0.5 for the uniform yarn with complete migration, the mean fiber position values are lower in the low torque ring yarn and the conventional ring yarn with normal twist level, which indicates that the density is greater near the yarn axis in these two yarns.

The amplitude of migration of tracer fibers is best expressed by the Root Mean Square Deviation (RSM). Table 4-5 shows that the values of RSM deviation are higher for low torque ring yarns than for conventional ring yarns. It means that fiber migration and fluctuations of the fiber positions from their mean value are higher in low torque ring yarns than in conventional ring yarns. The values of RSM deviation ranging from 0.183 to 0.233, compared to the value of 0.29 for the yarn with ideal

migration, indicate that fibers do not migrate fully in the real yarns and are constricted to a certain cross-sectional zone.

The rate of change of migration or the slope of the helix envelop is a measure of the intensity of migration. As shown in Table 4-5, the low torque ring yarn has the highest value of the mean migration intensity, followed by the conventional ring yarn with normal twist level. The value for the conventional ring yarn with low twist level is the lowest. It indicated that the fibers alter their positions faster and more frequently in the low torque ring yarn when compared with that of conventional ring yarns. The equivalent migration frequency value of the low torque ring yarn did not differ considerably from that of conventional ring yarn with normal twist level since the increase in the mean migration intensity was compensated by the increase in the RSM deviation.

Fiber migration seems to be closely related to the method of twisting and the level of tension present during yarn formation. In low torque ring yarn spinning, as mentioned in Chapter 3, the geometry of the spinning triangle exhibits different characteristics such as symmetric structure, short height and multi-bundle of fibers when compared with that of conventional ring yarn. Moreover, the introduction of false-twisting operation during low torque ring yarn formation is important for yarn structure, which provides the chance for fibers to be rearranged in yarn. All these changes resulted in a higher migration effect in low torque ring yarn in comparison with that of conventional ring yarns, as revealed from the experimental results of migration parameters. It is likely that the higher rate of migration in low torque ring

yarns could be beneficial in promoting high yarn tenacity, low yarn snarling and less yarn hairiness, particularly when low twist level is adopted in yarn spinning.

Table 4-5 Parameters Characterizing Low Torque and Conventional Ring Yarn Structure

Yarn sample	Mean fiber position	RSM deviation	Mean migration intensity, cm^{-1}	Equivalent migration frequency, cm^{-1}
Low Torque Ring Yarn 10Ne, TF=3.2, FTF=0.43	0.248	0.233	4.832	2.984
Conventional Ring Yarn, 10Ne, TF=4.2	0.472	0.183	3.948	3.132
Conventional Ring Yarn, 10Ne, TF=3.2	0.508	0.214	2.760	1.860

4.6 Summary and Conclusion

With the help of SEM and tracer fiber technique, structures of low torque ring yarn were analyzed and characterized by yarn surface structure, 3D configuration of tracer fiber in the yarn and fiber migration behavior of the yarn in this Chapter.

The work started from the development of a measuring system for investigation of the fiber configuration in staple yarns, based on the tracer fiber technique. The major components of the tracer fiber measuring system include a tracer fiber observation device, an automatic moveable platform with motion velocity and length control system for specimen, a high resolution digital camera with high performance zoom lens, and the measuring procedure controller and data analysis system by a personal

computer equipped with image capturing and analysis software. The main features of the system is that it can capture and store consecutive images of single tracer fiber, thus the image acquisition becomes faster and more accurate, and the problems in manual operation such as slow movement, larger random error can be solved. It is also helpful for the analysis and processing of the tracer fiber image information such as transfer of the obtained images into a set of data. Moreover, the regeneration of the 3D configuration and radial position variation of the tracer fiber in a real yarn and the analysis of yarn structural characteristics can be achieved.

Yarn surface structure was observed under the SEM and some structural features were found in the low torque ring yarn such as ring-yarn-like appearance, compact structure, wrapper fibers in vertical or opposite direction and less yarn hairiness, which may contribute to the reduction of yarn residual torque and yarn hairiness, as well as to the increase of yarn strength when low twist level was adopted in low torque ring yarns.

The analysis of 3D configuration and radial position variation of the tracer fiber regenerated with the data obtained from the tracer fiber technique indicated that the tracer fiber in the low torque ring yarn is located in the core area with more sections than that of conventional ring yarn and the migratory pattern shows apparently higher magnitude of fluctuation. Unlike conventional ring yarn, the low torque ring yarn exhibits different migratory patterns in which the big fiber migration includes some small fiber migration with various configurations. Moreover, some parts of tracer fibers in low torque ring yarns arrange in opposite direction to the yarn twist,

which is rarely occurred in conventional ring yarn.

An attempt for the investigation of fiber migration behavior demonstrated that a higher migration effect occurred in low torque ring yarn with lower value of mean fiber position as well as higher values of RSM deviation and the mean migration intensity when compared with those of conventional ring yarn, which can be attributed to the introduction of false-twisting operation in the low torque ring yarn spinning. It is likely that the higher rate of migration in low torque ring yarns could be beneficial in promoting high yarn tenacity and less yarn hairiness, particularly when low twist level is adopted in yarn spinning. The parts of fibers twisted in the opposite direction of the yarn twist are one of the reasons for low yarn snarling.

CHAPTER 5 STATISTIC MODELS FOR RELATIONSHIPS BETWEEN YARN PROPERTIES AND SPINNING PARAMETERS

5.1 Introduction

Yarn properties depend on not only fiber properties and spinning method, but also spinning parameters such as the spinning tension, the twist and spinning draft in ring spinning. As we mentioned earlier, low torque ring yarn spinning method is a modified ring spinning technology with an attachment of torque reduction device installed on the conventional ring spinning frame. During yarn processing, a false-twisting operation is induced and thus yarn structure is modified accordingly, which results in some characteristics of low torque ring yarn different from those of conventional ring yarn. In the previous research (Sengupta and Kapoor, 1973; Tarfder, Sutradhar and Mishra, 2002), the influence of process parameters on properties of conventional ring yarn was investigated. However, with the false-twisting operation induced in the low torque yarn spinning, spinning parameter like yarn twist probably exhibits different effects on the yarn properties and, more importantly, some new parameters will be introduced to describe the false-twisting operation. Therefore, it is necessary to carry out experiments to investigate the effects of various parameters on the properties of low torque ring yarn.

In this Chapter, in order to carry out the experimentation more rapidly and efficiently, the strategy of experiment research was adopted as illustrated in Figure 5-1, in which the Fractional Factorial Methodology (FFM) was used for experiment design and to determine those processing parameters having significant effects on yarn properties. Then a two-factor Response Surface Methodology (RSM) was used to investigate the effects of yarn twist and speed ratio on low torque ring yarn properties and second-order polynomial response surface models were set-up to predict and explain their relationship. The developed RSM model was further coupled with the desirability function and overlaid contour plot to find the optimum spinning parameters leading to the desirable yarn properties.

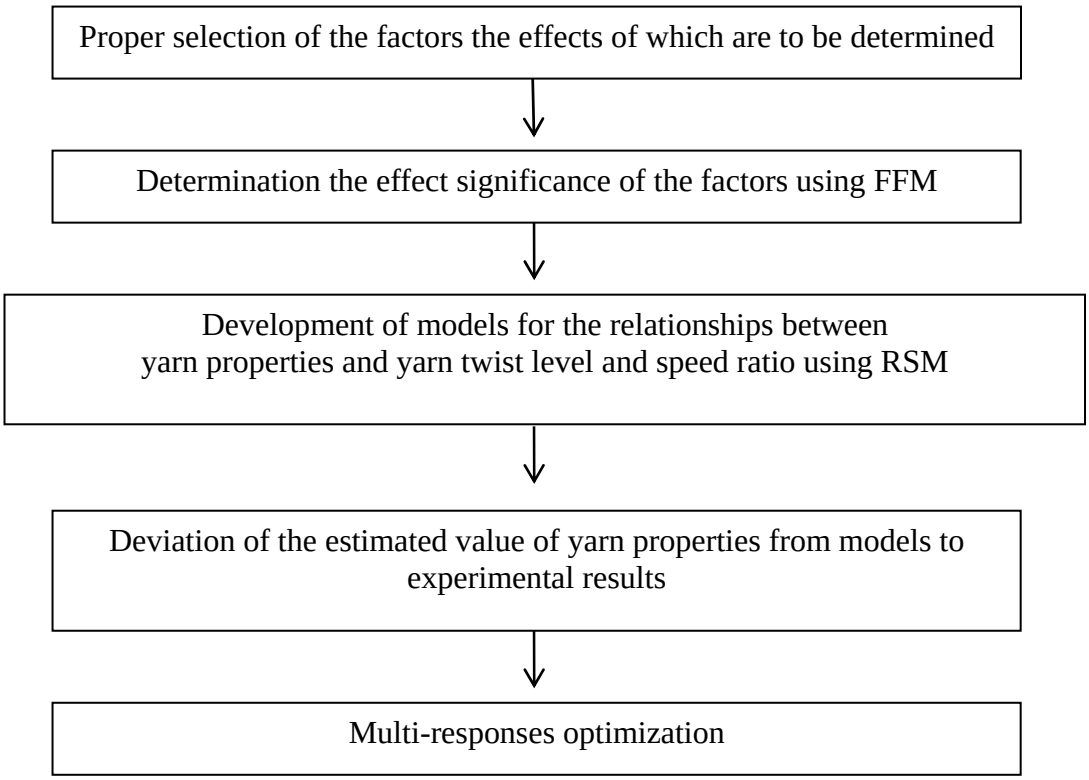

Figure 5-1 The Strategy of Experiment Research

5.2 Experimental Work

5.2.1 Yarn Sample Preparation

Carded cotton rovings of 952tex for low torque ring yarn spinning process were used on the modified Ring Spinning Frame. The cotton fibers had a micronaire value of 4.0, a 2.5% span length of 28.7mm, a bundle strength of 22cN/tex, and a breaking extension of 5.3%. All these fiber parameters were measured by the Spinlab 900.

In accordance with experimental design, two weaving yarns were spun, namely 84tex (7Ne) and 58tex (10Ne). In each experiment, six bobbins of each yarn were spun simultaneously under the same conditions. Then the yarn samples were conditioned for at least 24 hours under standard conditions (20 ± 2°C and 65 ± 2% RH) and tested for yarn properties.

5.2.2 Test Methods

Yarn snarling and tenacity are major concern in evaluating yarn performance for modification. Other yarn properties such as hairiness and evenness are also required to reach the requirements of yarn quality standard. Therefore, yarn tenacity, snarling, hairiness and evenness used as experimental responses were examined in the experiment.

An Uster Tensorapid instrument was used to examine yarn tensile properties at a speed of 5000mm/min and a specimen length of 500mm. Fifty readings for each

sample were recorded. Yarn snarling was measured with a newly developed yarn snarling tester by adopting a principle similar to ISO Standard 3343-1984. Thirty readings were taken on each sample.

In this study, a Zweigle G566 Hairiness Tester was used to measure the hairiness of yarns per 100m yarn at different length groups. Yarn evenness was measured using Uster Evenness Tester III.

5.3 Determination of Effect Significance of Spinning Parameters

5.3.1 Design of Experiment

In many process development and manufacturing applications, potentially influential input variables (factors) are numerous. Screening (process characterization) reduces the number of variables by identifying the key input variables or process condition that affects product quality. This reduction allows the focus of process improvement effects on the really important variables, or the 'vital few'. In practice, two-level full and Fractional Factorial Designs (Minitab^{TM}, 2000; Nelson, 2003) are often used to screen for the really important factors because the factorial approach is an efficient method to reduce experimental size considerably without losing important information about the response.

In the present study, based on the investigation of low torque ring yarn spinning mechanism and the preliminary experiment on the low torque ring yarn, some

spinning parameters such as twist factor (TF), speed ratio (FTF), weight of traveler (Tr) and the position of the torque-reduction device (H and V) are selected as potentially influential input variables (factors).

The position of the torque-reduction device is shown in Figure 5-2. In view of the length of time required to perform the experiment and test the spun yarns, it was considered expedient to use the Fractional Factorial Methodology (FFM) with 2^{k-2} design in the present study. Since FFM can reduce the number of runs to a manageable size, while still making it possible to examine a number of factors. A major use of FFM is in screening experiments in which many factors are considered with the purpose of identifying those factors, if any, that have significant effects. The factors which are identified as important are then investigated more thoroughly in subsequent experiments.

In the fractional factorial experiment set out in Table 5-1, the levels were chosen to cover the wide multivariable operating ranges of the process available on the spinning machine.

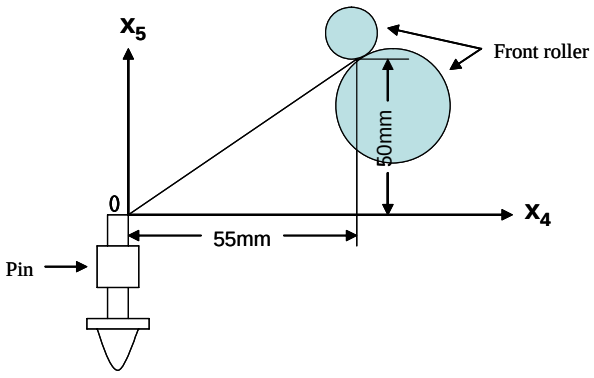

Figure 5-2 Schematic of the Position of the Torque-reduction Device

Table 5-1 Experimental Variables and Levels of Low Torque Ring Yarn for Weaving

Levels	Variables				
				Position of pin	
	X_1: Twist factor	X_2: Speed ratio	X_3: Traveler (g)	X_4: Horizontal distance (mm)	X_5: Vertical distance (mm)
1	3.8	0.43	0.40	12	12
-1	3.2	0.35	0.28	0	0

5.3.2 Results and Discussion

The response data of low torque ring yarn for weaving are shown in Table 5-2 and the effects of spinning process parameters on the yarn properties are shown in Figure 5-3 to Figure 5-7.

From the Table and Figures as just mentioned, it can be seen that the significance of the factors to the yarn tenacity is revealed as follows:

Level of importance = TF > H > FTF > FTF×V > V > FTF×Tr > Tr

It can also be seen that twist factor has significant effect on yarn tenacity at $\alpha = 0.15$.

The figures also show that the significance of the factors to the yarn elongation is as follows:

Level of importance = Tr > FTF > H > TF > FTF×Tr > V > FTF×V

Among the five factors, Tr, FTF and H are important to the yarn elongation.

The significance of the factors to the yarn snarling is revealed as follows:

Level of importance = TF >FTF > Tr > V = H = FTF×V = FTF×Tr

TF and FTF have significant effects on the yarn snarling at $\alpha = 0.05$.

The figures also show the significance of the factors to the yarn hairiness and evenness respectively as follows:

Level of importance to yarn hairiness =TF >Tr > H > FTF×Tr > FTF > FTF ×V > V

Level of importance to yarn evenness =Tr>TF > V > FTF ×Tr > H > FTF > FTF ×V

At $\alpha = 0.2$, Tr and TF are important to the yarn hairiness. For yarn evenness, there are no significant effects.

Based on the analysis above, identified as the most important factors to the yarn properties particularly on yarn snarling and tenacity, TF and FTF were chosen for more thorough investigation in subsequent experiments with the help of Respond Surface Methodology.

Table 5-2 Design Matrix and Response Data of Low Torque Ring Yarn for Weaving

Test no.	X_1	X_2	X_3	X_4	X_5	Y_1 Tenacity [cN/tex]	Y_2 Elongation [%]	Y_3 Snarling [turns/25cm]	Y_4 Hairiness [S3/100m]	Y_5 Evenness [CV%]
1	3.2	0.35	0.28	12	12	16.28	5.88	25	924	11.42
2	3.2	0.35	0.40	12	0	15.93	4.99	25	1316	11.79
3	3.8	0.35	0.28	0	0	17.30	6.39	31	492	11.30
4	3.8	0.43	0.40	12	12	16.53	4.54	28	864	11.52
5	3.2	0.43	0.40	0	0	16.45	4.82	23	881	11.79
6	3.8	0.35	0.40	0	12	17.73	5.38	30	748	11.24
7	3.8	0.43	0.28	12	0	16.65	5.41	29	659	11.18
8	3.2	0.43	0.28	0	12	16.50	5.69	24	771	11.10

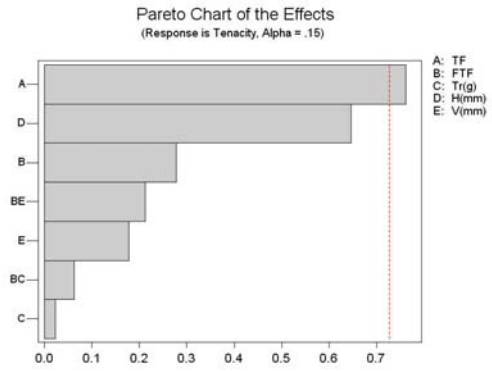

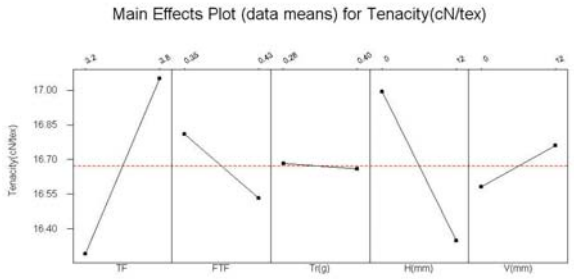

Pareto Chart Main Effects Plot

Figure 5-3 The Effects of Factors on Yarn Tenacity

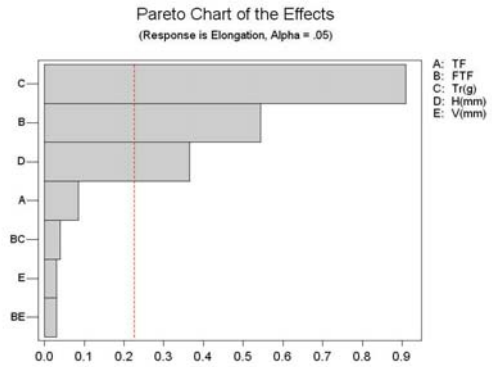

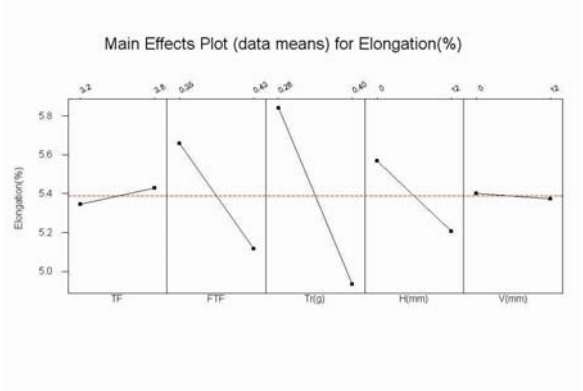

Pareto Chart Main Effects Plot

Figure 5-4 The Effects of Factors on Yarn Elongation

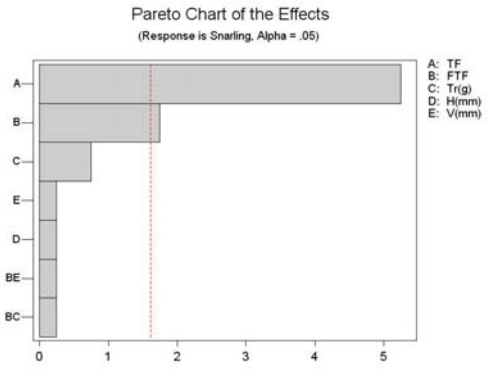

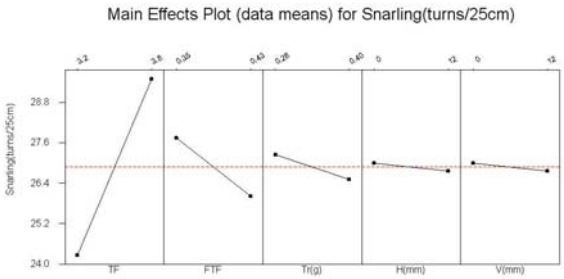

Pareto Chart Main Effects Plot

Figure 5-5 The Effects of Factors on Yarn Snarling

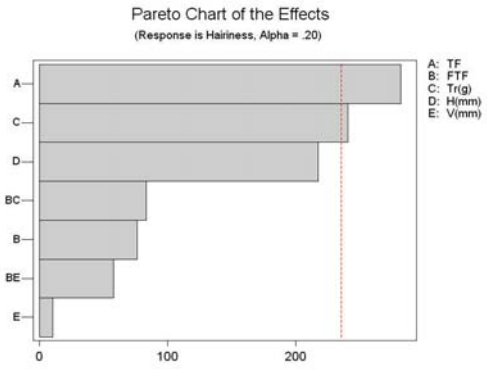

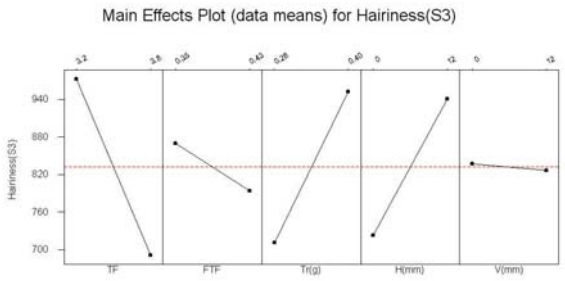

Pareto Chart Main Effects Plot

Figure 5-6 The Effects of Factors on Yarn Hairiness

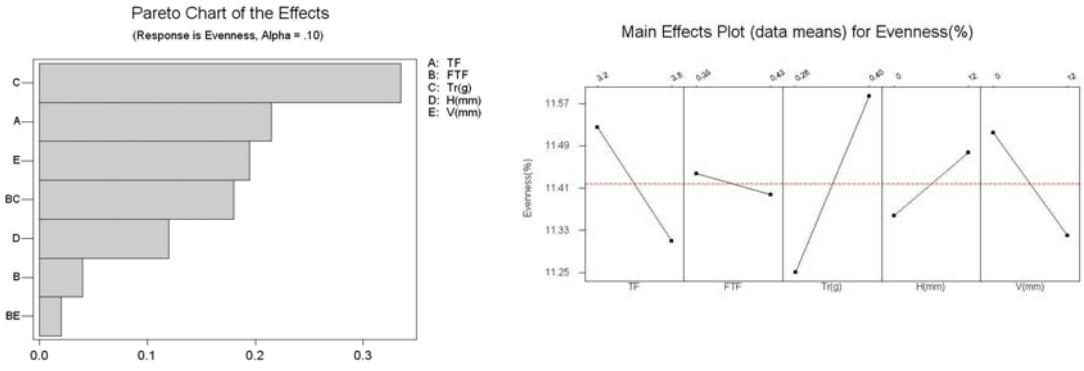

Pareto Chart Main Effects Plot

Figure 5-7 The Effects of Factors on Yarn Evenness

5.4 Development of Statistical Models for the Relationships between Yarn Properties and Yarn Twist Level and Speed Ratio

The fundamental investigation of effect significance of processing parameters such as yarn twist factor, speed ratio, travelers and the position of the torque-reduction device using FFM in previous section demonstrated that the yarn twist level and the speed ratio are the two most important processing parameters for the properties of low torque weaving yarn during yarn processing. Therefore, the need for exploring in depth the relationship between yarn properties and yarn twist factor and speed ratio becomes apparent for better understanding of yarn spinning process. In this Section, one of the renowned mathematical experimental design and analysis techniques,

namely “Response Surface Methodology”, is used to set up second-order polynomial response surface models, which predicts and explains the effects of yarn twist factor and speed ratio on the yarn properties for spinning process of low torque ring yarn.

5.4.1 Theoretical Consideration

Response Surface Methodology (RSM), first introduced by Box and Wilson (1951) and later developed by Box and Hunter (1957) and others, is a collection of statistical and mathematical techniques useful for developing, improving and optimizing processes (Box and Draper, 1987; Montgomery and Runger and Hubele, 2001; Tarafder, Sutradhar and Mishra, 2002). When studying continuous factors, after finding their effects to be significant, it is interesting to find conditions (levels of factors) that lead to a particular response, usually a maximum or a minimum. The responses of an experiment when considered as a function of the possible levels of the factors are called a response surface, and the designs used to study a response surface are called Response Surface Designs. This method is often employed after the “vital few” controllable factors have been identified. By careful design and analysis of experiments, RSM seeks to relate the responses to the levels of a number of variables which affect them and to optimize the response.

In general, the response value (μ) that depends on the controllable input variables $X_1, X_2, ..., X_k$ can be expressed by:

$$\mu = f(X_1, X_2, ..., X_k) + \varepsilon \qquad (5\text{-}1)$$

where ε represents the noise or error observed in the response (μ). It is often assumed that ε has a normal distribution with the mean zero and the variance σ^2. The expected response $E(\mu)$ is given by:

$$E(\mu) = E[f(X_1,X_2,...,X_k)] + E(\varepsilon) = f(X_1,X_2,...,X_k) = Y \quad (5\text{-}2)$$

The variables $X_1,X_2,...,X_k$ in Equation (5-2) are usually called the natural variables. The true response function is now written as

$$Y = f(X_1,X_2,...,X_k) \quad (5\text{-}3)$$

In most RSM problems, the form of the true response function f is unknown. Thus, the first step in RSM is to find a suitable approximation for the true relationship between Y and the independent variables, which is critically dependent upon the experimental ability. Usually, a low-order polynomial in some region of the independent variables is employed. If the response is well modeled by a linear function of the independent variables, then the approximating function is the first-order model:

$$Y = \beta_0 + \beta_1 X_1 + \beta_2 X_2 + \cdots + \beta_k X_k \quad (5\text{-}4)$$

If there is curvature in the system, then a polynomial of higher degree must be used, such as second-order model:

$$Y = \beta_0 + \sum_{i=1}^{k} \beta_i X_i + \sum_{i=1}^{k} \beta_{ii} X_i^2 + \sum_{i=1}^{k-1} \sum_{j=2}^{k} \beta_{ij} X_i X_j \quad (i < j) \tag{5-5}$$

where β_0, β_i, β_{ii}, and β_{ij} are the regression coefficients of each monomial.

The method of least squares is used to estimate the parameters in the approximating polynomials. The response surface is then done in terms of the fitted surface. If the fitted surface is an adequate approximation of the true response function, then analysis of the fitted surface will be approximately equivalent to the analysis of the actual system.

5.4.2 Design of Experiment

In creating Response Surface Design, the Central Composite Design (CCD) is used in the present study. CCD is a very popular design for fitting second-order response surface and often recommended when the design plan calls for sequential experimentation because these designs can incorporate information from a properly planned factorial experiment. The CCD design consists of a 2^2 design centered at 3.35 twist factor and 0.380 speed ratio, five center point, and four runs along the coordinate axes called axial runs. Four response variables were measured during this phase of the experiment, namely yarn tenacity, yarn snarling, yarn hairiness and yarn evenness. The design points are presented graphically in Figure 5-8. Tables 5-3 and 5-4 give the experimental variables and levels, and the design matrix respectively in the present work.

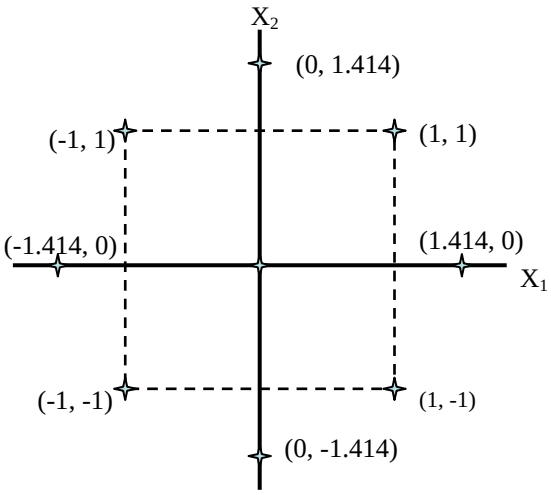

Figure 5-8 A Central Composite Design in k = 2 Variables

Table 5-3 Experimental Variables and Levels of Low torque Ring Yarn

Levels	Variables	
	X_1: Twist factor	X_2: Speed ratio
+1.414	3.99	0.450
+1	3.80	0.430
0	3.35	0.380
-1	2.90	0.330
-1.414	2.71	0.309

Table 5-4 Design Matrix of Low Torque Ring Yarn

Test no.	X_1	X_2
1	3.80	0.330
2	3.35	0.380
3	3.99	0.380
4	2.71	0.380
5	3.80	0.430
6	3.35	0.380
7	3.35	0.380
8	3.35	0.380
9	3.35	0.450
10	2.90	0.430
11	3.35	0.309
12	3.35	0.380
13	2.90	0.330

5.4.3 Results and Discussion

The response data of low torque ring yarn are given in Tables 5-5 and 5-6. According to Response Surface Methodology, the relationships between yarn properties and the two controllable processing factors were analyzed using Minitab Statistical Software (2003). Second-order polynomial response surface models to predict and explain the relationship of yarn properties to yarn twist and speed ratio within the scope of the experiments are shown in Equation 5-7 to Equation 5-14, where Y_1, Y_2, Y_3, Y_4, X_1 and X_2 stand for yarn tenacity (cN/tex), snarling (turns/25cm), hairiness (S3), evenness (%), yarn twist factor and speed ratio, respectively.

Table 5-5 Response Table of Low Torque Ring Yarn (84 tex)

Test no.	Y_1 Tenacity (cN/tex)	Y_2 Snarling (turns/25cm)	Y_3 Hairiness (S3/100m)	Y_4 Evenness (CV%)
1	17.21	31	604	11.19
2	16.08	28	1044	10.70
3	16.09	32	678	11.15
4	14.89	22	1476	10.78
5	16.26	28	780	11.10
6	15.91	28	1221	10.54
7	16.10	28	1200	10.41
8	16.19	28	1238	10.77
9	15.46	25	1086	10.55
10	15.69	23	1242	10.54
11	16.71	32	1233	10.76
12	16.02	28	1067	10.41
13	15.98	26	1728	10.71

Table 5-6 Response Table of Low Torque Ring Yarn (58 tex)

Test no.	Y_1 Tenacity (cN/tex)	Y_2 Snarling (turns/25cm)	Y_3 Hairiness (S3/100m)	Y_4 Evenness (CV%)
1	16.41	35	382	12.50
2	15.58	29	375	12.42
3	15.62	34	360	12.35
4	14.86	25	960	12.21
5	15.47	31	369	12.33
6	15.92	31	380	12.50
7	16.05	30	465	12.53
8	15.81	29	393	12.51
9	15.46	27	440	12.46
10	15.24	27	840	12.05
11	15.78	31	495	12.75
12	15.77	30	510	12.45
13	15.08	29	1122	12.26

Equations 5-6 and 5-7 show the relation between yarn tenacity (Y_1) and yarn twist factor(X_1) and speed ratio(X_2):

$$Y_1 = 5.332 + 9.073X_1 - 24.563X_2 - 0.793X_1^2 + 54.75X_2^2 - 7.333X_1X_2 \quad (5\text{-}6)$$

(R^2=0.845 R=0.919) (84tex)

$$Y_1 = -19.806 + 14.078X_1 + 60.055X_2 - 1.299X_1^2 - 29.2X_2^2 - 12.222X_1X_2 \quad (5\text{-}7)$$

(R^2=0.905 R=0.951) (58tex)

Equations 5-8 and 5-9 show the relation between yarn snarling (Y_2) and yarn twist factor(X_1) and speed ratio(X_2):

$$Y_2 = -13.852 + 29.453X_1 - 58.749X_2 - 3.395X_1^2 + 25X_2^2 \quad (5\text{-}8)$$

(R^2=0.954 R=0.977) (84tex)

$$Y_2 = -4.613 + 9.381X_1 + 71.902X_2 + 0.803X_1^2 - 35X_2^2 - 22.222X_1X_2 \quad (5\text{-}9)$$

(R^2=0.923 R=0.961) (58tex)

Equations 5-10 and 5-11 show the relation between yarn hairiness (Y_3) and yarn twist factor(X_1) and speed ratio(X_2):

$$Y_3 = 10719.1 - 2029.24X_1 - 24510.8X_2 - 226.852X_1^2 - 1875X_2^2 + 7355.56X_1X_2$$

(R^2=0.945 R=0.972) (84tex) (5-10)

$$Y_3 = 17501.7 - 6549.24X_1 - 26167.5X_2 + 722.593X_1^2 + 20030X_2^2 + 2988.89X_1X_2$$

(R^2=0.92 R=0.959) (58tex) (5-11)

Equations 5-12 and 5-13 show the relation between yarn evenness (Y_4) and yarn twist factor(X_1) and speed ratio(X_2):

$$Y_4 = 26.521 - 7.125X_1 - 23.598X_2 + 1.078X_1^2 + 25.3X_2^2 + 0.889X_1X_2 \quad (5\text{-}12)$$

(R^2=0.817 R=0.904) (84tex)

$$Y_4 = 6.629 + 4.675X_1 - 10.19X_2 - 0.693X_1^2 + 8.85X_2^2 + 0.444X_1X_2 \quad (5\text{-}13)$$

(R^2=0.804 R=0.897) (58tex)

It is necessary to examine the fitted model to ensure that it provides an adequate approximation to the true system and verifies that none of the least squares

regression assumptions are violated. The residual from the least squares fit play an important role in judging model adequacy, which is the actual response value minus the predicted response value. In the present study, the residual analysis is used to assess the model adequacy. Figures 5-9 and 5-10 show the normal probability plot of the residuals and the plot of residuals versus the order of the data. From the Figures, it can be seen that the normal probability plots are approximately along a straight line and the residuals scatter randomly on the plot of residuals versus the order of the data, which indicates that the model is found adequate.

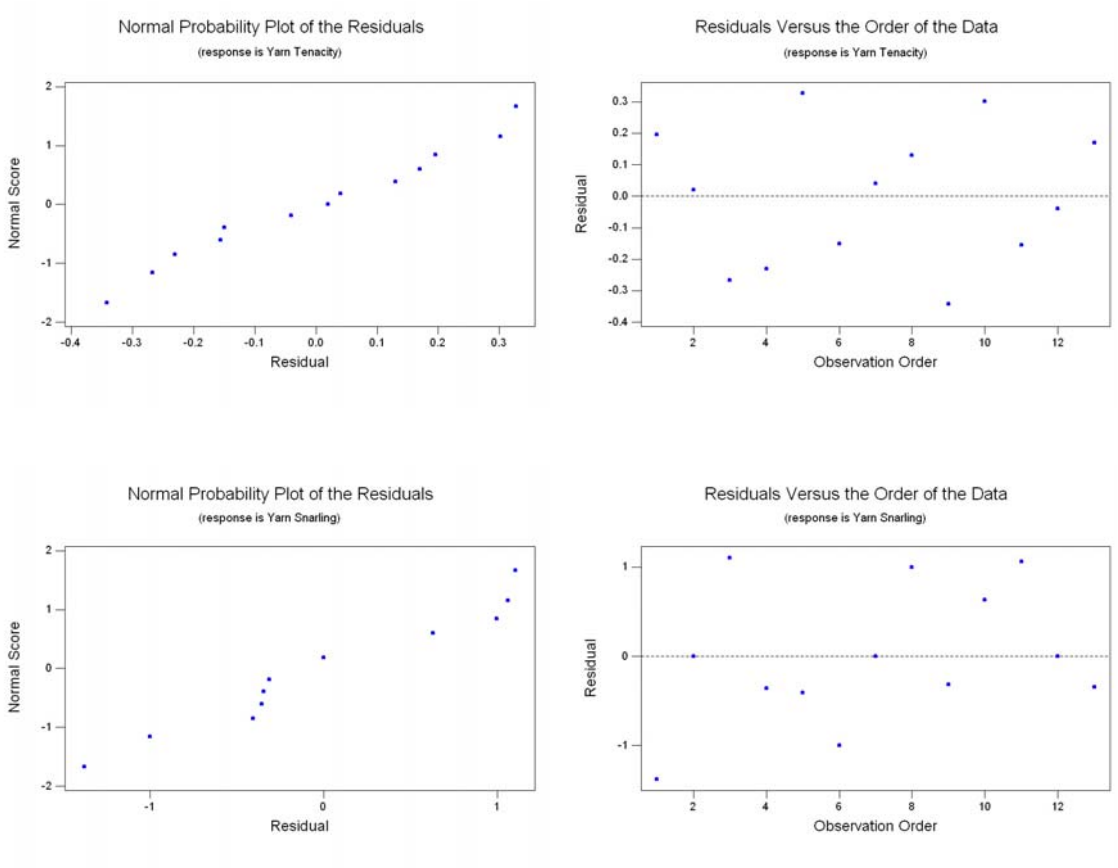

Figure 5-9a Residual Analysis for Model Adequacy Checking of Yarn Tenacity and Snarling (84 tex)

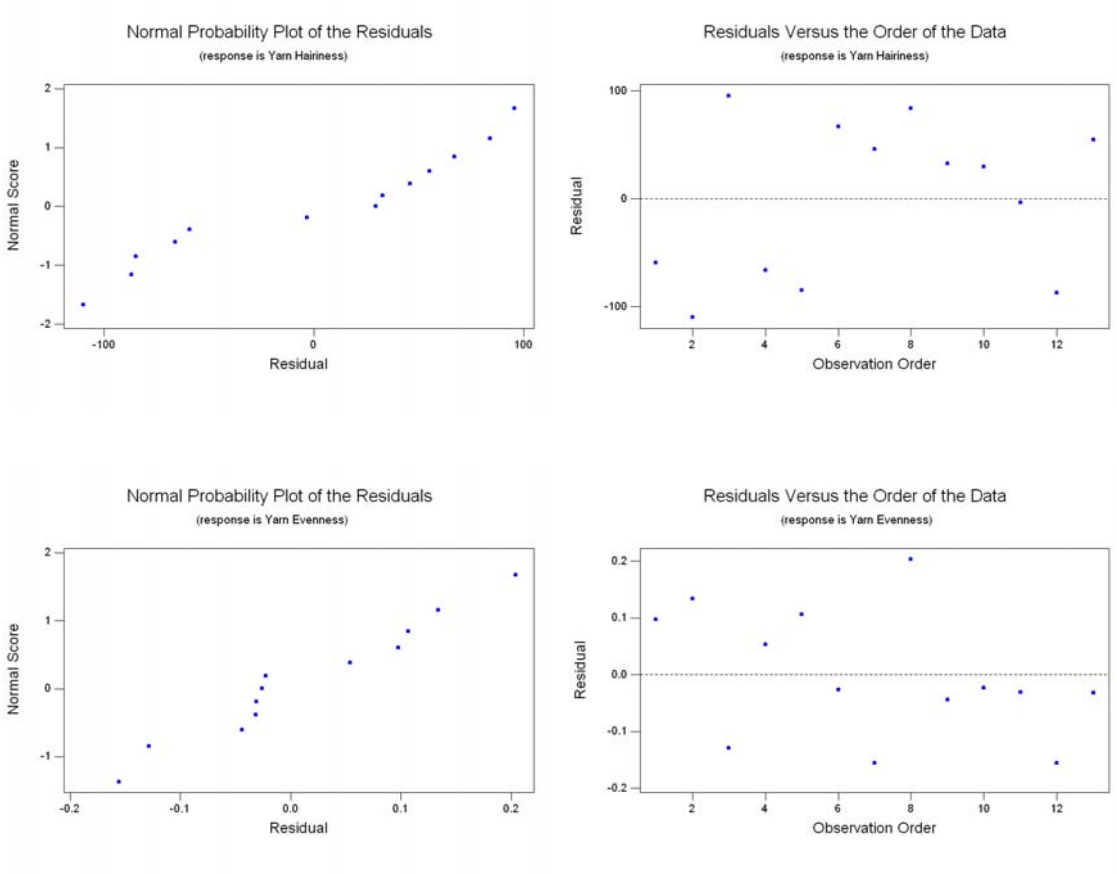

Figure 5-9b Residual Analysis for Model Adequacy Checking of Yarn Hairiness and Evenness (84 tex)

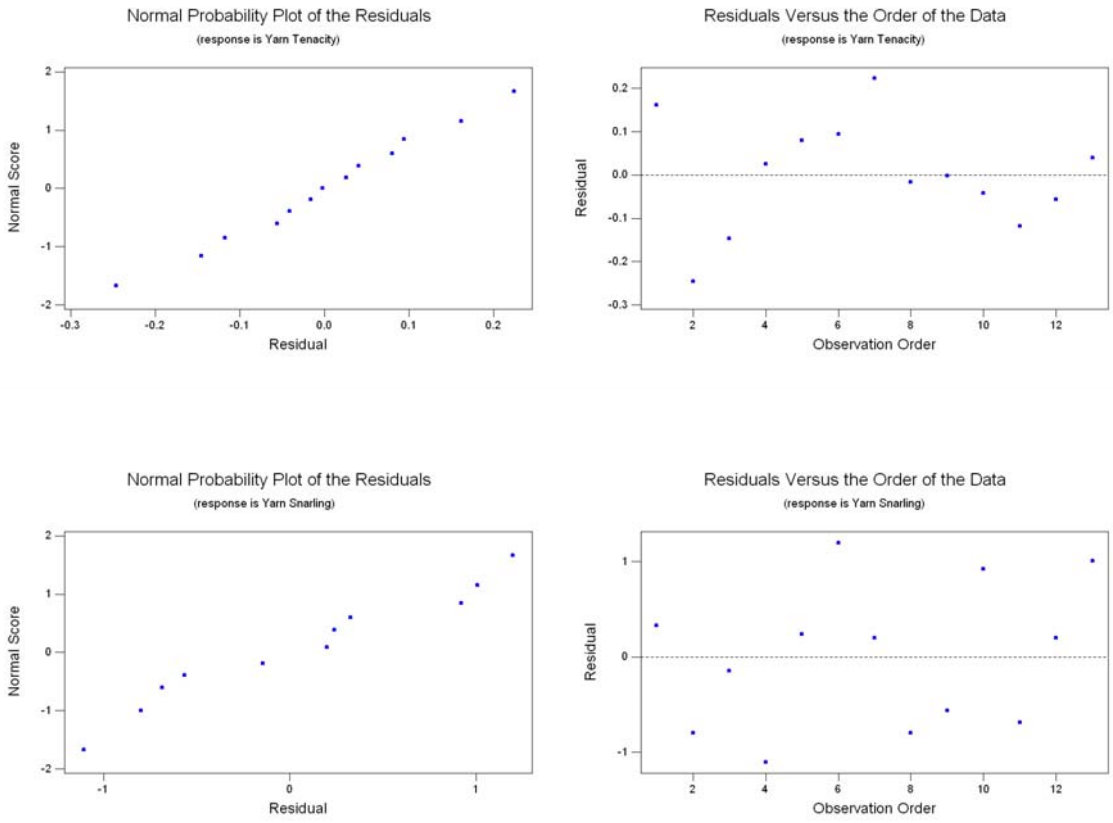

Figure 5-10a Residual Analysis for Model Adequacy Checking of Yarn Tenacity and Snarling (58 tex)

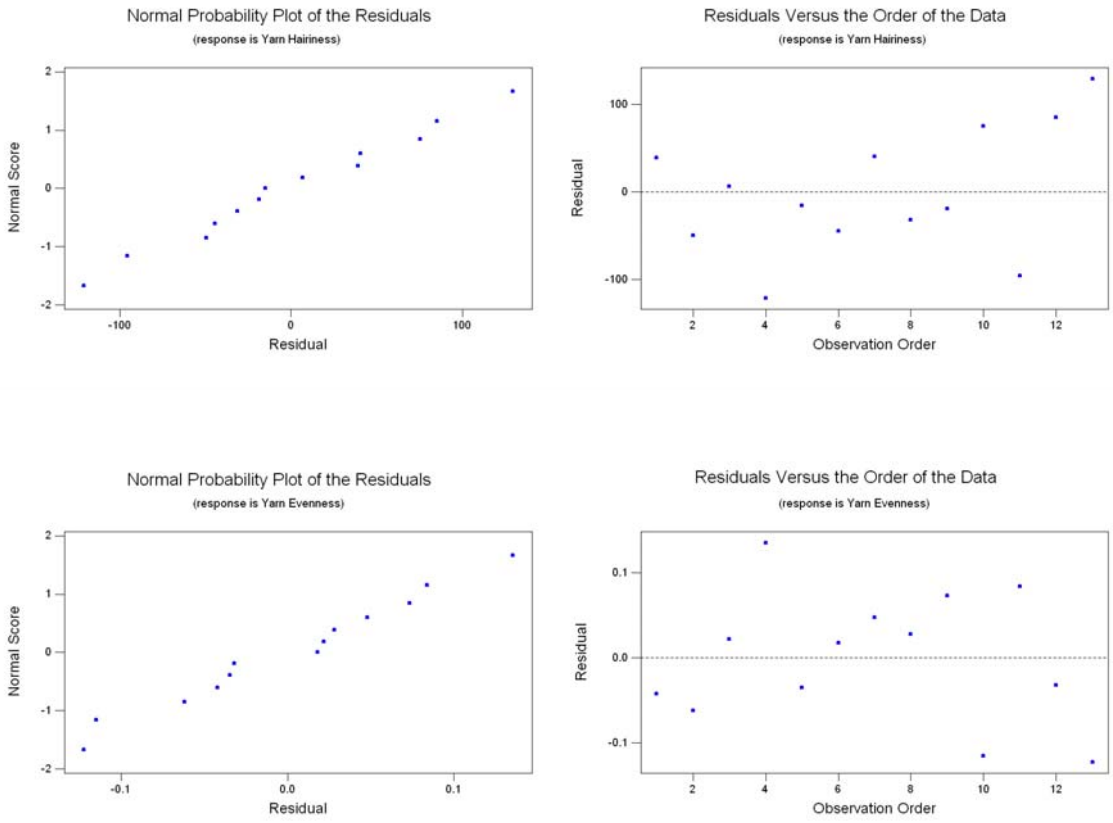

Figure 5-10b Residual Analysis for Model Adequacy Checking of Yarn Hairiness and Evenness (58tex)

5.4.3.1 Effects of Yarn Twist and Speed Ratio on the Tenacity of Low Torque Yarns

Figures 5-11 and 5-12 show the effects of yarn twist and speed ratio on the tenacity of low torque ring yarns. It can be seen that the tenacity of low torque ring yarns increases with increase in yarn twist factor. This trend is similar to that for conventional ring yarns. As the twist increases, the individual fibers assume helical paths and wrap around each other. The normal pressure and total friction of the individual fibers pressing against each other progressively increase, with accompanying yarns strength increase. Figures 5-11 and 5-12 also show that as yarn speed ratio increases, yarn tenacity decreases, particularly on higher twist range. The reason why yarn tenacity is reduced may be ascribed to the combined effects of fiber migration, fiber packing density, fiber deformation and fiber arrangement in yarns. With increase in yarn speed ratio, despite the possibility of fiber migration and packing density increase, an increase of fiber deformation especially of plastic deformation and a decrease in the uniformity of fiber arrangement along yarn lengthwise results in decreased yarn tenacity.

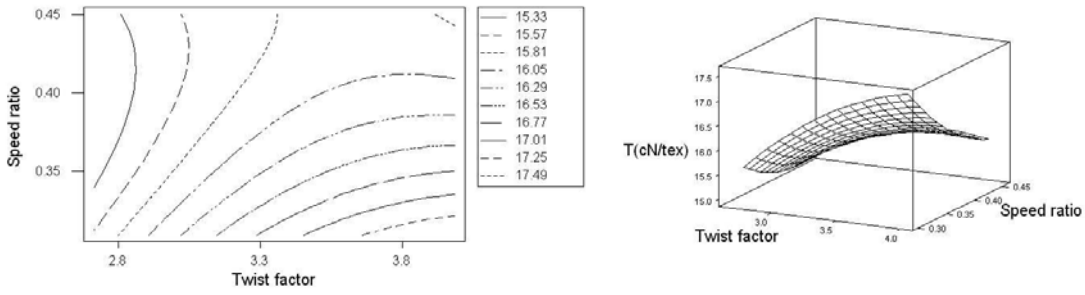

Figure 5-11 Contour and Surface Plot of Yarn Twist and Speed Ratio on Yarn Tenacity (84 tex)

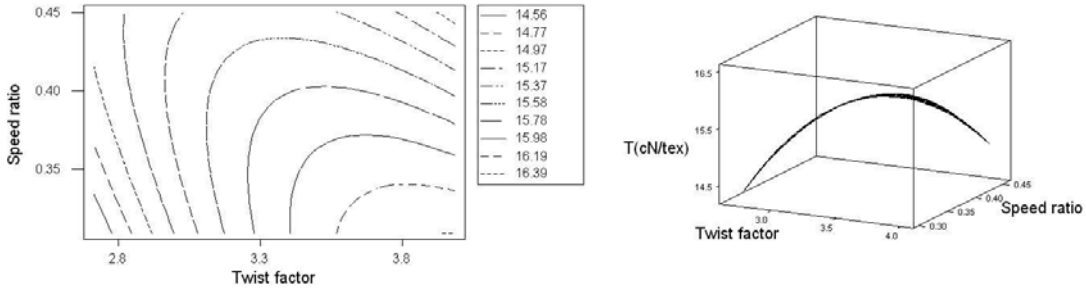

Figure 5-12 Contour and Surface Plot of Yarn Twist and Speed Ratio on Yarn Tenacity (58 tex)

5.4.3.2 Effects of Yarn Twist and Speed Ratio on the Snarling of Low Torque Yarns

From Figures 5-13 and 5-14, it can be seen that the snarling of low torque ring yarns increase with increase in yarn twist factor. In staple yarns, twist is essential to hold the fibers together and to impart some degree of cohesiveness to the structure. When twist is inserted in yarns, the fibers will be bound into a helical path along the yarn,

and fiber internal stress and strain are created in the yarn. Since yarn twist is one of the most important factors governing the magnitude of yarn torque and the tendency of yarn to snarl, increase in yarn twist tends to increase the fiber internal stress and strain built in the yarn, thus increase the yarn torque.

Figures 5-13 and 5-14 also show that as yarn speed ratio increases, yarn snarling decreases. As mentioned early, the speed ratio relates to the level of yarn false-twisting during spinning. The structure investigation in Chapter 4 also exhibits some new structure characteristics of low torque yarn such as higher fiber migration, more compacted fiber packing manner and fibers with fiber section arranging in an opposite direction to the yarn twist direction, compared to that of conventional ring yarn, which mainly comes from the introduction of false-twisting operation during yarn formation. Therefore, it is seemed that when speed ratio increases, fiber migration and fiber sections with opposite arranging direction tend to increase and yarn tends to become compact, while radial bias of distribution of fiber tensile stress exists in the yarn tends to decrease, which have positive effects contributing to the reduction of yarn residual torque. Although fiber internal stress and strain may increase with increase in speed ratio, which tends to increase yarn torque, fiber plastic deformation and frictions among fibers in the yarn also increase. Therefore, the reduction of yarn torque may be ascribed to the combined effects of these factors.

In addition, as shown in Figures 5-13 and 5-14, with lower yarn twist and higher speed ratio, yarn tends to possess lower yarn snarling. For example, Tables 5-5 and

5-6 show that, with lower twist factors (2.71, 3.35 and 2.90) and higher speed ratios (0.38, 0.45 and 0.43), Tests No.4, No.9 and No.10 produce yarns with lower snarling (22 turns/25cm, 25 turns/25cm and 23 turns/25cm for 84tex yarns; and 25 turns/25cm, 27 turns/25cm and 27 turns/25cm for 58tex yarns).

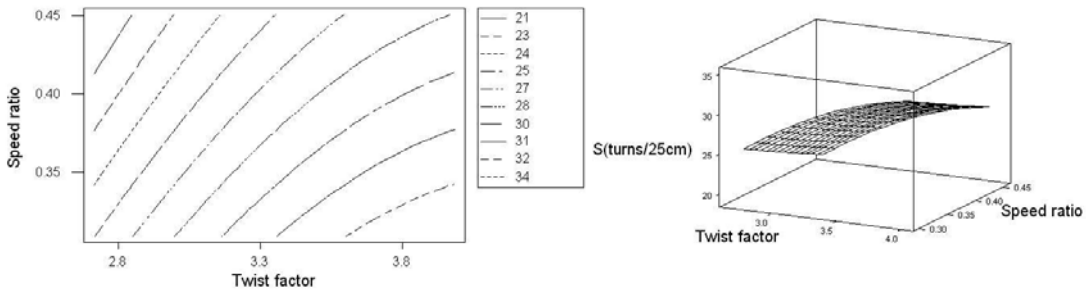

Figure 5-13 Contour and Surface Plot of Yarn Twist and Speed Ratio on Yarn Snarling (84 tex)

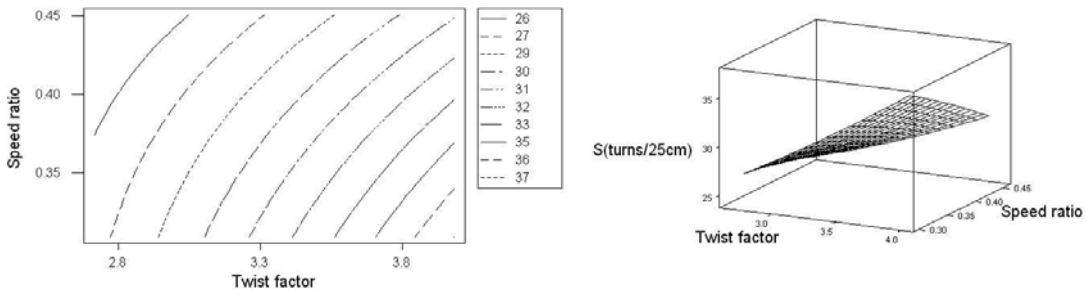

Figure 5-14 Contour and Surface Plot of Yarn Twist and Speed Ratio on Yarn Snarling (58 tex)

5.4.3.3 Effects of Yarn Twist and Speed Ratio on the Hairiness of Low Torque Yarns

Figures 5-15 and 5-16 show the effects of yarn twist and speed ratio on yarn hairiness. It can be found that hairiness decreases with increasing yarn twist because a greater binding force is exerted between the fibers owing to twist. Moreover, increase in yarn twist tends to shorten the length of the protruded fiber ends and loops. In addition, for 84 tex yarn, increase in speed ratio in lower yarn twist and decrease in speed ratio in high yarn twist will slightly reduce yarn hairiness. With the false-twisting operation induced in the low torque yarn spinning, the magnitude of speed ratio affects yarn hairiness to some extent. It is known that geometry of spinning triangle has an important influence on the occurrence of yarn hairiness (Rodiger, 1988; Stalder, 1991). The speed ratio partly determines the twist level of yarn section above the point of false-twisting and thus influences the geometry of spinning triangle and the incidence of yarn hairiness. In addition, the operation of false-twisting includes a process of twisting and detwisting. During detwisting, some edge fibers may be wrapped on the yarn, which also depends on the magnitude of speed ratio. Moreover, the magnitude of speed ratio perhaps influences the yarn packing density, thus affects bind force between fibers. Therefore, a proper selection of the speed ratio combined with twist factor probably results in lower yarn hairiness.

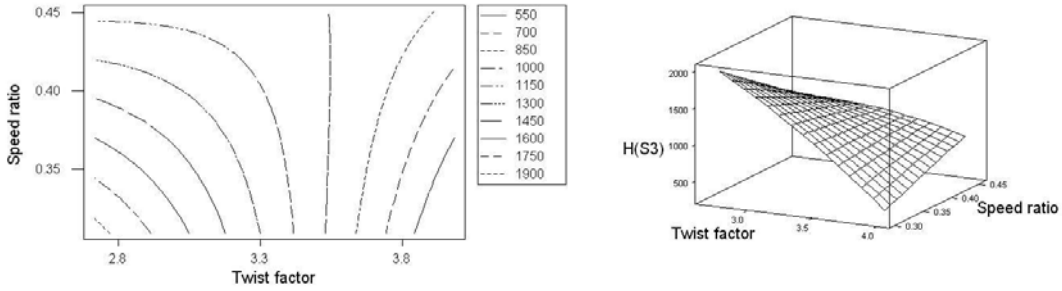

Figure 5-15 Contour and Surface Plot of Yarn Twist and Speed Ratio on Yarn Hairiness (84 tex)

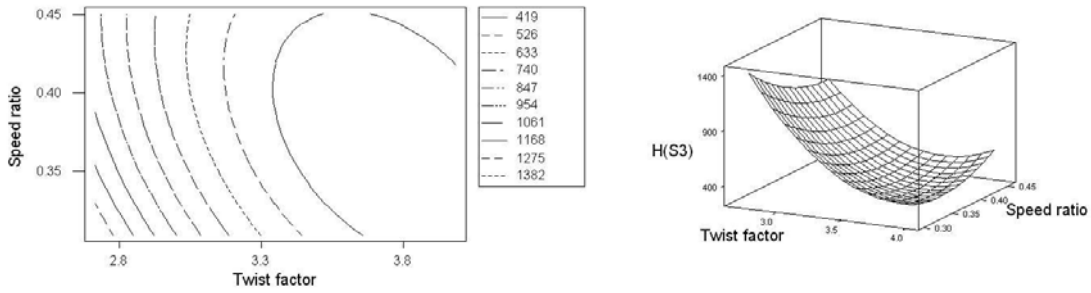

Figure 5-16 Contour and Surface Plot of Yarn Twist and Speed Ratio on Yarn Hairiness (58 tex)

5.4.3.4 Effects of Yarn Twist and Speed Ratio on the Evenness of Low Torque Yarns

It is known that yarn unevenness is mainly determined by the number of fibers in the yarn cross-section and the fiber motion and control during drafting. In addition, as shown in Figures 5-17 and 5-18, the modified system also has some effects on irregularity of the low torque ring yarn.

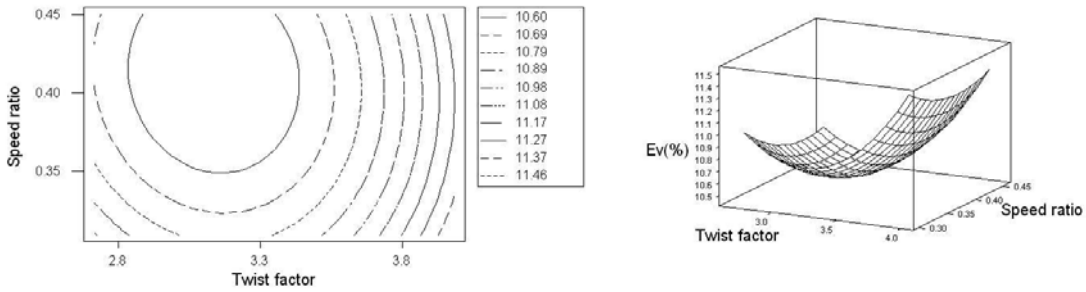

Figure 5-17 Contour and Surface Plot of Yarn Twist and Speed Ratio on Yarn Evenness (84 tex)

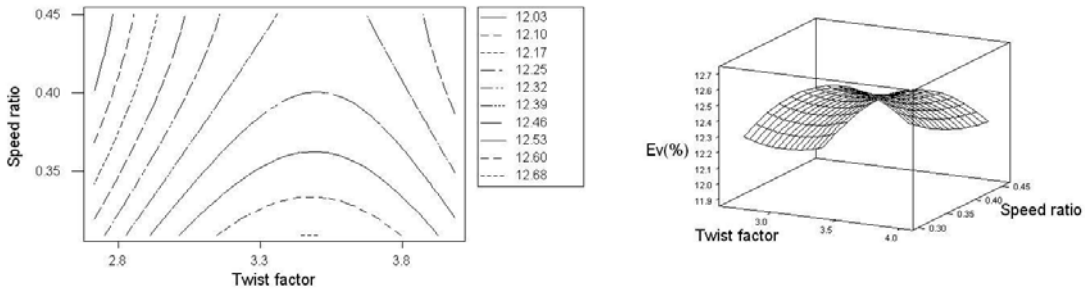

Figure 5-18 Contour and Surface Plot of Yarn Twist and Speed Ratio on Yarn Evenness (58 tex)

5.5 Deviation of the Estimated Value of Yarn Properties from Statistical Models to Experimental Results

In order to check the validity of mathematical model for predicting the effects of yarn twist factor and speed ratio on yarn properties, a set of processing conditions from the region of spinning process parameters were chosen to spin yarns. Then yarn

properties were measured and the experimental values were compared to the estimated values from model. The percentage error (P) between the actual experimental values (A) and the estimated values (E) obtained from mathematical model can be calculated according to Equation 5-14 with the results being summarized in Table 5-7.

$$P = \frac{D}{E} \times 100\% \tag{5-14}$$

where P is percentage error, D is difference between the estimated Y value and the experimental Y value and E is estimated value from the mathematical model.

It can be seen from Table 5-7 that the percentage error between the estimated value and the experimental value of yarn tenacity was less than 5% and the maximum accuracy error of yarn snarling is found to be about 5.4%. These indicate that RSM model generated has sufficient accuracy in predicting yarn tenacity and snarling. In addition, Table 5-7 shows that the percentage error of yarn evenness is less than 10% and yarn hairiness percentage error is less than 15%, implying that the mathematical models of yarn evenness and yarn hairiness were significant at the confident level of 90% and 85% respectively, and gave satisfactory accuracy for prediction. These confirm that the mathematical model can reflect the actual relationship between yarn properties and yarn twist factor and speed ratio.

Table 5-7 Percentage Error between the Estimated Values and the Experimental Values of Yarn Properties

Yarn count	Parameter		Y_1 Tenacity (cN/tex)			Y_2 Snarling (turns/25cm)			Y_3 Hairiness (S3/100m)			Y_4 Evenness (CV%)		
	TF	FTF	E	A	P (%)	E	A	P (%)	E	A	P (%)	E	A	P (%)
84tex	3.00	0.33	16.0	16.2	1.3	27	26	3.7	1579	1410	11.2	10.7	10.8	0.9
	3.20	0.33	16.3	16.2	0.6	29	29	0	1377	1307	5.1	10.7	11.1	3.7
	3.20	0.43	15.8	16.2	2.5	25	24	4.0	1137	984	13.5	10.5	11.2	6.7
	3.50	0.36	16.4	16.5	0.6	30	29	3.4	1038	899	13.4	10.6	11.3	6.6
	3.80	0.33	17.0	17.2	1.2	32	31	3.1	663	604	8.9	11.1	11.2	0.8
	3.98	0.30	17.7	16.9	4.5	34	33	2.9	310	350	12.9	11.5	10.8	6.1
58tex	3.00	0.33	15.3	14.9	2.6	29	28	3.4	862	739	14.2	12.5	13.0	4.0
	3.20	0.33	15.7	15.3	2.5	30	30	0	646	696	7.7	12.6	13.2	4.8
	3.20	0.43	15.6	15.5	0.6	27	26	3.7	507	431	15.0	12.4	12.2	1.6
	3.50	0.36	16.0	15.7	1.9	31	32	3.1	372	341	8.3	12.5	12.7	1.7
	3.80	0.33	16.3	16.4	0.6	35	35	0	343	382	11.4	12.6	12.5	0.4
	3.98	0.30	16.4	16.7	1.8	37	35	5.4	403	371	7.9	12.4	12.7	1.7

5.6 Optimization of Spinning Processing Parameters

With the help of RSM, second-order polynomial response surface models are set-up to predict and explain the relationship between yarn properties and yarn twist and speed ratio. Besides this, one of the primary objectives in this Chapter is the determination of operating conditions on a set of input variables that result in an optimum response. In many instances there are several properties of the product output that must be considered in the definition of "desirable". In this study, yarn snarling is the major concern in evaluating yarn performance for modification, but other yarn properties such as yarn tenacity, hairiness and evenness are also required to reach the requirements of yarn quality standard. Up to now several approaches can be used for the multiply response optimization such as making use of desirability function and overlaying the contour plots for each response in the optimization. Therefore, using a computer, it is possible to specify the desired response values and search the experimental space for the optimum conditions to provide the best compromise to meet these specifications.

5.6.1 Optimization Using the Desirability Function

One useful approach for optimization of multiply responses is to use the simultaneous optimization technique popularized by Derringer and Suich (1980). The procedure makes use of desirability functions. The general approach is to first convert each response into an individual desirability function d_i. The d_i, which

ranges from 0 to 1 (least to most desirable), represents the desirability of each individual (i) response.

The individual desirability functions for the various responses under consideration are next incorporated into a single function by calculating the geometric mean which gives the overall assessment of the desirability of the combined responses. The overall desirability function is:

$$D = (d_1 \times d_2 \times \ldots \times d_n)^{\frac{1}{n}} \quad (5\text{-}15)$$

where n is the number of responses.

Once the overall desirability has been set up as a function of the input variables, the next step is to maximize this function over the experimental region using univariate optimization techniques.

In this study, yarn tenacity, snarling, hairiness and evenness are four responses and yarn snarling is the major indicator of evaluating yarn performance for modification. For low torque yarn, yarn snarling value is desired to be as low as possible with acceptable level of yarn tenacity, hairiness and evenness for industry application. This objective can be achieved efficiently by adjusting spinning parameters with the help of an appropriate optimization method using desirability function. For this, the optimization problem can be formulated in the standard mathematical format as

follows:

Find: TF, FTF

Minimize: S (TF, FTF) (turns/25cm)

Subjected to constraints: S (turns/25cm), T (cN/tex), H (S3), Ev (%)

S (TF, FTF) is the RSM model developed in Section 5.3 and constraints of each response depend on the actual requirements of yarn properties.

In order to calculate the numerical optimal solution, it is necessary to specify the target and lower and/or upper bounds for each response. Table 5-8 lists the target and boundaries of each response. With the help of Minitab Statistical Software, response optimization of 84tex yarn and 54 tex yarn were worked out and presented in Figures 5-19 and 5-20, respectively.

From the Figures, it can be see that the individual desirability and composite desirability of these four responses are close to 1, which indicates that one of the best combination of parameters (TF=3.2 and FTF=0.43) leads to the optimum multiply responses in the present work.

Table 5-8 Target and Boundaries of Each Response

Yarn count	Response	Goal	Lower bound	Target	Upper bound
84tex	T (cN/tex)	Target	15.5	15.7	20.0
	S (turns/25cm)	Minimize	-	25	30
	H (S3)	Target	0	1150	1500
	Ev (%)	Target	0	10.50	12.00
58tex	T (cN/tex)	Target	15.0	15.4	20.0
	S (turns/25cm)	Minimize	-	28	30
	H (S3)	Target	0	500	1000
	Ev (%)	Target	0	12.35	12.60

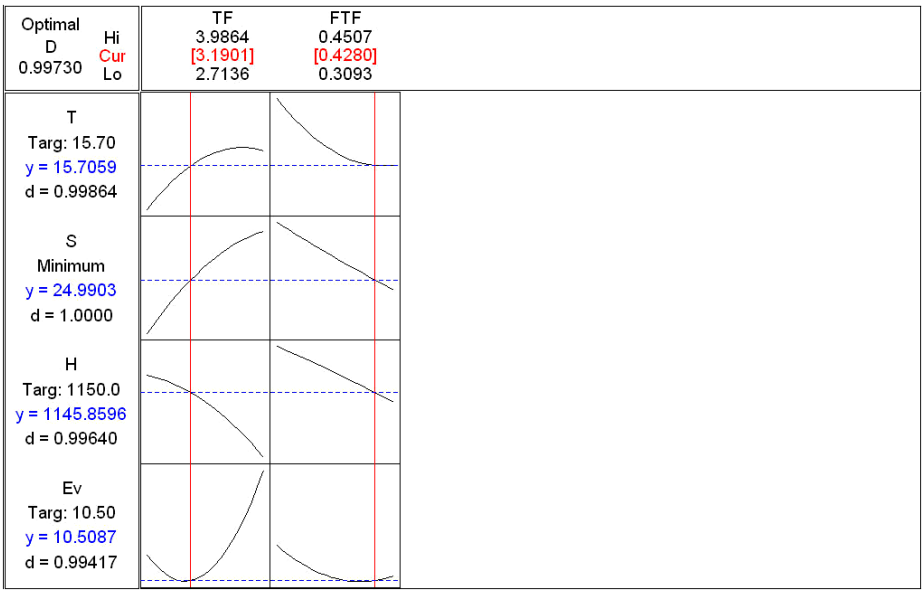

Figure 5-19 Response Optimization of 84tex Yarn

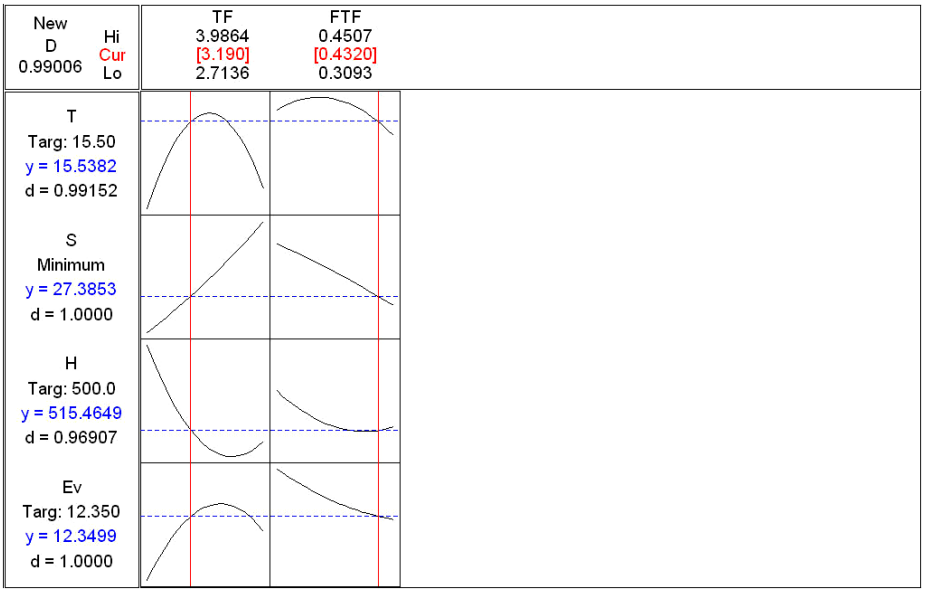

Figure 5-20 Response Optimization of 58tex Yarn

5.6.2 Optimization Using Overlaid Contour Plot

In the present study, only two design variables of twist factor and speed ratio are considered in the responses optimization. Therefore, another relatively straightforward approach to optimizing several responses that works well is to overlay the contour plots for each response.

Lower bound and upper bound of each yarn property need set up before analysis. For 84tex yarn, the tenacity was between 15.5 cN/tex and 20.0 cN/tex, the snarling was between 0 turns/25cm and 26 turns/25cm, the hairiness was between 0 and 1300, and the evenness was lower than 12.0%. For 58 tex yarn, the tenacity was between 15.4

cN/tex and 20.0 cN/tex, the snarling was between 0 turns/25cm and 28 turns/25cm, the hairiness was between 0 and 1100, and the evenness was lower than 12.6%. With the help of Minitab Statistical Software, the overlaid contour plot of yarn properties is gathered and shown in Figures 5-21 and 5-22, where the white area is the feasible region in which optimized parameters can be chosen to meet requirements of all four yarn properties.

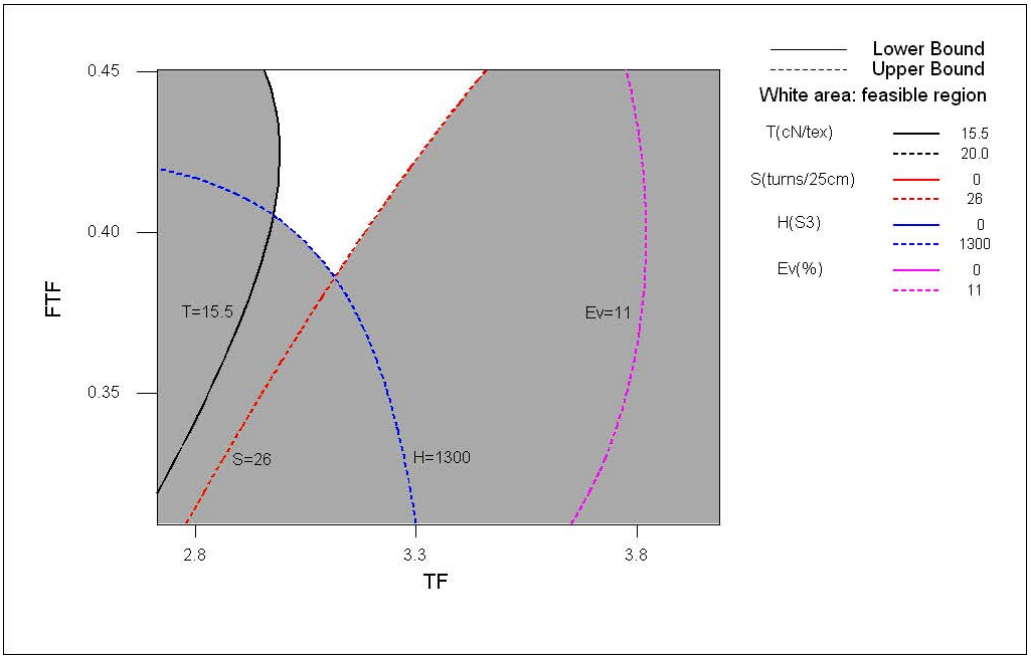

Figure 5-21 Overlaid Contour Plot of Yarn Properties (84tex)

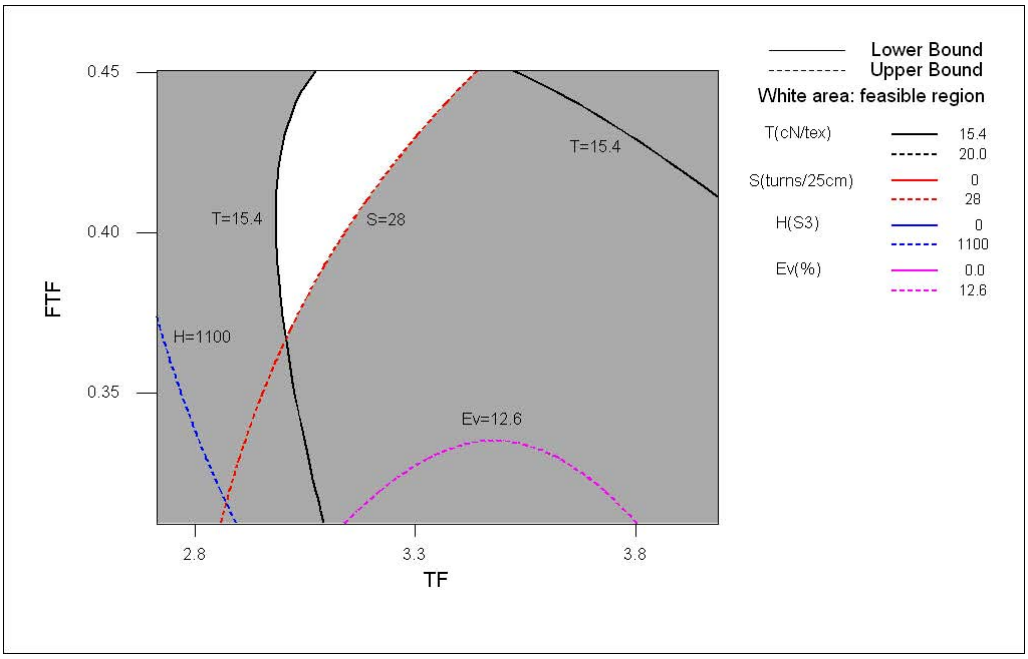

Figure 5-22 Overlaid Contour Plot of Yarn Properties (58tex)

With the help of the plot in combination with the optimization plot shown in Figures 5-19 and 5-20, the best parameters are found for giving the desirable yarn properties. Table 5-9 shows the optimized spinning parameters and the measured and estimated yarn properties.

Table 5-9 The Optimized Spinning Parameters and Yarn Properties

Yarn count	Parameters		Response							
	TF	FTF	S (turns/25cm)		T (cN/tex)		H (S3)		Ev (%)	
			E	M	E	M	E	M	E	M
84 tex	3.19	0.428	25	24	15.7	16.2	1146	985	10.5	11.1
58 tex	3.19	0.432	27	26	15.5	15.6	515	435	12.4	12.2

5.7 Summary and Conclusion

During low torque ring yarn spinning, a false-twisting operation is induced and a new parameter, namely speed ratio, is introduced. The relationship between yarn properties and spinning parameters differs from that of conventional ring spinning. The work reported in this Chapter has been concerned with the development of statistic models for predicting and explaining the relationship between low torque ring yarn properties and spinning processing parameters.

With the help of Fractional Factorial Methodology, the effect significance of spinning parameters such as twist factor (TF), speed ratio (FTF), weight of traveler (Tr) and the position of the torque-reduction device (H and V) is determined. The analysis indicates that twist factor (TF) and speed ratio (FTF) are the two most important spinning parameters contributing to the low torque yarn properties, particularly on yarn snarling and tenacity. Therefore, TF and FTF are chosen for more thorough investigation in subsequent experiments.

The second-order polynomial response surface models have been developed to predict and explain the relationships between yarn properties and yarn twist factor and speed ratio using Response Surface Methodology (RSM). The results of RSM investigation show that yarn tenacity increases with increase in yarn twist and decrease in speed ratio, and yarn snarling decreases with the reduction of yarn twist and increase of speed ratio. The reason for these trends may be ascribed to the combined effects of the change of fiber migration, fiber packing density, fiber deformation and fiber arrangement in yarns due to the modification.

The model adequacy assessment by the residual analysis and the checking of model validity, through assessing the deviation of the estimated values obtained from mathematical model to the actual experimental values, all demonstrate that the developed model exhibits a good predicating accuracy and this model can reflect the actual relationship between yarn properties and yarn twist and speed ratio.

The developed RSM model is further coupled with the desirability function and overlaid contour plot to find the optimum spinning parameters leading to the desirable yarn properties. Optimization using desirability function indicates that one of the best combination of parameters is TF = 3.2 and FTF = 0.43, which results in lower yarn snarling with acceptable level of yarn tenacity, hairiness and evenness for industrial application. Optimization using overlaid contour plot also gives a feasible operating region where a number of combination of twist factor and speed ratio can be adopted to obtain desirable yarn properties.

CHAPTER 6 PROPERTIES OF LOW TORQUE RING YARN AND CHARACTERISTICS OF RESULTANT WOVEN FABRIC

6.1 Introduction

Yarn properties are determined by not only fiber properties but also yarn structures. Different spinning methods will form yarns of different yarn structure. Therefore, as a modified ring spinning method, a false-twisting operation is induced during low torque ring yarn formation and thus yarn structure is modified accordingly. The introduction of false-twisting operation during yarn formation gives low torque ring yarn a new fiber and yarn configuration, and thus causes different characteristics of low torque ring yarn from that of conventional ring yarn. Just as predicted, the preliminary experiment shows the encouraging results of low torque ring yarn such as lower yarn snarling, less yarn hairiness, and normal yarn tenacity and evenness. All these improvement of yarn properties would be reported in depth in this Chapter, in which the investigation mainly involves structure properties and physical properties of low torque ring yarn.

In addition, the new characteristics of low torque ring yarn will no doubt be brought into downstream fabrics in subsequent production. Therefore, fabric characteristics become another focus of the investigation in this Chapter. Characterization of woven

fabric from low torque ring yarns investigated includes fabric structural characteristics, mechanical characteristics and fabric performance. The emphasis is placed on fabric properties most related to the characteristics of the low torque ring yarns.

With results of objective measurements on fabrics, a study was carried out to evaluate the comparative performance of the end-product (Jeans and Trousers) produced by low torque ring yarns, conventional ring yarns and rotor yarns through actual wearing and washing trials in this Chapter.

6.2 Experimental

6.2.1 Sample Preparation

6.2.1.1 Yarn Sample Preparation

A carded cotton roving of 952tex (0.62 Ne) was used to spin 84tex (7Ne) conventional ring yarns (C) and low torque ring yarns (NS) with twist factors of 3.2, 3.8 and 4.2, and 58tex (10Ne) conventional ring yarns (C) and low torque ring yarns (NS) with twist factors of 3.2, 3.3 and 4.2 on the modified Ring Spinning Frame. The fiber properties and main spinning parameters are listed in Table 6-1. The details of yarn sample specifications are shown in Table 6-2. In addition, two rotor yarns used in this study, 7Ne with twist factor 4.3 and 10Ne with twist factor 4.7, were made by Central Textiles.

Table 6-1 Fiber Properties and Process Parameters of Spinning

Fiber properties		
Micronaire value		4.0
Fiber 2.5% span length		28.7 mm
Fiber bundle strength		22cN/tex
Fiber breaking extension		5.3%
Process parameters		
Yarn count		7Ne (84tex), 10Ne (58tex)
Yarn twist factor		3.2, 3.3, 3.8, 4.2
Speed ratio		0.33, 0.36, 0.43
Spinning speed		7000-10000 rpm
Total draft	7Ne	11.29
	10Ne	16.13
Back draft		1.14

Table 6-2 Specifications of Yarn Samples

Yarn sample.	Yarn type	Yarn count		Twist factor	Speed ratio
		Ne	Tex		
7-3.2-A	C	7	84	3.2	-
7-3.2-NS $_{0.33}$	NS	7	84	3.2	0.33
7-3.2-NS $_{0.43}$	NS	7	84	3.2	0.43
7-3.8-A	C	7	84	3.8	-
7-3.8-NS $_{0.33}$	NS	7	84	3.8	0.33
7-4.2-A	C	7	84	4.2	-
7-4.2-NS $_{0.33}$	NS	7	84	4.2	0.33
10-3.2-A	C	10	58	3.2	-
10-3.2-NS $_{0.43}$	NS	10	58	3.2	0.43
10-3.3-A	C	10	58	3.3	-
10-3.3-NS $_{0.36}$	NS	10	58	3.3	0.36
10-4.2-A	C	10	58	4.2	-
10-4.2-NS $_{0.33}$	NS	10	58	4.2	0.33

6.2.1.2 Fabric Sample Preparation

Nine denim fabrics were produced using the low torque ring yarns, conventional ring yarns and rotor yarns as weft yarns. The fabric specifications are listed in Table 6-3. Among them, Samples 4, 5 and 6 were made by Toyota air-jet loom and the rest were produced by Picanol rapier loom. Fabrics then underwent finishing and enzyme pumice washing. With 29tex ring warp yarns, three twill fabrics were woven using the low torque ring yarns, conventional ring yarns and rotor yarns as weft yarns on a Toyota air-jet loom. The greige fabrics were desized, bleached, and dyed Khaki. Samples 13, 14 and 15 are the same fabrics as Samples 10, 11 and 12 but treated for wrinkle free effect. The treatment was carried out by a commercial company.

Table 6-3 Fabric Specifications

Fabric sample	Fabric content		Yarn count (Ne)		Yarn twist factor		Fabric count (no./2.54cm)		Weave	Fabric type
	warp	weft	warp	weft	warp	weft	warp	weft		
1	C	NS	7	7	4.2	3.2	68	46	3/1 twill	denim
2	C	C	7	7	4.2	3.2	68	46	3/1 twill	denim
3	C	C	7	7	4.2	4.2	68	46	3/1 twill	denim
4	C	NS	7	7	4.2	3.2	63	53	3/1 twill	denim
5	C	C	7	7	4.2	4.2	63	53	3/1 twill	denim
6	C	OE	7	7	4.2	4.3	63	53	3/1 twill	denim
7	C	NS	7	10	4.2	3.3	68	44	3/1 twill	denim
8	C	C	7	10	4.2	3.3	68	44	3/1 twill	denim
9	C	C	7	10	4.2	4.2	68	44	3/1 twill	denim
10	C	NS	20	10	4.2	3.2	117	58	3/1 twill	dyed twill
11	C	C	20	10	4.2	4.2	117	58	3/1 twill	dyed twill
12	C	OE	20	10	4.2	4.7	117	58	3/1 twill	dyed twill
13	C	NS	20	10	4.2	3.2	117	58	3/1 twill	wrinkle free treated twill
14	C	C	20	10	4.2	4.2	117	58	3/1 twill	wrinkle free treated twill
15	C	OE	20	10	4.2	4.7	117	58	3/1 twill	wrinkle free treated twill

Note: NS, C and OE indicate the low torque ring yarn, conventional ring yarn and rotor yarn, respectively.

6.2.2 Test Methods

6.2.2.1 Yarn Test

The yarn and fabric samples were conditioned for at least 24 hours under standard conditions (20 ± 2°C and 65 ± 2% RH) and tested for yarn and fabric properties.

In this study, the yarn diameter was measured on the Projectina Microscope (Model: CH-9435 Heerburgg) at 30 randomly selected places along the length of the yarn. Electronic Yarn Twisting Tester was used to measure the low torque ring yarn and conventional ring yarn twist. According to the structure characteristics of low torque ring yarn, Method B, the method of Untwist-Retwist, was selected following ASTM D1422-99. The hairiness of per 100m yarn was tested using the Zweigle G566 Hairiness Tester and yarn evenness was measured by the Uster III Evenness Tester (400mm/min, 2.5minute for each bobbin).

In the study of yarn torsional property, a yarn snarling tester was used to measure yarn twist liveliness by adopting the principle similar to ISO Standard 3343-1984. A yarn with a higher residual torque will have a higher potential of snarling and thus can be considered more twist lively. Thirty readings were taken on each sample. In addition, the torque of twisted yarn was measured by KES-YN1 Yarn Torsion and Intersecting Torque Tester, a torsion-balance type of torque testing apparatus. The yarn test length was 3cm and the yarn tension was kept constant 2cN. Ten specimens were tested for each yarn sample. The Uster Tensorapid Instrument was used to

examine yarn tensile properties at a speed of 5000 mm/min and a specimen length of 500mm. Fifty readings for each sample were recorded. Yarn bending property was measured on the KES-FB2 Bending Tester. Yarn samples were prepared on a rectangular paper frames with a 15cm by 1 cm wide hollow portion in the center (Radhakrishaiah, 2005). Then yarn samples were mounted between the front and back sets of clamps at a distance of 1 cm. After this, the yarns were bent between the clamps by rotating the movable clamp to achieve yarn curvatures of +2.5 cm^{-1} and -2.5 cm^{-1}.

6.2.2.2 Fabric Test

Dimensional stability of denim fabrics and twill fabrics were examined based on AATCC 135. Denim fabric skewness and twill fabric skewness were measured following Levi Strauss Standard LS&CO.11 (Levi Strauss, 2002) and AATCC 179 respectively.

The fabric breaking strength and tear strength were measured following ASTM D5034 and ASTM D1424 respectively. Fabric mechanical and surface properties were mainly conducted on KES-FB Tester. The tensile behavior and shear behavior of all fabric samples were studied on KES-FB1, while the bending behavior of all fabrics was investigated on a KES-FB2, the compression properties were measured with KES-FB3 and surface roughness and friction were identified by KES-FB4. All the sixteen parameters describing fabric mechanical properties were measured following the test procedure. Then these measured results were used to compute the

primary and total hand qualities of the fabrics.

Air permeability of all fabrics was tested on Shirley Air Permeability Tester according to BS 5636. The test was measured at a constant pressure drop across a given area (508mm^2) of fabric of 100 Pa. The wicking property of fabrics was determined by The Vertical Wicking Strip Test Method in accordance to DIN 53924 (1978). The result of the test is a wicking curve, expressing the wicking height (mm) in a vertical positioned sample as function of wicking time (up to 600 seconds). Besides, from the difference between initial and final weights of the strip, the amount of water taken up by the sample was calculated, expressing this as the percentage of the weight of water gained by the fabric stripe to the initial weight of the stripe. The sample strip, 3cm in width and 22cm in length, was suspended in its weft direction with one of the ends clamped on to a camping bar. The other end had attached to a clamp weighted 5g with a 3cm length dipping into the 250ml of reservoir of water. For each fabric, four samples were tested and the average wicking height of the four fabric samples at regular intervals of time was determined. With reference to AATCC 124, denim fabric smoothness appearance was also evaluated subjectively. The evaluation of fabric smoothness appearance is based on following 5 grade scales: 5 - no ‘small snake’; 4 - slight ‘small snake’; 3 - moderate ‘small snake’; 2 - severe ‘small snake’; 1 - very severe ‘small snake’. A grade midway between those whole-number standard is also assigned to represent the fabric appearance if the appearance of the test specimen warrants it.

6.3 Results and Discussion

6.3.1 Yarn Properties

The introduction of false-twisting operation during yarn formation gives low torque ring yarns a new fiber and yarn configuration, and thus causes different characteristics of low torque ring yarns from that of conventional ring yarns. As a result, low torque ring yarns exhibit lower yarn snarling, less yarn hairiness and normal yarn tenacity, as reported below together with other yarn structural and mechanical properties.

6.3.1.1 Yarn Diameter

After yarn structure modification process, low torque ring yarns show pronounced decrease in yarn diameter compared to conventional ring yarn with same twist level, as presented in Figure 6-1. Apparently, this reduction of yarn diameter comes from the increased compactness of yarn structure. With the introduction of false-twisting operation during yarn formation, the high-twisting process of yarn section above the point of false-twisting endows the yarn with a compact structure before untwisting. After that, even though the yarn will be untwisted to the same twist level as conventional ring yarn finally, low torque ring yarn still can maintain its tightness of structure to some extent which is more compact than that of conventional ring yarn with low twist level.

On the other hand, as mentioned early, low twist level will be mainly used in the low

torque ring yarn spinning. From Figure 6-1, the diameters of low torque ring yarns with low twist level is bigger than that of normal twist conventional ring yarn samples such as Sample 7-4.2-A and Sample 10-4.2-A, probably due to the adoption of low twist level in low torque ring yarn.

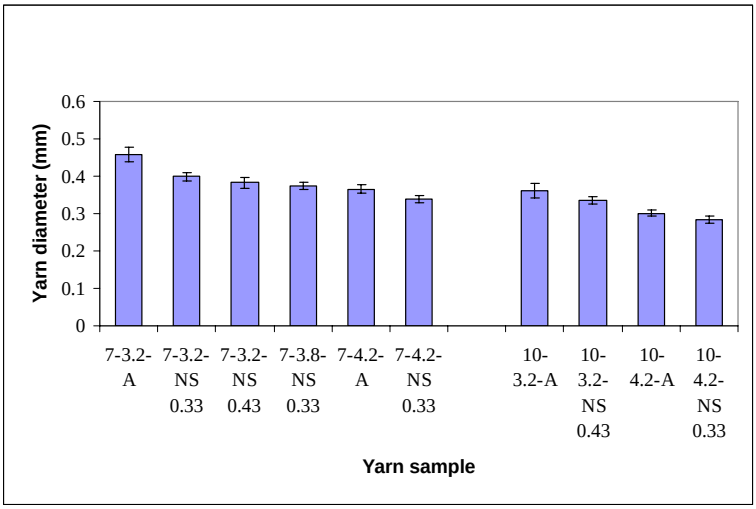

Figure 6-1 Yarn Diameter Profile

6.3.1.2 Yarn Twist

During low torque ring yarn spinning, the false-twisting operation was induced into the yarn formation. As revealed in Figure 6-2, there are no significant changes in yarn twist after this modification. However, in order to achieve a lower yarn residual torque, low twist level was adopted for yarn spinning in the present study. It is known that yarn twist is a main structure factor to the yarn properties and thus influences fabric performance. A reduction in yarn twist level might contribute to the improvement of fabric surface smoothness and fabric soft and full handle. In

addition, other yarn and fabric properties such as yarn bulky and fabric air permeability are also expected to change with twist decrease.

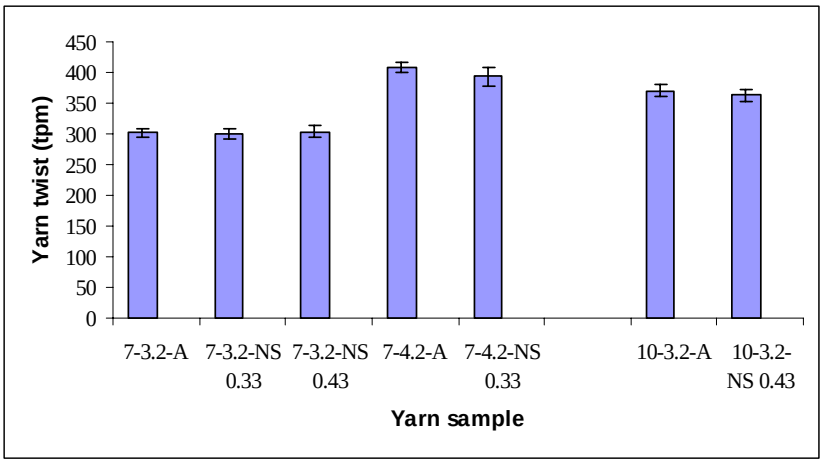

Figure 6-2 Yarn Twist Profile

6.3.1.3 Yarn Hairiness

Yarn hairiness is a key factor affecting yarn and fabric processes and properties. Previous research (Barella, 1957; Pillay, 1964; Wang, Miao and How, 1997; Wang and Chang, 2003; Wang and Chang, 2006) revealed that yarn hairiness may be due to the materials and processes. The study conducted by Barella (1957) indicated that yarn twist is one of the most important parameters influencing yarn hairiness. Barella found that hairiness increased with decreasing yarn twist level. However, the experiment results of yarn hairiness listed in Table 6-4 showed that even though lower twist level is mainly used in low torque ring yarn spinning, the hairiness of low torque ring yarns is still close to or even less than that of conventional ring yarns with normal twist level; while the conventional ring yarns using lower twist level

show a significant increase in yarn hairiness after yarn twist decrease. Moreover, after winding process, low torque ring yarns show the same trend in hairiness as that in cop. In an attempt to explain this result it could be stated that with the false-twisting operation being induced in the low torque yarn spinning, the geometry of spinning triangle is changed which influences the incidence of yarn hairiness. The symmetric structure, short height and multi-bundle fiber form exhibited in the geometry of spinning triangle in low torque ring yarn probably result in the reduction of yarn hairiness. In addition, the operation of false-twisting includes a process of twisting and detwisting. During detwisting, some edge fibers may be wrapped on the yarn body. Moreover, fiber migration is enhanced and yarn structure becomes more compact in low torque ring yarns. Compared to conventional ring yarns, low torque ring yarns possess less yarn hairiness, which is of great benefit to the post-spinning yarn process and fabric appearance and performance.

Table 6-4 Yarn Hairiness

Yarn sample	Value (S3)		Hairiness index (N3)	
	Cop	Cone	Cop	Cone
7-3.2-A	2008	6734	203	571
7-3.2-NS $_{0.33}$	1307	4965	100	435
7-3.2-NS $_{0.43}$	771	3733	71	238
7-3.8-A	1249	4641	173	273
7-3.8-NS $_{0.33}$	604	2354	47	168
7-4.2-A	1049	4108	148	251
10-3.3-A	590	3196	45	307
10-3.3-NS $_{0.36}$	417	2048	33	175
10-4.2-A	496	2527	56	335

6.3.1.4 Yarn Evenness

Yarn evenness is also important for yarn and fabric performance. Table 6-5 lists experiment results of coefficient of variation of yarn mass of low torque ring yarns and conventional ring yarns measured by Uster III Tester. From the Table, it can be seen that the evenness of low torque ring yarns is similar to that of conventional ring yarns with normal twist level. 7Ne low torque yarns can reach 25% Uster Statistics quality level (2001) and 10 Ne yarns also achieve 50% Uster Statistics quality level (2001). Compared to low twist conventional ring yarns, a pleasant improvement is found in low torque ring yarn evenness, due probably to less loose fiber ends and more compact yarn structure in low torque ring yarns.

Table 6-5 Yarn Evenness

Yarn sample	7-3.2-A	7-3.2-NS 0.33	7-3.2-NS 0.43	7-3.8-A	7-3.8-NS 0.33	7-4.2-A	7-4.2-NS 0.33	10-3.2-A	10-3.2-NS 0.43	10-4.2-A
Evenness (CV_m, %)	12.15	11.10	11.20	12.57	11.19	11.43	10.72	14.13	13.30	13.32

6.3.1.5 Yarn Torsional Property

Yarn torque has practical significance for a number of the characteristics of yarns, fabrics, and carpets. Development of low torque ring yarns for industrial application becomes the aim of this study. Table 6-6 and Table 6-7 present test results of yarn torsion properties based on yarn snarling and yarn torque measured respectively in low torque ring yarn samples and conventional ring yarn samples.

Yarn snarling is a better term for representing the residual torque in the yarns, in which the number of turns of snarling formed is counted when the two ends of specified pre-tensioned length yarn segment completely in contact and reach equilibrium. As revealed in Table 6-6, low torque ring yarns have a significant reduction in yarn snarling compared to conventional yarns with normal twist level (Sample 7-4.2-A and Sample 10-4.2-A), even compared with yarns of same twist level. In the case of low torque ring yarn (7Ne) with twist factor 3.2, when compared to conventional yarn with normal twist level, the yarn has a snarling reduction of around 40% from 39 to 24 turns/25cm and for low torque ring yarn (10Ne) with twist factor 3.2, the yarn also has a snarling reduction of around 45% from 47 to 26 turns/25cm. Using low twist level, conventional yarn can also achieve yarn snarling reduction to some extent, but the level of snarling reduction is less than that of low torque ring yarn. As shown in Table 6-6, conventional yarn (7Ne) with twist factor 3.2 only has snarling reduction of about 15% compared to conventional yarn with normal twist level.

It is known that yarn twist is one of the most important factors governing the magnitude of yarn torque and the tendency of yarn to snarl, and decreasing yarn twist tends to decrease the fiber internal stress and strain built in the yarns, thus reducing the yarn torque. Therefore, it seems that the great torque reduction of low torque ring yarns mainly comes from the adoption of low twist in yarn spinning. In addition, the increment of fiber migration and fiber sections with opposite arranging direction to the yarn twist and more compact structure in low torque ring

yarns probably also contribute to the reduction of yarn residual torque.

Table 6-7 shows the results of yarn torque tested by KES-YN Tester where the yarn torque was measured by twisting yarn samples until 3 turns. As revealed in Table 6-7, yarn samples present same trend in yarn torque as that in yarn snarling exhibited in Table 6-6. Low torque ring yarn possesses the lowest yarn torque among three yarns with same yarn count.

Table 6-6 Yarn Snarling

Yarn sample	7-3.2-A	7-3.2-NS 0.33	7-3.2-NS 0.43	7-3.8-A	7-3.8-NS 0.33	7-4.2-A	7-4.2-NS 0.33	10-3.2-A	10-3.2-NS 0.43	10-3.3-A	10-3.3-NS 0.36	10-4.2-A	10-4.2-NS 0.33
Snarling (turns/ 25cm)	33	29	24	39	31	39	33	37	26	39	32	47	36

Table 6-7 Yarn Torsional Property

Yarn sample	7-3.2-A	7-3.2-NS 0.43	7-4.2-A	10-3.2-A	10-3.2-NS 0.43	10-4.2-A
Torque (1×10^{-2}cN.cm)	17.2	9.5	19.9	9.6	5.9	13.0

6.3.1.6 Yarn Tensile Property

Yarn strength is one of the major yarn properties in evaluating yarn performance for modification and further textile processing. Table 6-8 lists the yarn tenacity of low torque ring yarns and conventional yarns. From the Table, it is easy to see that the

tenacity of low torque ring yarns is only slightly lower than that of conventional yarns with normal-twist level (Sample 7-4.2-A and Sample 10-4.2-A). The lowest value of yarn tenacity of low torque ring yarn is around 16.2cN/tex among the four 7Ne yarn samples and 15.33cN/tex for 10Ne low torque ring yarns, which is acceptable for industrial application. It is known that yarn tenacity largely depends on yarn twist level and yarn tenacity tends to decrease as yarn twist level decreases. However, with enhanced fiber migration and more compact yarn structure, low torque ring yarns can still keep their strength at acceptable level when using low twist level, while the conventional ring yarns in low twist level get a great reduction in yarn strength, especially after winding processing, which may bring problems in the following yarn processing, weaving and fabric properties.

The elongation of low torque ring yarns shows a reduction tendency after yarn structure modification, as presented in Table 6-8. Reduced yarn twist in low torque ring yarns may give some explanation to this phenomenon. In addition, after false-twisting operation during yarn formation, some fiber deformation may occur which also results in the reduction of yarn breaking elongation.

Table 6-8 Yarn Tensile Property

Yarn sample	Tenacity				Elongation	
	Mean (cN/tex)		CV (%)		Mean (%)	
	Cop	Cone	Cop	Cone	Cop	Cone
7-3.2-A	15.72	15.21	6.09	7.62	6.72	6.05
7-3.2-NS $_{0.33}$	16.20	15.94	4.29	6.31	6.13	6.29
7-3.2-NS $_{0.43}$	16.50	16.28	4.16	6.00	5.69	6.64
7-3.8-A	17.04	16.16	4.69	6.51	6.59	6.21
7-3.8-NS $_{0.33}$	17.21	16.55	5.31	6.32	5.75	7.07
7-4.2-A	17.58	18.28	4.59	5.53	7.14	7.63
7-4.2-NS $_{0.33}$	16.23	16.51	4.93	5.69	6.59	6.81
10-3.3-A	15.58	14.67	4.94	9.91	5.41	5.44
10-3.3-NS $_{0.36}$	15.33	15.33	5.18	7.26	5.50	5.08
10-4.2-A	17.42	17.32	5.29	6.54	6.38	6.25
10-4.2-NS $_{0.33}$	16.12	16.32	5.26	6.29	5.73	5.86

6.3.1.7 Yarn Bending Property

Bending property of a yarn is one of the important yarn properties for fabrics, as the bending property of a yarn will affect yarn crimp level within a fabric and thus influence fabric properties and performance. Yarn structure factors such as yarn packing density and thickness, as well as the properties of its constituent fibers, are main factors that determines the bending behavior of a yarn. KES-Bending Tester is therefore used to measure both the bending rigidity (B) and hysteresis (2HB) of low torque ring yarns and conventional ring yarns, as shown in Table 6-9. Bending

rigidity (B) is a measure of the ability of a yarn to resist to bending movement while bending hysteresis (2HB) represents the recovery ability of a yarn after being bent. In the present research, low torque ring yarns present a lower yarn bending rigidity compared to that of conventional ring yarns with normal twist level, while slightly higher than that of same twist level conventional ring yarns. These changes in yarn bending properties probably bring benefits for the improvement of fabric thickness, fabric cover, as well as fabric handle of softness and fullness.

Table 6-9 Yarn Bending Property

Yarn sample	7-3.2-A	7-3.2-NS $_{0.33}$	7-3.2-NS $_{0.43}$	7-4.2-A
B ($gf.cm^2/cm$)	0.0052	0.0055	0.0058	0.0066
2HB(gf.cm/cm)	0.0048	0.0044	0.0044	0.0052

6.3.2 Fabric Properties

With notable changes in yarn structure and properties, the fabrics produced from low torque ring yarns show different characteristics from that of conventional ring yarn and rotor yarn fabrics such as improvement of surface smoothness and fullness of low torque ring yarn fabrics, which is reported as follows.

6.3.2.1 Structure Characteristics

- Dimensional Stability and Skewness

Dimensional stability and skewness of fabrics are of great importance for apparel

cotton products. Table 6-10 presents fabric dimensions and skewness before and after washing. From the Table, it can be seen that the fabric samples using low torque ring yarns as weft yarns possess slightly lower dimensional change after washing and fabric skewness also slightly reduced compared to conventional ring yarn fabrics. As far as woven fabrics are considered, the two main reasons for dimensional instability are hygral expansion and relaxation shrinkage. Relaxation shrinkage is caused by the loosening of cohesive or temporarily fixed stress created during spinning, weaving and finishing processes. Therefore, the decrease of dimensional change of fabric with low torque ring yarns as wefts seems deviating from the reduction in yarn residual torque when low torque ring yarns were used. In addition, since a tighter twill structure is adopted in the present study, there have not exhibit remarkable deference between the dimensional changes of fabric samples. Skewness is another type of dimensional change commonly occurred in twill woven fabrics, which can be described as the movement of vertical and horizontal alignment away from perpendicular. Fabric weave, fabric density, yarn twist direction, the level of yarn twist and finishing method all influence the level of fabric skewness. Thus, like the effect of yarn residual torque on dimensional stability, the reduction of yarn twist liveliness or yarn torque may also be helpful in the decrease of fabric skewness.

Table 6-10 Dimensional Stability and Skewness of Fabric Samples

Fabric sample	Dimensional change (%)		Skewness movement (%)
	Warp	Weft	
1	-2.7	-2.4	1.2
2	-3.2	-2.5	2.4
3	-3.7	-3.1	0.8
4	-1.2	-2.0	1.7
5	-1.2	-2.4	3.4
6	-0.4	-2.0	1.4
10	-2.4	-1.6	2.0
11	-3.2	-2.1	5.8
12	-1.2	-1.1	3.7
13	-3.5	-0.9	0.1
14	-4.3	-1.6	2.3
15	-3.7	-0.8	0.9

6.3.2.2 Mechanical Characteristics

- Tensile and Tear Properties

Fabric tensile strength and tear strength are important for the durability of garment. Particularly, after fabric finishing, denim will undergo hard garment washing such as stone washing or enzyme and stone washing. During this process, denim fabric should have enough strength to endure the process. More importantly, after garment washing, denim fabric should still have better strength to meet the needs of the end use.

Table 6-11 Fabric Tensile and Tear Properties

Fabric sample	Tensile strength (N)		Tear strength (N)	
	Warp	Weft	Warp	Weft
1	1151.3	681.6	91.2	69.6
2	1141.4	644.5	87.2	61.7
3	1102.4	733.4	87.2	75.5
4	983.2	849.2	90.2	88.2
5	989.0	840.0	87.8	84.9
6	1053.8	681.4	86.2	59.4
7	1071.5	537.9	87.2	46.1
8	1115.8	462.3	90.1	39.2
9	1146.8	551.2	91.1	47.0
10	609.9	592.5	43.3	64.1
11	620.4	622.4	38.6	62.6
12	626.3	495.1	37.8	46.4
13	401.1	380.8	26.1	39.8
14	446.2	402.9	24.3	37.5
15	372.8	327.9	20.4	24.1

The test results of fabric tensile strength in Table 6-11 show that by using low torque ring yarns as weft yarns, the tensile strength of low torque ring yarn fabrics in weft direction is only slightly lower than that of fabrics using conventional ring yarns with normal twist level as weft yarns, but it is higher than that of the fabrics using rotor yarns and conventional low twist ring yarns as weft yarns. This is because fabric tensile strength is directly proportional to yarn tensile strength.

Tear strength, which is usually more critical in many applications than tensile strength, is also presented for all fabric samples in Table 6-11. As shown in the Table, fabric tear strength using low torque ring yarns as weft yarns is similar to or even

slightly higher than that of conventional ring yarn fabrics, and much higher than that of rotor yarn fabrics and conventional ring fabrics with low twist yarns. The possible reason is that the low torque ring yarn fabrics have a good extensibility due to lower yarn bending rigidity and higher yarn crimp level within the fabric. The crimp levels alter the extensibility of the yarns in the del zone and thus change the number of yarns taking load.

- Bending Property and Compression

Bending rigidity of a fabric depends largely on the bending rigidity of the yarns and the yarn mobility within the fabric and the fabric thickness. KES-FB2 test results in Table 6-12 show that fabrics with the low torque ring weft yarns possess a slightly higher bending rigidity than that of the fabrics with conventional ring weft yarns. On one hand, low torque ring yarns, being the yarns with lower bending rigidity compared to conventional ring yarns, would give lower fabric bending rigidity. However, on the other hand, it is also logical to suggest that the remarkable increase in the thickness of fabrics produced from low torque ring yarns as weft yarns, as revealed in Table 6-12, results in a higher resistance to fabric bending deformation.

Fabric compression property is one of the most important factors assessing a fabric's mechanical properties. It is also a property highly related to fabric handle such as fullness and softness. Based on the test results of fabric compression property, the compression energy (WC) of low torque ring yarn fabrics is higher than that of conventional ring yarn fabrics and rotor yarn fabrics. The increase of fabric

compression energy, when low torque ring yarns were used, may come from the improvement in bulkiness of the yarn and thickness of the fabrics. Hence, accompanied with an increased fabric thickness as presented in Table 6-12, the relative high compression energy of fabrics using low torque ring yarns as weft yarns endows low torque ring yarn fabrics with a softer and full handle feeling compared with the fabrics using conventional ring yarns and rotor yarns as weft yarns.

- Surface Characteristics

Fabric surface, a characteristic integrated by the fabric structure as well the constituent fiber and yarn surface property, is one of the important factors related to fabric appearance and handle of fabric smoothness. Three parameters are used to represent the fabric surface properties in Kawabata Evaluation System, which includes coefficient of friction (MIU), mean deviation of friction (MMD) and geometrical roughness (SMD).

From the test results as shown in Table 6-12, it can be seen that the value of mean deviation of friction (MMD) and geometrical roughness (SMD) of fabrics using low torque ring yarns as weft yarns is lower compared to that of fabrics using conventional ring yarns and rotor yarns as weft yarns, which may indicate that the smoothness and the evenness of the low torque ring yarn fabric surface is better than that of other conventional fabrics. For denim fabric, the improvement of smoothness may come from the decrease of ‘small snake’ pattern on fabric surface, a group of white and light color warp streaks on the fabric surface after garment

washing. The improvement of surface smoothness of low torque yarn fabrics is also related to different characteristics of low torque ring yarns from that of conventional ring and rotor yarns exhibited in yarn bending and compression aspects and fabric compression property.

Table 6-12 Fabric Mechanical Characteristics Measured by KESF

Fabric sample	Tensile				Bending		Shear		Surface			Compression			Thickness	Weight
	EMT (%)	LT (-)	WT (gf.cm /cm^2)	RT (%)	B (gf.cm^2 /cm)	2HB (gf.cm /cm)	G (gf/ cm^2.deg)	2HG (gf /cm)	MIU	MMD	SMD	LC	WC (g.cm/ cm^2)	RC (%)	T (mm)	W (mg/ cm^2)
4	9.39	0.689	16.20	31.31	0.482	0.5271	4.32	10.57	0.214	0.0266	6.06	0.312	0.468	36.54	1.710	44.553
5	9.25	0.693	15.95	34.28	0.465	0.5408	4.10	9.65	0.224	0.0294	5.66	0.321	0.442	35.75	1.610	46.028
6	8.76	0.659	14.40	30.24	0.475	0.5350	4.17	10.39	0.253	0.0312	6.45	0.416	0.447	30.43	1.530	44.880
10	6.07	0.653	9.93	36.33	0.385	0.4245	4.64	12.03	0.182	0.0235	5.64	0.343	0.308	32.22	0.985	29.175
11	6.47	0.644	10.38	36.19	0.335	0.3994	4.39	11.10	0.185	0.0279	6.27	0.354	0.246	35.06	0.877	29.075
12	5.33	0.742	9.88	36.42	0.366	0.4110	4.45	10.83	0.180	0.0315	6.00	0.312	0.244	38.09	0.919	28.975
13	5.86	0.548	7.97	55.07	0.216	0.1797	2.30	4.69	0.169	0.0287	5.61	0.343	0.313	39.45	0.910	29.125
14	5.26	0.637	8.38	53.74	0.196	0.1504	2.30	4.19	0.168	0.0288	5.77	0.338	0.293	42.11	0.884	28.400
15	5.31	0.635	8.43	53.44	0.214	0.1912	2.53	5.07	0.172	0.0301	5.87	0.315	0.294	37.35	0.911	28.250

6.3.2.3 Fabric Performance

The analysis of fabric structural and mechanical characteristics above demonstrates that, just as predicted, the notable change in structural and mechanical properties of low torque ring yarns gives the downstream fabric an improved appearance and modified properties. Among them, the fabric surface smoothness and fabric fullness and softness exhibit a desirable improvement.

- Hand

The objective evaluated handle values listed in Table 6-13 are a true reflection of the low-stress mechanical and surface properties of the fabrics. The applicable range of values for the primary hand qualities presented in the Table is 0 to 10, and the higher the value within this range, the greater the intensity of this particular hand . The range of the total hand quality is between 0 and 5, and also the higher the total handle value within this range, the better the hand quality.

Table 6-13 presents the various hand attributes of the fabric and fabric total hands associated with the men's winter jacket and slacks. From Table 6-13, it can be seen that the fabrics representing low torque ring yarns used as wefts give higher values in fabric Numeir and Fukurami in all samples compared with fabrics with conventional ring yarns and rotor yarns as wefts. The higher value in fabric Numeir of low torque ring yarn fabrics may be attributed to the lower values of mean deviation of friction (MMD) and geometrical roughness (SMD) of fabrics and higher

value of fabric compression energy (WC) using low torque ring yarns as weft yarns. Also the higher compression energy (WC) and lower mean deviation of friction (MMD) of fabrics give low torque ring yarn fabrics a higher value in fabric Fukurami.

Although low torque yarns show a lower bending rigidity revealed in the analysis of yarn properties, higher fabric bending rigidity and thickness may result in a higher value of Koshi in low torque ring yarn fabrics when compared to conventional ring yarn and rotor yarn fabrics. Table 6-13 also shows that fabrics using low torque ring yarns as weft yarns exhibit better total hand quality than those of fabrics from conventional ring yarns and rotor yarns except wrinkle-free treated twill fabric samples. The total hand quality of the wrinkle-free treated twill fabric Sample 13 with low torque ring yarns is similar to conventional ring yarn fabric Sample 14, but it is still better than that of rotor fabric Sample 15.

Table 6-13 Objective Evaluated Handle Values for Men's Winter Jacket and Slacks

Fabric sample	Value of hand attribute (KN-101-W)			THV (KN-301-W)
	Koshi (stiffness)	Numeri (smoothness)	Fukurami (fullness and softness)	
4	9.53	2.60	6.41	2.88
5	9.52	2.16	5.87	2.80
6	9.60	1.49	5.35	2.72
10	9.37	2.50	5.34	2.40
11	9.06	1.73	4.38	2.29
12	9.27	1.31	4.05	2.06
13	7.70	2.48	4.84	2.71
14	7.42	2.39	4.55	2.72
15	7.64	2.10	4.49	2.58

- Air Permeability

Table 6-14 lists the results of air permeability for denim fabric and twill fabric samples. From the Table, it can be seen that the air permeability of denim fabrics and twill fabrics with low torque ring yarns as weft yarns is lower than that of the fabrics made by conventional ring yarns and rotor yarns at normal twists as weft yarns. This discrepancy seems to be from the fact that the low torque ring yarns when compared to conventional ring yarns and rotor yarns of normal twist level, being the lower bending rigidity yarn, and the bulkier yarn due to using lower twist level, results in the thicker fabric and better cover and is therefore less permeable to air.

Table 6-14 Air Permeability of Fabric Samples

Fabric sample	1	2	3	10	11	12	13	14	15
Air permeability ($ml/cm^2.s$)	2.9	2.5	4.0	14.63	20.00	19.69	14.88	17.56	19.35

- Wicking Property

Wicking is an important property relating to clothing comfort. Figure 6-3 shows the average wicking curve for three types of fabric samples. As shown in Figure 6-3, the rate of water rise of Sample 12 is slower than that of Samples 10 and 11, particularly at the beginning of the water absorption, which is probably due to the reduction of capillary channel by the presence of randomly arranged fibers in the rotor yarns.

There is no significant difference in the rate of water rise among these three types of fabric samples. On one hand, the lower yarn twist level was adopted in low torque ring yarns and yarn diameter increased compared to that of normal twist conventional ring yarns and rotor yarns, which probably increases the number and diameter of the capillary channels between the fibers in the low torque ring yarns and thus increase the rate of water rise in fabric when low torque ring yarns were used as weft yarns. However, on the other hand, it is also logical to suggest that the increase in the thickness and cover of fabric produced from low torque rings as weft yarns, as reveled in Table 6-12, may result in the decrease of the rate of water rise in fabric.

Table 6-14 presents the amount of water absorbed by fabric during wicking. From the Table, it can be seen that the amount of water taken up by Sample 10 in which low torque ring yarns were used as weft yarns is more than those of Samples 11 and 12 where normal twist conventional ring yarns and rotor yarns were used as weft yarns respectively. The results of multiply comparison LSD test indicate that there is significant difference on the amount of water absorbed by fabric between Sample 10 and Sample 11 at the 0.05 level. It is known that the mass of the water that is taken up by fabric depends on the height the water has raised to, the thickness of the fabric and the water-holding power of the fabric structure. With similar wicking height after wicking time of 600 seconds, Sample 10 shows a higher absorption of the mass of water compared with Sample 11 and Sample 12. The increase of the mass of water absorbed by fabric when low torque ring yarns were used may come from the

improvement in bulkiness of the yarn and thickness of the fabric.

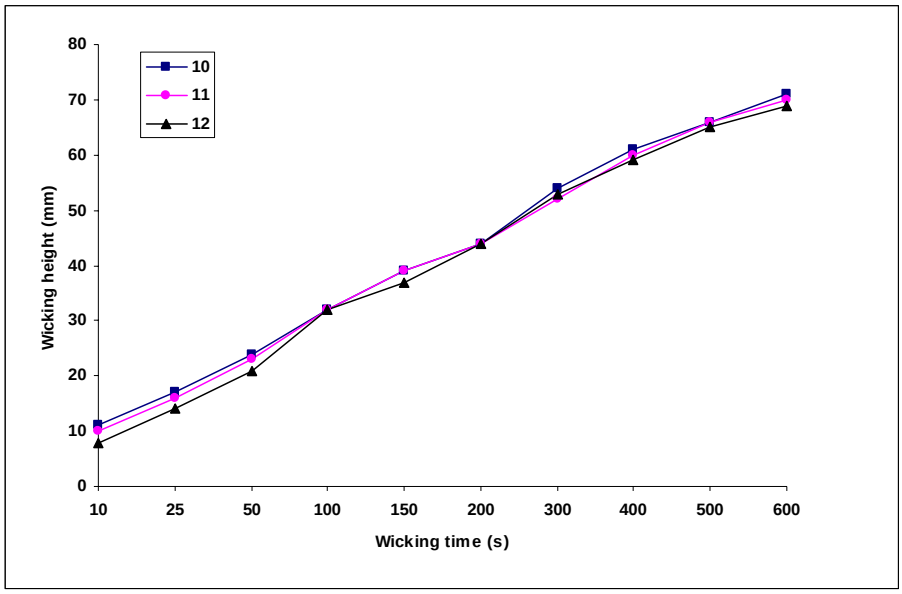

Figure 6-3 Average Wicking Curve for Fabric Samples

Table 6-15 The Amount of Water Absorbed by Fabric Samples during Wicking

Fabric sample	10	11	12
Water absorbed by stripe (%)	40.7	38.2	38.5

- Appearance

Conventionally, denim is a heavy 3/1 twill fabric made from 100% cotton with dyed warp yarn and undyed weft yarn. The surface of denim fabric has the possibility of becoming uneven after garment washing. A group o f white and light color warp

streaks forms what is usually called ‘small snake’ pattern on the fabric surface (Figure 6-4). Yarn residual torque particularly on weft yarns is believed to be one of the prominent factors contributing to the surface unevenness of denim fabric. Therefore, the reduction of weft yarn residual torque brings benefits to the internal stress balance in the denim fabric, thus improving the surface smoothness appearance of denim. Figure 6-5 presents photographs of two denim fabric samples and the fabric smoothness appearance is evaluated based on 5 grade scales. The evaluation shows that the smoothness grade of Fabric Sample 1 reaches grade 4 while Fabric Sample 3 only gets grade 2, which means that the ‘small snake’ pattern decreased greatly and thus the appearance of denim fabrics improved significantly when using the low torque ring yarns as weft yarns due to lower yarn residual torque in Sample 1. Moreover, this smoothness improvement concomitantly brings a more prominent slub effect in warp direction of denim when slub yarns are used as warps. An investigation of effect of yarn residual torque on the denim fabric surface smoothness will be reported in detail in the following Chapter. In addition, the better fabric surface smoothness of low torque ring yarn fabric, as revealed by KES-FB examination, may bring benefits to the improvement of fabric luster.

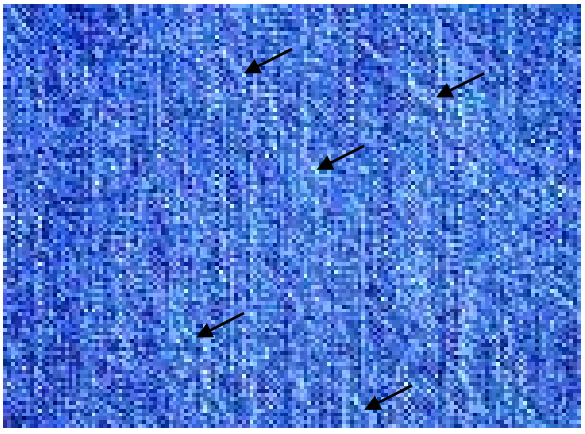

Figure 6-4 ‘Small Snake’ Pattern on the Fabric Surface (as arrows indicate)

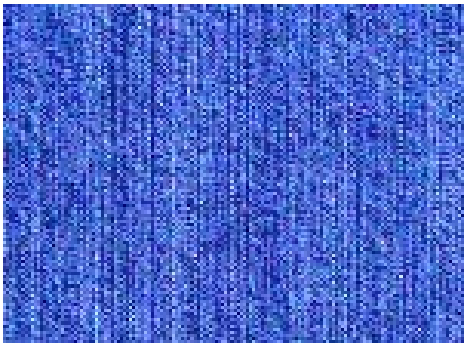

Fabric Sample 1

(slight ‘small snake’)

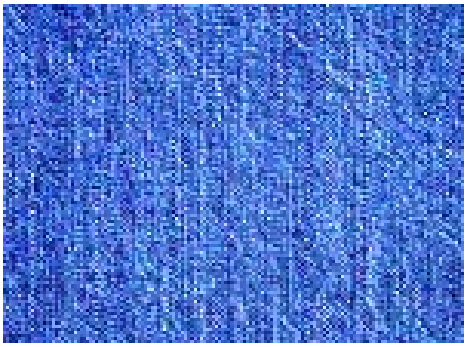

Fabric Sample 3

(severe ‘small snake’)

Figure 6-5 Photographs of Denim Fabric Appearance

6.4 Subjective Evaluation of Denim Jeans and Twill Trousers

Low torque ring yarns differ from conventional ring yarns and rotor yarns in both structure and properties**.** These new characteristics of low torque ring yarns will no doubt be brought into downstream fabrics in subsequent production. The objective tests in the previous section revealed that the surface smoothness and fullness of low torque ring yarn fabrics are better than those of conventional ring yarn fabrics and rotor yarn fabrics. The fabrics made from low torque ring yarns are also found to be thicker than that of fabrics produced by conventional ring yarns and rotor yarns. The air permeability of low torque ring yarn fabrics is lower than those of conventional ring yarn and rotor yarn fabrics.

The results of objective measurements on fabrics are not always well correlated with end-use performance, and this relationship is a special problem when new products are developed. Wear studies are frequently used to evaluate the end-use performance of garments and to verify the value of objective tests that are routinely used to predict performance (Morris and Prato, 1978; Lau and Fan, 2002). Therefore, a study was carried out to evaluate the comparative performance of the end-products (jeans and trousers) produced by low torque ring yarns with conventional ring yarns and rotor yarns through actual wearing and washing trials in the following Section.

6.4.1 Methods

6.4.1.1 Clothing and Subjects

Three jean samples were tested in the study. The low torque ring yarn jeans were produced by fabrics with low torque ring yarns as weft yarns, the conventional ring yarn jeans were made by denim fabric using conventional ring yarns as weft yarns, while the rotor yarn jeans were made from fabric by rotor yarns as weft yarns. The specification of these three types of fabrics (Sample 4, Sample 5 and Sample 6) is listed in Table 6-3.

In this study, three types of fabrics for trousers were also produced using low torque ring yarns, conventional ring yarns and rotor yarns as weft yarns, respectively. Table 6-3 presents the specification of three types of twill fabrics namely Samples10, 11 and 12. Ten pieces of twill trousers were made from each of the fabrics for use in the wear phase of the study.

All these six types of fabrics were measured objectively on fabric properties and performance in the earlier study.

For jeans investigation, one male research student was asked to participate in the wear phase. Then ten male and ten female research students and staffs were invited to evaluate appearance and performance of jeans before and after wearing and washing.

Ten male research students and staffs were invited to take part in the wear phase of twill trousers. After that, twenty subjects (ten male and ten female research students and staffs) were asked to do the subjective and comparative assessments on twill trousers performance.

All research students and staffs came from The Hong Kong Polytechnic University with experience in fabric performance assessment. Table 6-16 shows the background of the subjects.

Table 6-16 Background of the Subjects

Sex	Male (10)	Female (10)	
Age range	Below 25 (6)	26 to 40 (10)	41 or above (4)
Wearing time with similar jeans per week	Not very often (6)	1-3 days a week (5)	4 days or above (9)
Wearing time with similar trousers per week	Not very often (7)	1-3 days a week (10)	4 days or above (3)

6.4.1.2 Procedures

- Wear Procedures

One participant was given three pieces of jeans for the jeans wear trial, while each of the other ten participants received three pieces of trousers for the trousers wear trial. The period of wearing time for each sample was around 10 hours and the wearing sequence was not specified. The wearing conditions can be varied from clerical work to active work etc. Measurements were conducted on before wearing and washing

and after five wearing and washing cycles. The washing cycle comprised machine wash hot 49°C and tumble dry high for jeans and machine wash cold 27°C and tumble dry low for trousers following AATCC 135.

- Wear Evaluation

Before wearing and after five wearing and washing cycles, ten male and ten female participants were asked to do the subjective and comparative assessments on jeans and trousers performance. In addition, ten male wearers of trousers were asked to do the subjective and comparative assessments on trousers wear comfort after every wear cycle.

During subjective assessment, subjects were asked to arrive at an air-conditioned testing laboratory (20 ± 2°C and 65 ± 2% RH) 15 min before the assessment started so as to become familiar with the environment and the pertinent evaluation information such as the special attributes of jeans and trousers to be evaluated as listed in Table 6-17, the rating scale to be used and the number of jeans and trousers to be rated and compared. Assessment was made under AATCC 124 standard lighting and viewing environment in the testing laboratory.

Table 6-17 Attributes of Jeans and Trousers

Attributes evaluation of jeans	
Before wearing and washing	After five wearing and washing cycles
The smoothness is good.	The smoothness is good.
The ‘small snake’ pattern is not significant.	It does not fuzz.
The slub effect in warp direction is obvious.	The ‘small snake’ pattern is not significant.
The softness is good.	The slub effect in warp direction is obvious.
The overall quality is good.	The softness is good.
-	The overall quality is good.
Attributes evaluation of trousers	
Before wearing and washing	After five wearing and washing cycles
The luster is good.	The luster is good.
The smoothness is good.	The smoothness is good.
The fullness is good.	It does not fuzz.
The stiffness is acceptable.	The fullness is good.
The overall quality is good.	The stiffness is acceptable.
-	The overall quality is good.

According to the 5-point Likert Scale of Summated Rating, 0-5 scale was used for jeans and trousers evaluation with the description being summarized in Table 6-18. The level of agreement can be rated by select the appropriate rating of choice.

Table 6-18 Scale of the Level of Agreement

Scale	1	2	3	4	5
Level	strongly disagree	disagree	neutral	agree	strongly agree

The samples of jeans and trousers were on the hangers and hung at the centre of the viewing board. Standing in a close range from the samples, the subjects viewed the surface appearance of jeans and trousers and touched them with the fingers, thumb and palm of the hand. Ratings were then given by subjects according to the degree of agreement from 1 to 5. During evaluation, comparative ratings should be considered to indicate if there were any differences between the samples. One-way analyses of variance were performed on the data and the sample means were compared with each other. The results were evaluated using significant test at 0.05 level and a multi-comparison test called LSD was performed using SPSS packet program.

Before wearing and after five wearing and washing cycles, dimensional stability and skewness of jeans and trousers were measured according to AATCC 135 (Method A) and AATCC 179 (Method A) respectively.

At the conclusion of the subjective evaluation, a questionnaire was given to the subjects. With three pieces of jeans and trousers, the questions were answered about their performance.

6.4.2 Results and Discussions

6.4.2.1 Subjective Evaluation of Appearance and Performance

Subjective rating on jeans appearance and performance is shown in Figure 6-6 to Figure 6-11. One-way analysis of variance was performed on the data in order to test and assess if there was a significant difference between the means of samples with different types of weft yarns at 0.05 level. In the analysis, the sample means were compared and the data referring to the samples are given in Table 6-19. From the Figures and Table, it is found that the jean sample produced by the low torque ring weft yarn fabric has significant advantages of better jean smoothness appearance, less 'small snake' pattern, more prominent slub effect in warp direction and overall quality than the samples produced by the conventional ring yarns and rotor yarns. When low torque ring yarns with low residual torque were introduced into denim fabrics used as weft yarns, the 'small snake' pattern on fabric surface, which is largely caused by high weft yarn residual torque, is greatly reduced and thus the fabric surface smoothness improved significantly. The objective measurement of denim fabric and subjective assessment of fabric appearance in the previous Section showed a similar trend. The results measured by KES-FB Surface Tester demonstrated that the value of mean deviation of friction (MMD) and geometrical roughness (SMD) of fabrics using low torque ring yarns as weft yarns is lower compared to that of fabrics using conventional ring yarns and rotor yarns as weft yarns, which probably indicate that the smoothness and the evenness of the low torque ring yarn fabric surface are better than that of other conventional fabrics.

The objective evaluated handle also means that the fabric representing low torque ring yarns used as wefts obtained higher value in Numeir compared with that of fabrics with conventional ring yarns and rotor yarns as wefts. Moreover, with less 'small snake' pattern and better smoothness of fabric, the jeans exhibits a better prominent slub effect in the warp direction of denim when slub yarns were used as warp yarns. The distinguished jeans appearance improvement with less 'small snake' pattern and better prominent slub effect on the denim surface is a success for low torque ring yarns being applied in denim.

In addition, the softness of low torque ring weft yarn woven fabric is better than that of rotor weft yarn woven fabric. But the softness of jeans made by low torque ring weft yarn woven fabrics does not show any significant advantages over the jeans made by conventional weft yarn woven fabric. The possible reason is that even though the measurement of KES- FB Tester showed a higher value in Fukurami of low torque ring yarn denim fabric compared to other conventional denim fabrics, probably due to the higher compression energy (WC) and lower mean deviation of friction (MMD) of low torque ring yarn fabric, the higher fabric bending rigidity, shear rigidity and thickness in low torque ring yarn fabric presented by KES-FB measurement also affect handle feeling in such an evaluation.

Figures 6-12, 6-13, 6-14, 6-15, 6-16 and 6-17 present the subjective rating on trousers appearance and performance and Table 6-20 shows the results of multiply comparison LSD test for trousers' subjective evaluation. As shown in the Figures

and Table, the low torque ring twill trousers has significant advantages of better luster, better smoothness appearance and better overall quality than the other two trousers made from conventional ring yarn fabric and rotor yarn fabric particularly after five cycle wearing and washing. Like jeans, the objective test results from KES-FB Surface Tester indicated that the fabric, when low torque yarns were used as weft yarns, possesses lower value of mean deviation of friction (MMD) and geometrical roughness (SMD) and higher value of fabric compression energy (WC) of fabric. In addition, the change for the better luster of the low torque ring twill trousers exhibited in subjective evaluation is also related to this surface smoothness improvement.

The Figures also show that the fullness of trousers produced by low torque ring twill fabric is slightly better than that of trousers made from the conventional ring yarn and rotor yarn twill fabrics, however, no significant difference was found among them. In addition, all three trousers showed less fuzzy appearance.

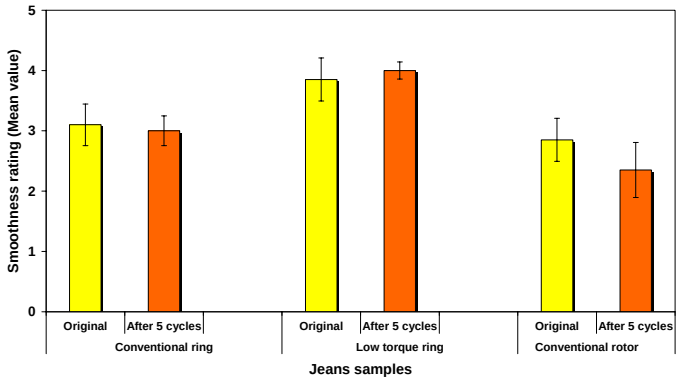

Figure 6-6 Subjective Evaluation on Smoothness of Jeans

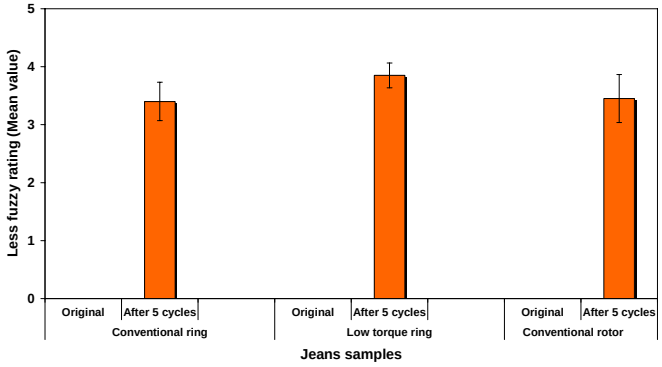

Figure 6-7 Subjective Evaluation on Fuzz of Jeans

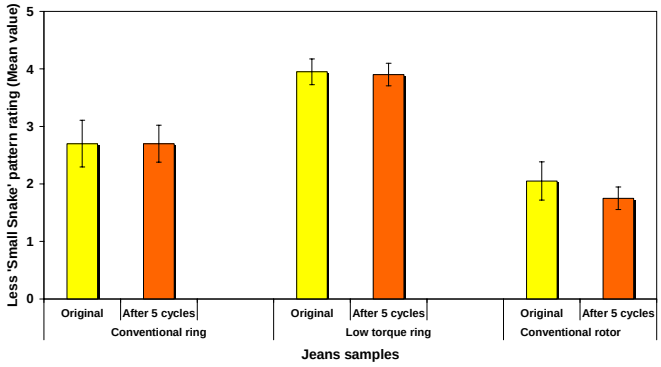

Figure 6-8 Subjective Evaluation on ‘small snake’ Pattern of Jeans

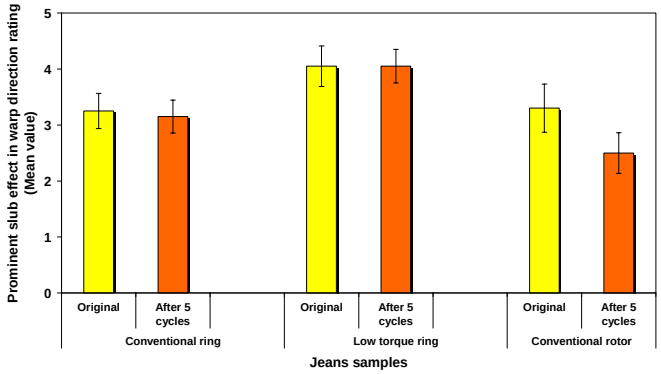

Figure 6-9 Subjective Evaluation on Prominent Slub Effect of Jeans

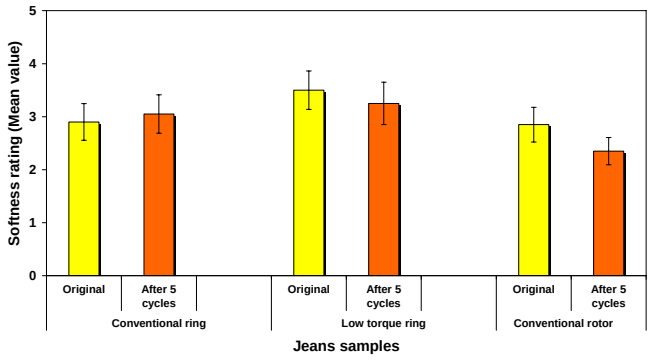

Figure 6-10 Subjective Evaluation on Softness of Jeans

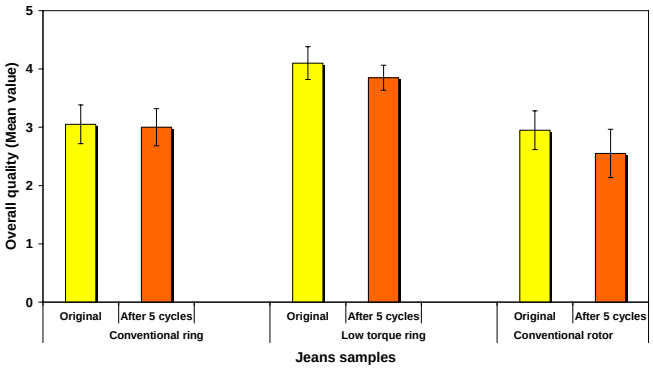

Figure 6-11 Subjective Evaluation on Overall Quality of Jeans

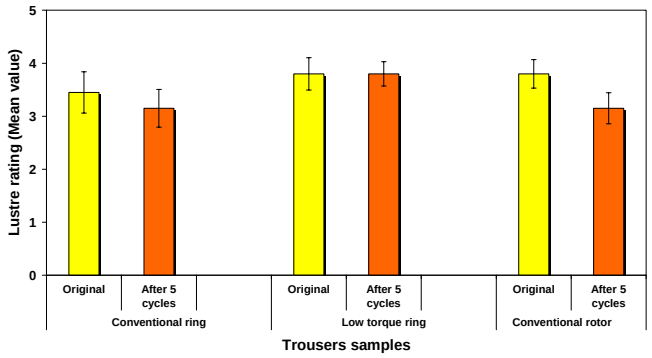

Figure 6-12 Subjective Evaluation on Luster of Trousers

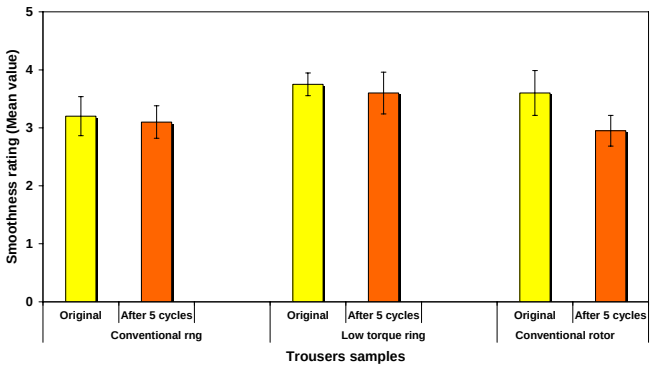

Figure 6-13 Subjective Evaluation on Smoothness of Trousers

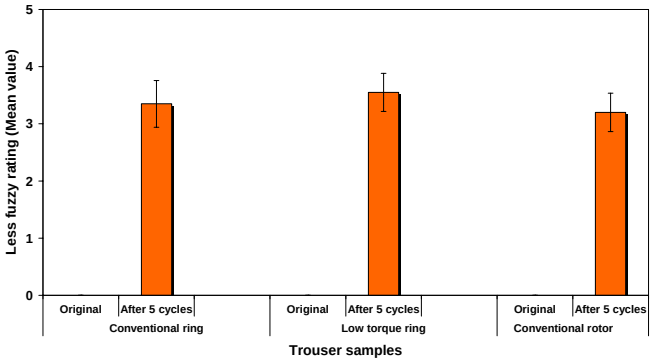

Figure 6-14 Subjective Evaluation on Fuzz of Trousers

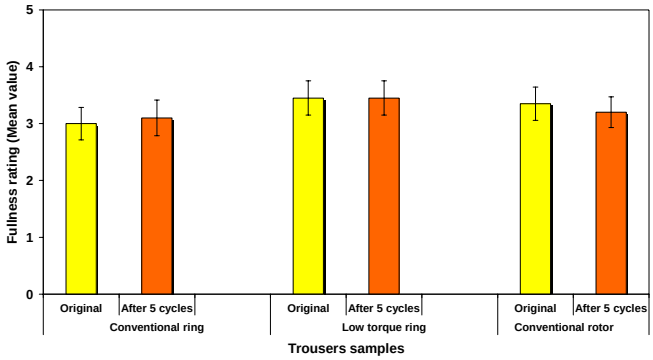

Figure 6-15 Subjective Evaluation on Fullness of Trousers

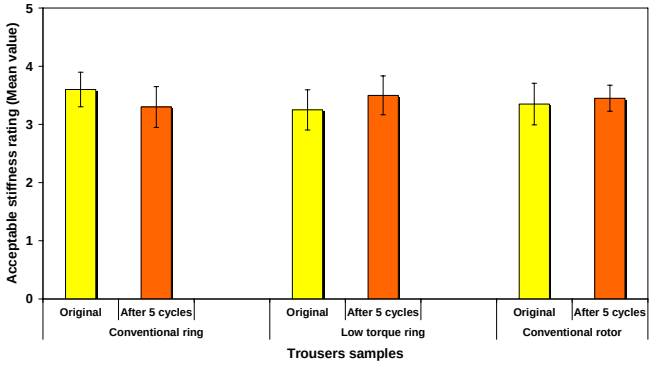

Figure 6-16 Subjective Evaluation on Acceptable Stiffness of Trousers

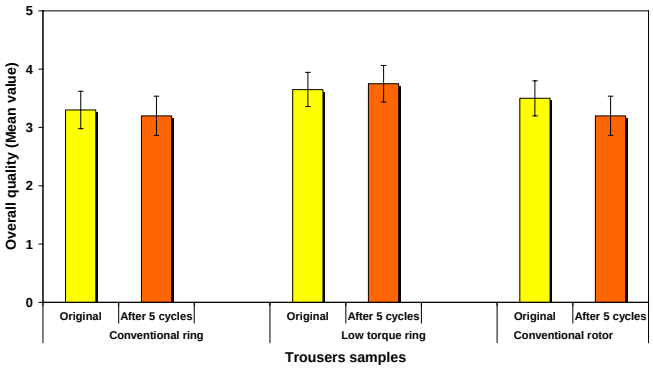

Figure 6-17 Subjective Evaluation on Overall Quality of Trousers

Table 6-19 Results of Multiple Comparisons LSD Test for Jeans' Subjective Evaluation

Original jeans									
Sample	Sample	Smoothness		Small snake		Slub effect		Overall quality	
		Mean Dif.	Sig.	Mean Dif.	Sig.	Mean Dif.	Sig.	Mean Dif.	Sig.
Low torque ring jeans[a]	Ring jeans[a]	0.75*	0.005	1.25*	0.000	0.80*	0.004	1.05*	0.000
	Rotor jeans[a]	1.00*	0.000	1.90*	0.000	0.75*	0.007	1.15*	0.000
Jeans after 5 cycle wearing and washing									
Sample	Sample	Smoothness		Small snake		Slub effect		Overall quality	
		Mean Dif.	Sig.	Mean Dif.	Sig.	Mean Dif.	Sig.	Mean Dif.	Sig.
Low torque ring jeans	Ring jeans[a]	1.00*	0.000	1.20*	0.000	0.90*	0.000	0.85*	0.001
	Rotor jeans[a]	1.65*	0.000	2.15*	0.000	1.55*	0.000	1.30*	0.000

[a] Low torque ring jeans, ring jeans and rotor jeans are jeans produced by low torque ring yarn fabrics, conventional ring yarn fabrics and conventional rotor yarn fabrics respectively.

* The mean difference is significant at the 0.05 level

Table 6-20 Results of Multiple Comparisons LSD Test for Trousers' Subjective Evaluation

Original trousers							
Sample	Sample	Luster		Smoothness		Overall quality	
		Mean Dif.	Sig.	Mean Dif.	Sig.	Mean Dif.	Sig.
Low torque ring trousers[a]	Ring trousers[a]	0.35	0.141	0.55*	0.019	0.35	0.118
	Rotor trousers[a]	0.00	1.000	0.15	0.514	0.15	0.499
Trousers after 5 cycle wearing and washing							
Sample	Sample	Luster		Smoothness		Overall quality	
		Mean Dif.	Sig.	Mean Dif.	Sig.	Mean Dif.	Sig.
Low torque ring trousers	Ring trousers[a]	0.65*	0.004	0.50*	0.027	0.55*	0.024
	Rotor trousers[a]	0.65*	0.004	0.65*	0.005	0.55*	0.024

[a] Low torque ring trousers, ring trousers and rotor trousers are jeans produced by low torque ring yarn fabrics, conventional ring yarn fabrics and conventional rotor yarn fabrics respectively.

* The mean difference is significant at the 0.05 level.

As revealed in Table 6-21 and Table 6-22 about the consistency of the subject's ratings, very extreme ratings given by one subject compared to others can not be found. In comparison with the lowest rating given by M5 for jeans and F8 for trousers, there was only 0.5 grade lower than the average rating (2.7 compared to 3.2) for jeans and (2.9 compared to 3.4) for trousers, therefore, the rating given by subjects can be considered as relatively consistency.

Table 6-21 The Consistency of the Subject's Ratings of Jeans

Subjects	Total amount of the ratings given by the individual subject						Overall Total	Average of 33 answers
	Smoothness (30)	Fuzz (15)	Small snake (30)	Slub (30)	Softness (30)	Overall (30)		
M 1	18	12	18	18	18	18	102	3.1
M 2	18	12	21	18	18	18	105	3.2
M 3	18	12	19	22	18	18	107	3.2
M 4	19	9	18	19	18	18	101	3.1
M 5	16	8	16	16	18	16	90	2.7
M 6	16	9	18	18	17	18	96	2.9
M 7	18	10	18	22	22	22	112	3.4
M 8	24	11	19	20	20	21	115	3.5
M 9	23	12	17	24	15	17	108	3.3
M 10	15	12	16	22	14	24	103	3.1
F 1	23	12	18	24	21	26	124	3.8
F 2	20	11	20	21	18	18	108	3.3
F 3	17	8	15	18	16	18	92	2.8
F 4	19	12	14	25	19	25	114	3.5
F 5	18	13	16	24	15	21	107	3.2
F 6	18	12	16	18	14	18	96	2.9
F 7	22	12	16	21	20	20	111	3.4
F 8	22	12	17	20	20	20	111	3.4
F 9	18	6	12	17	17	15	85	2.6
F 10	21	9	17	19	20	19	105	3.2
						Average	105	3.2
						CV%	7.0	7.0

Table 6-22 The Consistency of the Subject's Ratings of Trousers

Subjects	Total amount of the ratings given by the individual subject						Overall Total	Average of 33 answers
	Fuzz (15)	Luster (30)	Smoothness (30)	Fullness (30)	Stiffness (30)	Overall (30)		
M 1	8	24	23	20	19	21	115	3.5
M 2	12	22	16	19	18	16	103	3.1
M 3	12	22	22	20	20	20	116	3.5
M 4	9	19	22	20	21	21	112	3.4
M 5	10	24	22	22	23	20	121	3.7
M 6	10	18	19	20	19	23	109	3.3
M 7	12	22	20	21	21	20	116	3.5
M 8	12	24	24	21	21	23	125	3.8
M 9	12	22	18	19	22	22	115	3.5
M 10	9	21	20	20	19	20	109	3.3
F 1	12	20	20	20	22	19	113	3.4
F 2	12	25	22	19	24	25	127	3.8
F 3	9	18	18	18	18	18	99	3.0
F 4	6	26	21	21	24	24	122	3.7
F 5	9	18	21	18	18	24	108	3.3
F 6	10	20	18	17	22	20	107	3.2
F 7	12	22	20	22	20	22	118	3.6
F 8	8	17	19	21	20	18	103	3.1
F 9	7	20	18	16	17	17	95	2.9
F 10	11	19	21	17	21	19	108	3.3
					Average		112	3.4
					CV%		7.5	7.5

6.4.2.2 Measurement of Dimensional Stability and Skewness

The experimental results of the dimensional stability and skewness of jeans and trousers after five wearing and washing cycles are shown in Table 6-23 and Table 6-24 respectively. From the Tables, it can be seen that the jeans produced by denim fabric using low torque ring yarns as weft yarns possesses similar or slightly lower dimensional change and skewness after five wearing and washing cycles compared to jeans made by fabrics using conventional ring yarns and rotor yarns as weft yarns. It is because the dimensional stability and skewness of garment mainly depend on the dimensional stability and skewness of fabric used if no distortion is caused by garment manufacturing.

Like jeans, the trousers produced by low torque ring twill fabric exhibits similar trend in the dimensional stability and skewness compared with trousers made by conventional ring and rotor weft yarn woven fabrics. No significant difference has been found among these three types of trousers.

Table 6-23 Dimensional Stability and Skewness of Jeans

Jeans	After five wearing and washing cycle				
	Length of jean		Width of leg		Skewness (%)
	Inlength	Outlength	Length of crease line	Length of seam	
Conventional ring yarn jeans	-1.51	-1.83	-1.92	-1.63	1.43
Low torque ring yarn jeans	-0.67	-1.78	-1.07	-1.18	0.72
Conventional rotor yarn jeans	-1.44	-2.13	-1.92	-1.20	1.26

Table 6-24 Dimensional Stability and Skewness of Trousers

Trousers	After five cycle wearing and washing				
	Length of jean		Width of leg		Skewness (%)
	Inlength	Outlength	Length of crease line	Length of seam	
Conventional ring yarn jeans	-2.6	-2.7	-0.8	-0.9	1.0
Low torque ring yarn jeans	-2.5	-2.2	-0.9	-0.4	0.8
Conventional rotor yarn jeans	-2.6	-2.5	-1.0	-0.7	1.3

6.4.2.3 Overall Subjective Evaluation

Copy of the questionnaire given to the subjects of the jeans, with the responses summarized, is shown in Table 6-25. The majority of subjects preferred the jeans produced by low torque ring weft yarn denim fabric to jeans made from conventional ring weft yarn and rotor weft yarn fabrics since the jeans made from low torque ring yarn fabrics possesses more even and lighter fabric colour, less 'small snake' pattern, more prominent slub effect, better softness and better surface smoothness and evenness when compared to jeans produced by conventional weft yarn fabrics and rotor weft yarn fabrics.

Based on the assessments of wearing comfort and subject's answers revealed in Table 6-26, twill trousers produced by low torque ring weft yarn fabrics show slightly better wear comfort than that of the other two twill trousers.

Table 6-25 Questions Given to Subjects and Summary of Their Answers on Jeans

Questions given to subjects	Which pair of jeans do you prefer?		
Jean samples	Conventional ring jeans[a]	Low torque ring jeans[a]	Conventional rotor jeans[a]
Number of subjects	4	15	1
Reasons for preference (number of subjects)	Preferred dark colour of fabric (2)	Preferred more even and lighter fabric colour (9)	Preferred old fashion (1)
	Preferred ‘small snake’ pattern (2)	Didn’t preferred ‘small snake’ pattern (8)	
	Preferred fabric appearance (2)	Preferred prominent slub effect (7)	
		Preferred better softness (6)	
		Preferred surface evenness and smoothness (6)	
		Preferred better over quality (2)	

[a] Low torque ring jeans, conventional ring jeans and conventional rotor jeans are jeans produced by low torque ring yarn fabrics, conventional ring yarn fabrics and conventional rotor yarn fabrics respectively.

Table 6-26 Questions Given to Subjects and Summary of Their Answers on Trousers

Questions given to subjects		Which pair of trousers is more comfort to wear?					
Wear cycle		1	2	3	4	5	Total
Answers and number of subjects	Same	5	6	5	3	2	21
	Low torque ring trousers[a] was better than conventional ring trousers[a]	3	2	3	4	5	17
	Low torque ring trousers was better than rotor trousers[a]	3	2	3	5	6	19
	Conventional ring trousers was better than low torque ring trousers	2	2	2	3	2	11
	Rotor trousers was better than low torque ring trousers	2	2	2	2	1	9

[a] Low torque ring trousers, conventional ring trousers and rotor trousers are trousers produced by low torque ring yarn fabrics, conventional ring yarn fabrics and conventional rotor yarn fabrics respectively.

6.5 Summary and Conclusion

This Chapter reports the properties of low torque ring yarn and characteristics of fabrics produced. The introduction of false-twisting operation during yarn formation gives low torque ring yarn a new fiber and yarn configuration, and thus the characteristics of low torque ring yarn are different from those of conventional ring

yarn. The yarn properties presented in this Chapter exhibit some exciting features of low torque ring yarn that, after modification, yarn snarling is greatly reduced and yarn hairiness shows a remarkable decrease. Even at low twist level, low torque ring yarn can still maintain its yarn tenacity and evenness comparable to conventional ring yarn with normal twist level. Compared to conventional ring yarn at the same low twist level, low torque ring yarn presents significant advantages of lower yarn snarling, less yarn hairiness and higher yarn strength particularly after yarn winding process.

A detailed depiction of characteristic changes generated in the fabrics as well as the reasons for these changes are presented in this Chapter, demonstrated by improved denim fabric and twill fabric appearance, a fuller, thicker and more smooth hand. The distinguished jeans appearance improvement with less ‘small snake’ pattern and more prominent slub effect on the denim surface is a success for low torque ring yarn being applied in denim. In fabric wicking property test, the low torque ring yarn fabric shows similar wicking rate but higher wicking amount of water. The fabric also exhibits satisfactory levels of mechanical properties such as tensile strength and tearing strength when low twist level was adopted in weft yarn.

Subjective evaluation of jeans and twill trousers, produced by low torque ring yarn fabrics, is made and compared to those made from conventional ring yarn fabric and rotor yarn fabric through actual wear trial. It is further confirmed that the low torque ring weft yarn fabric has advantages of better jean smoothness appearance, less

'small snake' pattern, better prominent slub effect in warp direction and overall quality than the samples produced by the conventional ring yarns and rotor yarns. The twill trousers produced by low torque ring fabrics also show some benefits such as better luster, better smoothness appearance and better overall quality than the other two conventional ring and rotor yarn trousers.

In addition, since low torque ring yarns are only used as weft yarns of the fabrics in the present study, there are needs to further investigate the fabrics made from low torque ring yarns in both the warp and weft direction.

CHAPTER 7 EFFECT OF YARN TORQUE ON SURFACE SMOOTHNESS OF DENIM FABRIC

7.1 Introduction

Denim is perhaps the most used item of clothing and is the single fabric which has been produced in such large quantities. Conventionally, denim is a heavy 3/1 twill fabric made from 100% cotton with indigo dyed warp yarn and undyed weft yarn. Through modern technology, denims have been improved in quality and provided a satisfactory level of comfort and durability to consumers. However, the surface of denim fabric has the possibility of becoming uneven after garment washing, particularly when heavier count yarns are used. A group of white and light color warp streaks forms what is usually called ‘small snake’ pattern on the fabric surface. It affects the fabric’s appearance, smoothness and soft handle and thus the aesthetics and comfort of apparel made from it.

The ‘small snake’ pattern of denim is a complex phenomenon arising from many factors such as yarn count, yarn twist multiple, twist direction, weave, direction of twill and fabric count. The main factor contributing to the formation of ‘small snake’ pattern is the yarn residual torque particularly on weft yarns. After yarn dyeing and sizing, the warp yarn residual torque is greatly reduced. When fabrics are subject to water, hygral expansion and relaxation shrinkage occur. Moreover, the local yarn buckling is activated which distorts the fabric and results in the formation of ‘small snake’ pattern on the denim surface. As we know, when a cotton yarn is dyed with indigo, ring dyeing effect is created. The outer layer of the warp yarn is coated with indigo and the core of the yarn remains undyed, which gives the indigo denim the unique characteristic of washdown effect. During washing, the raised parts (warp yarn) of fabric surface get greater washing effect than the other parts of the fabric. Some portions of surface fibers and dyes of the raised parts of fabric surface are rub off by abradant, thus the ‘fad look’ of denim became uneven. Therefore, the reduction of weft yarn residual torque probably brings benefits to the internal stress balance in the denim fabric, thus improving the surface smoothness appearance of denim.

Although research work has been conducted to determine the effect of washing technology on the surface appearance of denim fabric (Tyndall, 1992; Yu, Szeto, Tao, Chong and Choy, 2001), no study on the effect of yarn residual torque on the ‘small snake’ pattern of denim has been reported. In Chapter 6, we reported that the low torque ring yarns were applied to denim fabrics and jeans with the excited results of improved denim fabric appearance in which less ‘small snake’ pattern and more

prominent slub effect were presented on the denim surface. Therefore, a theoretical probe and experimental study of the effect of yarn torque on the surface smoothness of denim fabric is of great significance, which forms the subject of this Chapter.

7.2 Theoretical Study of Surface Smoothness of Denim Fabric

In the past, several research works had been done on the effects of yarn twist or yarn torque on woven fabric properties and appearance. Whitman (1947) reported that the curl of woven textile fabrics is caused by the additive torque effects of the warp and filling sets of yarns. And if the warp and weft sets of yarns are similar in direction of twist and state of finish, the torque effect of one is opposite to that of the other. Backer (1953) and Backer, Zimmerman and Best (1956) investigated the relationship between the structural geometry of a textile fabric and its physical properties, particularity on the interaction of twist and twill direction as related to fabric structure and properties. They pointed out that the effects of twist and twill direction on fabric properties are ascribed to fiber nesting at the contact points between warp and weft yarns, and the nonsymmetric pressures at the side of a twill float promote later yarn displacement. Platt, Klein and Hamburger (1959) found that when one bends a twist yarn in a plane, it tends to develop a couple directed toward bucking the yarn out of that plane. And if there is no restraining matrix present, this three-dimensional bucking will take place as the usual accompaniment of ordinary bending of twisted structures. But when the yarn twist is extremely low, the motivation towards buckling is less and when the surrounding matrix resists the three-dimensional movement, the yarn will be restrained to bending in a plane. In the

study of yarn bending and buckling in fabric, Hearle, Grosberg and Backer (1969) gave an example of a fairly open fabric woven with a highly twisted yarn. The warp yarn in this example is highly bucked and has in effect assumed a helical configuration in the fabric. In another case, they explained the principle of puckered surface created in crepe fabrics with the yarns highly unstable from torsional point of view, but were woven into a fabric with a moderate degree of matrix restraint. If these yarns were made of a swellable fiber, immersing them in water will greatly increase their torsional energy. With such wetting, the torsional buckling which has been subdued before will take over, distorting the yarn structure, and, if similar instabilities occurred in the adjacent yarns, distorting the fabric structure into a puckered effect. In 1991, Ishikura, Kase and Nakajima investigated the crinkling mechanism of crepe in which the elastic curve of elastic body under distortion and tension was theoretically analyzed, and the relationship between torsional moment and tensile force, and buckling, when it occurred, was figured. A mechanical model was proposed by Komori and Itoh (2002) where the formation of pucker in a crepe fabric was analyzed as a post-buckling phenomenon which is induced by self-untwisting torque in the constituent yarns over-twisted.

Therefore, the studies indicate that the high twist liveliness or residual torque of the yarn causes yarn torsional buckling when yarn is bent in the fabric and no restraining matrix exists, which results in the puckering and distortion of the fabric surface. Figure 7-1 shows denim fabric surface in the closeup view. The grey fabric does not display obvious yarn buckling on the fabric surface. After this fabric was immersed in water and underwent enzyme pumice washing, the torsional energy of yarns was

greatly released and local yarn buckling was activated, which distorted the fabric and resulted in the formation of ‘small snake’ pattern on the denim surface.

Grey fabric

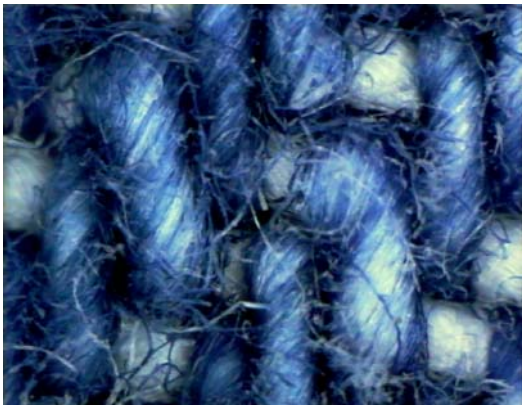

Enzyme pumice washed fabric

Figure 7-1 Denim Fabric Surface in the Closeup View

In this study, we attempt to theoretically analyze the effect of yarn residual torque on the surface smoothness of denim fabric. A typical 3/1 twill structure is considered in the present analysis since this weave structure is conventionally adopted in denim manufacture. Figure 7-2 presents an original shape of orthogonal 3/1 right-hand twill structure and a deformed shape of skewed 3/1 right-hand twill structure. Besides, because denim was made of dyed indigo warp yarns and grey weft yarns, the skew is affected by this imbalance (Deloach, 1976).

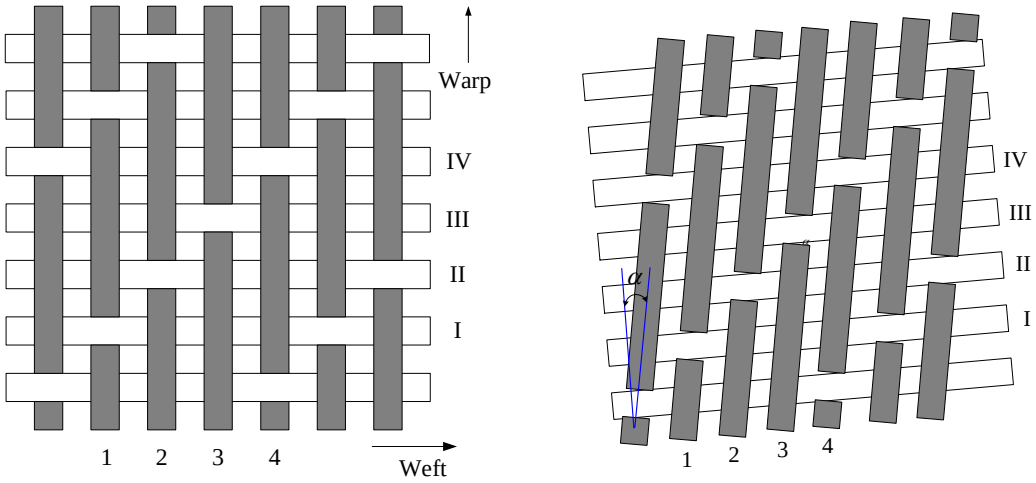

Original shape Deformed shape with skewness

Figure 7-2 Typical Shape of Denim Fabric (3/1 right hand-twill)

Figure 7-3 shows Peirce's structural model for a typical 3 up-1down weave structure where subscripts 1 and 2 represent warp and weft yarns respectively, x is the spacing of the weft yarns in one weave repeat, a_2 is the spacing of the weft yarns at the crossover point, b_2 is the spacing of adjacent sinking weft yarns, l_1 is the modular length of the warp yarn at the crossover point, h_1 and h_2 are the crimp height of the warp and weft yarns respectively, θ_1 and θ_2 are the crimp angles of the warp and weft yarns respectively, d_1 and d_2 are the diameters of the warp and weft yarns respectively, and D is the sum of diameters of the warp and weft yarns. In order to investigate theoretically the mechanism by which yarn residual torque affects 'small snake' pattern on the fabric surface, which may be a reflection of interaction of yarn residual torque between warp yarns and weft yarns, assumptions must be made. If it is assumed that warp yarn and weft yarn at the crossover points

closely contact each other, the adapted model for warp yarn float can be a fixed-ends rod with the weft yarn contacting at the point B, as showed in Figure 7-4. In addition, the yarn is assumed to behave as a cylindrical elastic rod and the force acting at the contacting region between warp yarn and weft yarn is assumed to be point force only.

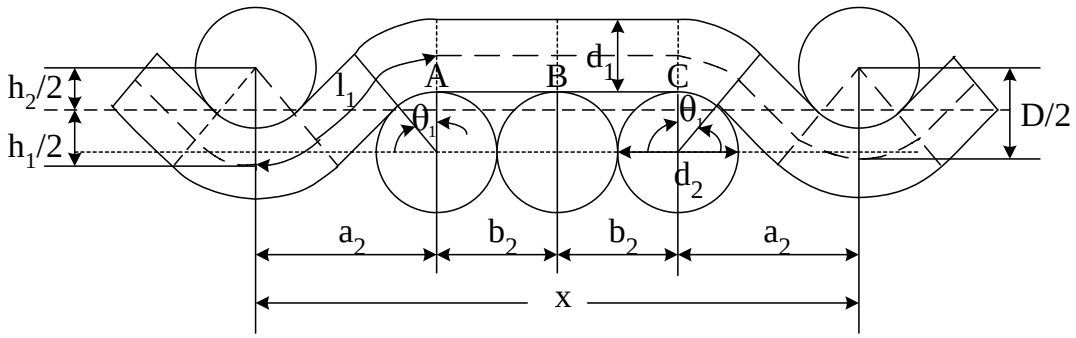

Figure 7-3 Geometry of Woven Fabric

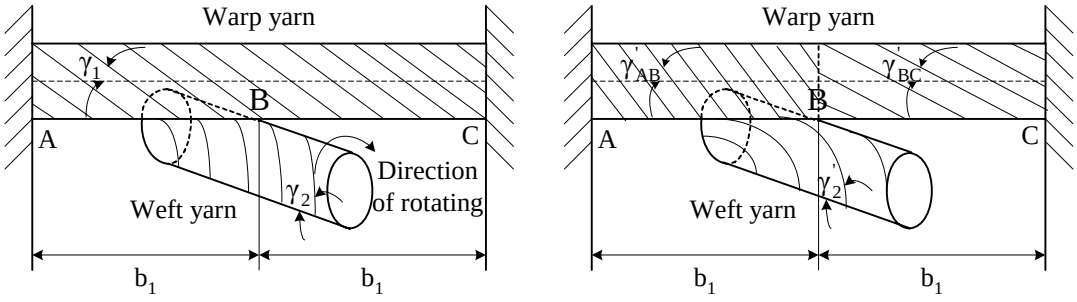

a. Original state b. State after weft yarn rotating

Figure 7-4 Schematic Diagram of a Fixed-ends Rod for Warp Yarn with Weft Yarn Contacting at Point B

The torsional deformation of a circular rod under a torque is well treated in the classical literature (Carig, 2000). For a cylindrical elastic rod, if the rod is subjected to a torque, the angle of the twist of the rod (ϕ) and the helix angle of the deformed surface (γ) are expressed as

$$\phi = \frac{ML}{IG} \tag{7-1}$$

$$\gamma = \arctan[\frac{R\phi}{L}] = \arctan[\frac{MR}{IG}] \tag{7-2}$$

where M is the torque exerted on the rod, L is the length of the rod, R is the radius of the rod, and I and G are rod polar moment of inertia and shear modulus of elasticity respectively.

In woven fabric, twisted warp yarn and weft yarn possess residual torques. Thus the torsional deformations of warp yarn and weft yarn shown on Figure 7-5a can be given by:

$$\phi_1 = \frac{M_1 L_1}{I_1 G_1} \tag{7-3}$$

$$\gamma_1 = \arctan[\frac{M_1 R_1}{I_1 G_1}] \tag{7-4}$$

$$\phi_2 = \frac{M_2 L_2}{I_2 G_2} \tag{7-5}$$

$$\gamma_2 = \arctan[\frac{M_2 R_2}{I_2 G_2}] \tag{7-6}$$

where ϕ_1 and ϕ_2 are the angles of twist of the warp and weft yarns respectively, M_1 and M_2 are the residual torques of the warp and weft yarns respectively, L_1 and L_2 are the lengths of the warp and weft yarns respectively, I_1 and G_1 are warp yarn polar moment of inertia and shear modulus of elasticity respectively, and I_2 and G_2 are weft yarn polar moment of inertia and shear modulus of elasticity respectively, γ_1 and γ_2 are the helix angles of the deformed surface of the warp and weft yarns respectively, R_1 and R_2 are the radius of the warp and weft yarns respectively,

Compared with warp yarns, weft yarns possess higher yarn residual torques in denim fabric due to warp yarn sizing and dyeing. When the highly unstable weft yarns from the torsional point of view were woven into a fabric and if there is no restraining

matrix present, the torsional energy of weft yarns will be released. As a result, the weft yarn probably rotates around its yarn axis to some extent and then reaches a new equilibrium condition of torque with its restraining matrix. If it is assumed that the original weft yarn torque is M_2 and the corresponding angle of twist of the weft yarn is ϕ_2, and after weft rotation the yarn torque decreases to M_2' and the angle of twist reduces to ϕ_2', the difference of the ϕ_2 and ϕ_2' can be given by:

$$\Delta\phi_2 = \phi_2 - \phi_2' = \frac{(M_2 - M_2')L_2}{I_2 G_2} \tag{7-7}$$

where $\Delta\phi_2$ is an additional angle of twist of the weft yarn due to weft yarn rotating.

It is further assumed that the pressure at contact point of warp and weft yarns (points B in Figure 7-5) is high and no relative rotating slippage occurs. Hence, the warp yarn probably rotates around its axis due to reactive torque from weft yarn. The additional angle of twist of the warp yarn due to weft yarn rotating depends on the additional angle of twist of the weft yarn and the inclination angle of warp yarn to the perpendicular line of weft yarn. The additional angle of twist of the warp yarn can be expressed as:

$$\Delta\phi_1 = C \cdot \Delta\phi_2 \tag{7-8}$$

where $\Delta\phi_1$ is an additional angle of twist of the warp yarn, $\Delta\phi_2$ is an additional angle of twist of the weft yarn, and C is the transmission coefficient between the rotation of weft yarn and warp yarn.

In the present model presented in Figure 7-5a, the relative angle of twist of the warp yarn between A and C is given by:

$$\phi_{AC} = \phi_1 = \frac{M_1 L_1}{I_1 G_1} \tag{7-9}$$

where $L_1 = 2b_1$.

Then the angle of twist of the warp yarn between A and B, and B and C can be obtained as follows:

$$\phi_{AB} = \phi_{BC} = \frac{M_1 b_1}{I_1 G_1} \tag{7-10}$$

After warp yarn rotates around its axis due to reactive torque from weft yarn, the angle of twist of the warp yarn between A and B, and B and C are given by:

$$\phi_{AB}' = \phi_{AB} + \Delta\phi_1 \tag{7-11}$$

$$\phi_{BC}' = \phi_{BC} - \Delta\phi_1 \tag{7-12}$$

where ϕ_{AB}' and ϕ_{BC}' are the relative angles of twist between A and B, and B and C respectively. Substituting for $\Delta\phi_1$ from Equation (7-8), ϕ_{AB} and ϕ_{BC} from Equation (7-10), and $\Delta\phi_2$ from Equation (7-7) gives:

$$\phi_{AB}' = \frac{M_1 b_1}{I_1 G_1} + C \cdot \frac{(M_2 - M_2')L_2}{I_2 G_2} \tag{7-13}$$

$$\phi_{BC}' = \frac{M_1 b_1}{I_1 G_1} - C \cdot \frac{(M_2 - M_2')L_2}{I_2 G_2} \tag{7-14}$$

Hence, the helix angles of the deformed surface shown on Figure 7-5b are expressed as:

$$\gamma_{AB}' = \arctan\left[\frac{M_1 R_1}{I_1 G_1} + C \cdot \frac{(M_2 - M_2')L_2 R_1}{I_2 G_2 b_1}\right] \tag{7-15}$$

$$\gamma_{BC}' = \arctan\left[\frac{M_1 R_1}{I_1 G_1} - C \cdot \frac{(M_2 - M_2')L_2 R_1}{I_2 G_2 b_1}\right] \tag{7-16}$$

The difference of the angle of twist between warp yarn sections AB and BC can be given by:

$$\Delta\phi_1' = \phi_{AB}' - \phi_{BC}' = 2C \cdot \frac{(M_2 - M_2')L_2}{I_2 G_2} \tag{7-17}$$

where $\Delta\phi_1'$ is the difference of the angle of twist between warp yarn sections AB and BC.

For circular yarns, the polar moment of inertia of cross section is given by:

$$I_2 = \frac{\pi R_2^4}{2} \tag{7-18}$$

where R_2 is the weft yarn radius.

Then, we obtain:

$$\Delta\phi_1' = \phi_{AB}' - \phi_{BC}' = 4C \cdot \frac{(M_2\text{-}M_2')L_2}{\pi R_2^4 G_2} \tag{7-19}$$

From the Equation (7-19), it can be seen that $\Delta\phi_1'$ is directly proportional to the magnitude of torque release in weft yarn (M_2-M_2'), the transmission coefficient between the rotation of weft yarn and warp yarn C, and the length of weft yarns L_2 while $\Delta\phi_1'$ is inverse proportional to weft yarn radius R_2 and shear modulus of elasticity G_2. The weft yarn radius R_2 and the length of weft yarns L_2 are determined by the fabric specification. The transmission coefficient C depends on the inclination angle of warp yarn to the perpendicular line of weft yarn α. For reduction of fabric skewness, α needs to be reduced for better fabric performance. M_2' also depends on the fabric specification. Therefore, reducing weft yarn residual torque M_2 will decrease the difference of the angle of twist between warp yarn sections AB and BC. As a result, the yarn buckling unevenness in warp yarn float may be decreased, which endows denim a more smooth surface and thus decrease the problem of 'small snake' pattern on denim fabric.

7.3 Experimental Study of Surface Smoothness of Denim Fabric

As indicated in the theoretical study, the reduction of weft yarn residual torque may bring benefits for the improvement of denim fabric surface appearance. Therefore, an experimental investigation was carried out for the improvement of surface

smoothness in denim fabric.

7.3.1 Yarn and Fabric Sample Preparation

A carded cotton roving of 952tex (0.62Ne) was used to spin 84tex conventional ring yarns (C) and low torque ring yarns (NS) with twist factors of 4.2, 3.8, 3.5, 3.2 and 3.0, and 58tex yarns with twist factors 4.2, 3.8, 3.6, 3.3 and 3.1 on the modified Ring Spinning Machine. Details of the yarns are listed in Table 7-1. The cotton fibers had a micronaire value of 4.0, a 2.5% span length of 28.7mm, a bundle strength of 22cN/tex, and a breaking extension of 5.3%, all parameters were measured by Spinlab 900.

Twelve denim fabrics were produced by a Picanol rapier loom using the low torque ring yarns and conventional ring yarns as weft yarns. The fabric specifications are given in Table 7-2. From fabric Samples No 1 to 6, 84tex conventional ring slub yarns were used as warp yarns, while 84tex conventional ring yarns were used as warp yarns of fabric Samples No 7, 8, 9, 10, 11 and 12. After weaving, the fabric Samples underwent finishing and enzyme pumice washing.

Table 7-1 Specifications of Yarn Samples

Yarn sample	Yarn type	Yarn count (Ne)	Twist factor	Speed ratio
7-3.0-NS $_{0.43}$	NS	84	3.0	0.43
7-3.2-NS $_{0.43}$	NS	84	3.2	0.43
7-3.5-NS $_{0.38}$	NS	84	3.5	0.38
7-3.8-NS $_{0.33}$	NS	84	3.8	0.33
7-4.2-NS $_{0.33}$	NS	84	4.2	0.33
7-3.0-A	C	84	3.0	-
7-3.2-A	C	84	3.2	-
7-3.5-A	C	84	3.5	-
7-3.8-A	C	84	3.8	-
7-4.2-A	C	84	4.2	-
10-3.1-NS $_{0.43}$	NS	58	3.1	0.43
10-3.3-NS $_{0.36}$	NS	58	3.3	0.36
10-3.6-NS $_{0.36}$	NS	58	3.6	0.36
10-3.8-NS $_{0.36}$	NS	58	3.8	0.36
10-4.2-NS $_{0.33}$	NS	58	4.2	0.33
10-3.1-A	C	58	3.1	-
10-3.3-A	C	58	3.3	-
10-3.6-A	C	58	3.6	-
10-3.8-A	C	58	3.8	-
10-4.2-A	C	58	4.2	-

Table 7-2 Fabric Specifications

Fabric sample	Fabric content		Yarn count (tex)		Yarn twist factor		Fabric count (no./2.54cm)		Weave
	Warp	Weft	Warp	Weft	Warp	Weft	Warp	Weft	
1	C	NS	84	84	4.2	3.0	61	49	3/1 twill
2	C	NS	84	84	4.2	3.2	61	49	3/1 twill
3	C	NS	84	84	4.2	3.8	61	49	3/1 twill
4	C	C	84	84	4.2	3.2	61	49	3/1 twill
5	C	C	84	84	4.2	3.5	61	49	3/1 twill
6	C	C	84	84	4.2	4.2	61	49	3/1 twill
7	C	NS	84	58	4.2	3.3	68	44	3/1 twill
8	C	NS	84	58	4.2	3.6	68	44	3/1 twill
9	C	NS	84	58	4.2	3.8	68	44	3/1 twill
10	C	C	84	58	4.2	3.3	68	44	3/1 twill
11	C	C	84	58	4.2	3.6	68	44	3/1 twill
12	C	C	84	58	4.2	4.2	68	44	3/1 twill

7.3.2 Test Methods

All yarn and fabric samples were conditioned for at least 24 hours under standard conditions (20 ± 2°C and 65 ± 2% RH) and then tested for yarn and fabric properties. Yarn tensile properties were tested on an Uster Tensorapid instrument at a speed of 5,000 mm/min and a specimen length of 500 mm. Fifty readings for each sample were recorded. Yarn evenness was measured using Uster III tester. Yarn snarling was measured by a yarn snarling tester by using the principle similar to ISO Standard 3343-1984. Thirty readings were taken on each sample. In this study, a Zweigle G566 hairiness tester was used to measure the hairiness of yarns at different length groups. For each yarn bobbin, three different parts were measured. Yarn evenness

was measured using Uster Evenness tester III.

After enzyme pumice washing, the fabric weight was measured following Levi Strauss Standard LS&CO.12 (Levi Strauss, 2002). The fabric breaking strength and tear strength were measured based on ASTM D5034 and ASTM D1424, respectively. Data were analyzed by one-way analysis of variance to compare the sample means. The significance level was set at 0.05 level and a multiple comparisons LSD test was performed using the SPSS statistical software.

With reference to AATCC 124, fabric smoothness appearance was also evaluated subjectively. The evaluation of fabric smoothness appearance was based on the following 5 grade scales: 5 - no ‘small snake’; 4 - slight ‘small snake’; 3 - moderate ‘small snake’; 2 - severe ‘small snake’; 1 - very severe ‘small snake’. A grade midway between those whole-number standard was also assigned to represent the fabric appearance if the appearance of the test specimen warranted it.

7.3.3 Results and Discussion

7.3.3.1 Yarn Properties and Comparison

Table 7-3 shows yarn properties such as yarn snarling, tenacity, elongation, hairiness and evenness of low torque and conventional yarns. The snarling of low torque ring yarns is much lower than that of conventional ring yarns with a normal twist factor (4.2 for 84tex and 58tex), even that of yarns of the same twist level. In the case of

low torque ring yarn (84tex) with twist factor 3.2, when compared to conventional yarns with a normal twist, the yarn has a snarling reduction of around 40% from 39 to 24 turns/25cm; for low torque ring yarn (58tex) with twist factor 3.3, the yarn also has a snarling reduction of around 32% from 47 to 32 turns/25cm. Using low twist level, conventional ring yarn can also achieve yarn snarling reduction to some extent, but the level of snarling reduction is less than that of low-torque yarn. As shown in Table 7-3, conventional ring yarn (84tex) with twist factor 3.2 only has snarling reduction of about 15% compared to conventional ring yarns with a normal twist level.

Table 7-3 Properties of Low Torque Ring Yarns and Conventional Ring Yarns

Sample no.	Tenacity (cN/tex)	Elongation (%)	Snarling (turns/25cm)	Hairiness (S3/100m)	Evenness (CV%)
7-3.0-NS $_{0.43}$	16.24	5.95	21	935	10.75
7-3.2-NS $_{0.43}$	16.50	5.69	24	771	11.10
7-3.5-NS $_{0.38}$	16.51	5.85	28	749	11.56
7-3.8-NS $_{0.33}$	17.21	5.75	31	604	11.19
7-4.2-NS $_{0.33}$	16.23	6.59	33	413	10.72
7-3.0-A	14.91	6.32	31	2142	12.61
7-3.2-A	15.72	6.72	33	2008	12.15
7-3.5-A	16.43	6.31	35	1638	12.41
7-3.8-A	17.04	6.59	39	1249	12.57
7-4.2-A	17.58	7.14	39	1049	11.43
10-3.1-NS $_{0.43}$	14.98	5.20	27	423	12.97
10-3.3-NS $_{0.36}$	15.33	5.41	32	417	12.96
10-3.6-NS $_{0.36}$	15.59	5.58	33	399	12.74
10-3.8-NS $_{0.36}$	16.41	5.46	35	382	12.50
10-4.2-NS $_{0.33}$	16.12	5.73	36	352	12.21
10-3.1-A	14.41	5.15	34	587	14.01
10-3.3-A	15.58	5.50	39	590	13.93
10-3.6-A	16.58	5.84	44	696	14.21
10-3.8-A	16.82	5.92	47	590	13.77
10-4.2-A	17.42	6.38	47	496	13.32

Table 7-3 lists the yarn tenacity and other typical yarn properties of low torque and conventional ring yarns. From the comparison, it is easy to see that the tenacity of low torque ring yarns is only slightly lower than that of conventional ring yarn with normal twist factor (4.2 for 84tex and 58tex). The lowest value of yarn tenacity of low torque ring yarn is around 16.5cN/tex among the six 84tex yarn samples and 15.0cN/tex for 58tex low torque ring yarns, which is acceptable for industrial

application. As we know, the snarling decrease of conventional ring yarn can also be achieved through reducing yarn twist level. However, the yarn tenacity will decrease concomitantly. As shown in Table 7-3, the level of tenacity reduction occurs at a faster rate for the conventional yarns than for low torque ring yarns, especially in lower yarn twist level. In the 84tex conventional ring yarn with twist factor 3.0, the value of yarn tenacity is only 14.91cN/tex, which may result in the increase of end break in yarn spinning and bring problems in the following yarn processing, weaving and fabric properties. Moreover, yarn hairiness of conventional ring yarns increases significantly in yarns of low twist level, which will deteriorate the fabric appearance.

Possessing lower yarn snarling and less yarn hairiness as well as normal yarn tenacity and evenness, low torque ring yarns will contribute to the improvement of fabric appearance of denim produced.

7.3.3.2 Fabric Properties and Appearance

In order to improve fabric appearance and evaluate the effect of weft yarn torque on the ‘small snake’ pattern of the denim fabric, six fabric samples were produced by using the low torque ring yarns as weft yarns, and six conventional fabrics with normal twist level yarn and low twist level yarn as wefts were also woven for comparison of fabric properties and appearance. The photographs of denim fabric appearance using low torque ring yarns and conventional ring yarns as wefts are shown in Figures 7-5 and Figure 7-6. Figure 7-7 shows the grade of fabric smoothness appearance of twelve samples.

As shown in Figure 7-7, the appearance of denim fabrics is improved significantly when using the low torque ring yarns as weft yarns. Conventional fabrics with a normal twist factor (4.2 for 84tex and 58tex) yarns as weft yarns have severe ‘small snake’ pattern, while fabrics using the low torque ring yarns as weft yarns only have moderate, or even slight ‘small snake’ pattern on the fabric surface. Moreover, using slub yarn as warp yarn in Samples No 1 to No 6, the fabrics made by low torque ring yarns as wefts show a more prominent slub effect in the warp direction of denim due to less ‘small snake’ pattern and better smoothness of fabric. When using a low twist factor (3.2 for 84tex and 3.3 for 58tex), that is, lower yarn residual torque, the conventional fabrics also achieve better fabric appearance with slight ‘small snake’ pattern on the denim surface such as Sample No 4.

In addition, the experimental results demonstrate that the ‘small snake’ pattern of the fabric decreases with the reduction of weft yarn snarling. Figure 7-8 shows the relationship between weft yarn snarling and fabric ‘small snake’ pattern of the twelve fabric samples. Among the six Fabric Samples No 1 to No 6, with lowest weft yarn snarling, Fabric Samples No 1 has the best fabric smoothness appearance, while Fabric Samples No 6 has the most severe ‘small snake’ pattern because of the highest weft yarn snarling among the six weft yarn samples (84tex) in this study. Similarly, Fabric Sample No 7 presents the slight ‘small snake’ pattern and Sample No 12 shows server ‘small snake’ pattern on denim surface among six fabrics using the low torque ring yarns (58tex) and conventional yarns as weft yarns. As indicated in the theoretical study, reducing weft yarn residual torque will decrease the difference of the angle of twist between warp yarn sections. As a result, yarn

buckling unevenness may be decreased, which endows denim a more smooth surface and thus decreases the problem of ‘small snake’ pattern on denim fabric. Following the same trend, Figure 7-8 also shows the difference of effect of yarn snarling on the fabric ‘small snake’ between fabrics using low torque ring yarns and conventional ring yarns as weft yarns. For example, with higher yarn snarling, the Sample No 4 achieves higher ‘small snake’ grade than that of Sample No 3. Based on the experiment results and analysis above, it can be confirmed that the weft yarn residual torque is the main factor contributing to the ‘small snake’ pattern of denim fabric, but other yarn properties also make contributions to the fabric appearance to some extent. After the modification of the yarn structure, low torque ring yarn not only differs from conventional ring yarn in terms of yarn residual torque but also in bulk, other mechanical properties and surface properties. Mechanical and bulking properties and surface properties of yarn are also related to the fabric appearance.

The experiment shows that fabric made from the coarse weft yarns (84tex) has higher level of ‘small snake’ pattern than that from the finer yarns (58tex), which may be explained by the fact that if the twist angles are identical for both coarse and fine yarns (identical twist multipliers), the coarse yarn has a higher tendency to release its strain. For fabrics using low torque ring yarns (84tex) as weft yarns, improvement of smoothness appearance of denim is more significant than that of fabrics with low torque ring yarns (58tex) as weft yarns.

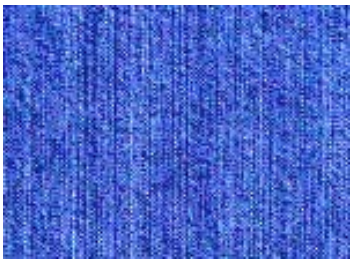

Fabric Sample No 1

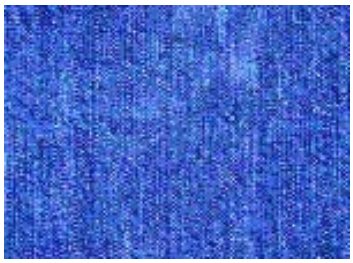

Fabric Sample No 2

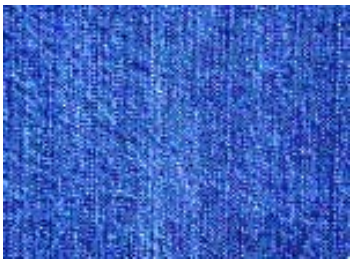

Fabric Sample No 3

Fabric Sample No 4

Fabric Sample No 5

Fabric Sample No 6

Figure 7-5 Photographs of Denim Fabric Appearance (84tex weft yarns)

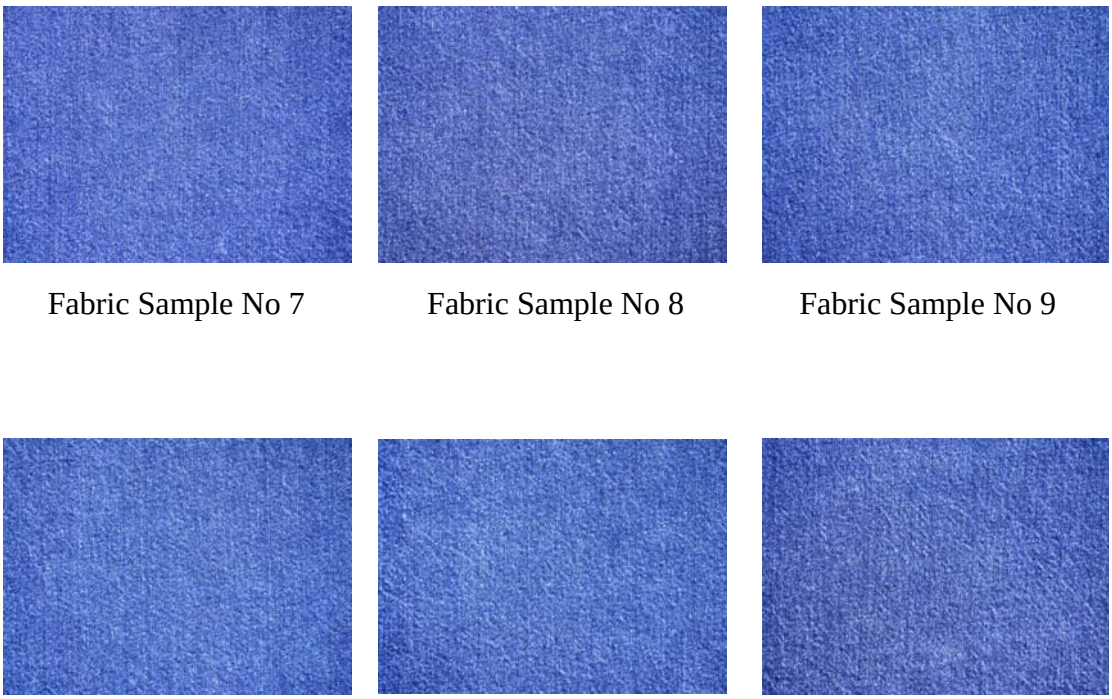

Fabric Sample No 7 Fabric Sample No 8 Fabric Sample No 9

Fabric Sample No 10 Fabric Sample No 11 Fabric Sample No 12

Figure 7-6 Photographs of Denim Fabric Appearance (58tex weft yarns)

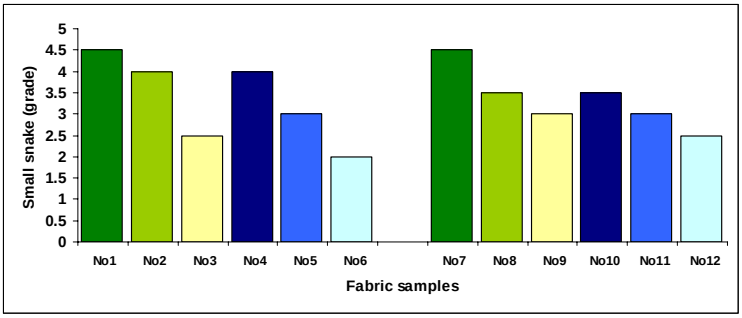

Figure 7-7 Grade of 'Small Snake' Pattern of the Denim Fabrics

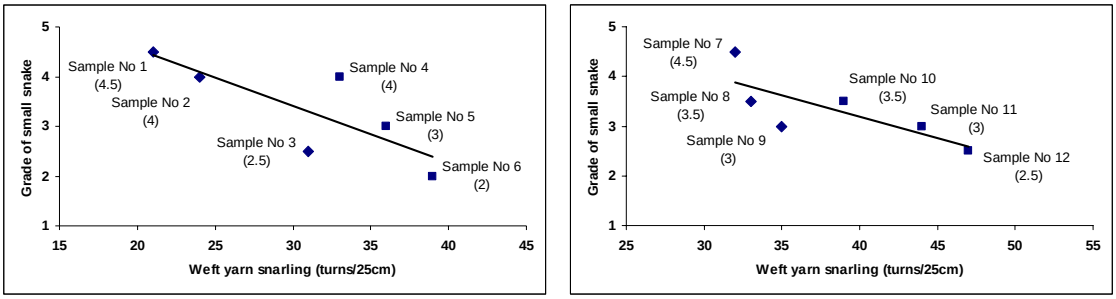

84tex weft yarn 58tex weft yarn

Figure 7-8 Relationship between Weft Yarn Snarling and Fabric 'Small Snake' Pattern

Table 7-4 presents typical properties of denim fabrics using the low torque ring yarns and conventional yarns as weft yarns. In this study the appearance of denim fabric is improved through using low torque ring yarns as weft yarns, hence the analysis of fabric will be placed on the fabric properties in the weft direction. One-way analysis of variance was performed on the data in order to test and assess if there was a significant difference between the means of samples with different types of weft yarns at 0.05 level. Compared to normal denim fabric produced in the factory such as Sample 6 and Sample 12, the fabric appearance is improved at equal or more than one grade in the Samples 1, 2, 4, 7, 8 and 10. Therefore, the means of those Samples were compared and the results of multiply comparison LSD test are given in Table 7-5. It is obvious that there is no significant difference on tensile strength and tear strength between fabric samples using the low torque ring yarns as weft yarns and conventional fabrics with normal twist factor (4.2 for 84tex and 58tex) yarns as wefts. However, the tensile strength and tear strength of fabrics using conventional

low twist yarns as weft yarns shows a significant decrease compared to normal conventional yarn fabric and majority of fabric samples using low torque weft yarns. The possible reason is that the structure of low twist conventional yarn is easy to become loose during winding and weaving processes, which results in a further decrease of yarn tensile stress, while low torque ring yarn can still maintain its twist structure at low twist due to its better fiber migration and cohesion in the yarn. Therefore, even though the fabric appearance can be improved greatly using low twist conventional yarns as weft yarns, the weft tear strength and tensile strength loss of fabric are serious, which can not meet the quality requirements of denim standard.

Table 7-4 Fabric Properties

Fabric sample	Weight (g/m^2)	Tensile strength (N)		Tear strength (N)	
		warp	weft	warp	weft
1	441	937.8	777.4	82.4	63.6
2	459	979.8	773.3	83.3	62.9
3	466	1044.3	805.6	85.2	64.1
4	453	985.4	748.8	89.8	53.9
5	458	977.5	754.3	87.3	57.8
6	467	982.3	797.6	86.9	62.8
7	434	1071.3	537.9	84.4	46.1
8	437	1075.8	551.2	85.4	48.0
9	441	1186.9	520.1	89.2	49.0
10	427	1160.2	462.3	90.1	39.2
11	434	1066.9	493.4	87.2	43.1
12	434	1146.9	551.2	91.1	47.0

Table 7-5 Results of Multiple Comparisons LSD Test

Fabric sample no.	Fabric sample no.	Tensile strength in weft direction		Tear strength in weft direction	
		Mean difference (I-J)	Sig.	Mean difference (I-J)	Sig.
6	1	19.900	0.364	-0.820	0.733
	2	24.280	0.272	-0.080	0.973
	4	48.840*	0.036	8.860*	0.002
4	1	-28.940	0.193	-9.680*	0.001
	2	-24.560	0.266	-8.940*	0.002
	6	-48.840*	0.036	-8.860*	0.002
12	7	13.320	0.414	0.940	0.573
	8	-0.060	0.997	-0.960	0.565
	10	88.960*	0.000	7.860*	0.000
10	7	-75.640*	0.000	-6.920*	0.001
	8	-89.020*	0.000	-8.820*	0.000
	12	-88.960*	0.000	-7.860*	0.000

* The mean difference is significant at the 0.05 level.

7.4 Summary and Conclusion

This Chapter presents a theoretical probe and experimental study of the effects of yarn torque on the surface smoothness of denim fabric. It starts from a theoretical analysis on the effect of yarn residual torque on the surface smoothness of denim fabric based on a woven fabric with typical 3/1 twill structure. The theoretical analysis results indicate that reducing weft yarn residual torque will decrease the

difference of the angle of twist between warp yarn sections. As a result, yarn buckling unevenness may be decreased, which endows denim a more smooth surface and thus decrease the problem of ‘small snake’ pattern on denim fabric.

Based on the theoretical analysis results, the low torque ring yarns were applied to the denim fabric to improve fabric smoothness appearance. The experimental study has demonstrated that the appearance of the denim fabrics has been greatly improved by using the low torque ring yarns as weft yarns as a result of lower yarn residual torque. Thus the fabric shows a more prominent slub effect in the warp direction of denim when slub yarn is used as warp yarn due to less ‘small snake’ pattern and better smoothness of fabric. Moreover, multiply comparison LSD test of fabric properties manifests that there is no significant difference on tensile strength and tear strength between fabric samples using the low torque ring yarns as weft yarns and conventional fabrics with normal twist level yarns as wefts, while the losses in the weft tear strength and tensile strength are serious when using low twist conventional yarns as weft yarns. In addition, investigation on the relationship between weft yarn snarling and fabric ‘small snake’ pattern indicates that the ‘small snake’ pattern of the fabric decreases with the reduction of weft yarn snarling.

CHAPTER 8 CONCLUSION AND RECOMMENDATION

8.1 Conclusion

Ring spinning technology is the most widely used spinning method at present due to its flexibility with respect to types of material and count range, and particularly its optimal yarn structure, which results in outstanding yarn strength. However, along with these positive aspects, there was a growing realization that this system still has imperfections that cause quality problems in yarns and thus influence some fabric performance. One of the disadvantages related to the conventional ring spinning process is that ring spun yarn possesses high residual torque. The residual torque may cause distortion in knitted fabric and woven fabric such as spirality of knitted fabrics and skewness of woven fabrics, bring about difficulties in handling any post-spinning operation such as winding, sizing, dyeing and weaving, and also produce defects like pucker in fabrics.

The present work aims to probe the possibility of producing low torque ring weaving yarns for industrial application with the adoption of a torque reduction device attached on the conventional ring spinning machine. Extensive experimental studies

and some theoretical exploration were conducted to investigate the process and torque reduction device for low torque ring yarn, the spinning mechanism by the geometry of ring spinning triangle and its effect on the yarn torque, yarn structures characterized based the geometrical arrangement of the fibers in the yarn, the relationship between yarn properties and spinning parameters, properties and performance of low torque ring yarn and fabric, and effect of yarn snarling on surface smoothness of denim fabric.

8.1.1 The Process and the Torque Reduction Device

The significance and background of the present study are provided in Chapter 1. Chapter 2 details the explanation of the process of the low torque ring yarn spinning technology in which a modification system is attached to a ring spinning machine.

The principal mechanism of this method is to produce modified yarn structure, wherein the yarn residual torque can be reduced because of the introduction of false-twisting operation during yarn formation, which is based on the analysis of nature of yarn torque and factors affecting yarn torque. The possible method to reduce yarn torque is proposed on the basis of the following aspects. Firstly, reducing yarn twist level may result in the reduction of the magnitude of the fiber bending, fiber torsion and fiber tension created during yarn twisting and thus reduces yarn torque and the tendency of yarn to snarl. Secondly, changing fiber tensile stress distribution within the yarn to avoid its radial bias and to bring about some fibers and fiber sections arranging in opposite direction to the yarn twist, through altering

fiber arrangement in the yarn, i.e. modifying yarn structure, probably also reduce yarn torque. In addition, the increase of fiber migration which improves the equalization of fiber tensile stress and interfiber friction within the yarn, and the forming of a more compact yarn structure will contribute to the reduction of yarn residual torque.

A preliminary study of the torque reduction device was made. The torque reduction device is composed mainly of a false-twisting system including a pair of spaced rotors, a false-twister in tangential frictional contact with each of rotors and magnetic means. The experimental results show that the resultant yarns had reduced residual torque through modifying yarn structure directly during yarn formation, which eliminates any additional step after the spinning process and makes this technology more practical and economical for industrial application. In addition, the yarn strength in the spinning triangle zone can be enhanced, thus the yarn spinnability was improved. Moreover, false-twisting operation probably results in a higher migration effect in low torque ring yarn and endows low torque ring yarn more fiber entanglement as well as a tight yarn structure even though the final yarn twist level is low. Positive results were achieved in the preliminary experiment where low torque ring yarn exhibits lower yarn snarling, less yarn hairiness and normal yarn tenacity.

8.1.2 Investigation on the Geometry of the Ring Spinning Triangle and Its Effect on Yarn Torque

The work in Chapter 3 has been concerned with the investigation of the geometry of ring spinning triangle and its effects on the yarn torque. The study starts with the geometry of spinning triangle with the help of an experimental device for spinning triangle observation. The experimental device includes a special designed transparent roller, the CCD Micro-Camera and a frame for camera-mounting and photo-taking. The observation of spinning triangle indicates that the geometry of spinning triangle in low torque ring yarn exhibits some characteristics such as symmetric structure, short height and multi-bundle of fibers.

Following that, a theoretical investigation of the effect of shape of spinning triangle on the distribution of the fiber tension stress is carried out using the principle of stationary total potential energy. A shape parameter (β) which describes the symmetric level of the geometry of spinning triangle is introduced in the analysis. The typical shape of spinning triangle and then two special cases of spinning, as well as multi-bundle form of fibers are analyzed for the distribution of the fiber tension stress at the spinning triangle.

The theoretical analysis indicates that the individual fiber tension at the spinning triangle is determined by yarn spinning tension, fiber properties, number of fibers, the shape of spinning triangle and the yarn twist angle. To evaluate and simulate the

theoretical results, a case study was carried out on the investigation of the distribution of fibers tension stress at the spinning triangle of 58tex cotton yarn. The simulation results showed that the distribution of fiber tension force depends on the shape of the spinning triangle. As the value of shape parameter increases, the tension force distribution of fibers at the spinning triangle becomes more uniform. Besides, as yarn twist increases, more fiber tension developed in the spinning triangle. For fibers distributed at the spinning triangle in the form of multi-bundle, it was observed that the maximum value of fiber tension at the spinning triangle decreased when compared with that of fiber distribution without multi-bundle form in the present analysis.

On the basis of some assumption, an attempt on linking the fiber tension stress at the spinning triangle to yarn torque is also included in Chapter 3. A case of simulation of the distribution of fiber tensile stresses within a twisted yarn suggested that the yarn shows a more uniform tensile stress distribution of fibers in the form of symmetric spinning triangle, and lower fiber tensile stress distributed across the whole yarn when lower yarn twist level is adopted. Besides, the calculated results of yarn torque for 58tex cotton yarn showed that in the form of symmetric spinning triangle, the yarn exhibits a lower yarn torque when compared to that of yarn with shape of right-angled spinning triangle, and the torque of the yarn with twist factor 3.2 is much lower than that of the yarn using twist factor 4.2 in the present examples.

8.1.3 Structures of Low Torque Ring Yarn for Weaving

Chapter 4 concerns structures of low torque ring yarn for weaving. With the help of SEM and tracer fiber technique, structures of low torque ring yarn were analyzed and characterized by yarn surface structure, 3D configuration of tracer fiber in the yarn and fiber migration behaviors of the yarn in this Chapter.

The work starts from the development of a measuring system for investigation of the fiber configuration in staple yarns, based on the tracer fiber technique. The main features of the system is that it can capture and store consecutive images of single tracer fiber, thus the image acquisition becomes faster and more accurate, and the problems in manual operation such as slow movement, larger random error can be solved. It is also helpful for the analysis and processing of the tracer fiber image information such as transfer of the obtained images into a set of data. Moreover, the regeneration of the 3D configuration and radial position variation of the tracer fiber in a real yarn and the analysis of yarn structural characteristics can be achieved.

Under the SEM, some structural features were found in the low torque ring yarn such as ring-yarn-like appearance, compact structure, wrapper fibers in vertical or opposite direction and less yarn hairiness, which contributes to the reduction of yarn residual torque and yarn hairiness, as well as to the increase of yarn strength when low twist level was adopted in low torque ring yarns.

The analysis of 3D configuration and radial position variation of the tracer fiber

regenerated with the data obtained from the tracer fiber technique indicated that the tracer fiber in the low torque ring yarn is located in the core area with more sections than that of conventional ring yarn and the migratory pattern shows apparently higher magnitude of fluctuation. Unlike conventional ring yarn, the low torque ring yarn exhibits different migratory patterns in which the big fiber migration includes some small fiber migration with various configurations. Moreover, some parts of tracer fibers in low torque ring yarns arrange in opposite direction to the yarn twist, which is rarely occurred in conventional ring yarn.

Another attempt for the investigation of fiber migration behavior demonstrated that a higher migration effect occurred in low torque ring yarn with lower value of mean fiber position as well as higher values of RSM deviation and the mean migration intensity when compared with that of conventional ring yarn, which can be attributed to the introduction of false-twisting operation in the low torque yarn spinning. It is likely that the higher rate of migration in low torque ring yarns could be beneficial in promoting high yarn tenacity and less yarn hairiness, particularly when low twist level is adopted in spinning. The parts of fibers twisted in the opposite direction of the yarn twist are one of the reasons for low yarn snarling.

8.1.4 Statistic Models for the Relationships between Yarn Properties and Spinning Parameters

With a false-twisting operation introduced into spinning, the relationship between low torque ring yarn properties and spinning parameters differs from that of

conventional ring spinning. Thus the statistic models have been developed to predict and explain their relationship.

The analysis based on the Fractional Factorial Methodology indicates that twist level (TF) and speed ratio (FTF) are the two most important spinning parameters contributing to the low torque yarn properties, particularly on yarn snarling and tenacity. Therefore, TF and FTF are chosen for more thorough investigation in subsequent experiments.

With twist level (TF) and speed ratio (FTF) as variables and yarn properties as responses, the second-order polynomial response surface models are developed to predict and explain the relationships between yarn properties and yarn twist level and speed ratio using Response Surface Methodology (RSM). The results of RSM investigation show that yarn tenacity increases with increase in yarn twist and decrease in speed ratio, and yarn snarling decreases with the reduction of yarn twist and increase of speed ratio. The reason for these trends may be ascribed to the combined effects of the change of fiber migration, fiber packing density, fiber deformation and fiber arrangement in yarns due to the modification.

The model adequacy assessment by the residual analysis and the checking of model validity, through assessing the deviation of the estimated values obtained from mathematical model to the actual experimental values, all demonstrate that the developed model exhibits a good predicating accuracy and this model can reflect the

actual relationship between yarn properties and yarn twist and speed ratio.

The optimum spinning parameters leading to the desirable yarn properties are found, based on the developed RSM model coupled with the desirability function and overlaid contour plot. Optimization using desirability function indicates that one of the best combination of parameters is TF = 3.2 and FTF = 0.43, which results in lower yarn snarling with acceptable level of yarn tenacity, hairiness and evenness for industrial application. Optimization using overlaid contour plot also gives a feasible operating region where a number of combination of twist factor and speed ratio can be adopted to obtain desirable yarn properties.

8.1.5 Characteristics of Low Torque Ring Yarn and Its Woven Fabric

The properties of low torque ring yarn and characteristics of fabrics produced are comprehensively depicted in Chapter 6. The test and analysis of yarn properties in the Chapter exhibit some exciting results of low torque ring yarn with great reduction of yarn snarling and yarn hairiness. Even at low twist level, low torque ring yarn can still maintain its yarn tenacity and evenness comparable to conventional ring yarn with normal twist level. Compared to conventional ring yarn at the same low twist level, low torque ring yarn presents significant advantages of lower yarn snarling, less yarn hairiness and higher yarn strength particularly after yarn winding process.

As for the fabrics generated, they demonstrate improved denim fabric and twill fabric appearance, a fuller, thicker and more smooth hand. The distinguished jeans appearance improvement with less ‘small snake’ pattern and more prominent slub effect on the denim surface is a success for low torque ring yarn being applied in denim. The fabric also exhibits satisfactory levels of mechanical properties such as tensile strength and tearing strength. In addition, with yarn at low twist level, low torque ring yarn fabric possesses acceptable tensile strength and tear strength for industrial application. These improvements no doubt indicate the commercial potential of low torque ring spinning technology applied on ring spun yarns.

Subjective evaluation of jeans and twill trousers produced by low torque ring yarn fabrics further confirmed that the jeans produced by the low torque ring weft yarn fabric has significant advantages of better jean smoothness appearance, less ‘small snake’ pattern, more prominent slub effect in warp direction and better overall quality than the samples produced by the conventional ring yarns and rotor yarns. The twill trousers produced by low torque ring fabrics also show some benefits such as better luster, better smoothness appearance and overall quality than the other two conventional ring and rotor yarn trousers.

In addition, since low torque ring yarns are only used as weft yarns of the fabrics in the present study, there are needs to further investigate the fabrics made from low torque ring yarns in both the warp and weft direction.

8.1.6 Effect of Yarn Snarling on Surface Smoothness of Denim Fabric

Chapter 7 provides the investigation theoretically and experimentally of the effect of yarn torque on the surface smoothness of denim fabric. The theoretical analysis results indicate that reducing yarn residual torque, particularly weft yarn residual torque will decrease the difference of the angle of twist between warp yarn sections. As a result, yarn buckling unevenness may be decreased, which endows denim a more smooth surface and thus decrease the problem of 'small snake' pattern on denim fabric. The experimental study has demonstrated that the appearance of the denim fabrics has been greatly improved by using the low torque ring yarns as weft yarns as a result of lower yarn residual torque. Thus the fabric shows a more prominent slub effect in the warp direction of denim when slub yarn is used as warp yarn due to less 'small snake' pattern and better smoothness of fabric. Moreover, multiply comparison LSD test of fabric properties manifests that there is no significant difference on tensile strength and tear strength between fabric samples using the low torque ring yarns as weft yarns and conventional fabrics with normal twist level yarns as wefts, while the losses in the weft tear strength and tensile strength are serious when using low twist conventional yarns as weft yarns. In addition, investigation on the relationship between weft yarn snarling and fabric 'small snake' pattern indicates that the 'small snake' pattern of the fabric decreases with the reduction of weft yarn snarling.

8.2 Recommendation for Future Work

In the present study, cotton is the primarily material involved and thus the variety of

fiber types is limited. For further study, it is recommended that a wide selection of fibers can be exploited in the low torque ring yarn spinning. Of these fibers, wool and polyester are of prime interest due to their great popularity in yarn manufacture. In addition, it is worth to apply low torque ring yarn spinning technology on other yarns such as core-spun yarn, slub yarn and blend yarn.

The concept of introducing shape of spinning triangle into spinning mechanism study is innovative. However, in the real situation, the spinning triangle is under the combined influence of the tensile force due to spinning tension and torque because of the twist propagation though its improvement in spinning triangle study is quite clear. A more extensive study of this might be helpful for an in-depth understanding of the mechanism of spinning triangle.

The development of a measuring system for the investigation of the fiber configuration in staple yarns brings about benefits for the analysis of yarn structure with improved accuracy and efficiency of measurement. For future work, it is suggested that the system be further refined to the point where it will automatically detect, measure and process tracer fibers without any operator intervention. Besides, although the longitudinal distribution of individual fibers in the yarn is obviously of great importance in yarn structure analysis, the fiber distribution in yarn cross section can provide additional important information on the yarn structure, for example the fiber packing density distribution in a yarn. The work on yarn cross section is quite time-consuming and yarn sample preparation is rather complex, thus calls for a better method to investigate yarn structure.

REFERENCES

1. AATCC Test Method 124-2001 Appearance of Fabrics after Repeated Home Laundering, 2001.

2. Araujo, M., and Smith, G., Spirality of Knitted Fabric, Part II: The Effect of Yarn Spinning Technology on Spirality, Textile Res. J. 59(6), 350-356 (1989).

3. ASTM Designation: D1424-96 Standard Test Method for Tearing Strength of Fabrics by Falling-Pendulum Type (Elmendorf) Apparatus, 1996.

4. ASTM Designation: D5034-95 Standard Test Method for Breaking Strength and Elongation of Textile Fabrics (Grab Test), 2001.

5. Backer, S., The Effect of the Direction of Yarn Twist and Twill on the Properties of Woven Cloth, J. Textile Inst. 44(10), T477-T479 (1953).

6. Backer, S., Zimmerman, J., and Best-Gordon, H.W., The Relationship between the Structural Geometry of a Textile Fabric and Its Physical Properties Part V: The Interaction of Twist and Twill Direction as Related to Fabric Structure, Textile Res. J. 26(2), 87-107 (1956).

7. Baird, M., Laird, W., and Weedall, P., Effects of Yarn Twist on the dimensional Stability of Light Weight Worsted Fabrics, Proc. of the 9th International Wool

Textile Research Conference, 1995.

8. Baird, M., Laird, W., and Weedall, P., Effects of Yarn Twist on the dimensional Stability and Tailorability of Light Weight Worsted Fabrics, Proc. of the 75th world conference of the Textile Institute, 1994.

9. Bajaj, P., and Agarwal, R., Innovations in Denim Production, American Dyestuff Reporter, 88(5), 26-37 (1999).

10. Balls, W. L., Studies of Quality in Cotton, Macmillan, London, P168 (1928).

11. Barella, A., Some Factors Affecting the Hairiness of Worsted Yarns, J. Textile Inst. 48(5), P311-316 (1957).

12. Barella, A., and Manich, A.M., Friction Spun Yarns Versus Ring and Rotor Spun Yarns- Resistance to Abrasion and Repeated Extensions, Textile Res. J. 59(12), 767-769 (1989).

13. Behera, B.K., Ishtiaque, S.M., and Chand, S., Comfort Properties of Fabrics Woven from Ring-, Rotor-, and Friction- Spun Yarns, J. Textile Inst. 88(3), 255-264 (1997).

14. Bennett, J. M., and Postle, R., A Study of Yarn Torque and Its Dependence on the Distribution of Fiber Tensile Stress in the Yarn, Part I: Theoretical Analysis, J. Textile Inst. 70(4), 121-132 (1979).

15. Bennett, J. M., and Postle, R., A Study of Yarn Torque and Its Dependence on the Distribution of Fiber Tensile Stress in the Yarn, Part II: Experimental, J. Textile Inst. 70(4), 133-141 (1979).

16. Box, G. E.P., and Draper, N. R., Empirical Model-building and Response Surfaces, John Wiley & Sons, Inc., NY, 1987.

17. Buhler, G., and Haid, H., What Distinguishes Fabrics Knitted from Ring or Rotor Spun Yarns, Textil. Prax. Int. 46(4), 316-317 (1991).

18. Carig, Roy R., Mechanics of Materials, John Wiley and Sons, Inc., NY, 2000.

19. Cheng, K. P. S., and Yu, C., A Study of Compact Spun Yarns, Textile Res. J. 73(4), 345-349 (2003).

20. Cheng, K. P. S., and Li, C. H. L., JetRing Spinning and its Influence on Yarn Hairiness, Textile Res. J. 72(12), 1079-1087 (2002).

21. Choi, K.F., and Lo, T.Y., An Energy Model of Plain Knitted Fabric, Textile Res. J. 73(8), 739-748 (2003).

22. Choi, K.F., and Lee, K.K., The Effect of Frontzone Condenser Width on the Abrasion Resistance in terms of Migration, B.S.D Thesis, The Hong Kong Polytechnic University, 2003

23. CTI Year Book, Spinning/Twisting/Winding: Spinning in the Nineties, 41 (1990).

24. DeLoach, J.R., Twisted Legs in Jeans Causes and Cures as Viewed by the Fabric Manufacturer, American Society for Quality Control Conference Proceedings, Vol.4,101-104 (1976).

25. El-Shiekh, A., On the Mechanics of Twist Insertion, Mech. Eng. Sc.D. Thesis, M.I.T. 1965.

26. Emmanuel, A., and Plate, D.E.A., An Alternative Approach to Two-fold Weaving Yarn Part II: The Theoretical Model, J. Textile Inst. 73(3), 107-116 (1982).

27. Fehrer, E., New Spinning Process Comforspin, Melliand Int. 1(3), 22-25 (2000).

28. Fraser, W.B., and Stump, D.M., Yarn Twist in the Ring-spinning Balloon, Proc. R. Soc. Lond. A, 454 (1970), 707-723 (1998).

29. Fraser, W.B., On the Theory of Ring Spinning, Phil. Trans. R. Soc. Lond. A, 342 (1665), 439-468 (1993).

30. Fujino, K., Uno, M., Shiomi, A., Yanagawa, Y., and Kitada, Y., A Study on the Twist Irregularity of Yarns Spun on the Ring Spinning Frame, J. Text. Mach. Soc. Japan, 8(3), 51-62 (1962).

31. Gegauff, C., Force et Elasticite des Files en Coton, Bull. Soc. Ind., Mulhouse, 77, 153 (1907)

32. Goswami, B. C., Martindale, J. G., and Scardino, F. L., Textile Yarns, Technology, Structure, and Applications, A Wiley-Interscience, Publication, U.S.A. 1969.

33. Grosberg, P., and Iype, C., Yarn Production, The Textile Institute, UK, 1999.

34. Gursoy, N., and Dayioglu, H., 2.2' Bipyridine Catalyzed Peracetic Acid Bleaching of Cotton, Textile Res. J. 73(4), 297-304 (2003).

35. Hearle, J.W.S., and Goswami, B. C., Migration of Fibers in Yarns: Part VIII: Experimental Study on a 3-Layer Structure of 19 Filaments the Combination of Mechanisms of Migration, Textile Res. J. 40(7), 598-607 (1970).

36. Hearle, J.W.S., Grosberg, P., and Backer, S., Structure Mechanics of Fibers, Yarns, and Fabrics, Vol.1, Wiley-Interscience, NY, 1969.

37. Hearle, J.W.S., Gupta, B. S., and Goswami, B. C., Migration of Fibers in Yarns: Part V: The Combination of Mechanisms of Migration, Textile Res. J. 35(10), 972-978 (1965).

38. Hearle, J.W.S., Gupta, B. S., and Merchant, V. B., Migration of Fibers in Yarns: Part I: Characterization and Idealization of Migration Behavior, Textile Res. J. 35(3), 329-334 (1965).

39. Hearle, J.W.S., and Shanahan, W.J., Energy Method for Calculations in Fabric Mechanics. Part I. Principles of the Method, J. Textile Inst. 69(4), 81-91(1978).

40. Hearle, J.W.S., and Shanahan, W.J., Energy Method for Calculations in Fabric Mechanics. Part II. Examples of Application of the Method to Woven Fabrics, J. Textile Inst. 69(4), 92-100 (1978).

41. Hearle, J.W.S., Potluri, P., and Thammandra, V.S., Modelling Fabric Mechanics, J. Textile Inst. 92(3), 53-69 (2001).

42. Hickie, T.S., & Chaikin, M., The Configuration and Mechanical State of Single Fiber in Woolen and Worsted Yarns, J. Textile Inst. 51(12), 1120-1130 (1960).

43. Hickie, T.S., & Chaikin, M., Aspects of Worsted-yarn Structure, Part IV: The Application of Fourier Analysis to the Study of Single-fiber Configurations in a Series of Worsted Yarns, J. Textile Inst. 65(5), 537-551 (1974).

44. Hosseini Ravandi, S.A., and Ghane, M., Study of Fundamental Factors Affecting Fabric Surface Protrusion, J. Textile Inst. 91(1), 100-106 (2000).

45. Hu, J.L., Theories of Woven Fabric Geometry, Textile Asia, 26(1), 58-60 (1995).

46. Huh, Y., Kim, Y.R., and Ryu, W., Y., Three-dimensional Analysis of Migration and Staple Yarn Structure, Textile Res. J. 71(1), 81-90 (2001).

47. Huh, Y., Kim, Y.R., and Oxenham, W., Analyzing Structural and Physical Properties of Ring, Rotor, and Friction Spun Yarns, Textile Res. J. 72(2), 156-163 (2002).

48. Ishikura, H., Kase, S., and Nakajima, M., Study on Crinkle Design of Crepe, Part I: Crinkling Mechanism of Crepe, Journal of the Textile Machinery Society of Japan, 44(12), T260-T267 (1991).

49. ISO 3344 Textile Glass - Yarns - Determination of Twist Balance Index, 1984.

50. Jeddi, Ali A. A., Shams, S., Nosraty, H., and Sarsharzadeh. A., The Effect of Fabric Structure and Weft Yarn Properties on the Frictional Behavior of Woven Fabrics, The 6th Asian Textile Conference, Hong Kong, 2001.

51. Kim, Y.R., Huh, Y., and Ryu, W.Y., Comparison of Fiber Migration Behaviors According to Ring, Rotor, and Friction Spin Methods, Proc. 5th Asian Textile Conference, Vol. 1, 197-200, 1995.

52. Klein, W., A Practical Guide to Ring Spinning. The Textile Institute Manual of Textile Technology, MFP Design & Print, Manchester, UK, 1887.

53. Klein, W., The Technology of Short Staple Spinning, The Textile Institute, Manual of Textile Technology, Short-staple Series, Vol. 1, 34-36 (1987).

54. Klein, W., New Spinning Systems. The Textile Institute Manual of Textile Technology, Stephen Austin and Sons Limited, UK, 1993.

55. Klein, W., Spinning Geometry and its Significance, International Textile Bulletin: Yarn + Fabric Forming, 139(3), 22-26(1993).

56. Komori, T., and Itoh, M., A Mechanical Model Analysis of Crepe Puckering, Sen'i Gakkaishi, 58(5), 176-181 (2002).

57. Krause, H. W., Soliman, H. A., and Tian, J. L., Investigation of the Strength of the Spinning Triangle in Ring Spinning, Melliand Textilberichte, 72(6), 499-502

(1991).

58. Lau, L., and Fan, J., Comfort Sensations of Polo Shirts With and Without Wrinkle-Free Treatment, Textile Res. J. 72(11), 949-953 (2002).

59. Lau, Y. M., Tao, X. M., and Dhingra, R.C., Spirality in Single Jersey Fabric, Textile Asia, 31(8), 95-102 (1995).

60. Lau, Y. M., and Tao, X. M., Torque-balanced Singles Knitting Yarns Spun by Unconventional Systems, Part II: Cotton Friction Spun Yarn, Textile Res. J. 67(11), 815-828 (1997).

61. Levi Strauss Ltd., Levi Strauss & Co, Product Performance Standard, 2002.

62. Lord, P.R., The Structure of Open-End Spun Yarn, Textile Res. J. 41(9), 778-784 (2002).

63. Lord, P. R., Mohamed, M.H., and Ajgaonkar, D. B., The Performance of Open-End, Twistless, and Ring Spun Yarns in Weft Knitted Fabrics, Textile Res. J. 44(7), 405-414 (1974).

64. Louis, G. L., Salaun, H. L., and Kimmel, L. B., Comparison of Properties of Cotton Yarns Produced by the DREF-3, Ring, and Open-End Spinning Methods, Textile Res. J. 55(6), 344-351 (1985).

65. Miles, L.W.C., and Hearle, J.W.S., The Setting of Fibers and Fabrics, Merrow Publishing Co.Ltd, Watford, England, 1971.

66. Milosavljevic, S., and Tadic, T., A Contribution to Residual-torque Evaluation by the Geometrical Parameters of an Open Yarn Loop, J. Textile Inst. 86(4), 676-681 (1995).

67. Minitab Statistical Software Release 13 for Windows: User Guide, 2003.

68. Mitchell, P., Naylor, G.R.S., and Phillips, D.G., Torque in Worsted Wool Yarns, Textile Res. J. 76(2), 169-180 (2006).

69. Montgomery, D. C., Runger, G. C., and Hubele, N. F., Engineering Statistics, John Wiley & Sons, Inc., NY, 2001.

70. Mohamed, M.H., and Lord, P.R., Comparison of Physical Properties of Fabrics Woven from Open-End and Ring Spun Yarns, Textile Res. J. 43(3), 154-166 (1973).

71. Morris, M. A., and Prato, H. H., End-Use Performance and Consumer Acceptance of Denim Fabrics Woven from Open-End and Ring-Spun Yarns, Textile Res. J. 48(3), 177-183 (1978).

72. Neckar, B., Ishtiaque, S.M., and Svehlova, L., Rotor Yarn Structure by Cross-sectional Microtomy, Textile Res. J. 58(11), 625-632 (1988).

73. Nelson, P. R., Coffin, M., and Copeland, K.A.F.C., Introductory to Statistics for Engineering Experimentation, Elsevier Academic Press, San Diego, USA, 2003.

74. Pavlov, Y. V., Structural Transformations in the Fiber Assembly at the Twist Threshold at the Instant of Rupture, Tech. of Textile Ind., USSR, No 4, 57-63 (1965).

75. Peak. S.L., Pilling, Abrasion, and Tensile Properties of Fabrics from Open-end and Ring-spun Yarns, Textile Res. J. 59(10), 577-583 (1989).

76. Peak. S.L., Effect of Yarn Type and Twist Factor on Air Permeability, Absorbency, and Hand Properties of Open-end and Ring-spun Yarn Fabrics, J. Textile Inst. 86(4), 581-589 (1995).

77. Peirce, F.T., The Geometry of Clothing Structure, J. Textile Inst. 28(3), T45-T96 (1937).

78. Pillay, K. P. R., A Study of the Hairiness of Cotton Yarns, Part I: Effect of Fiber and Yarn Factors, Textile Res. J. 34(8), 663-674 (1964).

79. Platt, M.M., Klein, W.G., and Hamburger, W.J., Mechanics of Elastic Performance of Textile Materials, Part XIII: Torque Development in Yarn System: Singles Yarn. Textile Res. J. 28(1), 1-13 (1958).

80. Plate, D.E.A., and Lappage, J., An Alternative Approach to Two-fold Weaving Yarn Part I: Control of Surface Fibers, J. Textile Inst. 73(3), 99-106(1982).

81. Plate, D.E.A., An Alternative Approach to Two-fold Weaving Yarn Part I: The Properties of Two-strand Yarns, J. Textile Inst. 73(4), 321-328 (1983).

82. Postle, R., Burton, P., and Chaikin, M., The Torque in Twisted Singles Yarns. J. Textile Inst. 55(11), 448-461 (1964).

83. Postle, R., Carnaby, G. A., and Jong, S. de, The Mechanics of Wool Structures, Ellis Horwood Limited, Chichester, England, 1988.

84. Primentas, A., Direct Determination of Yarn Snarliness, Indian Journal of Fiber & Textile Research, 28(3), 23-28 (2003).

85. Primentas, A., Spirality of Weft Knitted Fabrics: Part II-Methods for The Reduction of The Effect, Indian Journal of Fiber & Textile Research. 28(3), 60-64 (2003).

86. Primentas, A., and Iype, C., Spirality of Weft Knitted Fabrics: Part III- An Innovative Method for The Reduction of The Effect, Indian Journal of Fiber & Textile Research, 28(6), 202-208 (2003).

87. Primentas, A., and Iype, C., Spirality of Weft Knitted Fabrics: Part IV-Effect of Yarn Partial Detwisting on Yarn and Fabric Properties, Indian Journal of Fiber & Textile Research, 28(6), 209-215 (2003).

88. Prins, M., Lamb, P., and Finn N., Solospun, The Long Staple Weavable Singles Yarn, Textile Institute 81st World Conference, April 2001.

89. Radhakrishnaiah, R., He, J.W., Cook, F. L., and Diller, G. B., Hand-Related Mechanical Behavior of Enzyme-Treated Yarns, Part I: Role of the Spinning System, Textile Res. J. 75(3), 265-273 (2005).

90. Realff, M.L., and Seo, M., Boyce, M.C., Schwartz, P., and Backer, S., Mechanical Properties of Fabrics Woven from Yarns Produced by Different Spinning Technologies: Yarn Failure as a Result of Gauge Length, Textile Res. J. 61(9), 517-530 (1991).

91. Riding, G., Filament Migration in Single Yarns, J. Textile Inst. 55(1), T9-17 (1964).

92. Rodiger, U., Variation in Hairiness of Worsted Yarns, Text. Praxis International, 43(3), 706-710 (1988).

93. Sawhney, A.P.S., and Kimmel, L.B., Tandem Spinning, Textile Res. J. 65(9), 550-555 (1995).

94. Sawhney, A.P.S., Kimmel, L.B., Tyndall, M., and Radhakrishnaiah, P., Properties of a Fabric Made with Tandem Spun Yarns, Textile Res. J. 66(10), 607-611 (1996).

95. Sawhney, A.P.S., Robert, K. Q., Ruppenicker, G. F., and Kimmel, L.B., Improved Method of Producing a Cotton/polyester Staple-core Yarn on a Ring Spinning Frame, Textile Res. J. 62(1), 21-25 (1992).

96. Schwarz, E. R., Textile and the Microscope, New York, McGraw-Hill, 1934.

97. Schwarz, E. R., Certain Aspects of Yarn Structure, Textile Res. J. 21(3), 125-136 (1951).

98. Schonung, B., First Results with Individual Motor-Driven Ring Spindles, Lecture on the Occasion of the 4th Ring Spinning Colloquium, SKF Report, 13-17 (1989).

99. Sengupta, A.K. and Kapoor, M., Effect of Drafting Speed at Ring Frame on Yarn Strength and Irregularity, Textile Res. J. 43 21-22 (1973)

100. Sengupta, A.K., and Sreenivasa, Murthy, H.V., Structure of Fiber Assembly During Yarn Formation in Rotor Spinning, Textile Res. J. 64(10), 692-694 (1994).

101. Shaikhzadeh Najar, S., An Analysis of the Twist Triangle in Ring Spinning, Ph.D. Thesis, University of New South Wales (Australia), 1996.

102. Stalder, H., High Performance Ring Spinning, Melliand Textilber., 72(8), 585-588 (1991).

103. Sun, M.N., and Cheng, K.P.S., Denim Performance, Textile Asia, 24(6), 38-40 (1993).

104. Tandon, S. K., Carnaby, G. A., Kim, S. J., and Choi, F. K. F., The Torsional Behaviour of Singles Yarns, Part I: Theory, J. Textile Inst. 86(2), 185-199 (1995).

105. Tandon, S. K., Kim, S. J., and Choi, F. K. F., The Tensional Behaviour of Singles Yarns. Part II: Evaluation, J. Textile Inst. 86(2), 200-217 (1995).

106. Tao, X. M., Mechanical Properties of a Migrating Fiber, Textile Res. J. 66(12), 754-762 (1996).

107. Tao, X. M., Lo, W. K., and Lau, Y. M., Torque-Balanced Singles Knitting Yarns Spun by Unconventional Systems, Part I: Cotton Rotor Spun Yarn, Textile Res. J. 67(10), 739-746 (1997).

108. Tao, X. M., and Xu, B. G., Manufacturing Method and Apparatus for Torque-free Singles Ring Spun Yarns, US Patent Pub. No.: 2003/0200740 A1, 2003.

109. Tao, X. M., Xu, B. G., and Wong, S. K., Method and Apparatus for Manufacturing a Singles Ring Yarn, US Patent Appl. No.: 10/858,400, 2004.

110. Tarafder, N., Sutradhar, C., and Mishra, S., Effect of Speed, Twist, Draft on Ring-spun Yarn, The Indian Textile Journal, 113(2), 19-28 (2002).

111. Tavanai, H., Denton, M.J., and Tomka, J.G., Direct Objective Measurement of Yarn-torque Level, J. Textile Inst. 87(1), 50-57 (1996).

112. The Woolmark Company (TWC), CSIRO and WRONZ, Solospun^{TM}, Introduction and Technical Manual, 1998.

113. Tyndall, R.M., Improving the Softness and Surface Appearance of Cotton Fabrics and Garments by Treatment with Cellulose Enzymes, Textile Chemist and Colorist, 24(6), 23-26 (1992).

114. Yao, M., Zhou, J.F., Huang, S.Z., Shao, L.H., An, R.F., and Fan, D,X., Textile Material, Textile Industry Press, Beijing, China, 1988.

115. Yu, J.M., Szeto, Y.S., Tao, X.M., Chong, C.L., and Choy, C.L., Surface Morphology of Natural Pumice Stone and its Abrading Effect on Denim Fabrics, The 6th Asian Textile Conference, Hong Kong, 2001.

116. Wang, X.G., and Chang, L.L., Reducing Yarn Hairiness with a Modified Yarn Path in Worsted Ring Spinning, Textile Res. J. 73(4), 327-332 (2003).

117. Wang, X.G., and Chang, L.L., The Hairiness of Worsted Wool and Cashmere Yarns and the Impact of Fiber Curvature on Hairiness, Textile Res. J. 76(4), 281-287 (2006).

118. Wang, X.G., Miao, M., and How, Y., Studies of JetRing Spinning, Textile Res. J. 67(4), 253-258 (1997).

119. Whitman, R., Curl in Woven Textile Fabrics: Its Cause and Control, Textile Res. J. 17(3), 148-157(1947).

120. Wu, X.Y., Wang, F.M., and Wang, S.Y., Study on the Torsional Properties and Torque-relaxation Behavior of Wool/PET Composite Yarns, Journal of Dong Hua University, 27(6) 99-104 (2001).

APPENDICES

Appendix A

Determination of the Maximum Fiber Angle with
the Twist Point Axis AT the Spinning Triangle

With the help of the experimental set-up for geometry photograph, the maximum fiber angles with the twist point axis in two typical examples of the spinning triangle ($\beta = 1$ and $\beta = 0$) were measured in the experiment. Besides, for simplify of analysis, it is assumed that the maximum fiber angle ($\theta_{n(\beta)}$) with the twist point axis is liner related to the shape parameter (β) of the spinning triangle. Then we have:

$$\theta_{n(\beta)} = \theta_{n(0)} + (\theta_{n(1)} - \theta_{n(0)})\beta$$

where $\theta_{n(\beta)}$ is the maximum fiber angle with the twist point axis when β takes the value between 0 to 1. $\theta_{n(0)}$ and $\theta_{n(1)}$ are the angles when $\beta = 1$ and $\beta = 0$ respectively.

Then, we also have:

$$\theta_{m(\beta)} = \arctan(\beta \tan \theta_{n(\beta)})$$

where $\theta_{n(\beta)}$ is the maximum fiber angle with the twist point axis in the other side of spinning triangle when β takes the value between 0 to1.

Table A-1 List the Results of Angle Measurement in the Experiment.

Yarn sample	Yarn twist factor	β	$\theta_{n(\beta)}$ (degree)
58 tex cotton yarn	4.2	1	26.5
		0	30
	3.2	1	20.8
		0	23.6

Appendix B

Program List

Appendix B1	Program for Capturing and Storing Images of Tracer Fiber
Appendix B2	Program for Distribution of Fiber Stress in Spinning Triangle Calculation

Appendix B1

Program for Capturing and Storing Images of Tracer Fiber

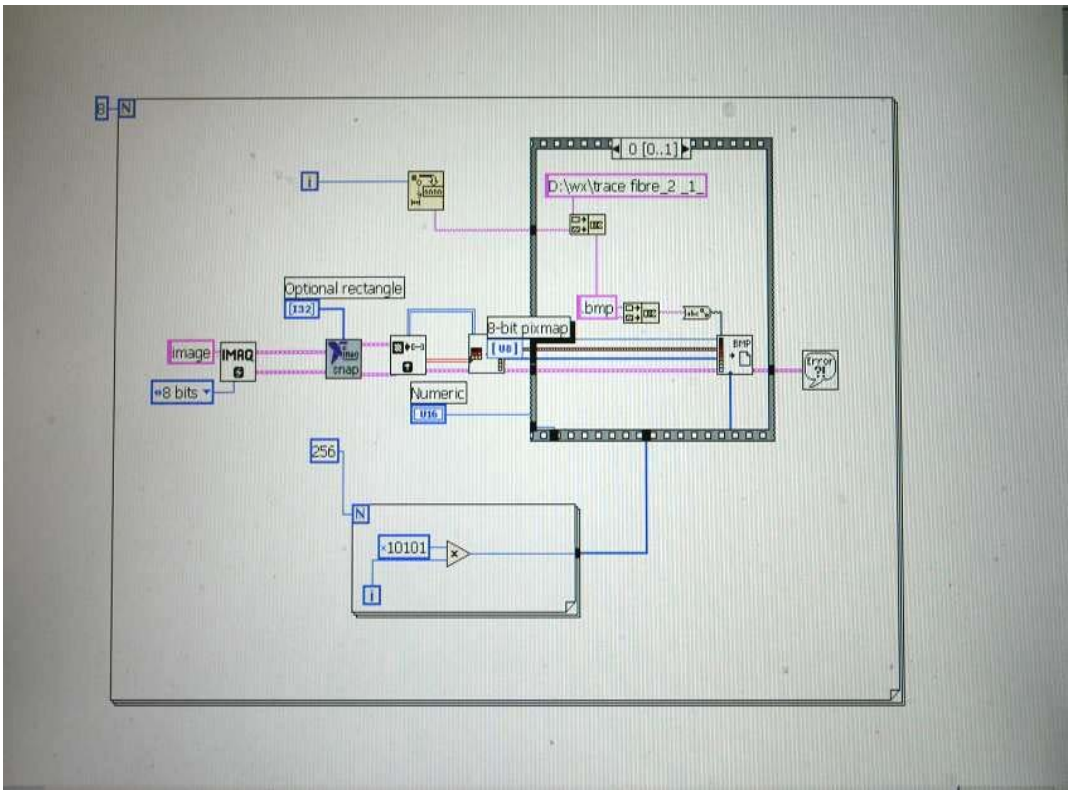

Figure B1-1 Program for Capturing and Storing Images of Tracer Fiber

Appendix B2

Program List for Spinning Triangle Study

Program for Distribution of Fiber Stress in Spinning Triangle Calculation

1. TF=4.2

```
clear
c=1; u=384,v=pi/6,z=53*pi/360,Y=30,A=1.5,E=50;
i=0:u/(1+c);
s=sum((1+(tan((i*(1+c)*(((1-c)*(v-z))+z))/u)).^2).*(tan((i*(1+c)*(((1-c)*(v-z))+z))/u)).^
2)
i=0:u/(1+c);
k=sum((1+(tan((i*(1+c)*(((1-c)*(v-z))+z))/u)).^2).^2)
j=0:c*u/(1+c);
p=sum((1+(tan(j*(1+c)*(atan(c*(tan(((1-c)*(v-z))+z))))/(c*u))).^2).*(tan(j*(1+c)*(atan(c
*(tan(((1-c)*(v-z))+z))))/(c*u))).^2)
j=0:c*u/(1+c);
q=sum((1+(tan(j*(1+c)*(atan(c*(tan(((1-c)*(v-z))+z))))/(c*u))).^2).^2)
for i=0:u/(1+c); h=i+1;
F(h)=((Y-A*E*(s+p)/2)*(1+(tan((i*(1+c)*(((1-c)*(v-z))+z))/u)).^2))/((k+q)-1)+((A*E*(ta
n((i*(1+c)*(((1-c)*(v-z))+z))/u)).^2/2))
r(h)=(i*(1+c)*(((1-c)*(v-z))+z)/u)
end
for j=0:c*u/(1+c); g=j+1;
T(g)=((Y-A*E*(s+p)/2)*(1+(tan(j*(1+c)*(atan(c*(tan(((1-c)*(v-z))+z))))/(c*u))).^2))/((k
+q)-1)+((A*E*(tan(j*(1+c)*(atan(c*(tan(((1-c)*(v-z))+z))))/(c*u))).^2/2))
w(g)=(-j*(1+c)*(atan(c*(tan(((1-c)*(v-z))+z))))/(c*u))
end
plot(r*180/pi,F,w*180/pi,T);hold on; text(16,2,['β= 1']); grid on
end


c=0; u=384,v=pi/6,z=53*pi/360,Y=30,A=1.5,E=50;
i=0:u/(1+c);
s=sum((1+(tan((i*(1+c)*(((1-c)*(v-z))+z))/u)).^2).*(tan((i*(1+c)*(((1-c)*(v-z))+z))/u)).^
2)
i=0:u/(1+c);
k=sum((1+(tan((i*(1+c)*(((1-c)*(v-z))+z))/u)).^2).^2)
for i=0:u/(1+c); h=i+1;
F(h)=((Y-A*E*s/2)*(1+(tan((i*(1+c)*(((1-c)*(v-z))+z))/u)).^2))/(k)+((A*E*(tan((i*(1+c)
*(((1-c)*(v-z))+z))/u)).^2/2))
```

```
r(h)=(i*(1+c)*(((1-c)*(v-z))+z)/u)
end
plot(r*180/pi,F); text(16,-2,['β= 0']); grid on
end


clear
c=1/9; u=384,v=pi/6,z=53*pi/360,Y=30,A=1.5,E=50;
i=0:u/(1+c);
s=sum((1+(tan((i*(1+c)*(((1-c)*(v-z))+z))/u)).^2).*(tan((i*(1+c)*(((1-c)*(v-z))+z))/u)).^
2)
i=0:u/(1+c);
k=sum((1+(tan((i*(1+c)*(((1-c)*(v-z))+z))/u)).^2).^2)
j=0:c*u/(1+c);
p=sum((1+(tan(j*(1+c)*(atan(c*(tan(((1-c)*(v-z))+z))))/(c*u))).^2).*(tan(j*(1+c)*(atan(c
*(tan(((1-c)*(v-z))+z))))/(c*u))).^2)
j=0:c*u/(1+c);
q=sum((1+(tan(j*(1+c)*(atan(c*(tan(((1-c)*(v-z))+z))))/(c*u))).^2).^2)
for i=0:u/(1+c); h=i+1;
F(h)=((Y-A*E*(s+p)/2)*(1+(tan((i*(1+c)*(((1-c)*(v-z))+z))/u)).^2))/((k+q)-1)+((A*E*(ta
n((i*(1+c)*(((1-c)*(v-z))+z))/u)).^2/2))
r(h)=(i*(1+c)*(((1-c)*(v-z))+z)/u)
end
for j=0:c*u/(1+c); g=j+1;
T(g)=((Y-A*E*(s+p)/2)*(1+(tan(j*(1+c)*(atan(c*(tan(((1-c)*(v-z))+z))))/(c*u))).^2))/((k
+q)-1)+((A*E*(tan(j*(1+c)*(atan(c*(tan(((1-c)*(v-z))+z))))/(c*u))).^2/2))
w(g)=(-j*(1+c)*(atan(c*(tan(((1-c)*(v-z))+z))))/(c*u))
end
plot(r*180/pi,F,w*180/pi,T);hold on; text(16,0,['β= 1/9']); grid on
end
```

2. TF=3.2

```
clear
c=1;u=384,v=59*pi/450,z=26*pi/225,,Y=30,A=1.5,E=50;
i=0:u/(1+c);
s=sum((1+(tan((i*(1+c)*(((1-c)*(v-z))+z))/u)).^2).*(tan((i*(1+c)*(((1-c)*(v-z))+z))/u)).^
2)
i=0:u/(1+c);
k=sum((1+(tan((i*(1+c)*(((1-c)*(v-z))+z))/u)).^2).^2)
j=0:c*u/(1+c);
 p=sum((1+(tan(j*(1+c)*(atan(c*(tan(((1-c)*(v-z))+z))))/(c*u))).^2).*(tan(j*(1+c)*(atan(c
 *(tan(((1-c)*(v-z))+z))))/(c*u))).^2)
j=0:c*u/(1+c);
q=sum((1+(tan(j*(1+c)*(atan(c*(tan(((1-c)*(v-z))+z))))/(c*u))).^2).^2)
```

```
for i=0:u/(1+c); h=i+1;
F(h)=((Y-A*E*(s+p)/2)*(1+(tan((i*(1+c)*(((1-c)*(v-z))+z))/u)).^2))/((k+q)-1)+((A*E*(ta
n((i*(1+c)*(((1-c)*(v-z))+z))/u)).^2/2))
r(h)=(i*(1+c)*(((1-c)*(v-z))+z)/u)
end
for j=0:c*u/(1+c); g=j+1;
T(g)=((Y-A*E*(s+p)/2)*(1+(tan(j*(1+c)*(atan(c*(tan(((1-c)*(v-z))+z))))/(c*u))).^2))/((k
+q)-1)+((A*E*(tan(j*(1+c)*(atan(c*(tan(((1-c)*(v-z))+z))))/(c*u))).^2/2))
w(g)=(-j*(1+c)*(atan(c*(tan(((1-c)*(v-z))+z))))/(c*u))
end
plot(r*180/pi,F,w*180/pi,T);hold o; text(16,2,['β= 1']); grid on;
end


c=0; u=384,v=59*pi/450,z=26*pi/225,,Y=30,A=1.5,E=50;
i=0:u/(1+c);
s=sum((1+(tan((i*(1+c)*(((1-c)*(v-z))+z))/u)).^2).*(tan((i*(1+c)*(((1-c)*(v-z))+z))/u)).^
2)
i=0:u/(1+c);
k=sum((1+(tan((i*(1+c)*(((1-c)*(v-z))+z))/u)).^2).^2)
for i=0:u/(1+c); h=i+1;
F(h)=((Y-A*E*s/2)*(1+(tan((i*(1+c)*(((1-c)*(v-z))+z))/u)).^2))/(k)+((A*E*(tan((i*(1+c)
*(((1-c)*(v-z))+z))/u)).^2/2))
r(h)=(i*(1+c)*(((1-c)*(v-z))+z)/u)
end
plot(r*180/pi,F); text(16,-2,['β= 0']); grid on
end


clear
c=1/9; u=384,v=59*pi/450,z=26*pi/225,,Y=30,A=1.5,E=50;
i=0:u/(1+c);
s=sum((1+(tan((i*(1+c)*(((1-c)*(v-z))+z))/u)).^2).*(tan((i*(1+c)*(((1-c)*(v-z))+z))/u)).^
2)
i=0:u/(1+c);
k=sum((1+(tan((i*(1+c)*(((1-c)*(v-z))+z))/u)).^2).^2)
j=0:c*u/(1+c);
p=sum((1+(tan(j*(1+c)*(atan(c*(tan(((1-c)*(v-z))+z))))/(c*u))).^2).*(tan(j*(1+c)*(atan(c
*(tan(((1-c)*(v-z))+z))))/(c*u))).^2)
j=0:c*u/(1+c);
q=sum((1+(tan(j*(1+c)*(atan(c*(tan(((1-c)*(v-z))+z))))/(c*u))).^2).^2)
for i=0:u/(1+c); h=i+1;
F(h)=((Y-A*E*(s+p)/2)*(1+(tan((i*(1+c)*(((1-c)*(v-z))+z))/u)).^2))/((k+q)-1)+((A*E*(ta
n((i*(1+c)*(((1-c)*(v-z))+z))/u)).^2/2))
r(h)=(i*(1+c)*(((1-c)*(v-z))+z)/u)
end
for j=0:c*u/(1+c); g=j+1;
T(g)=((Y-A*E*(s+p)/2)*(1+(tan(j*(1+c)*(atan(c*(tan(((1-c)*(v-z))+z))))/(c*u))).^2))/((k
```

```
+q)-1)+((A*E*(tan(j*(1+c)*(atan(c*(tan(((1-c)*(v-z))+z))))/(c*u))).^2/2))
w(g)=(-j*(1+c)*(atan(c*(tan(((1-c)*(v-z))+z))))/(c*u))
end
plot(r*180/pi,F,w*180/pi,T);hold on; text(16,0,['β= 1/9']); grid on
end
```

Program for Distribution of Fiber Stress in the Yarn Calculation

1. TF=4.2

```
clear
c=0; u=384,v=pi/6,z=53*pi/360,Y=30,A=1.5,E=50;
i=0:u/(1+c);
s=sum((1+(tan((i*(1+c)*(((1-c)*(v-z))+z))/u)).^2).*(tan((i*(1+c)*(((1-c)*(v-z))+z))/u)).^
2)
i=0:u/(1+c);
k=sum((1+(tan((i*(1+c)*(((1-c)*(v-z))+z))/u)).^2).^2)
for i=0:u/(1+c); h=i+1;
 F(h)=((Y-A*E*s/2)*(1+(tan((i*(1+c)*(((1-c)*(v-z))+z))/u)).^2))/(k)+((A*E*(tan((i*(1+c)
 *( ((1-c)*(v-z))+z))/u)).^2/2))
r(h)=(i*(1+c)*(((1-c)*(v-z))+z)/u)
end
plot(r*180/pi,F); text(16,-2,['β= 0']); grid on
end
h=0; m=11; bx=2:m; by=1:m;dx=ones(1,length(bx))*m; dy=ones(1,length(by))*m;
x=1+6*(sum(dx-bx)); y=6*(sum(dy-by));
N2=sum(F(x:y))/(6*(m-1))
```

```
clear
c=1; u=384,v=pi/6,z=53*pi/360,Y=30,A=1.5,E=50;
i=0:u/(1+c);
s=sum((1+(tan((i*(1+c)*(((1-c)*(v-z))+z))/u)).^2).*(tan((i*(1+c)*(((1-c)*(v-z))+z))/u)).^
2)
i=0:u/(1+c);
k=sum((1+(tan((i*(1+c)*(((1-c)*(v-z))+z))/u)).^2).^2)
j=0:c*u/(1+c);
p=sum((1+(tan(j*(1+c)*(atan(c*(tan(((1-c)*(v-z))+z))))/(c*u))).^2).*(tan(j*(1+c)*(atan(c
*(t an(((1-c)*(v-z))+z))))/(c*u))).^2)
j=0:c*u/(1+c);
q=sum((1+(tan(j*(1+c)*(atan(c*(tan(((1-c)*(v-z))+z))))/(c*u))).^2).^2)
for i=0:u/(1+c); h=i+1;
F(h)=((Y-A*E*(s+p)/2)*(1+(tan((i*(1+c)*(((1-c)*(v-z))+z))/u)).^2))/((k+q)-1)+((A*E*(ta
```

```
n((i*(1+c)*(((1-c)*(v-z))+z))/u)).^2/2))
r(h)=(i*(1+c)*(((1-c)*(v-z))+z)/u)
end
for j=0:c*u/(1+c); g=j+1;
T(g)=((Y-A*E*(s+p)/2)*(1+(tan(j*(1+c)*(atan(c*(tan(((1-c)*(v-z))+z))))/(c*u))).^2))/((k
+q)-1)+((A*E*(tan(j*(1+c)*(atan(c*(tan(((1-c)*(v-z))+z))))/(c*u))).^2/2))
w(g)=(-j*(1+c)*(atan(c*(tan(((1-c)*(v-z))+z))))/(c*u))
end
plot(r*180/pi,F,w*180/pi,T);hold on; text(16,2,['β= 1']); grid on
end
h=0; m=11; bx=2:m; by=1:m;dx=ones(1,length(bx))*m; dy=ones(1,length(by))*m;
x=1+3*(sum(dx-bx)); y=3*(sum(dy-by));
N=2*sum(F(x:y))/(6*(m-1))
```

1. TF=3.2

```
clear
c=0; u=384,v=59*pi/450,z=26*pi/225,,Y=30,A=1.5,E=50;
i=0:u/(1+c);
s=sum((1+(tan((i*(1+c)*(((1-c)*(v-z))+z))/u)).^2).*(tan((i*(1+c)*(((1-c)*(v-z))+z))/u)).^
2)
i=0:u/(1+c);
k=sum((1+(tan((i*(1+c)*(((1-c)*(v-z))+z))/u)).^2).^2)
for i=0:u/(1+c); h=i+1;
F(h)=((Y-A*E*s/2)*(1+(tan((i*(1+c)*(((1-c)*(v-z))+z))/u)).^2))/(k)+((A*E*(tan((i*(1+c)
*(((1-c)*(v-z))+z))/u)).^2/2))
r(h)=(i*(1+c)*(((1-c)*(v-z))+z)/u)
end
plot(r*180/pi,F); text(16,-2,['β= 0']); grid on
end
h=0; m=11; bx=2:m; by=1:m;dx=ones(1,length(bx))*m; dy=ones(1,length(by))*m;
x=1+6*(sum(dx-bx)); y=6*(sum(dy-by));
N2=sum(F(x:y))/(6*(m-1))
```

```
clear
c=1;u=384,v=59*pi/450,z=26*pi/225,,Y=30,A=1.5,E=50;
i=0:u/(1+c);
s=sum((1+(tan((i*(1+c)*(((1-c)*(v-z))+z))/u)).^2).*(tan((i*(1+c)*(((1-c)*(v-z))+z))/u)).^
2)
i=0:u/(1+c);
k=sum((1+(tan((i*(1+c)*(((1-c)*(v-z))+z))/u)).^2).^2)
j=0:c*u/(1+c);
p=sum((1+(tan(j*(1+c)*(atan(c*(tan(((1-c)*(v-z))+z))))/(c*u))).^2).*(tan(j*(1+c)*(atan(c
*(tan(((1-c)*(v-z))+z))))/(c*u))).^2)
j=0:c*u/(1+c);
```

```
q=sum((1+(tan(j*(1+c)*(atan(c*(tan(((1-c)*(v-z))+z))))/(c*u))).^2).^2)
for i=0:u/(1+c); h=i+1;
F(h)=((Y-A*E*(s+p)/2)*(1+(tan((i*(1+c)*(((1-c)*(v-z))+z))/u)).^2))/((k+q)-1)+((A*E*(ta
n((i*(1+c)*(((1-c)*(v-z))+z))/u)).^2/2))
r(h)=(i*(1+c)*(((1-c)*(v-z))+z)/u)
end
for j=0:c*u/(1+c); g=j+1;
 T(g)=((Y-A*E*(s+p)/2)*(1+(tan(j*(1+c)*(atan(c*(tan(((1-c)*(v-z))+z))))/(c*u))).^2))/((k
 + q)-1)+((A*E*(tan(j*(1+c)*(atan(c*(tan(((1-c)*(v-z))+z))))/(c*u))).^2/2))
w(g)=(-j*(1+c)*(atan(c*(tan(((1-c)*(v-z))+z))))/(c*u))
end
plot(r*180/pi,F,w*180/pi,T);hold on; text(16,2,['β= 1']); grid on
end
h=0; m=11; bx=2:m; by=1:m; dx=ones(1,length(bx))*m; dy=ones(1,length(by))*m;
x=1+3*(sum(dx-bx));y=3*(sum(dy-by));
N=2*sum(F(x:y))/(6*(m-1))
```

Appendix C

Yarn Properties

Appendix C1	Yarn Diameter
Appendix C2	Yarn Twist
Appendix C3	Yarn Hairiness
Appendix C4	Yarn Snaring
Appendix C5	Yarn Tenacity
Appendix C6	Yarn Bending Property

Appendix C1

Yarn Diameter

Yarn sample	7-3.2 -A	7-3.2 -$NS_{0.33}$	7-3.2 -$NS_{0.43}$	7-3.8 -$NS_{0.33}$	7-4.2 -A	7-4.2 -$NS_{0.33}$	10-3.2 -A	10-3.2 -$NS_{0.43}$	10-4.2 -A	10-4.2 -$NS_{0.33}$
	0.38	0.40	0.36	0.38	0.36	0.34	0.36	0.34	0.28	0.26
	0.48	0.44	0.40	0.36	0.32	0.36	0.32	0.34	0.30	0.30
	0.50	0.40	0.48	0.40	0.32	0.36	0.3	0.32	0.30	0.30
	0.40	0.38	0.40	0.32	0.42	0.36	0.34	0.32	0.26	0.26
	0.42	0.42	0.36	0.40	0.36	0.32	0.36	0.30	0.30	0.28
	0.44	0.40	0.40	0.36	0.38	0.34	0.34	0.32	0.28	0.26
	0.46	0.40	0.36	0.34	0.36	0.34	0.3	0.34	0.34	0.26
	0.50	0.38	0.34	0.38	0.38	0.32	0.38	0.32	0.28	0.32
	0.54	0.42	0.38	0.40	0.32	0.36	0.36	0.32	0.26	0.28
	0.40	0.42	0.38	0.40	0.40	0.32	0.40	0.32	0.32	0.24
	0.48	0.38	0.36	0.38	0.36	0.32	0.34	0.40	0.32	0.28
	0.46	0.44	0.34	0.38	0.40	0.32	0.38	0.28	0.30	0.26
	0.46	0.40	0.40	0.40	0.36	0.32	0.34	0.34	0.32	0.30
	0.52	0.38	0.36	0.38	0.34	0.36	0.40	0.36	0.30	0.30
	0.52	0.38	0.40	0.40	0.38	0.36	0.40	0.40	0.32	0.28
	0.46	0.36	0.44	0.34	0.36	0.40	0.40	0.32	0.28	0.32
	0.40	0.44	0.38	0.32	0.34	0.34	0.36	0.36	0.32	0.26
	0.40	0.36	0.36	0.40	0.40	0.30	0.44	0.32	0.32	0.30
	0.48	0.40	0.38	0.36	0.38	0.34	0.40	0.34	0.34	0.28
	0.46	0.38	0.38	0.36	0.38	0.30	0.32	0.34	0.28	0.36
Mean (mm)	0.458	0.399	0.383	0.373	0.366	0.339	0.362	0.335	0.301	0.285
CV (%)	10.11	6.19	8.68	7.23	7.75	7.28	10.44	8.64	7.91	9.89

Appendix C2

Yarn Twist

Yarn sample	7-3.2 -A	7-3.2 -$NS_{0.33}$	7-3.2 -$NS_{0.43}$	7-4.2 -A	7-4.2 -$NS_{0.33}$	10-3.2 -A	10-3.2 -$NS_{0.43}$
	322	332	314	455	450	396	378
	320	328	328	442	448	391	406
	330	328	358	448	439	428	399
	340	332	323	431	398	400	396
	346	334	342	446	412	402	416
	338	312	336	448	442	416	381
	324	342	346	452	440	414	400
	328	305	320	446	461	393	410
	332	338	332	453	394	414	403
	340	342	342	460	440	403	398
Mean (tpm)	302	300	304	408	394	370	363
CV (%)	4.07	4.88	5.13	3.50	6.25	4.24	4.26

Appendix C3

Yarn Hairiness (Cop)

Yarn sample	7-3.2 -A	7-3.2 -$NS_{0.33}$	7-3.2 -$NS_{0.43}$	7-3.8 -A	7-3.8 -$NS_{0.33}$	7-4.2 -A	10-3.3 -A	10-3.3 -$NS_{0.36}$	10-4.2 -A
	1806	1329	785	1470	698	1261	673	347	623
	1891	1250	744	1022	602	991	548	501	548
	2329	1341	862	1256	586	896	548	404	401
	2171	1248	649	1011	716	1002	693	419	489
	1852	1465	809	1325	572	895	521	452	446
	2001	1211	779	1412	451	1251	556	379	469
Mean (S3)	2008	1307	771	1249	604	1049	590	417	496
CV (%)	10.2	7.1	9.3	15.6	15.9	15.9	12.4	13.0	15.9

Appendix C4

Yarn Snaring

Yarn sample	7-3.2 -A	7-3.2 -$NS_{0.33}$	7-3.2 -$NS_{0.43}$	7-3.8 -A	7-3.8 -$NS_{0.33}$	7-4.2 -A	7-4.2 -$NS_{0.33}$	10-3.2 -A	10-3.2 -$NS_{0.43}$	10-3.3 -A	10-3.3 -$NS_{0.36}$	10-4.2 -A	10-4.2 -$NS_{0.33}$
	33	28	24	41	33	40	30	37	26	36	33	49	34
	33	28	23	42	31	38	34	38	27	35	32	47	32
	32	28	25	38	33	39	34	37	24	42	32	46	38
	32	29	25	39	30	41	33	36	26	42	33	45	36
	32	28	22	37	32	41	32	37	26	37	30	46	35
	35	30	25	38	29	43	34	40	25	39	30	46	36
	33	28	24	36	32	36	34	38	25	44	35	47	37
	27	31	23	39	32	36	34	41	27	40	30	44	38
	34	28	22	39	34	39	31	32	26	36	34	46	39
	35	30	23	40	28	41	34	37	26	36	28	49	39
Mean (turns /25cm)	33	29	24	39	31	39	33	37	26	39	32	47	36
CV (%)	6.96	3.94	4.97	4.61	6.04	5.76	4.52	6.45	3.56	8.18	6.82	3.40	6.24

Appendix C5

Yarn Tenacity (Cop)

Yarn sample	7-3.2 -A	7-3.2 -$NS_{0.33}$	7-3.2 -$NS_{0.43}$	7-3.8 -A	7-3.8 -$NS_{0.33}$	7-4.2 -A	7-4.2 -$NS_{0.33}$	10-3.3 -A	10-3.3 -$NS_{0.36}$	10-4.2 -A	10-4.2 -$NS_{0.33}$
	15.97	15.6	16.57	17.48	18.75	17.73	16.35	15.36	16.59	17.43	16.59
	16.55	16.49	16.27	16.99	16.45	17.42	16.35	15.9	15.84	17.04	18.21
	15.31	16.48	16.64	17.18	17.65	17.59	18.12	15.5	14.78	17.78	15.32
	16.06	16.65	17.3	17.28	17.21	18.52	16.32	15.61	14.98	18.19	16.24
	14.21	14.88	17.17	16.21	16.45	18.12	15.26	16.86	16.8	16.56	15.21
	13.89	17.25	16.74	15.24	16.12	18.83	16.25	15.12	14.75	17.25	15.66
	15.98	16.45	16.8	17.13	18.12	16.52	15.36	14.12	15.11	19.25	16.12
	16.35	16.19	15.9	17.09	17.3	16.21	15.59	16.25	15.01	16.12	16.12
	16.29	15.44	16.4	17.88	16.11	17.58	16.35	16.12	14.65	18.32	15.69
	16.61	16.57	14.9	17.95	17.96	17.31	16.38	14.91	14.79	16.25	16.01
Mean (cN/tex)	15.72	16.20	16.50	17.04	17.21	17.58	16.23	15.58	15.33	17.42	16.12
CV (%)	6.09	4.29	4.16	4.69	5.31	4.59	4.93	4.94	5.18	5.69	5.26

Appendix C6

Yarn Bending Property

Yarn sample	7-3.2-A		7-3.2-$NS_{0.33}$		7-3.2-$NS_{0.43}$		7-4.2-A	
	B	2HB	B	2HB	B	2HB	B	2HB
	0.0042	0.0056	0.0053	0.0047	0.0054	0.0043	0.0069	0.0042
	0.0058	0.0040	0.0055	0.0043	0.0062	0.0044	0.0064	0.0058
	0.0055	0.0047	0.0058	0.0041	0.0057	0.0044	0.0064	0.0056
Mean	0.0052	0.0048	0.0055	0.0044	0.0058	0.0044	0.0066	0.0052

Appendix D

Fabric Properties and Performance

Appendix D1	Fabric Dimensional Stability
Appendix D2	Fabric Skewness
Appendix D3	Fabric Tensile Properties
Appendix D4	Fabric Tear Properties
Appendix D5	Air Permeability
Appendix D6	Wicking Property
Appendix D7	Parameters Measured on The KES Apparatus
Appendix D8	Implication of Hand Terms

Appendix D1

Fabric Dimensional Stability

Fabric sample	1	2	3	4	5	6	10	11	12	13	14	15
Warp	-2.7	-3.2	-3.8	-1.1	-1.3	-0.2	-2.2	-2.9	-1.1	-3.5	-3.9	-3.2
	-2.8	-3.5	-3.5	-1.3	-1.2	-0.2	-2.6	-3.5	-1.2	-3.7	-4.1	-3.9
	-2.5	-3.1	-3.5	-1.2	-1.4	-0.4	-2.4	-3.2	-1.6	-3.6	-4.3	-3.7
	-2.9	-3.1	-3.6	-0.9	-0.9	-0.7	-2.4	-3.2	-0.8	-3.1	-4.7	-4.3
	-2.6	-3.2	-3.9	-1.5	-1.2	-0.5	-2.3	-3.0	-1.2	-3.5	-4.5	-3.3
Mean (%)	-2.7	-3.2	-3.7	-1.2	-1.2	-0.4	-2.4	-3.2	-1.2	-3.5	-4.3	-3.7
Weft	-2.6	-2.5	-2.9	-2.3	-2.3	-2.3	-1.6	-2.2	-1.0	-0.9	-1.4	-0.8
	-2.1	-2.3	-3.1	-2.1	-2.5	-1.8	-1.5	-2.1	-1.1	-0.9	-1.5	-0.8
	-2.3	-2.6	-3.1	-1.8	-2.4	-2.1	-1.4	-2.1	-1.2	-0.9	-1.8	-0.9
	-2.3	-2.6	-3.3	-2.1	-2.3	-1.9	-1.8	-1.9	-1.0	-1.2	-1.5	-1.0
	-2.5	-2.3	-3.1	-1.8	-2.6	-2.1	-1.6	-2.0	-1.1	-0.8	-1.7	-0.7
Mean (%)	-2.4	-2.5	-3.1	-2.0	-2.4	-2.0	-1.6	-2.1	-1.1	-0.9	-1.6	-0.8

Appendix D2

Fabric Skewness (Skewness Movement)

Fabric sample	1	2	3	4	5	6	10	11	12	13	14	15
	1.1	2.6	0.7	2.0	3.0	2.3	2.0	4.9	3.4	0.3	2.0	2.3
	1.4	2.0	1.0	1.5	3.8	1.8	2.0	5.8	4.7	-0.3	1.7	-0.3
	1.0	2.5	0.8	1.7	3.5	1.9	2.0	6.7	2.9	0.3	1.2	0.6
Mean (%)	1.2	2.4	0.8	1.7	3.4	1.4	2.0	5.8	3.7	0.1	2.3	0.9

Appendix D3

Fabric Tensile Properties

Fabric sample	1	2	3	4	5	6	7	8	9	10	11	12	13	14	15
Warp	1156.9	1146.8	1139.2	1005.8	942.1	1095.6	1074.4	1180.2	1172.7	624.4	610.2	589.8	411.7	491.8	343.8
	1198.7	1186	1159	1017	1034	1048	1064.2	1140.7	1124.7	598.1	587.7	623.4	383.6	443.2	357.6
	1039.2	1032	1001	1014	979.9	1074	1075.8	1058.9	1109.2	580.1	644.4	648.6	416.6	418.4	341.3
	1182.5	1198	1054.5	895.8	1001	995.3	1069.5	1101.3	1156	616.9	642.4	653.2	379.6	424.3	417.3
	1179	1144.3	1158.3	983.6	988.2	1056.3	1073.6	1098	1171.3	629.8	617.2	616.9	413.6	453.3	404.0
Mean (N)	1151.3	1141.4	1102.4	983.2	989.0	1053.8	1071.5	1115.8	1146.8	609.9	620.4	626.3	401.1	446.2	372.8
Weft	693.4	688.8	726.3	849.1	756.4	712.8	535.7	461.9	557.4	580.7	620.9	484.3	384.6	412.8	329.5
	679.6	621.1	799.2	846.6	839.7	689.9	540	465	544.1	589.8	598.4	513.0	381.7	406.0	348.6
	631.9	654.2	698.2	833.3	834.9	659.6	545.3	458.3	561.8	602.4	626.6	503.1	375.4	413.4	317.6
	701.2	655	699	888.6	921.1	681.4	534.1	457.1	539	581.5	637.0	484.6	393.2	392.8	324.2
	702	603.3	744.3	828.5	848.1	663.1	534.5	469.2	553.6	607.8	629.3	490.5	369.0	389.9	320.0
Mean (N)	681.6	644.5	733.4	849.2	840.0	681.4	537.9	462.3	551.2	592.5	622.4	495.1	380.8	402.9	327.9

Appendix D4

Fabric Tear Properties

Fabric sample	1	2	3	4	5	6	7	8	9	10	11	12	13	14	15
Warp	92.6	86.5	86.6	99.1	83.3	81.3	80.3	88.2	91.4	37.6	37.0	38.4	25.1	22.6	28.2
	91.2	89.2	85.6	85.3	83.3	105.8	82.3	92.1	92.1	47.7	37.0	3.64	26.3	25.1	18.8
	87.6	82.9	89.9	89.2	86.2	83.3	89.2	89.3	89.6	42.0	37.6	3.64	23.8	24.5	16.9
	87.5	91.2	82.9	87.2	95.1	81.3	88	89	95.2	47.7	39.5	39.5	29.5	24.3	18.7
	97.2	86	91	90.2	91.1	79.4	96.2	92.1	87	41.4	42.0	38.3	25.7	25.1	19.4
Mean (N)	91.2	87.2	87.2	90.2	87.8	86.2	87.2	90.1	91.1	43.3	38.6	37.8	26.1	24.3	20.4
Weft	66.9	59.3	79.6	98	83.3	68.6	48.6	40.2	48.1	63.3	61.5	43.9	40.8	35.8	25.7
	73.1	64.3	75.2	80.4	81.4	61.7	46.1	38.2	48	65.9	63.3	45.8	35.8	37.6	23.8
	68.5	60.8	71.8	96	88.2	48.2	45.6	39.2	45.1	64.0	60.8	47.0	40.8	40.1	22.6
	71.2	59	74	84.3	86.2	68.6	46.8	35.6	48.6	63.3	63.3	47.7	42.6	36.4	24.5
	68.5	65.3	76.8	82.3	85.3	49.8	43.5	43	45.2	64.0	64.0	47.6	38.9	37.6	23.8
Mean (N)	69.6	61.7	75.5	88.2	84.9	59.4	46.1	39.2	47.0	64.1	62.6	46.4	39.8	37.5	24.1

Appendix D5

Air Permeability

Fabric sample	1	2	3	10	11	12	13	14	15
	2.84	2.69	3.84	16.14	20.87	17.91	14.57	17.72	19.29
	2.91	2.81	3.94	12.40	21.26	18.70	15.75	17.72	19.69
	2.95	2.31	4.72	15.55	22.64	20.67	13.58	17.32	19.29
	2.81	2.71	3.98	15.94	17.72	19.69	14.96	19.69	21.06
	3.01	2.07	3.56	14.57	20.08	21.06	13.78	16.93	20.67
	3.12	2.32	3.74	15.75	18.90	20.08	14.76	16.73	19.88
	2.38	3.01	4.13	14.17	18.11	19.29	16.14	17.32	17.52
	3.74	2.54	4.31	13.78	21.65	19.69	15.16	18.70	19.88
	2.80	2.28	3.92	12.40	20.87	19.69	15.35	15.75	18.90
	2.60	2.19	4.17	15.55	21.26	20.08	14.76	17.72	17.32
Mean ($ml/cm^2.s$)	2.90	2.51	4.00	14.63	20.00	19.69	14.88	17.56	19.35
CV(%)	12.2	12.2	8.1	9.62	8.12	4.62	5.83	6.11	6.22

Appendix D6

Wicking Property

Wicking time (s)	Wicking height (mm)														
	10					11					12				
	1	2	3	4	Mean	1	2	3	4	Mean	1	2	3	4	Mean
10	12	10	10	10	11	10	10	10	10	10	9	7	7	9	8
25	16	18	16	16	17	17	16	16	15	16	13	14	13	16	14
50	23	25	23	23	24	24	23	23	22	23	20	22	20	22	21
100	32	33	32	32	32	31	31	33	31	32	32	33	31	31	32
150	38	40	38	38	39	39	40	39	38	39	36	38	37	38	37
200	43	45	44	45	44	43	44	44	43	44	43	44	44	44	44
300	53	55	53	55	54	52	52	53	52	52	52	53	53	53	53
400	60	62	60	61	61	59	60	60	59	60	59	60	59	58	59
500	65	67	66	67	66	65	66	66	65	66	64	66	66	64	65
600	70	72	71	71	71	68	71	71	70	70	68	71	70	68	69

Fabric sample	Water absorbed by stripe												
	Initial weight (g)				Final weight (g)				Water absorbed (%)				
	1	2	3	4	1	2	3	4	1	2	3	4	Mean
10	1.736	1.742	1.749	1.744	2.430	2.441	2.474	2.459	40.0	40.2	41.5	41.0	40.7
11	1.735	1.709	1.713	1.669	2.405	2.313	2.385	2.328	38.6	35.4	39.2	39.4	38.2
12	1.800	1.710	1.757	1.725	2.459	2.394	2.438	2.388	36.6	40.0	38.8	38.4	38.5

Appendix D7

Parameters Measured on the KES Apparatus

Properties	Parameters	Description	Units
Tensile	EMT	Extensibility	(%)
	LT	Linearity	-
	WT	Tensile energy per unit area	($gf.cm/cm^2$)
	RT	Tensile resilience	(%)
Bending	B	Bending rigidity	($gf.cm^2/cm$)
	2HB	Hysteresis of bending moment	(gf.cm/cm)
Shear	G	Shear stiffness	($gf/cm^2.deg$)
	2HG	Hysteresis at shear angle (0.5^o)	(gf/cm)
Surface	MIU	Coefficient of friction	-
	MMD	Mean deviation of MIU	-
	SMD	Geometrical roughness	-
Compression	LC	Linearity	-
	WC	Compression energy	($g.cm/cm^2$)
	RC	Compression resilience	(%)
Thickness	T	Fabric thickness	(mm)
Weight	W	Fabric weight	(mg/cm^2)

Appendix D8

Implication of Hand Terms

Parameters	Reflecting hand quality	Properties influencing hand quality
Koshi	Stiffness, springy property by bending	Bending, shearing, weight, thickness
Numeri	Smoothness, frictional force, smoothness surface	Surface, compression, shear
Fukurami	Softness, fullness, smoothness surface, soft extensibility	Compression, surface, tensile

Appendix E

Denim Washing Procedure

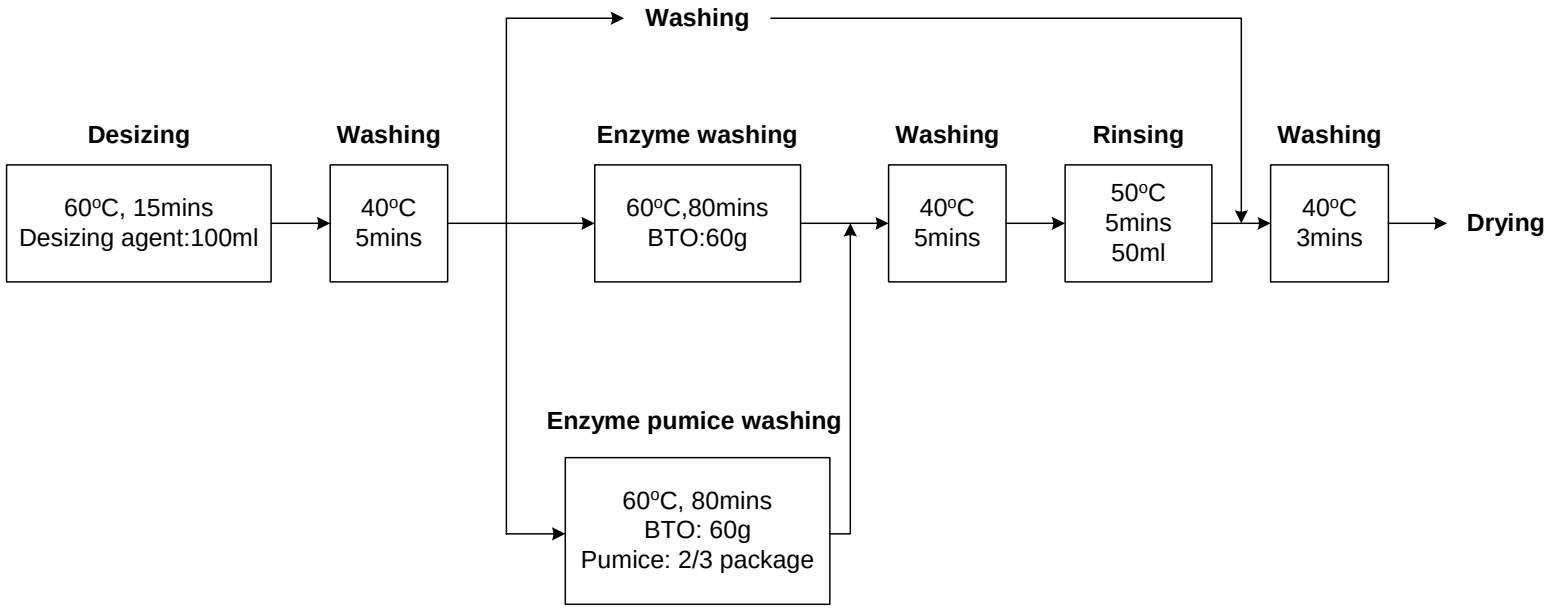

Figure E-1 Denim Washing Procedure